DOLOMITIC LIME MORTARS: CARBONATION COMPLICATIONS AND SUSCEPTIBILITY TO ACIDIC SULFATES

Heather Hartshorn

Submitted in partial fulfillment of the requirement for the degree
Master of Science in Historic Preservation

Graduate School of Architecture, Planning and Preservation

Columbia University

(May 2012)

ABSTRACT

Dolomitic Lime Mortars:
Carbonation Complications and Susceptibility to Acidic Sulfates

Heather Hartshorn

Prof. Norman R. Weiss, advisor

Dolomitic lime mortars, widely used in historic construction and as repair mortars today, are distinguished by their high magnesium content as well as their high plasticity, water retention, and workability. However, the dolomitic lime creates a more complicated chemistry in the resulting mortar in which the magnesium and calcium compounds carbonate at different rates. Although portlandite readily carbonates to calcite, the carbonation of brucite is delayed and could result in a variety of magnesium compounds in the cured mortar. The reaction of these magnesium compounds with acidic sulfates in the environment could lead to the formation of magnesium sulfate salts, which have the potential to deteriorate the mortar itself and surrounding materials. Mortar deterioration could also occur due to the dissolution of the magnesium compounds in the mortar and subsequent material losses.

A series of experiments have been conducted that examine the carbonation of dolomitic lime mortars as well as the extent to which these mortars interact with acidic sulfates. First the production of dolomitic lime was simulated in a laboratory setting, using XRD and SEM to determine the chemical and physical changes that occur during the calcining process. The same analytical techniques were used to examine the level of carbonation in dolomitic lime model mortars. The fundamental reactivity of acidic sulfate solutions with certain compounds in dolomitic mortars was explored using AA. Acidic sulfate attack via acid rain was also simulated on model mortars, and the effects of that exposure analyzed by AA and XRD.

Laboratory work for this thesis was conducted at Columbia University GSAPP's Architecture Conservation Laboratory, the Department of Scientific Research at the Metropolitan Museum of Art, and Highbridge Materials Consulting, Inc.

Heather Hartshorn 15 May 2012

ACKNOWLEDGEMENTS

I would first and foremost like to express my gratitude to my advisor, Prof. Norman R. Weiss, for his guidance and support during this thesis as well as in my conservation education. His unending enthusiasm for this topic and for my work has been a great encouragement throughout the entire process. I would also like to thank Prof. George Wheeler, who has gone above and beyond his duties as a reader and who has also offered much advice throughout my time in this program. For her insight and assistance in performing this thesis research, I also wish to thank my reader Magdalena Malaj.

I would like to extend many thanks to John Walsh and the staff at Highbridge Materials Consulting, Inc. for their generosity and interest in my work. I am also incredibly grateful to Federico Caro and everyone in the Department of Scientific Research at the Metropolitan Museum of Art for accommodating my thesis research and offering much support. Of course, I must also thank Jennifer Schork for beginning the thesis research on dolomitic lime mortars in this program several years ago.

Last, but definitely not least, I would like to thank my parents for their unending love and selfless encouragement.

CONTENTS

Chapter 1:

On Dolomitic Lime Mortars

On the most fundamental level, mortar consists of three components: binder, aggregate, and water. The binder is typically lime, cement, or some combination of the two while sand is commonly employed as the aggregate. For centuries mortars have been made with the primary binder as lime, which was often produced locally. Lime production involves the heating of limestone, a carbonate stone containing calcite ($CaCO_3$) and dolomite ($CaMg(CO_3)_2$). Chalk, coral rocks, and shells may also be calcined to produce lime; however, these sources contain only calcite or aragonite ($CaCO_3$ with an orthorhombic rather than rhombohedral crystal structure). Defined by its magnesium content, limestone containing an equivalent of 35-46% $MgCO_3$ (from dolomite) is classified as "dolomitic limestone" while "high-calcium limestone" contains an equivalent of less than 5% $MgCO_3$.[1]

The term "dolomitic" originates from the Dolomite Mountains in the Tyrol region of Austria and Northern Italy, where the limestone has a high magnesium content. However, dolomitic limestone can be found in many other regions of the world, including the United States, where the resulting lime has been used both in historic mortars and as a common repair mortar today. In fact, "Preservation Brief 2: Repointing of Mortar Joints in Historic Masonry Buildings" identifies Type S hydrated lime, which is typically dolomitic, as a proper lime in mortars for repointing masonry.[2]

The mechanism known as the *lime cycle* (see Figure 1-1), which describes the process of making lime mortars from high-calcium limestone, is well understood. However, the *dolomitic lime 'cycle'* is a somewhat more complicated model, in that the magnesium and calcium compounds hydrate and carbonate in a different manner, apparently leading to a wider variety of phases in the mortar (see Figure 1-2).

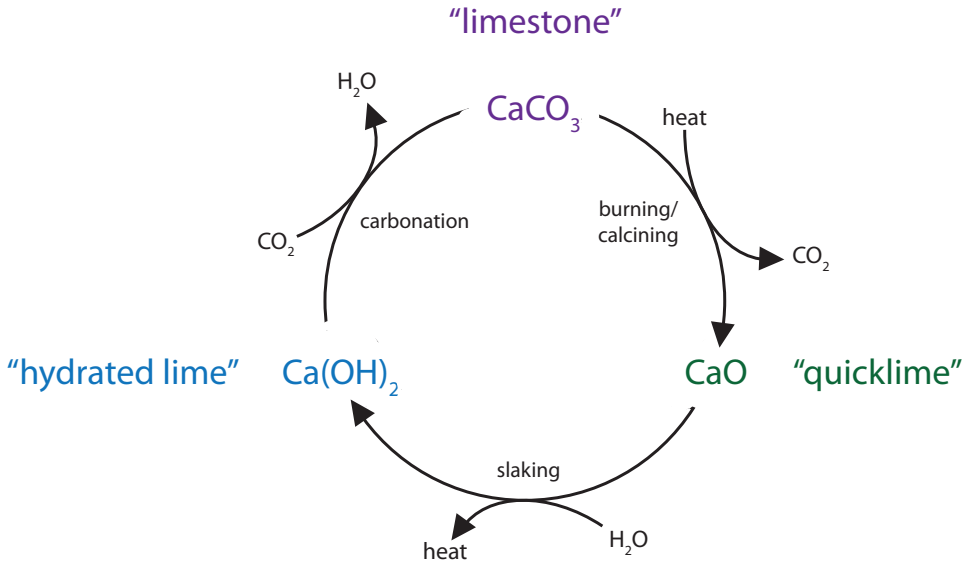

Figure 1-1. The Lime Cycle (for high-calcium limestone)

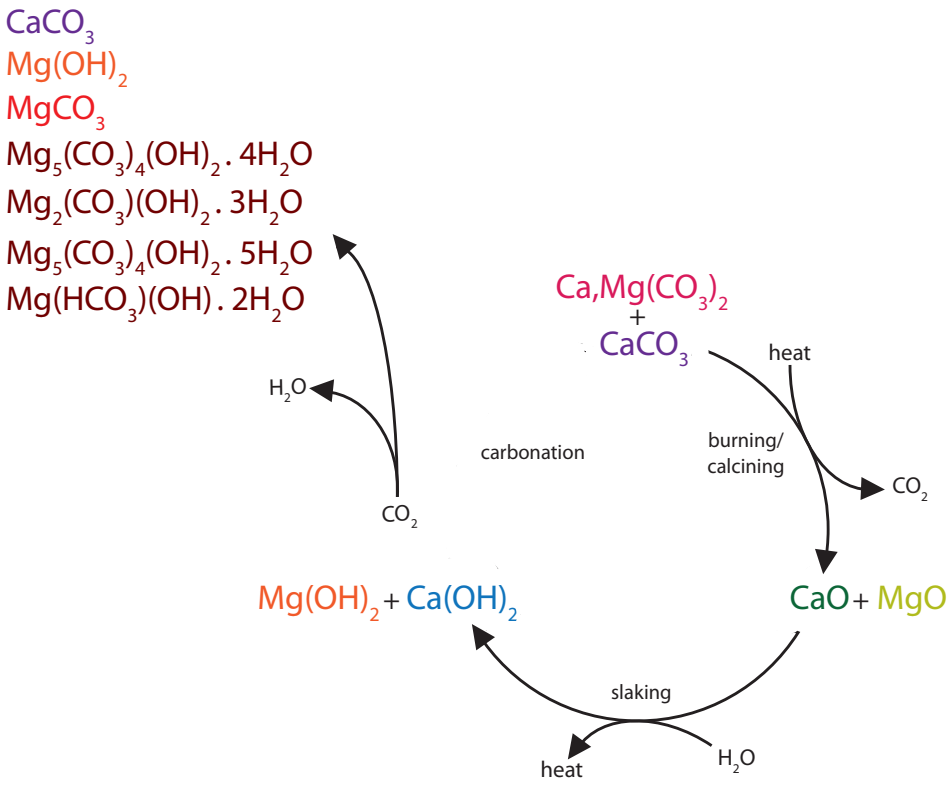

Figure 1-2. The Dolomitic Lime 'Cycle'

Just as the calcining of high-calcium limestone produces quicklime (CaO), dolomitic stone is calcined to produce both quicklime and periclase (MgO). The two oxides of dolomitic lime hydrate to portlandite ($Ca(OH)_2$) and brucite ($Mg(OH)_2$), although the hydration of periclase is much slower than that of quicklime. The carbonation of portlandite to calcite is unproblematic; however, the carbonation of brucite to magnesite ($MgCO_3$) occurs at a much slower rate, if at all. The resulting mortar could contain an assortment of compounds in varying ratios -- including residual periclase, brucite, magnesite, and a variety of hydroxycarbonates whose formation depends on the water content of the mortar as well as the carbon dioxide and moisture content of the air. Among the possible hydroxycarbonates formed are hydromagnesite ($Mg_5(CO_3)_4(OH)_2{\cdot}4H_2O$), nesquehonite ($Mg(HCO_3)(OH){\cdot}2H_2O$), artinite ($Mg_2(CO_3)(OH)_2{\cdot}3H_2O$), and dypingite ($Mg_5(CO_3)_4(OH)_2{\cdot}5H_2O$). Some scholars have also observed amorphous magnesium phases in dolomitic lime mortars, possibly as a result of overburning the lime.[3,4] The magnesium compounds, whether periclase, brucite, magnesite, or any of the hydroxycarbonates, may be significantly reactive with acid rain, which could lead to the formation of magnesium sulfate salts. This effect will be discussed later in this chapter in the section entitled “The Sulfate Problem.”

Some of the physical properties of dolomitic lime mortars have been explored by Schork (2009), and this thesis hopes to continue adding to the body of knowledge about these mortars.[5] Herein the chemical properties of dolomitic lime mortars are explored -- specifically the extent to which the high magnesium content of the dolomitic lime affects its carbonation and subsequent environmental reactivity.

History of Use and Standardization

Lime is one of the oldest building materials and has been used for construction purposes for millennia. Its properties and use in the Greco-Roman world have been recorded by scholars such as Pliny and Vitruvius. Other civilizations employed lime in construction from the Great Wall of China to the Egyptians to the cathedrals of medieval and renaissance Europe. Until the 19th century in Europe and the late 19th century in the United States, most mortars utilized a lime binder.[6,7]

Literature from the early 19th century onward described the use of dolomitic lime specifically, noting its higher long-term strength as compared to high-calcium limes.[8,9] Throughout the 19th and early 20th centuries mortars made of lime derived from dolomitic stone were used extensively in the United States, as craftsmen often preferred the workability of these mortars.[10] However, the dominance of dolomitic lime in mortars and plasters was seriously challenged at the turn of the 20th century by Portland cement, a binder which is less workable but sets faster with a higher initial strength.[11,12] Although builders from the 1910s onward often used mortars that were completely or mostly cement, by the 1930s research on masonry construction had shifted the preference back toward cement-lime combinations. Cement-lime mortars remain prevalent today while some in the preservation community are returning to the practice of using lime as the sole binder.

The first half of the 20th century saw the standardization of lime and other building materials by the National Bureau of Standards and the National Lime Association. In 1913 ASTM C6 was the first Standard for Hydrated Lime, which defined hydrated lime in four distinct categories based on magnesium content: high-calcium, calcium, magnesium, and high-magnesium. The Corson Pressure Hydrator, patented in 1943, afforded the lime industry a continuous process for making a dry hydrated lime of reproducible quality from dolomitic quicklime at high pressures. In 1946, ASTM C207 defined hydrated lime as Type S (special) or Type N (normal). Type S dry hydrates have early plasticity and high water retention, and the standard limits unhydrated oxide content to 8%.[13]

Although C207 specifies chemically only that 95% of the lime must consist of calcium and magnesium oxides, Type S limes are typically dolomitic.[14] In fact, the Type S designation grew out of the popularity of slaked dolomitic quicklimes for finishing work in the 19th century due to their high plasticity.[15]

Lime manufacture is the second largest use of limestone today. The use of Type S lime in particular grew rapidly since its standardization, as nearly 95% of hydrated lime for masonry construction was Type S by 1980. There are many producers of dolomitic lime in United States today (see Figures 1-3 and 1-4), and some have been in operation for over a century.

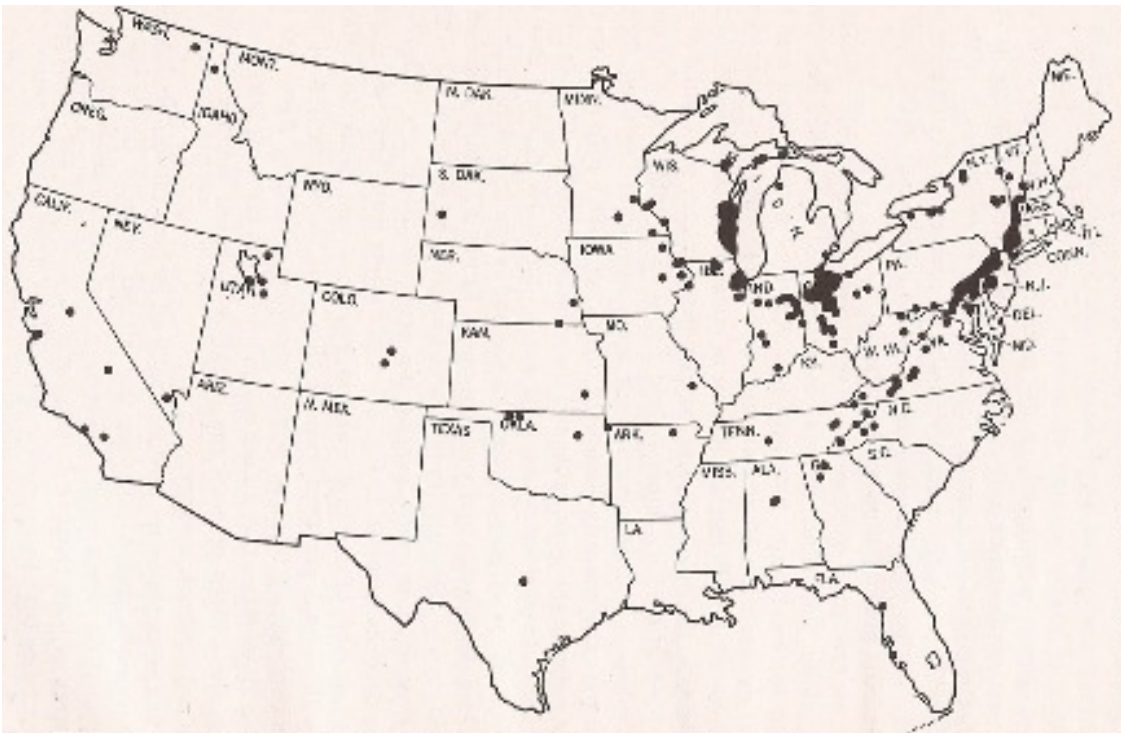

Figure 1-3. Location of dolomitic limestone deposits in the United States as published by Boynton (1980).[16]

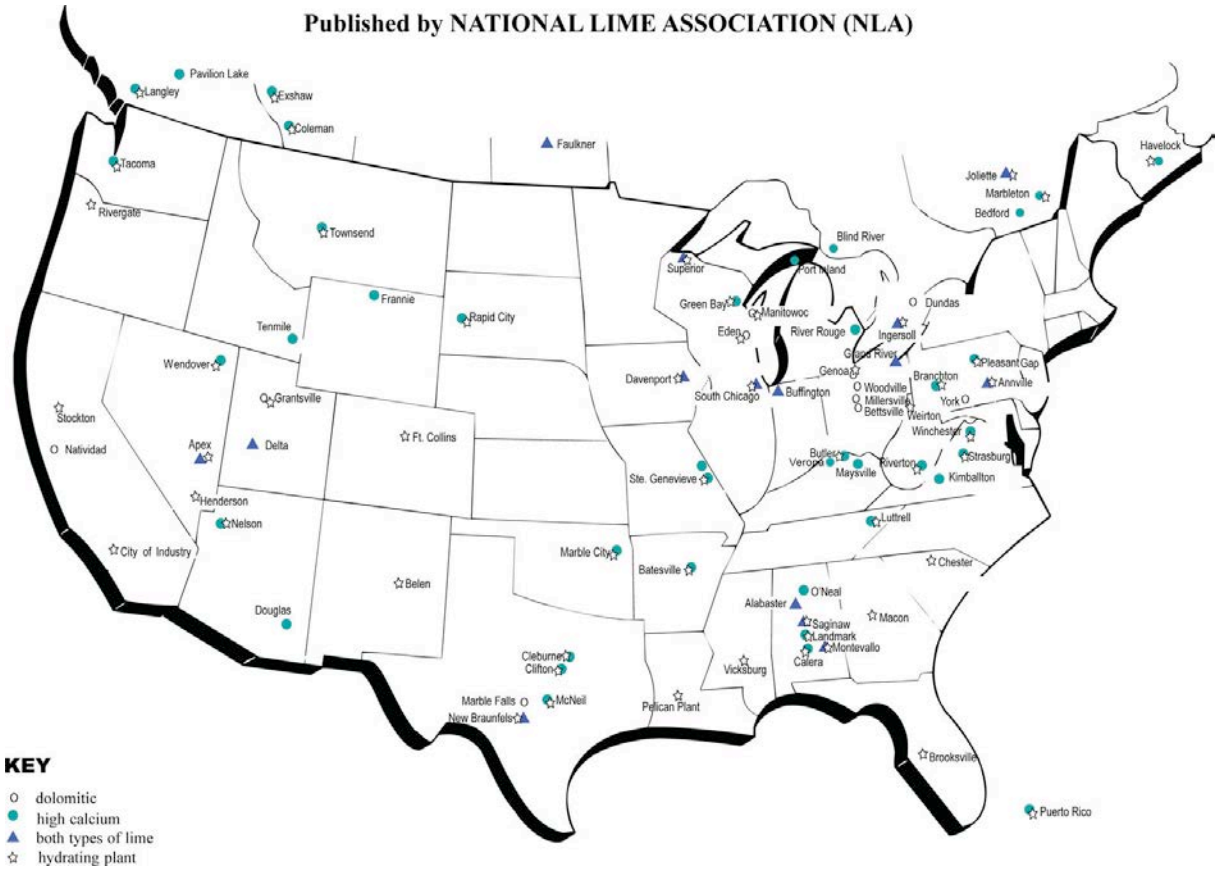

Figure 1-4. Lime producers in the United States, as published by the National Lime Association (2012).[17]

Although dolomitic lime has been widely used in modern construction the United States and Canada, a similar interest in it for this purpose does not seem to exist in other parts of the world.[18,19,20] However, the British standard Specification for Building Limes does specify two varieties of dolomitic lime for the use in building construction.[21]

Dolomitic lime has been found to be a common component of historic mortars in countries such as Great Britain, Ireland, Spain, Portugal, Austria, Italy, Switzerland, Estonia, Mexico, and India.[22,23,24] Because in-kind restoration is preferred by the preservation community, the use of dolomitic lime in repairs mortars may be advocated in these countries as well.[25] In general, it is difficult to detect and identify the magnesium phases in the mortar unambiguously without employing of a variety of analytical techniques. Therefore, it would not be surprising if the use of dolomitic lime mortar historically was far more widespread than is currently assumed.

The "Sulfate Problem"

Lime mortars, in general, are less resistant to freeze-thaw action and salt crystallization because they harden less readily than other mortars.[26] This is particularly intriguing in the case of dolomitic limes when examining their ability to withstand acid rain phenomena (including dry deposition). Their high magnesium content makes them susceptible to dissolution by acidic sulfate attack. The solubility of epsomite ($MgSO_4 \cdot 7H_2O$, 71.0 g/100 cc) is much greater than that of gypsum ($CaSO_4 \cdot 2H_2O$, 0.24 g/100 cc), which is a well-known reaction product in calcium carbonate materials. Thus, dissolution of dolomitic binders would be expected to have a considerable adverse effect on the cohesive properties of such mortars.

As explained previously, the magnesium components of dolomitic lime do not readily carbonate upon curing in the mortar. Due to the delayed rate or reduced extent of carbonation, a large component of the cured mortar is potentially brucite ($Mg(OH)_2$), which is highly reactive with sulfuric acid.[27] All of the magnesium compounds in dolomitic lime mortar -- whether periclase, brucite, magnesite, or any of the hydroxycarbonates -- are thought to be less stable and more reactive than calcite with environmental sulfur compounds.[28] This concept of reactivity will be discussed further in Chapters 4 and 5.

Subsequent evaporation leads to the formation of magnesium sulfate salts. These salts are described as harmful to building materials, and are credited as a large factor in the deterioration of mortar, stone, and brick.[29,30] In fact, magnesium sulfate is commonly used in standard tests to assess the durability of stone against sulfate attack.[31,32,33] The production of these salts results in a loss of material in the mortar itself, effectively reducing the strength of the bond between masonry units. Due to their high solubility, magnesium sulfates can potentially migrate through surrounding porous building materials, affecting both the mortar and the adjacent masonry. In fact, it is the recrystallization of magnesium sulfates upon drying that leads to extensive weathering of building materials due to the expansion of the salts crystals.[34]

Since the 19th century, there has been much contention about the appropriateness of dolomitic lime mortars because of this "sulfate problem." Pemberton observed the problem quite clearly in Philadelphia where he hypothesized that the dolomitic lime mortars absorbed the sulfur from the coal vapor in the air, converted to magnesium sulfate, and then were dissolved by rain and effloresced on the surface of the building. It was argued that dolomitic lime was unfit for making building mortar, and that "every 100 lbs of lime used contained enough magnesia to form 230 lbs of Epsom salts." However, Pemberton also noted that the Philadelphia mortars were not deteriorating as rapidly as would be expected for the amount of salts supposedly produced.[35]

Few investigations have been conducted on the formation of magnesium sulfate salts in dolomitic lime mortar, and the published research is rather contradictory. Four articles (all published within the past ten years) reach opposite conclusions. Research from a group in Spain suggested that dolomitic lime mortars produce sulfate salts and that their efflorescence is common.[36] Similar conclusions were reached by another group that examined the flaking and fracturing of dolomitic stone by magnesium sulfate salts in the walls of a monastery in Guadalajara (Spain). The second team of researchers argued against using dolomitic lime mortars (and dolomitic stone) in restoration work, as they credited the high magnesium content for the formation of the salts that were observed to deteriorate the buildings.[37]

Conversely, another Spanish group studied ancient dolomitic lime mortars in a church in Navarra (Spain) and concluded that such mortars did not release soluble salts. They recommended these mortars for use in restorations due to their chemical, structural, and mechanical compatibility with the ancient masonry.[38] In the United States, a group at Graymont Dolime similarly claimed that the interaction of sulfuric acid with brucite, simulating the reaction of acid rain with a major component of dolomitic lime mortars, does not produce magnesium sulfates in any significant capacity and that these salts do not appear as efflorescence.[39]

Due to the historic use of dolomitic lime mortar, its resurgence as a repair mortar, and the

contradictory nature of past research, it is important to further study interactions with the environment. This thesis explores 1) the carbonation of dolomitic lime mortars and 2) the extent to which such mortars interact with acid rain to produce magnesium sulfate salts.

[1] Maurenbrecher, A. H. Paul. "Mortars for Repair of Traditional Masonry," *Practice Periodical on Structural Design and Construction* (2004).
[2] Mack, Robert C. and John P. Speweik. "Preservation Brief 2: Repointing Mortar Joints in Historic Masonry Buildings." Technical Preservation Service, National Park Service, U.S. Dept of the Interior (1998).
[3] Diekamp, A., J. Konzett, W. Wertl, R. Tessadri, and P.W. Mirwald. "Dolomitic Lime Mortar – A Commonly Used Building Material for Medieval Buildings in Western Austria and Northern Italy." *Proceedings of the 11th International Congress on Deterioration and Conservation of Stone, 15-20 September 2008, Torun, Poland* 1. Eds. J. W. Lukaszewicz and P. Niemcewicz: (2008) 597–604.
[4] Montoya, C.; Lanas, J.; Arandigoyen, M.; Navarro, I.; García Casado, P.J.; Alvarez, J.I. "Study of Ancient Dolomitic Mortars of the Church of Santa María de Zamarce in Navarra (Spain): Comparison with Simulated Standards," *Thermochimica Acta* 398 (2003): 107-122.
[5] Schork, Jennifer. "Evaluation of the Physical and Chemical Properties of Dolomitic Lime Mortar." Masters Thesis, Columbia University, 2009.
[6] Boynton, Robert S. *Chemistry and Technology of Lime and Limestone,* 2nd edition. New York: John Wiley & Sons, Inc., 1980. p. 441-442.
[7] Lucas, A. *Ancient Egyptian Materials and Industries*. Great Britain: Kessinger, 2003. p. 96-97.
[8] Diekamp, A.; Konzett, J.; Mirwald, P.W. "Magnesian Lime Mortars – Identification of Magnesium-Phases in Medieval Mortars and Plasters with Imaging Techniques," *12th Euroseminar on Microscopy Applied to Building Materials.* Dortmund, Germany (September 2009).
[9] Vicat, Louis-Joseph. *A Practical and Scientific Treatise on Calcareous Mortars and Cements*. London: John Weale, 1837. p. 148.
[10] Seeley, Nigel. "Magnesian and Dolomitic Lime Mortars in Building Conservation." *Journal of Architectural Conservation* 2 (July 2000): 21-29.
[11] Pemberton, Henry. "On the Evil Effects Arising From the Use of Dolomitic Lime in Building Brick Walls." *Journal of the Franklin Institute* Vol. 106 Nos. 631- 636, Third Series, Vol. 76 July-Dec. (1878).
[12] Boynton, p. 443.
[13] Thomson, Margaret. "Why is Type S Hydrated Lime Special?" National Lime Association Building Lime Group, 2005.
[14] ASTM C207-06 "Standard Specification for Hydrated Lime for Masonry Purposes." West Conshohocken, PA: American Society for Testing Materials International, 2006.
[15] Thomson, 2005.
[16] Boynton, p. 14.
[17] "U.S. & Canadian Lime Companies >> Interactive Map," National Lime Association, 2012, http://www.lime.org/about_nla/find_a_lime_plant/us_canadian_lime_companies/interactive-map.asp.
[18] Boynton, p. 450, 460.
[19] Thomson, 2005.
[20] Maurenbrecher, 2004.
[21] "BS 890: Specification for Building Limes," *British Standard*. London: BSI, 1995.
[22] Diekamp, 2008.
[23] Diekamp, 2009.
[24] Seeley, 2000.

[25] "The Venice Charter: International Charter for the Conservation and Restoration of Monuments and Sites," *Second International Congress of Architects and Technicians of Historic Monuments*. Venice: ICOMOS, 1964.
[26] Maurenbrecher, A. H. Paul and Madeleine Rousseau. "Repointing Mortars for Older Masonry," *The Canadian Architect* 45 (2000): 44.
[27] Boynton, p. 209-226.
[28] Klemm, Werner and Heiner Siedel. "Evaluation of the Origin of Sulphate Compounds in Building Stone by Sulphur Isotope Ratio," *Geological Society, London, Special Publications* 205 (2002): 419-429.
[29] Klemm, 2002.
[30] Lopez-Arce, P.; Garcia-Guinea, J.; Benavente, D.; Tormo, L.; Doehne, E. "Deterioration of Dolostone by Magnesium Sulphate Salt: An Example of Incompatible Building Materials at Bonaval Monastery, Spain," *Construction and Building Materials* 23 (2009): 846-855.
[31] ASTM C88-05, "Standard Test Method for Soundness of Aggregates by Use of Sodium Sulfate or Magnesium Sulfate."
[32] ASTM C1012/C1012M – 10, "Standard Test Method for Length Change of Hydraulic-Cement Mortars Exposed to Sulfate Solution."
[33] ASTM D5240 – 04, "Standard Test Method for Test Rock Slabs to Evaluate Soundness of Riprap by Use of Sodium Sulfate or Magnesium Sulfate."
[34] Seeley, 2000.
[35] Pemberton, 1878.
[36] Coultrone, G.; Arizzi, A.; Rodriguez-Navarro, C; Sebastian, E. "Sulfation of Calcitic and Dolomitic Lime Mortars in the Presence of Diesel Particulate Matter." *Environmental Geology* Vol. 56, No. 3-4 (December 2008).
[37] Lopez-Arce, 2009.
[38] Montoya, 2003.
[39] Berman, Scott, Frage, Debera F.; Tate, Michael J. "The Effect of Acid Rain on Magnesium Hydroxide Contained in Cement-Lime Mortar," *Masonry: Opportunities for the 21st Century, ASTM STP 1432,* ed. D. Throop and R.E. Klingner (West Conshohocken, PA: ASTM International, 2003).

Chapter 2:

The Production of Dolomitic Lime

In order to get a better sense of how dolomitic lime mortars interact with acidic sulfates, the inherent properties of dolomitic lime, itself, were explored. Recall the lime cycle highlighted in Chapter 1. Dolomitic lime contains periclase (MgO) and quicklime (CaO) as a result of calcining dolomite $(Ca,Mg)(CO_3)_2$ and sometimes calcite ($CaCO_3$), the carbonate materials present in dolomitic stone. For a glossary of mineralogical terms and corresponding chemical formulas, please see Appendix A.

In a laboratory setting, the process of making dolomitic lime from stone was reproduced to examine how the chemical and physical characteristics of lime change as a factor of calcining temperature. Chemical grade representations of dolomitic lime, both unslaked (quicklime and periclase) and hydrated (portlandite, $Ca(OH)_2$, and brucite, $Mg(OH)_2$), were also evaluated in order to draw conclusions about their stability.

The set of experiments undertaken here is in no way meant to mimic a specific process for manufacturing lime. Rather it aims to gain knowledge about one step of the process – the calcining, or heating, of dolomitic stone to produce calcined lime that may be subsequently hydrated to produce hydrated lime. Lime production has evolved over time, and few manufacturers produce the same lime. Each plant has its own unique process, which may include varying the kiln type, calcining temperature, or duration of calcining. For each manufacturer, a compromise must be struck between the quality of the lime and an economy of cost. [1]

Vertical lime kilns have typically consisted of three zones: heating, calcining, and cooling, in which the lime is heated from 20-900°C, calcined up to 1200°C, and cooled down to 50°C. Rotary kilns often have operated at higher temperatures, usually in the range of 1250-1450°C.[2] But the temperature and duration of calcining are only two factors in the production of lime. The third involves the removal of evolved carbon dioxide through ventilation within the kiln.[3] Most kilns employ a draft, whether natural or induced, which increases and regulates the lime output.[4]

Likewise, the oven employed in the calcining of the materials for this thesis, a Thermolyne 4800 Furnace, allows for ventilation.

Over the years, dolomitic lime has consistently been produced at a much higher temperature than necessary to break down the dolomite. As a result of calcining temperature, all limes have the potential to be overburned or underburned, which can limit reactivity in the later steps of the lime cycle, including hydration and subsequent carbonation. The implications of such temperature effects will be discussed later in this chapter.

The following materials (described in the section "Effects of Calcining Temperature on Lime Production") were calcined to varying temperatures in order to mimic the process of burning dolomitic stone to produce lime. They were then examined via x-ray diffraction (XRD) and scanning electron microscopy-energy dispersive spectroscopy (SEM-EDS). The analysis of uncalcined and calcined samples offered insight into the decomposition, hydration, and carbonation of the components of the dolomitic lime 'cycle,' from dolomitic stone to lime in its unslaked and hydrated states used to make mortar.

XRD allowed for the identification of the individual crystalline components in the powdered materials. The resulting x-ray diffraction pattern, or diffractogram, was based upon the interplanar distances within each crystalline component. Therefore, each material had a unique pattern by which it could be identified.

To examine particle size and shape, images of the sample surface were captured via SEM at high magnification. A scanning electron microscope emitted a beam of electrons, which interacted with the surface atoms to emit a signal containing information about that surface. SEM essentially provided a highly magnified picture of the sample surface, which could be analyzed to assess the size of individual particles in the lime.

All of the materials examined in this chapter were analyzed at room temperature, and the time between calcining and analysis ranged anywhere from two hours to two months with XRD and

four to five months with SEM. In the interim, the materials were sealed in vials and placed in a container with desiccant to keep the materials dry and ensure the accuracy of data collected at later dates.

Each solid sample was ground with a mortar and pestle, mounted on a quartz slide with acetone, and analyzed to determine mineral content in a Philips PW1835 X-Ray Diffractometer. In preparation for SEM-EDS, solid powder samples were mounted on carbon tape adhered to aluminum stands. The samples were then gold-coated to ensure a clear topographic reading of the surface upon examination with a LEO 1455VP scanning electron microscope equipped with a Link Pentafet Si(Li) SATW EDS detector.

Effects of Calcining Temperature on Lime Production

In order to explore what happens in first step of the dolomitic lime 'cycle,' raw materials, including two dolomitic stones and crystalline dolomite, were calcined to varying temperatures and their chemical composition determined using XRD. Samples of Kasota stone (from the Mankato-Kasota quarries in Minnesota) and Tuckahoe marble (quarried in Westchester County just north of New York City) were acquired from the Columbia University Historic Preservation Conservation Laboratory. A pure dolomite crystal from Eugui, Pamplona, Spain was supplied by Ward's Natural Science Establishment.

Chemical grade calcite and magnesite were subjected to the same calcining regimen and XRD examination as the dolomitic stones and crystal described above. This was done in order to compare the decomposition of dolomite with that of calcite and magnesite. Chemical grade calcite was acquired from Acros Organics (CAS 471-34-1) while chemical grade magnesite was provided by Fisher Scientific (catalog #M27).

All of these materials were calcined to 400°C, 600°C, 750°C, and 900°C - sequentially removing samples for analysis. The materials were allowed to cool, then mounted and analyzed via

XRD (and some via SEM-EDS) along with samples of the same materials that were uncalcined. See Appendix C for x-ray diffractograms and Appendix E for scanning electron micrographs.

Decomposition of Dolomite

Dolomite Crystal

Full decomposition of the pure dolomite crystal occurred between 400°C and 600°C. Only dolomite was detected in the x-ray diffractogram for the sample calcined to 400°C. However, no dolomite was found in the sample calcined to 600°C, which contained only quicklime, portlandite, and calcite. Periclase was not detected, but was most likely present due to its detection in subsequent samples. This highlights the detection limitations of the instrument, particularly when dealing with the identification of multiple minerals. Upon calcining to higher temperatures, a greater proportion of the sample was composed of the oxides, periclase and quicklime, and portlandite was no longer present in the sample calcined to 900°C.

The following diagrams are not explicit phase diagrams, but rather are meant to function as a visual aid to understanding the decomposition of these materials. Chemical compositions were only determined for samples that were uncalcined (25°C) and calcined at 400°C, 600°C, 750°C, and 900°C. The graphics are not meant to extrapolate any data, as the compositions between these temperature points were not examined.

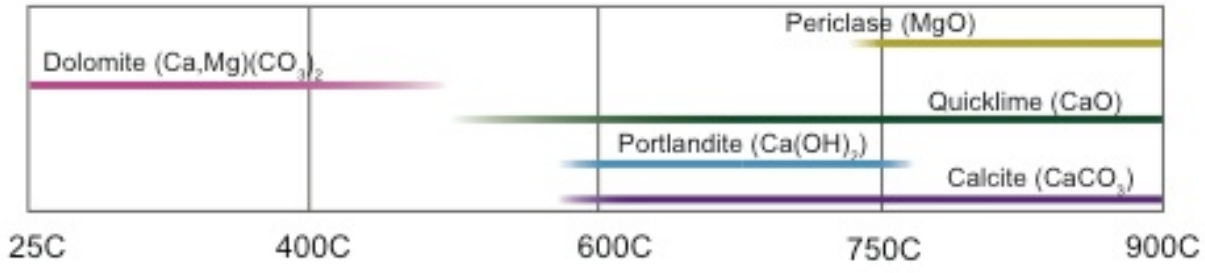

Figure 2-1. Diagram of decomposition of pure dolomite crystal.

To get a better picture of the physical state of the dolomite particles during the decomposition, samples of crushed dolomite crystal were examined with SEM-EDS. Similar to the XRD data on chemical composition, imaging by SEM supported the lack of dolomite decomposition in the uncalcined sample and the sample calcined to 400°C. Both contained characteristic rhombohedral crystals, which varied greatly in size (Figure 2-2). EDS determined that the crystals contained both calcium and magnesium, confirming the presence of dolomite.

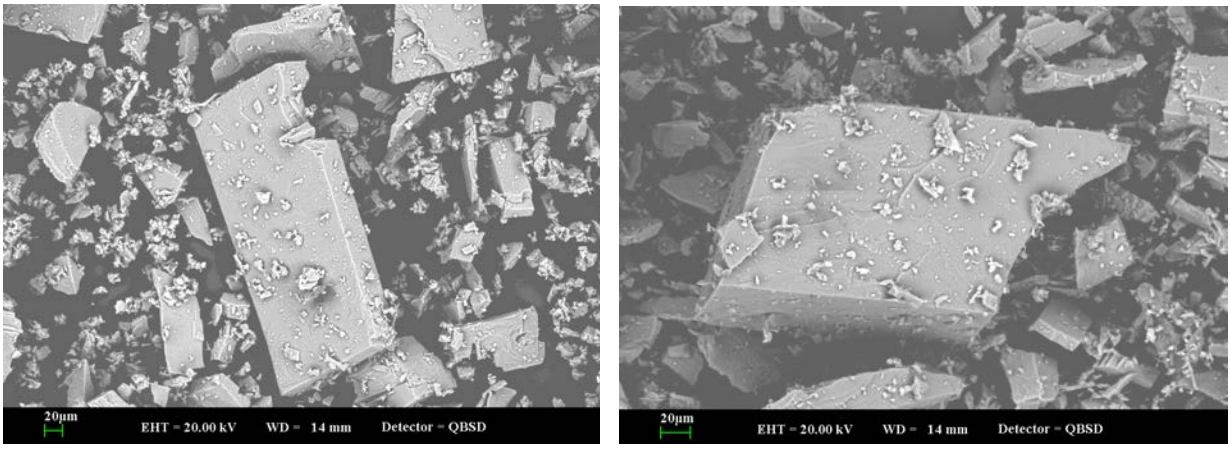

Figure 2-2. Crushed dolomite crystal, uncalcined at 362X (L) and calcined to 400°C at 646X (R).

According to XRD analysis, no dolomite was found in the sample calcined to 600°C, as it had fully decomposed. Upon examining the same sample with SEM, this decomposition of the dolomite was evident (Figure 2-3). Although the shape of the dolomite crystals remained, there was cracking and pitting along the planes of the crystalline structure, most likely from the release of carbon dioxide during decomposition to lime (Figure 2-4). While the shell of the crystal structure was maintained in these images, this would most likely not have been the case had the samples been ground further after calcining. EDS determined that both calcium and magnesium were still present within the interspersed particles, suggesting that each lump contained a mixture of quicklime and periclase.

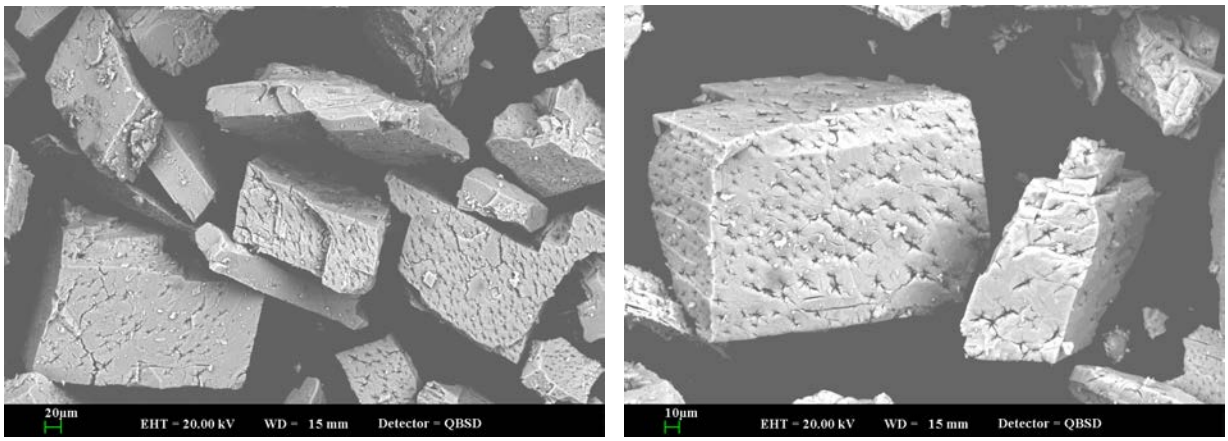

Figure 2-3. Crushed dolomite crystal, calcined to 600°C, at 348X (L) and 615X (R).

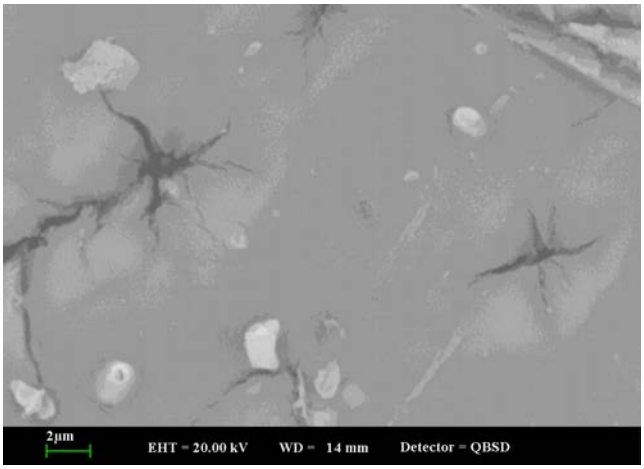

Figure 2-4. Pitting in crushed dolomite crystal, calcined to 600°C, at 9000X.

Dolomite calcined to both 750°C and 900°C were similar in morphology and composition. Each continued to exhibit a more greatly decomposed "ghost" of the original dolomite crystal, which was most likely a mixture of quicklime and periclase that had not yet been physically broken up (Figures 2-5 and 2-7). The limited resolution of the instrument prevented the imaging of individual particles. However, some particles were found to contain only periclase (Figure 2-6) and were not as pitted and cracked as the surrounding particles in the residual crystal shape that contained both calcium and magnesium components.

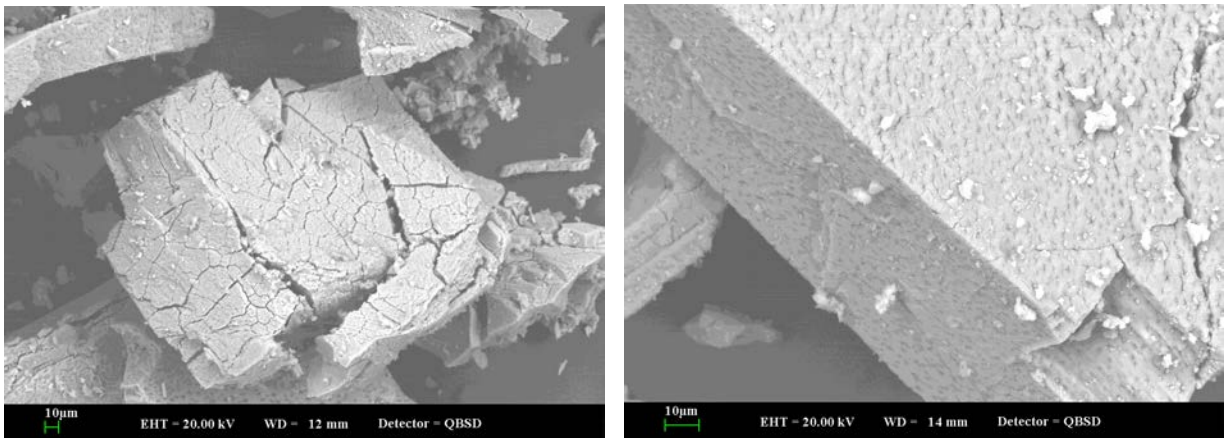

Figure 2-5. Crushed dolomite crystal, calcined to 750°C, at 611X (L) and 1500X (R).

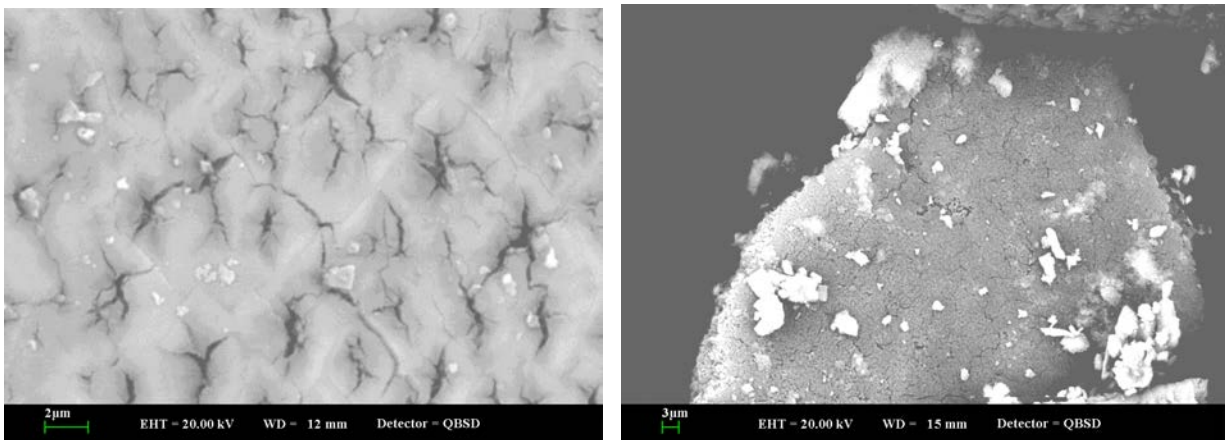

Figure 2-6. Crushed dolomite crystal, calcined to 750°C. Detail of pitting at 9600X (L) and periclase cluster at 2440X (R).

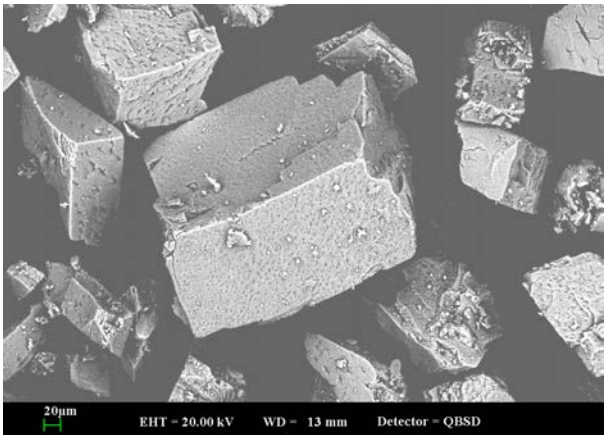

Figure 2-7. Crushed dolomite crystal, calcined to 900°C at 368X.

The examination with both XRD and SEM-EDS of the dolomite crystal, calcined to varying temperatures, allowed for greater insight into the decomposition of dolomite. However, lime has not been produced from the calcining of pure dolomite crystal, so it was also necessary to examine the decomposition of dolomitic stone into lime.

Dolomitic Stones

The chemical composition of Kasota stone and Tuckahoe marble were examined at 25°C (uncalcined) as well as after calcining to 400°C, 600°C, 750°C, and 900°C. Both stones contained muscovite, a micaceous material that has no bearing on the decomposition of the dolomitic stone and will be omitted from the description of each chemical composition for the sake of clarity.

In Kasota stone, the decomposition of dolomite began at calcining temperatures lower than 400°C and was complete at a calcining temperature of 750°C. In the samples calcined to both 400°C and 600°C, diminishing amounts of dolomite and increasing amounts of portlandite and periclase were detected. Only periclase, quicklime, and portlandite were detected in samples calcined to 750°C and 900°C.

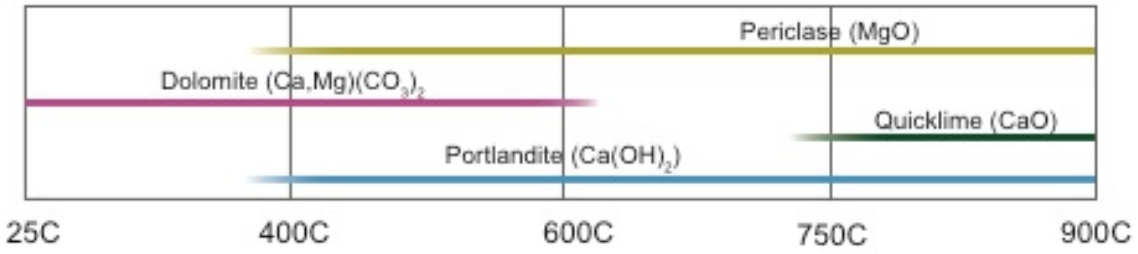

Figure 2-8. Diagram of dolomite decomposition in Kasota stone.

Images of Kasota stone calcined at 900°C were captured using SEM and compared with those of the dolomite crystal. Similarly, the Kasota stone was found to contain remnants of decomposed dolomite crystals, which had cracked and pitted (Figure 2-9).

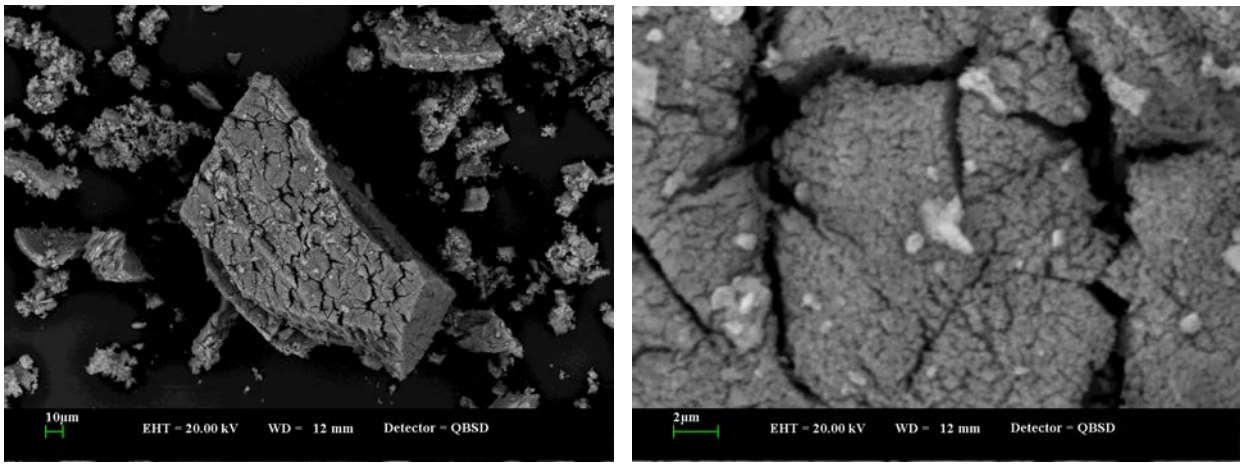

Figure 2-9. (L) "Ghost" of dolomite crystal in Kasota stone, calcined at 900°C at 752X magnification and (R) detail of cracking at 9770X.

Individual oxide particles could be imaged and were less than 1 µm in diameter. The periclase and quicklime particles appeared to be retained within the ghost of the dolomite crystal structure and were protected by a film of portlandite (Figure 2-10). EDS confirmed that the thin film contained much higher ratios of calcium to magnesium than the particles beneath. No distinct difference in particle size could be attributed to the overburning of periclase.

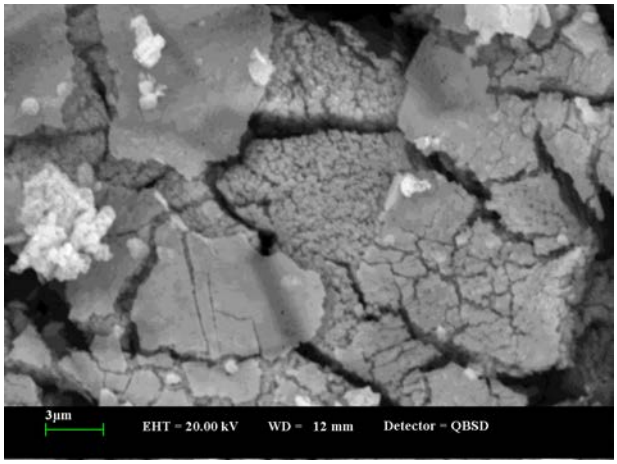

Figure 2-10. Kasota stone, calcined at 900°C at 8390X magnification displaying thin portlandite film over lumped periclase and quicklime particles.

As in the Kasota stone samples, the decomposition of Tuckahoe marble was observed to begin at calcining temperatures lower than 400°C, but it was not complete until 900°C. However,

the starting material was found to contain calcite as well as dolomite, which can occur in some dolomitic stones. The decomposition of calcite was complete by the calcining temperature of 750°C. At a calcining temperature of 900°C, only periclase and portlandite were detected and the decomposition of dolomite was complete.

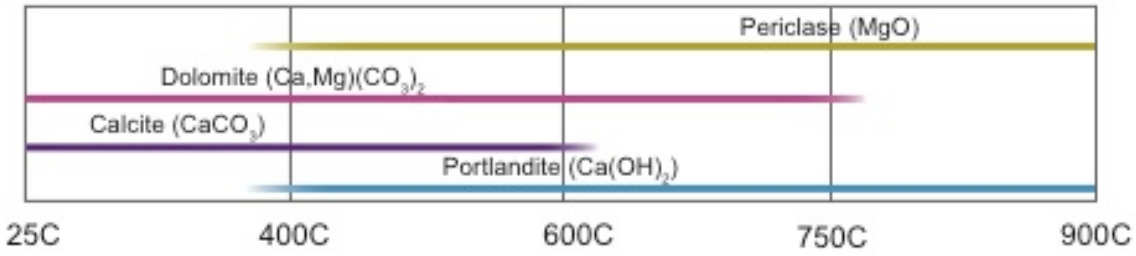

Figure 2-11. Diagram of dolomite decomposition in Tuckahoe marble.

The dissociation temperature of dolomite is not well established as it varies with the crystallinity of the dolomitic stone. More crystalline dolomitic stones require higher temperatures to break down the dolomite into periclase and quicklime. Historical sources observed the decomposition of dolomite in a range from 500-750°C, while more recent studies report the decomposition of dolomite at higher temperatures from 700-880°C.[5,6,7,8]

In the dolomitic stones examined here, the decomposition of dolomite began at temperatures as low as 400°C. Kasota stone decomposed completely by 750°C while the decomposition of Tuckahoe marble was not complete until 900°C. The difference in calcining temperature for complete dolomite dissociation can be attributed to the higher crystallinity, and therefore the higher decomposition temperature, of Tuckahoe marble.

Even in a more crystalline stone, dolomite decomposed completely into its lime components by 900°C. Historically, vertical kilns reached a calcining temperature of 1200°C, with even higher temperatures in rotary kilns, suggesting the prevalence of using higher temperatures than necessary for the production of lime.

On another note, the complete dissociation of the pure dolomite crystal by 600°C differed a great deal from the observed decomposition of dolomite in dolomitic stone. Perhaps this occurs because there are no other minerals present in the pure dolomite crystal. The presence of calcite, muscovite, or other minerals in the dolomitic stone examined could have increased the calcining temperature necessary to completely decompose the dolomite, as impurities often lead to a higher decomposition temperature.

Although the presence of quicklime and periclase was expected, the detection of portlandite in each of these samples indicates a complication of the dolomitic lime 'cycle' outlined in Chapter 1. When heated, carbon dioxide is driven off from the dolomite to give quicklime and periclase. The presence of portlandite suggests that quicklime readily hydrates in air, most likely upon the cooling of the sample. Due to the necessary slaking process, it has been observed that periclase hydrates less readily than quicklime. Therefore, it is unsurprising that no brucite was observed. Samples calcined to higher temperatures contained less portlandite, which could suggest overburning because the sample appeared to be less susceptible to hydration by water in the air.

Decomposition of Calcite

The decomposition of chemical grade calcite to quicklime began at a calcining temperature lower than 600°C, was almost complete at 750°C, and was fully decomposed by 900°C.

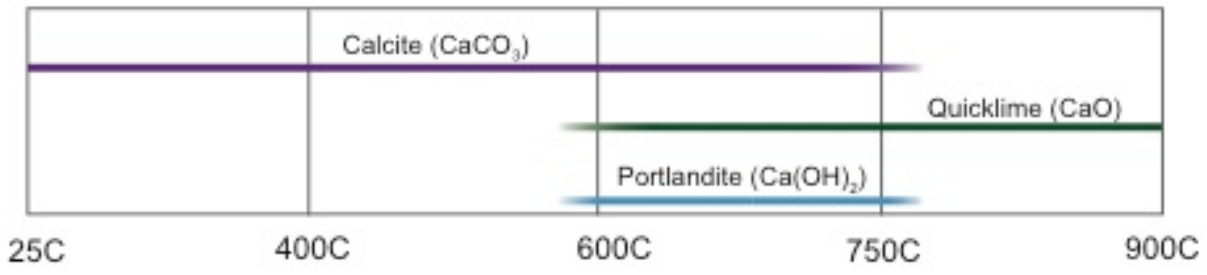

Figure 2-12. Diagram of dolomite decomposition of reagent grade calcite.

Just as the experiments performed for this thesis observed the complete decomposition of calcite between 750°C and 900°C, so have scholars reported the production of quicklime from calcite at anywhere from 800-900°C.[9,10,11,12,13] However, it must be noted that many of these numbers describe the calcining temperature necessary for the decomposition of pure calcite. Limestone can contain a number of impurities, which may constitute the need for a higher calcining temperature. Because of the presence of other minerals in limestone, it is not surprising that manufacturers historically subjected limestone to higher temperatures (1200°C for vertical kilns and up to 1450°C for rotary kilns) to produce quicklime.

In order to note any distinct physical differences in the decomposition of calcite and dolomite, chemical grade calcite calcined at 750°C was imaged with SEM. Due to the chemical grade nature of the calcite provided, all of the crystals had a rather uniform size distribution (Figure 2-13).

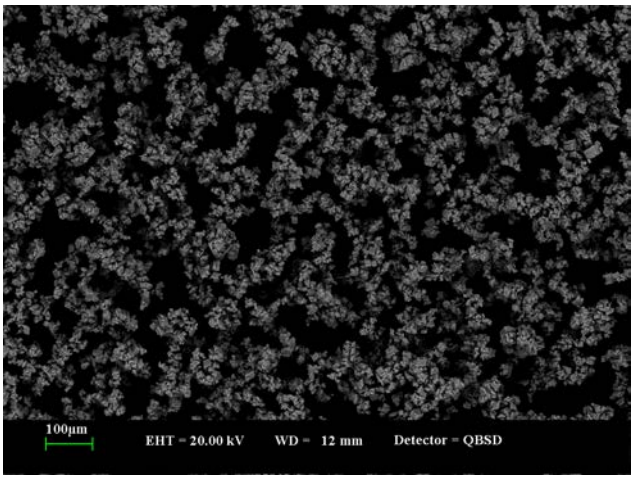

Figure 2-13. Chemical grade calcite, calcined at 750°C at 199X magnification with uniform size distribution.

As in the decomposition of dolomite, the calcite crystals appeared to keep their crystalline shape, although they cracked and pitted (Figure 2-14), as the interior decomposed into small quicklime particles.

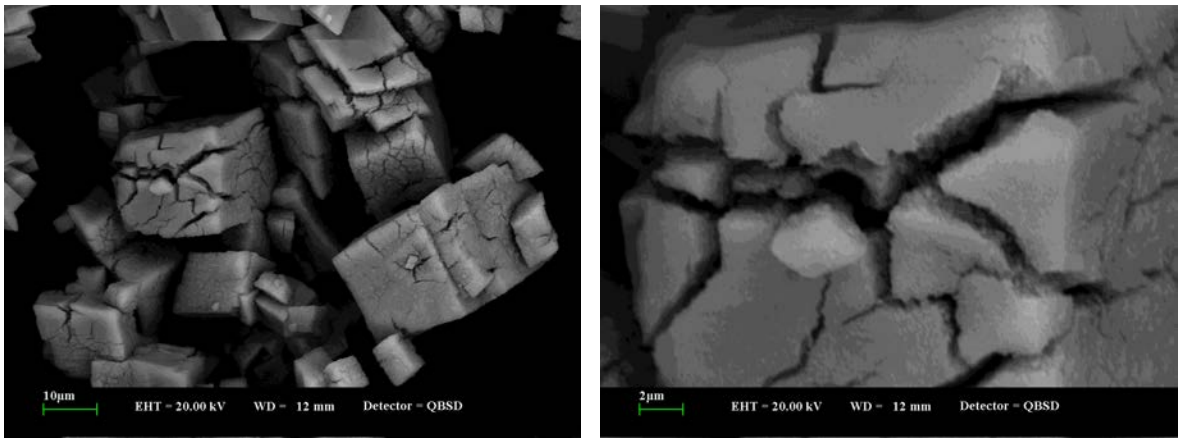

Figure 2-14. Chemical grade calcite, calcined at 750°C, with cracking at (L) 2480X and (R) 10,000X magnification.

Differing levels of decomposition were observed at this temperature (Figure 2-15), as the decomposition of calcite was not observed to be complete until 900°C.

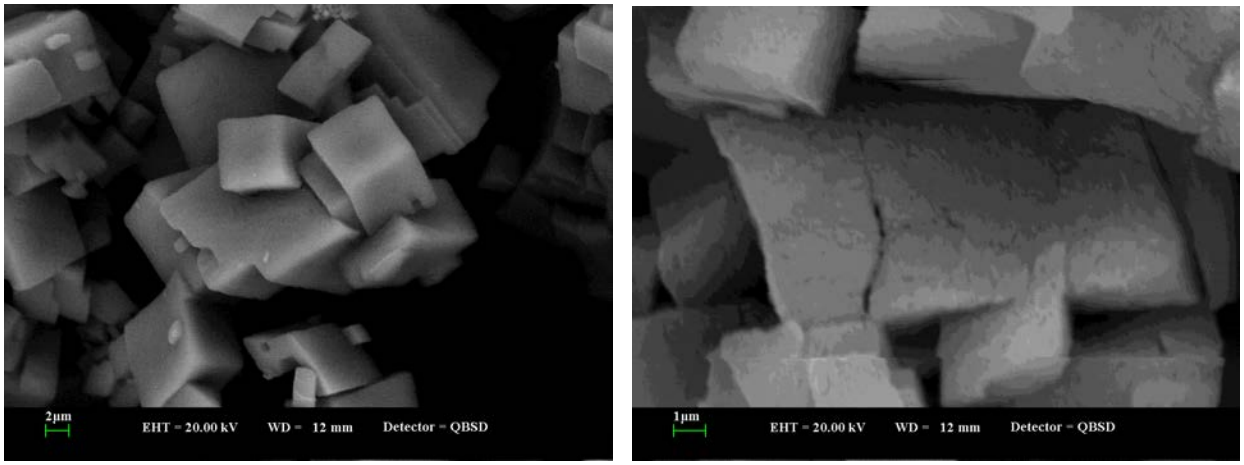

Figure 2-15. Chemical grade calcite, calcined at 750°C, exhibiting different levels of decomposition at (L) 5000X and (R) 14,000X magnification.

Decomposition of Magnesite

The decomposition of chemical grade magnesite was investigated for comparison to dolomite and calcite. It is not believed that dolomite dissociates into two separate carbonates, but the decomposition of magnesite may be compared to the decomposition of the magnesium component in dolomite to produce periclase.[14]

Interestingly, the chemical grade magnesite was identified as hydromagnesite at room temperature. The container had been opened previously and exposed to air, which contains water vapor that could have converted the magnesite to hydromagnesite. The presence of hydromagnesite could suggest a similar conversion of the magnesite, which might be found in dolomitic lime mortars, to this hydroxycarbonate form. This material was extremely sensitive to calcination as the hydromagnesite had decomposed completely to periclase by heating to 400°C.

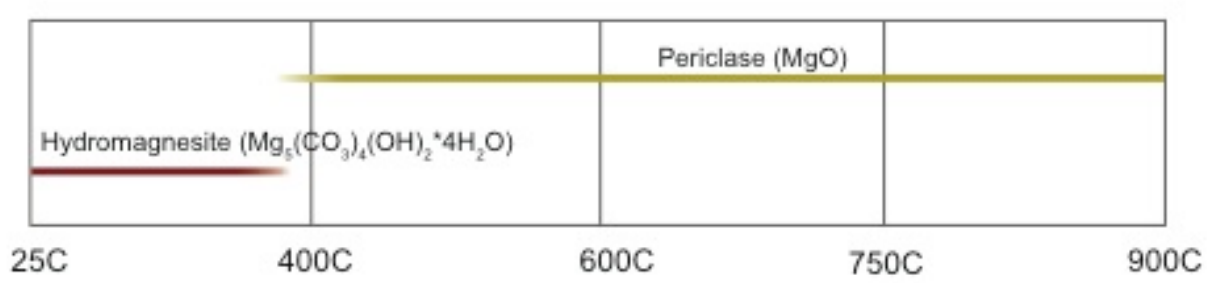

Figure 2-16. Diagram of dolomite decomposition of chemical grade magnesite.

The observed decomposition of magnesite, or in this case hydromagnesite, which decomposes to periclase by 400°C, reflects only a slightly lower temperature than expected from the multiple sets of data outlined by Boynton.[15] However, others observed the decomposition of magnesite at higher temperatures, anywhere from 600-750°C.[16,17,18,19]

The data gathered here supports the idea that dolomite will have a dissociation temperature lying between that of magnesite and calcite.[20] The dolomitic materials were fully decomposed by 600°C (in dolomite crystal), 750°C (in Kasota stone), and 900°C (in Tuckahoe marble). All of these values for the temperature of complete dolomite decomposition lie between 400°C (the observed temperature for the decomposition of hydromagnesite) and 900°C (observed decomposition of calcite). The variation in these values may be attributed to the purity and crystallinity of the dolomitic material. Historically and presently, the calcining of limestone (no matter the magnesium content) occurred at much higher temperatures than those explored here.

Calcining the dolomitic materials yielded the expected oxides of periclase and quicklime as well as some portlandite, which was most likely a result of the hydration of quicklime by moisture in the air. This reinforces the proficiency of the calcium component (quicklime) to hydrate, while the hydration of the magnesium component (periclase) occurs less readily.

Unslaked Lime Components

Chemical grade representations of other components of the dolomitic lime 'cycle' were examined with XRD. Samples of periclase and quicklime, both uncalcined and heated to 150°C, were analyzed to study the stability of the components of lime produced from the calcining of dolomitic stone. Chemical grade periclase was provided by Sigma-Aldrich (catalog #342792) while Fisher Scientific supplied chemical grade quicklime (catalog #C117).

Little change was observed in the composition of these oxides upon heating to 150°C. The chemical grade periclase samples (Figures 2-17 and 2-18) contained periclase, while chemical grade quicklime (Figures 2-19 and 2-20) was found to contain mostly quicklime as well as some portlandite. Again, this highlights the propensity of quicklime toward hydration. A portion of the quicklime was readily hydrated to portlandite by water in the air, which remained bound and was not driven off upon heating.

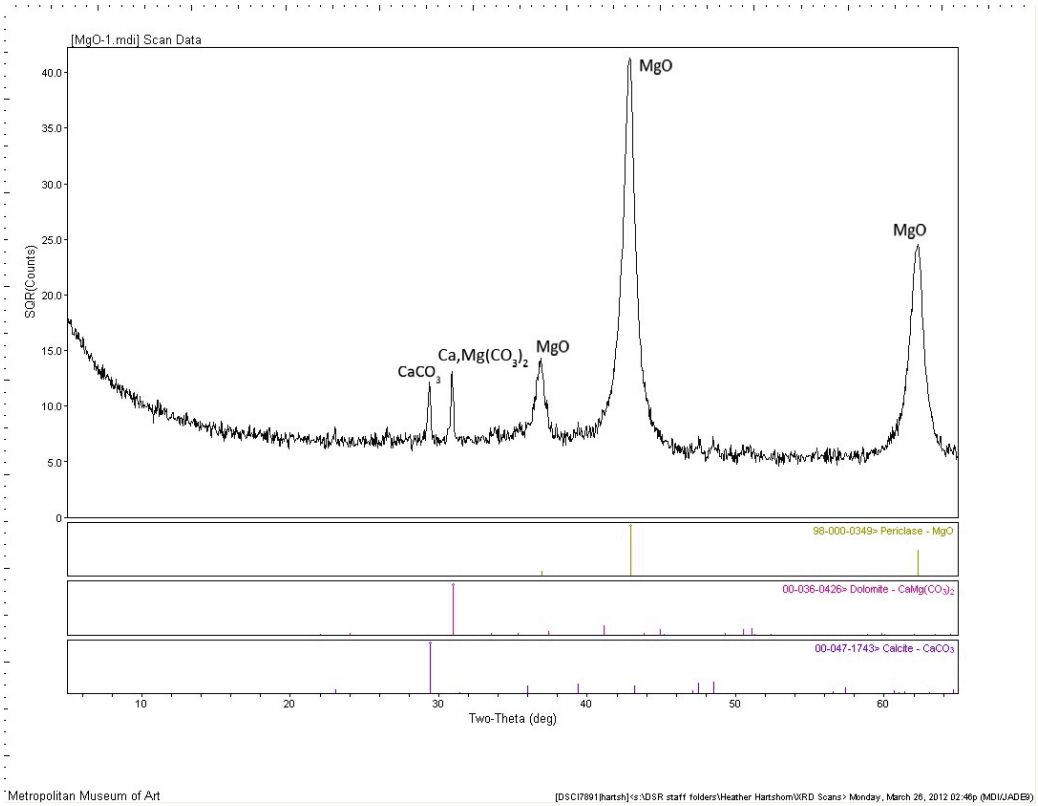

Figure 2-17. X-ray diffractogram of chemical grade periclase, uncalcined.

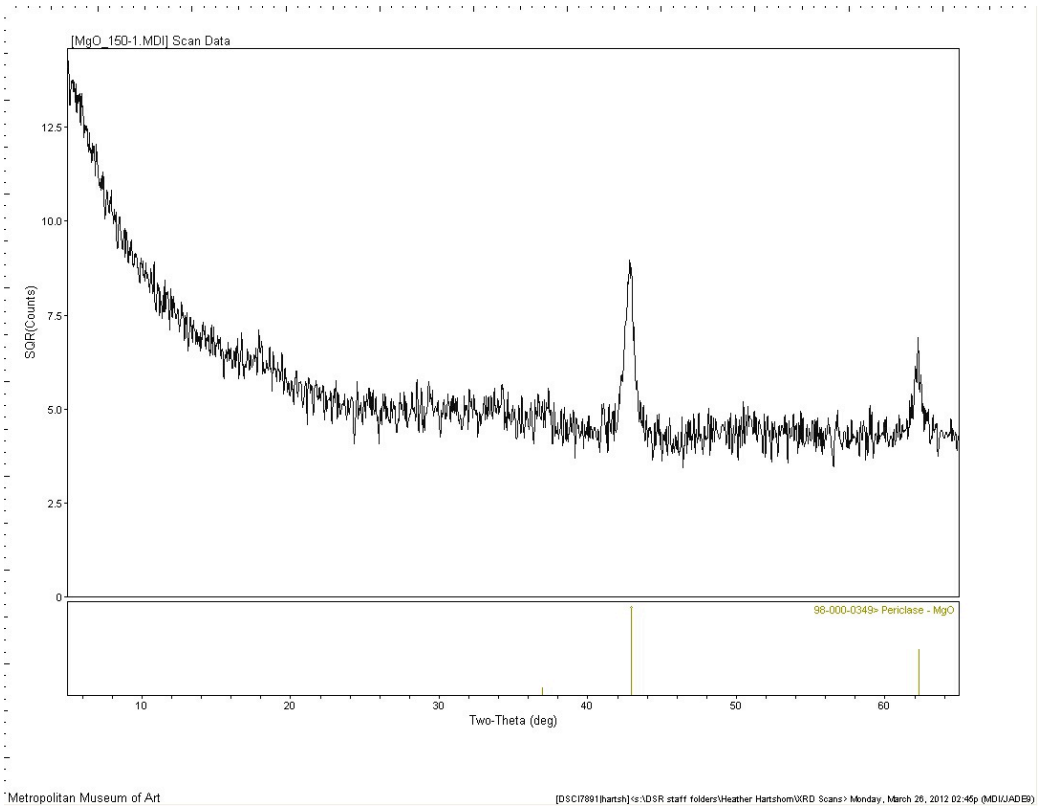

Figure 2-18. X-ray diffractogram of chemical grade periclase, calcined to 150°C.

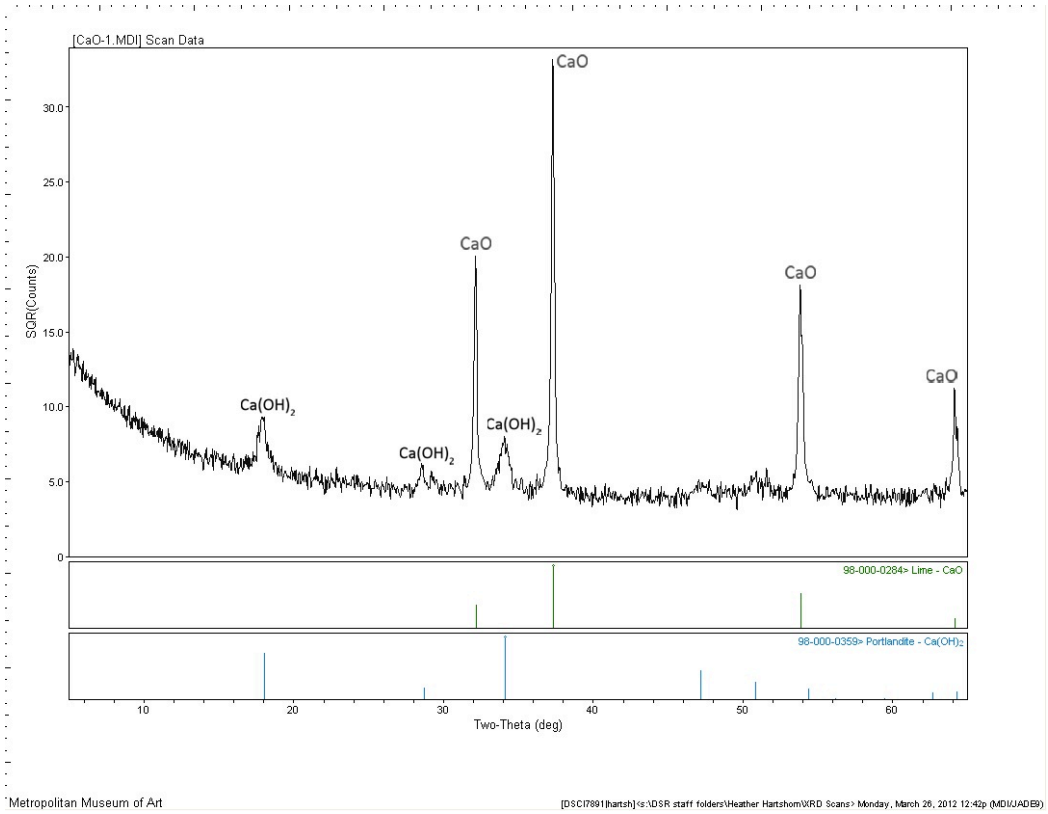

Figure 2-19. X-ray diffractogram of chemical grade quicklime, (L) uncalcined and (R) calcined to 150°C.

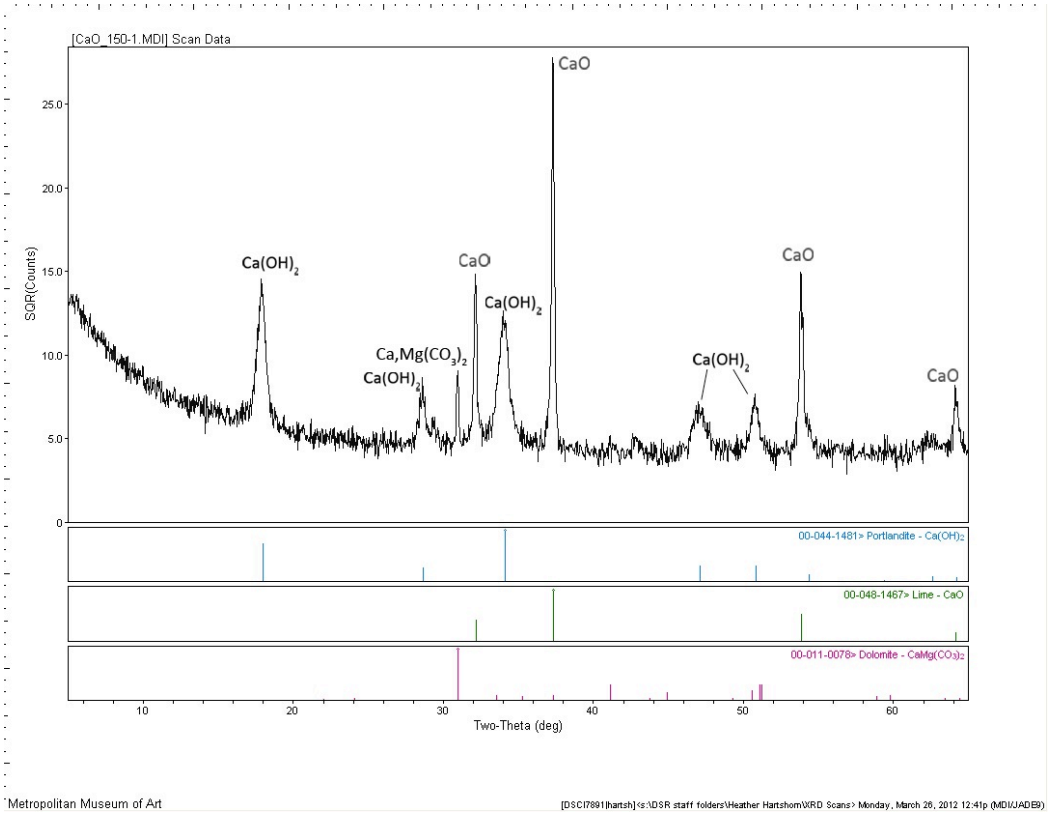

Figure 2-20. X-ray diffractogram of chemical grade quicklime, (L) uncalcined and (R) calcined to 150°C.

It has long been observed that dolomitic stone calcined at high temperatures yields an oxide material that is extremely difficult to hydrate. The opposite is true for lime derived from a high-calcium stone at the same temperature, which results in a very active oxide. It has been hypothesized that the presence of periclase hinders the rate of hydration of the quicklime.[21] However, according to observations made here, the quicklime still hydrates first and continues to readily hydrate even in the presence of periclase (as seen above in the section on the decomposition of dolomitic stones).

Hydrated Lime Components

To study the stability of the components of hydrated lime, which are most commercially available today, samples of brucite and portlandite (both uncalcined and heated to 150°C) were analyzed via XRD. Fisher Scientific supplied chemical grade brucite and portlandite (catalog # M342 and C88).

Much like the oxide components, little change was observed in the composition of these hydroxide components upon heating to 150°C. The chemical grade brucite samples (Figures 2-21 and 2-22) contained only brucite, while chemical grade portlandite (Figures 2-23 and 2-24) was found to contain mostly portlandite as well as some calcite.

The amount of calcite in the sample increased upon heating. The presence of calcite suggests that portlandite directly carbonates in the presence of carbon dioxide and water in the air. However, neither brucite sample showed any sign of carbonation. Such observations support the unproblematic carbonation of portlandite to calcite, particularly when compared to the complicated nature of brucite carbonation in dolomitic lime mortars.

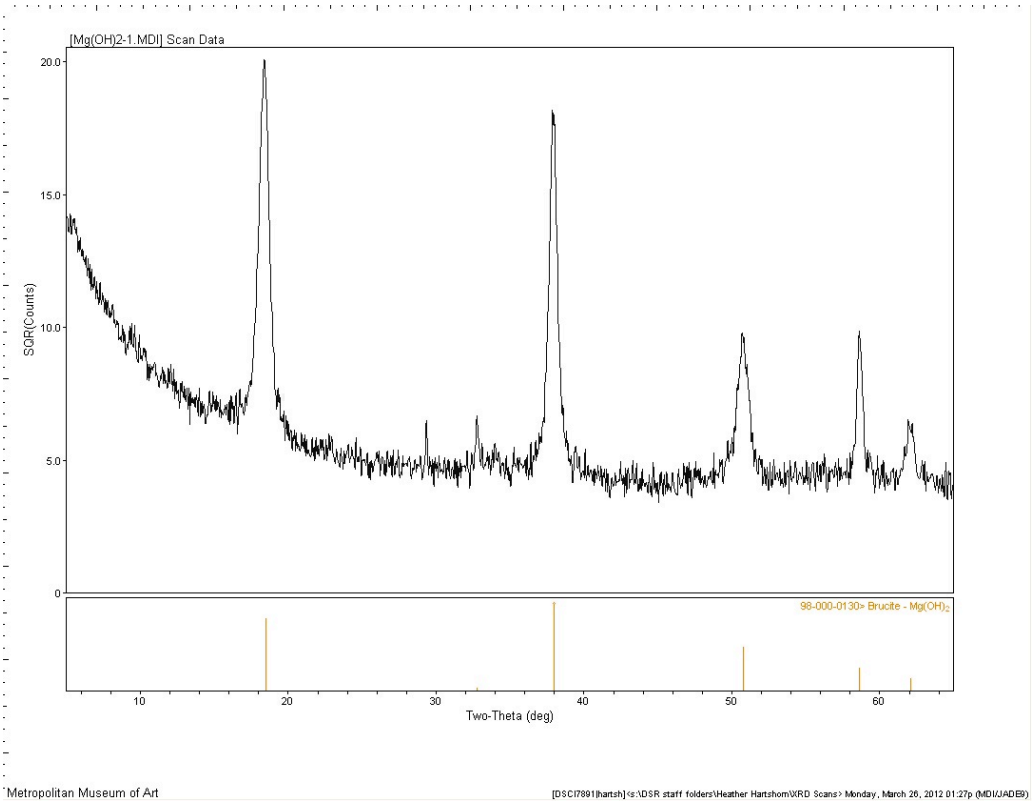

Figure 2-21. X-ray diffractogram of chemical grade brucite, uncalcined.

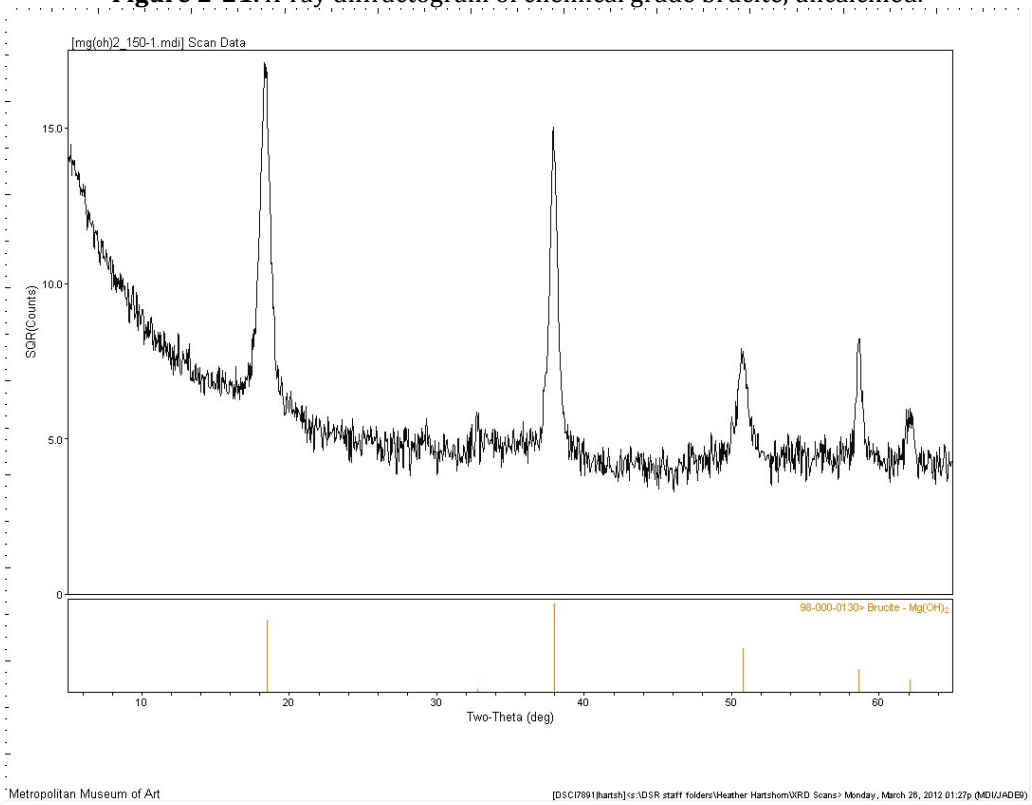

Figure 2-22. X-ray diffractogram of chemical grade brucite, calcined to 150°C.

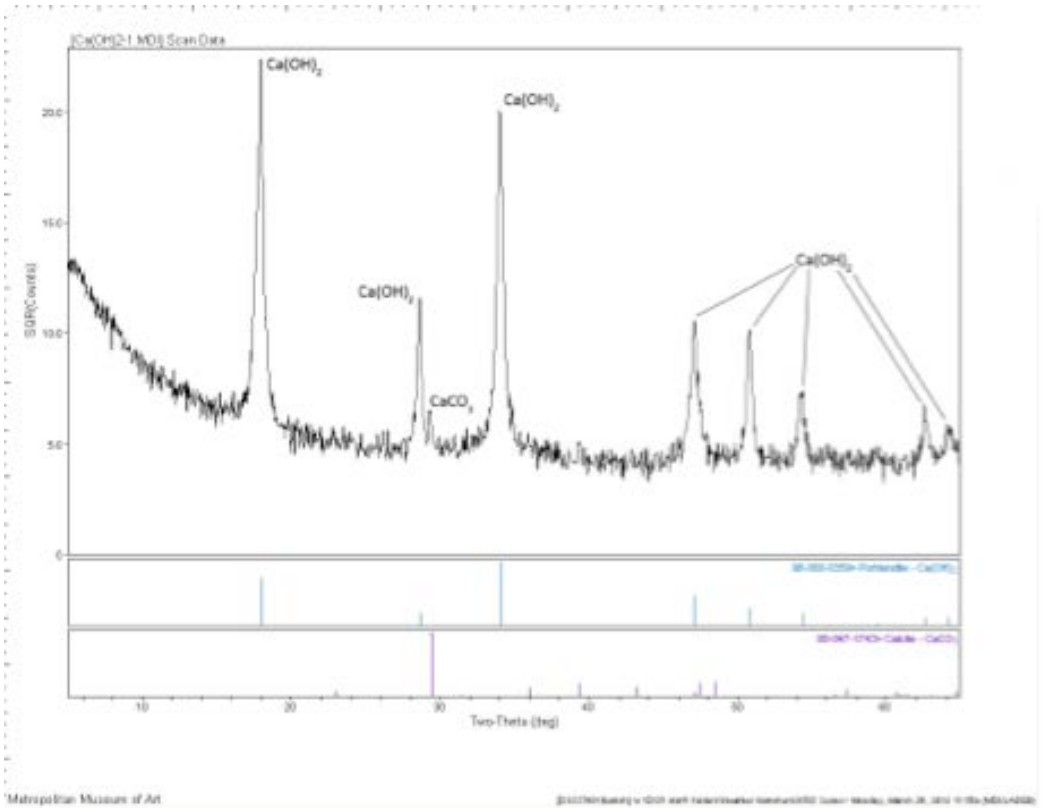

Figure 2-23. X-ray diffractogram of chemical grade portlandite, (L) uncalcined and (R) calcined to 150°C.

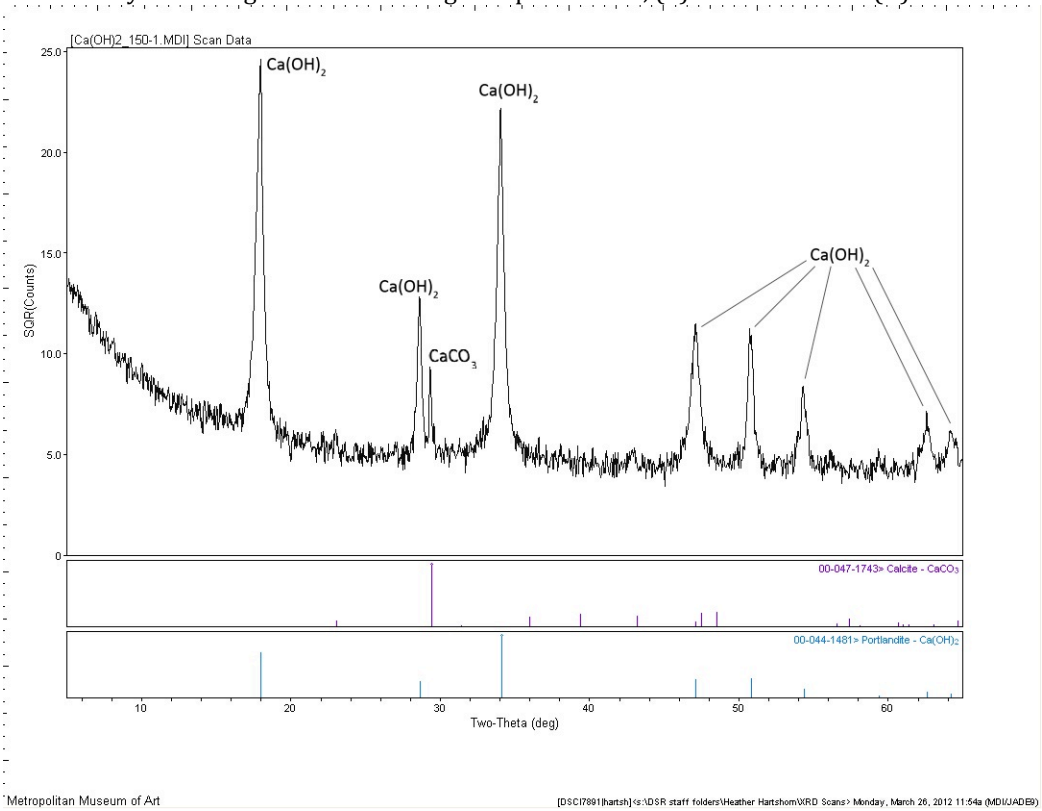

Figure 2-24. X-ray diffractogram of chemical grade portlandite, (L) uncalcined and (R) calcined to 150°C.

By recreating the manufacture of lime from dolomitic stone, some insight was provided into the decomposition of dolomite. The magnesium-containing component of dolomite decomposed to periclase at a much lower temperature than the calcium-containing component, whose decomposition product of quicklime easily hydrated to portlandite. Periclase was readily formed from calcining dolomite, but it was not easily hydrated to brucite. While portlandite exhibited a propensity toward carbonation, brucite did not, indicating the carbonation of portlandite occurs much more readily than that of brucite. This is not unexpected, as a variety of magnesium compounds (brucite, magnesite, and hydroxycarbonates) have been detected in dolomitic lime mortar.[22]

The carbonation of hydrated dolomitic lime, consisting of portlandite and brucite, will be explored further in Chapter 3. The observations on lime production made here will be applied to the examination of commercial limes and their subsequent carbonation in model dolomitic lime mortars.

---

[1] Boynton, Robert S. *Chemistry and Technology of Lime and Limestone,* 2nd edition. New York: John Wiley & Sons, Inc., 1980. p. 228-274.
[2] Knibbs, N.V.S. *Lime and Magnesia: The Chemistry, Manufacture and Uses of the Oxides, Hydroxides and Carbonates of Calcium and Magnesium*. London: Ernest Benn, 1924.
[3] Emley, Warren E. "Manufacture of Lime" in *Technologic Papers of the Bureau of Standards*, Department of Commerce. Washington: Government Printing Office, 1913.
[4] Knibbs, 1924.
[5] Boynton, p. 160-161.
[6] Seeley, Nigel. "Magnesian and Dolomitic Lime Mortars in Building Conservation." *Journal of Architectural Conservation* 2 (July 2000): 21-29.
[7] Montoya, C.; Lanas, J.; Arandigoyen, M.; Navarro, I.; García Casado, P.J.; Alvarez, J.I. "Study of Ancient Dolomitic Mortars of the Church of Santa María de Zamarce in Navarra (Spain): Comparison with Simulated Standards," *Thermochimica Acta* 398 (2003): 107-122.
[8] Knibbs, 1924.
[9] Boynton, p. 160-161.
[10] Emley, 1913.
[11] Seeley, 2000.
[12] Montoya, 2003.
[13] Eckel, Edwin C. *Cements, Limes, and Plasters; Their Materials, Manufacture and Properties,* 3rd ed. New York: John Wiley & Sons, Inc., 1928.

[14] Knibbs, 1924.
[15] Boynton, p. 160-161.
[16] Emley, 1913.
[17] Seeley, 2000.
[18] Montoya, 2003.
[19] Eckel, 1928.
[20] Emley, 1913.
[21] Knibbs, 1924.
[22] Diekamp, A., J. Konzett, W. Wertl, R. Tessadri, and P.W. Mirwald. "Dolomitic Lime Mortar – A Commonly Used Building Material for Medieval Buildings in Western Austria and Northern Italy." *Proceedings of the 11th International Congress on Deterioration and Conservation of Stone, 15-20 September 2008, Torun, Poland* 1. Eds. J. W. Lukaszewicz and P. Niemcewicz: (2008) 597–604.

Chapter 3:

Carbonation of Dolomitic Lime Mortars

Now that the decomposition of dolomitic stone into lime has been examined, this chapter explores the compounds present in commercially produced dolomitic and high-calcium limes. The carbonation of dolomitic lime mortars will then be examined using model mortars prepared with the same commercially produced limes.

Composition of Commercial Hydrated Limes

Three commercially produced limes, two dolomitic and one high-calcium were analyzed with x-ray diffraction (XRD) to determine their chemical composition. Scanning electron microscopy of the commercial limes was also performed, in order to make comparisons with the decomposition of dolomitic lime discussed in Chapter 2 and to provide insight into the materials used to make model mortars for experiments in this thesis.

Graymont Dolime Inc. supplied a dolomitic *Type S Hydrated Lime* from Genoa, OH where a pure Niagara Dolomite lies close to the ground surface.[1] Another dolomitic *Type S Hydrated Masonry Lime* was procured from the Western Lime Corporation in Eden, WI, which is also the site of the dolomitic limestone quarry.[2] Mercer Lime Company provided a high-calcium *Hydrated Lime* from Slippery Rock, PA.[3]

Dolomitic Limes

Upon examination, the two dolomitic limes appeared to have rather similar chemical compositions. Both limes were hydrated during production, so they were expected to contain portlandite and brucite, rather than periclase and quicklime. Graymont Dolime (Figure3-1) was found to contain mostly portlandite and brucite with small amounts of calcite and periclase. Western dolomitic lime (Figure 3-2) contained the same minerals (portlandite, brucite, some calcite and periclase), as well as small amounts of dolomite.

It can be assumed that the carbonates (calcite and dolomite) detected in these commercial hydrated limes were residual unburned starting material, which then remained unaffected by the hydrating process. The calcite could also be a product of the carbonation of portlandite exposed to carbon dioxide in the air over time. Since the carbonation of portlandite occurs much more readily than that of brucite, it is not surprising that no carbonation product of brucite was detected in the hydrated lime.

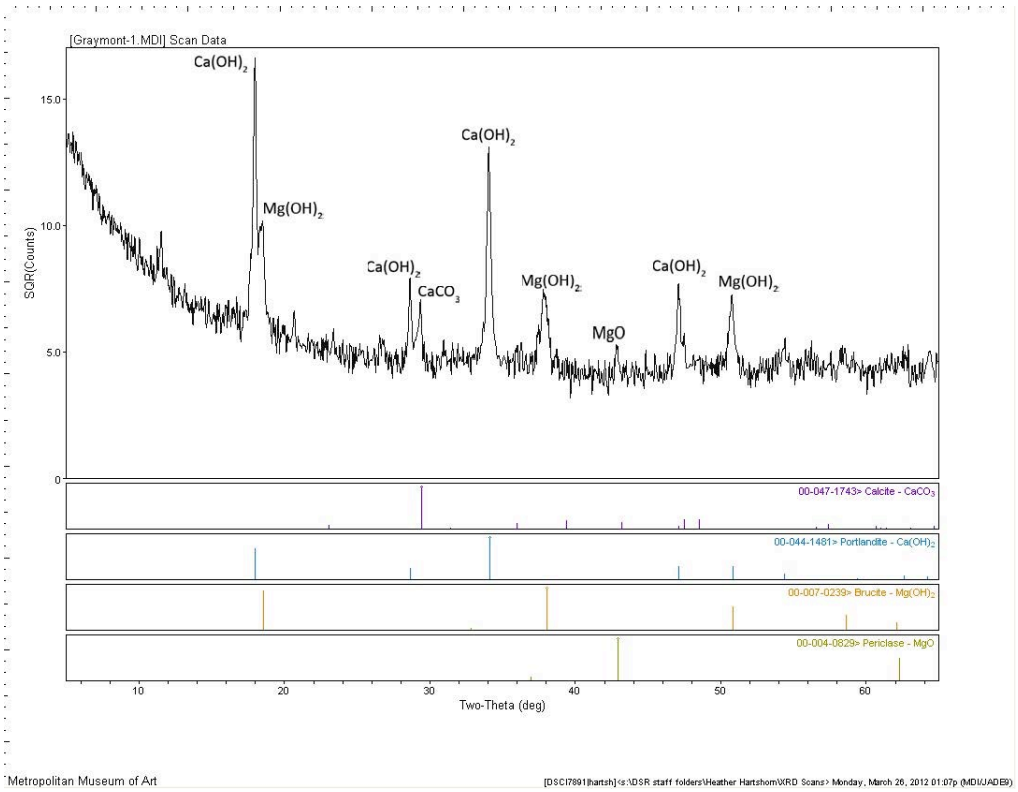

Figure 3-1. X-ray diffractogram of commercial Graymont Dolime.

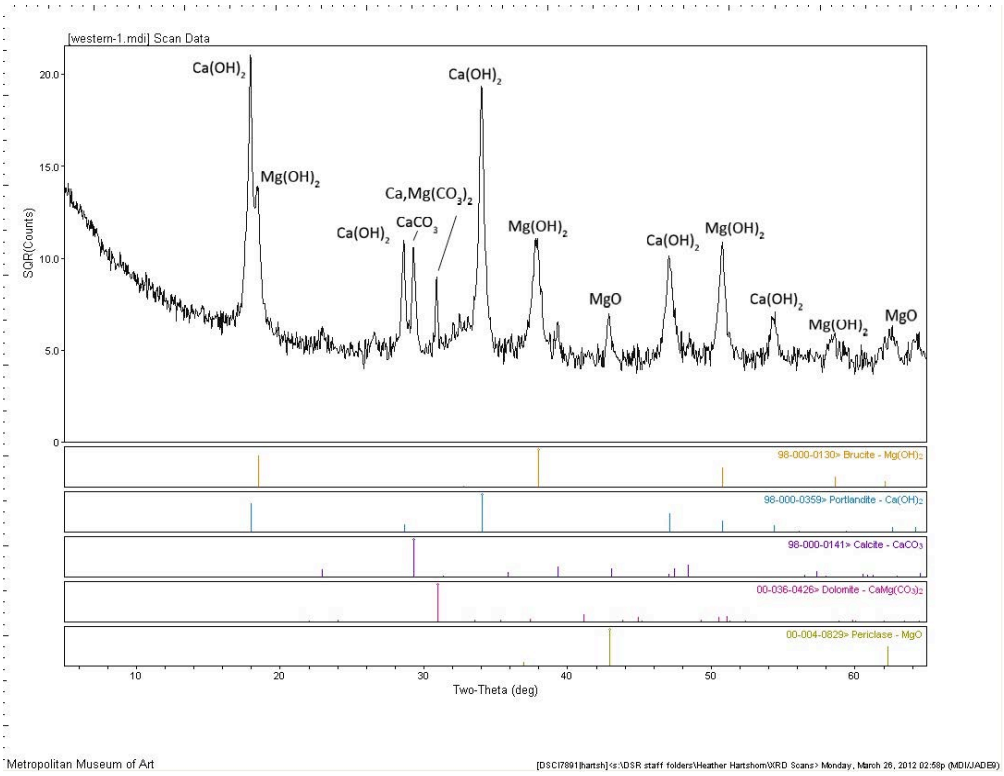

Figure 3-2. X-ray diffractogram of commercial Western dolomitic lime.

Graymont Dolime was produced by calcining stone in rotary kilns at ~1100°C, and then hydrating the resulting dolomitic lime under pressure. The dolomitic stone, extracted from an open pit quarry in Northwest Ohio, was sized between ¼" and 2" prior to calcining. Once the resulting lime had been hydrated, the hydrated lime was milled in order to isolate particle size.[4]

The commercial Graymont Dolime should not have included unhydrated or overburned periclase since the production accounts for the isolation of certain particle size by milling the lime after hydration. However, small amounts of periclase were detected in both samples suggesting that most dolomitic limes will contain some amount of periclase. Although Graymont's manufacturing process now includes a step to remove such undesired material, the same was not necessarily true for historic lime production. Recall that standard methods of hydration were not available for dolomitic lime until the 1940s with the invention of the Corson Pressure Hydrator. Before and even

within the past century, periclase content in dolomitic limes could have been much greater than that observed here, contributing to characteristics such as pitting in mortars and plasters.

SEM-imaging of these commercial dolomitic limes (Figure 3-3 and 3-4) revealed the presence of smaller clusters of hydrated lime particles. Unlike the calcined dolomite crystal and Kasota stone examined in Chapter 2, these limes were hydrated and contained mostly portlandite and brucite. However, the individual particles within the clusters appeared to be of a similar size (less than 1 μm). As expected, there were no observed remnants of the dolomite crystal structure, most likely due to the sizing of the hydrated lime during the production process.

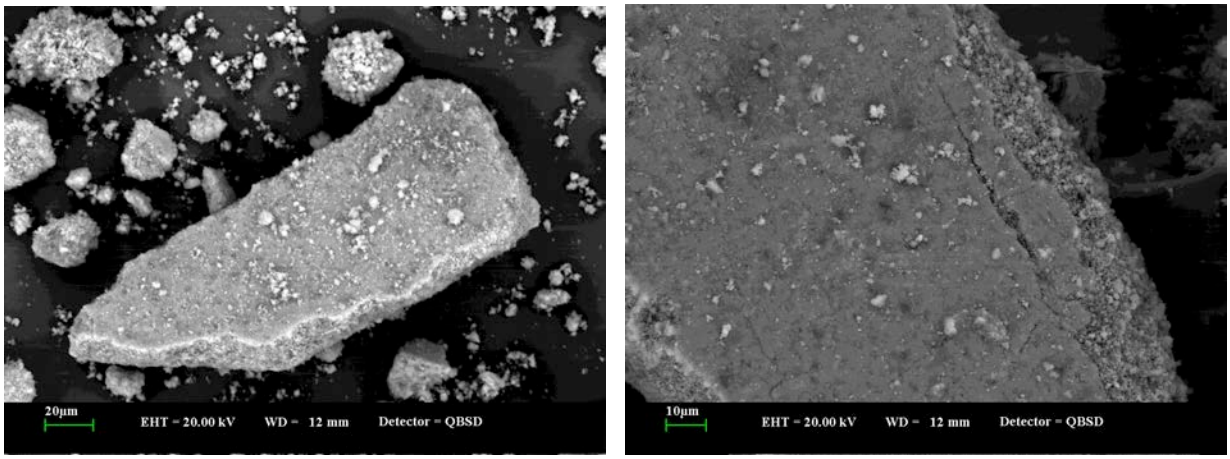

Figure 3-3. Graymont Dolime at (L) 1000X and (R) 1780X magnification.

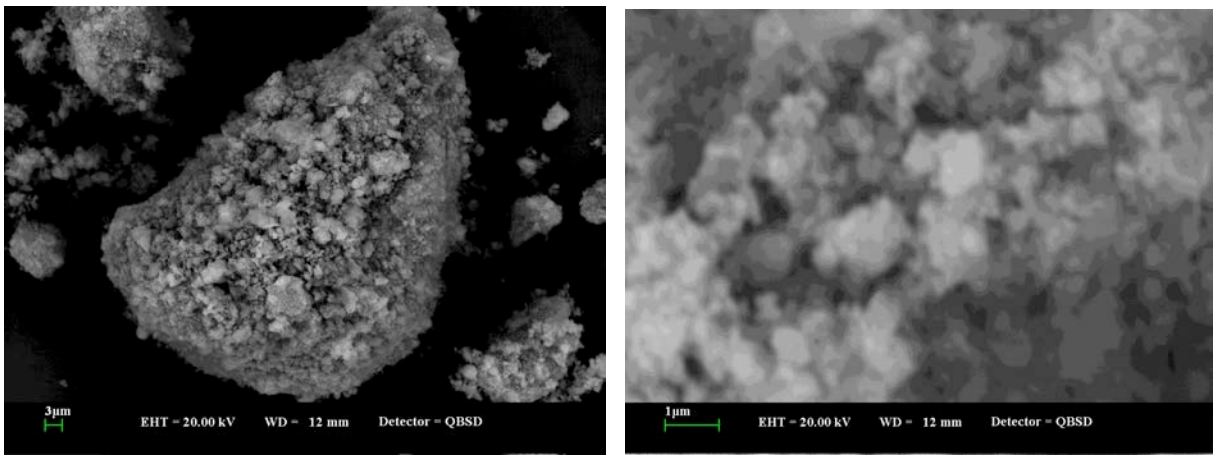

Figure 3-4. Graymont Dolime at (L) 2490X and (R) 24,500X magnification.

High-Calcium Lime

Mercer high-calcium lime was produced by calcining raw limestone in a rotary kiln at 1600-1800°C for four hours. Then the lumps of quicklime finer than ½" were hydrated and again isolated by particle size.[5]

While there were a variety of chemical compounds in the dolomitic lime, the hydrated high-calcium lime supplied by Mercer Lime Company contained only portlandite (Figure 3-5). Such an outcome was to be expected in hydrated high-calcium lime, calcined from calcite to quicklime, which was then hydrated to portlandite. Unlike in the commercial dolomitic limes, calcite was not detected here. This suggests that the calcite present in the dolomitic limes was residual starting material from the dolomitic stone, burned at a lower temperature. The temperatures employed in rotary kilns today are higher than that of historic vertical kilns, which could lead to a greater purity in high-calcium limes. The calcite could also result from the carbonation of portlandite; however, the lack of carbonation in the high-calcium lime (as opposed to its presence in the dolomitic limes) would suggest the faster carbonation of portlandite in the presence of brucite.

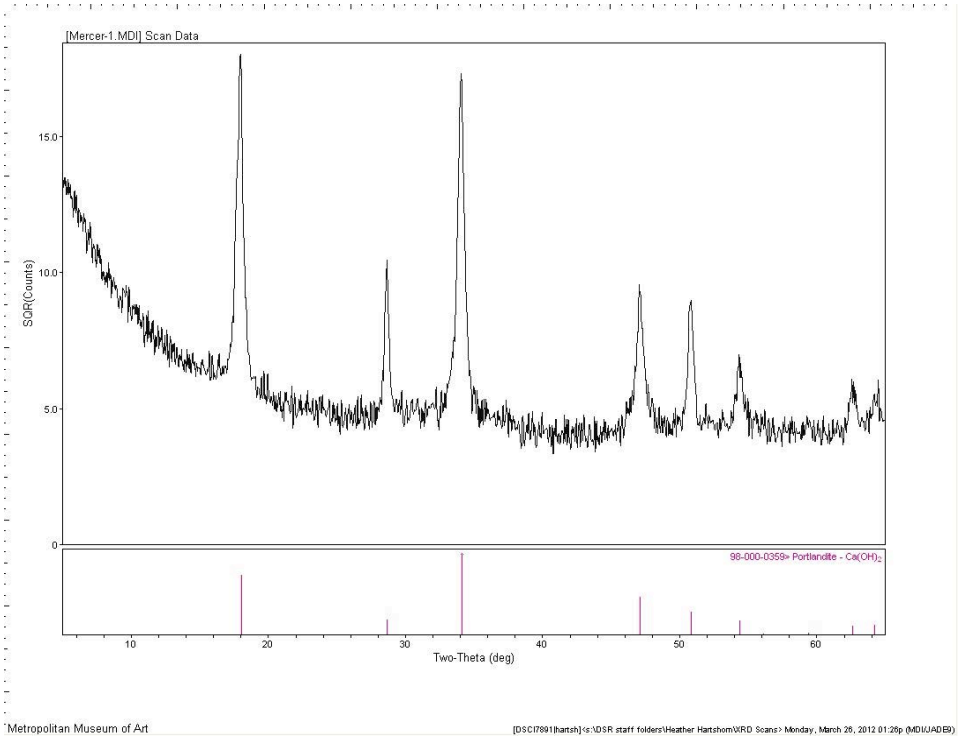

Figure 3-5. X-ray diffractogram of commercial Mercer high-calcium lime.

Although SEM-imaging of Mercer high-calcium lime (Figures 3-6 and 3-7) revealed fewer large clusters of the individual hydrated lime particles than in the dolomitic lime hydrate, the particles were similar in size (less than 1 μm). The homogeneity of size distribution within the high-calcium lime could be due to sizing during the manufacturing process.

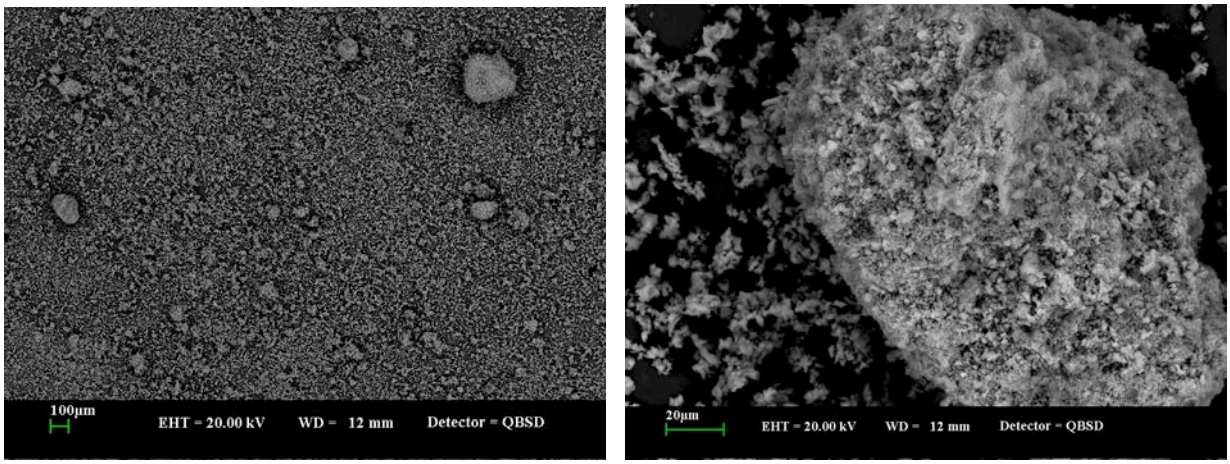

Figure 3-6. Mercer high-calcium lime at (L) 69X and (R) 1270X magnification.

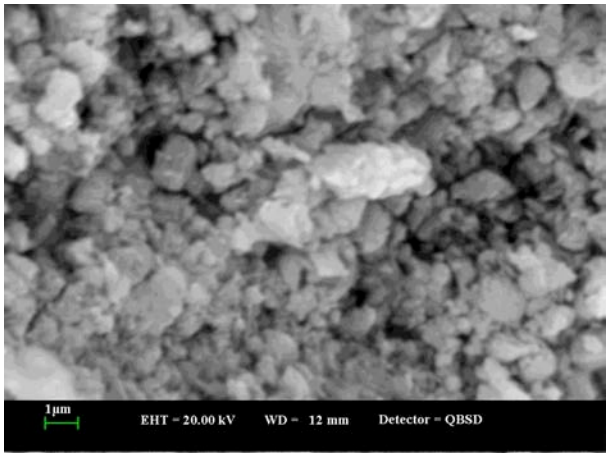

Figure 3-7. Mercer high-calcium lime at 14,600X magnification.

Preparation of Model Mortar Samples

First, the mortars were prepared with the commercial limes examined, and an appropriate curing method was developed. Three mortars, two with dolomitic and one with high-calcium lime, were mixed in a 1:2¼ (lime:sand) formulation. Although many mortars contain lime and cement as a dual binder, lime was the only binder used in these model mortars so that the direct effects of acid rain on the lime components could be examined. The common brown mason's sand, presumably from Long Island (and acquired from Extech Building Materials), should be chemically inert and have no effect on the carbonation of the mortar or on later acidic sulfate interactions.

Sieve Analysis

Before the mortar was mixed, a sieve analysis was performed to confirm that the sand consisted of properly sized sand grains to make adequate mortar. All sand was dried at ~115°C in a Precision Economy oven and all masses were measured using a Sartorius LP4200S balance. The mass of each individual sieve was recorded; then the sieves were assembled and sand (249.31 g) was added. After shaking the sieves for 5 minutes, the mass of each individual sieve was again measured to determine the mass of sand retained. The data, plotted in Figure 3-8 below, revealed that the common brown mason's sand fits within an acceptable range of particle size as 99.58% of the sand grains are between 0.074 mm (No. 200) and 4.76 mm (No. 4).

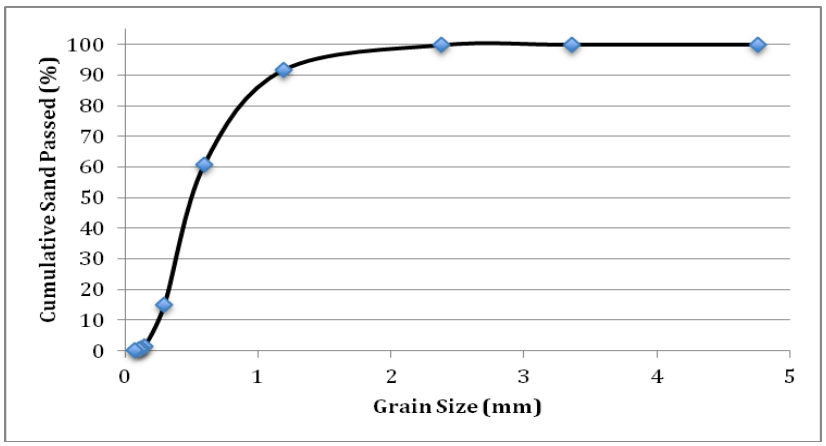

Figure 3-8. Sieve analysis showing the particle size distribution of the common brown mason's sand.

Mass and Volumetric Measurements

Measurement of the dry materials by mass is far more accurate than measurement by volume, especially due to the fine particle size of the lime. However, the mortar formulation (1:2¼) is based upon volumetric measurements. To produce reproducible samples, a correlation between mass and volumetric parts was determined. The same volume (1 cup, or 237 cc) of each dry material was weighed ten times to give an average bulk density of the material (Table 3-1). The average bulk density (g/cc) was then used to calculate the necessary amounts (g) of each material necessary to produce a 1:2¼ mortar formulation.

	Graymont Dolomitic	**Western Dolomitic**	**Mercer High-Cal**	**Common Brown Mason's Sand**
Recorded Masses (g)	0.60	0.51	0.47	1.38
	0.55	0.49	0.44	1.39
	0.55	0.49	0.41	1.38
	0.49	0.46	0.40	1.36
	0.46	0.49	0.40	1.38
	0.48	0.46	0.37	1.37
	0.48	0.47	0.37	1.39
	0.49	0.42	0.35	1.39
	0.47	0.42	0.36	1.39
	0.51	0.49	0.36	1.38
Average:	**0.51**	**0.47**	**0.39**	**1.38**

Table 3-1. Bulk densities (g/cc) of the commercial limes and sand.

Sample Mold and Mortar Groove

Samples were molded in 52 x 13mm plastic Petri dishes in order to create discs of mortar. A wooden tool, fashioned to fit the diameter of the Petri dish and sealed with two coats of linseed oil (boiled) with 4% Japan driers, was created to indent a uniform groove across the surface of each mortar sample. This groove area is intended to direct acidic sulfate attack in later experiments (Chapter 5), so that a consistent area is exposed to each attacking solution. Each Petri dish was

marked with a permanent marker on the outside to inform the placement of the groove tool and ensure the reproducibility of the groove from disc to disc.

Figure 3-9. Petri dish (L) marked for consistent placement of the wooden groove tool (R).

Mortar Mixing and Sample Molding

Lime and sand were added to a 2.5-quart plastic bucket, and the dry ingredients were mixed together in a folding motion until they were adequately mixed.

Figure 3-10. Dry ingredients, lime and sand, before (L) and after (R) mixing.

Deionized (DI) water was added and the mortar was mixed until a workable consistency was achieved. To determine if the mortar was the proper consistency, a trowel test was performed in which the mortar stuck to the trowel when scooped and inverted.

Figure 3-11. Mortar mixed with water (L), and trowel test (R) to ensure proper consistency.

The mortar was packed into the Petri dish and the top scraped with a trowel to create a flat uniform surface. The wooden tool was then inserted to create an indented groove in each mortar sample.

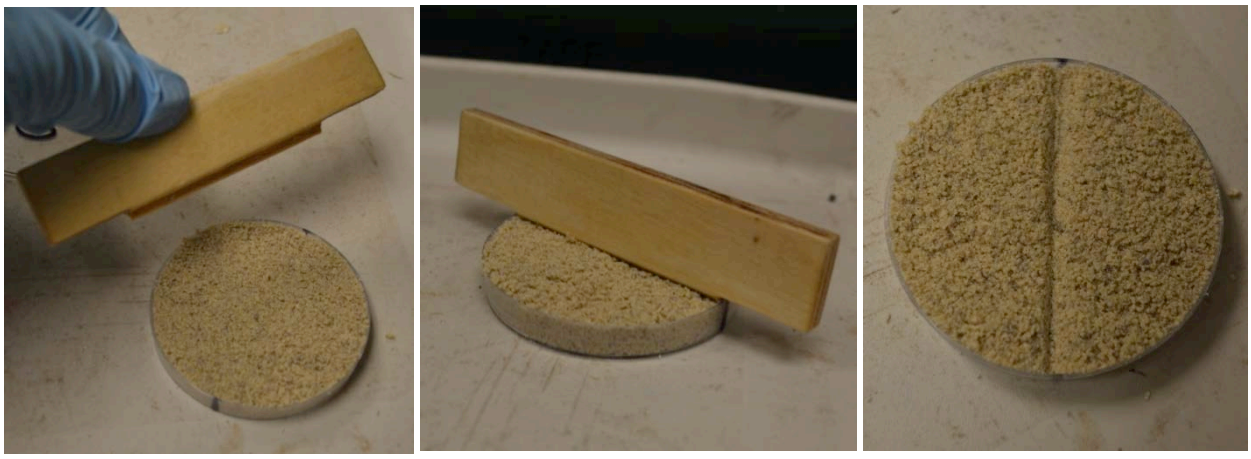

Figure 3-12. Mortar packed in the petri dish (L), wooden groove tool inserted (C), and resulting mortar sample disc (R).

Twenty-five samples were made of each mortar (three kinds: two with dolomitic and one with high-calcium lime).

Type of Lime	Mass of Lime (g)	Mass of Sand (g)	Volume of Water Added (mL)
Graymont	179.65	1102.74	84.1
Western	145.06	955.87	77.4
Mercer	139.95	1102.92	90.5

Table 3-2. Proportions of materials added for each type of mortar.

The high-calcium lime was much lighter, dustier, finer, and easier to mix with the sand than the dolomitic hydrated limes, which collected at the bottom of the container. However, the high-calcium hydrated limes were more difficult to mix with water, as they tended to form clumps.

Curing Regimen

For two weeks, mortar samples were placed in chambers equipped with Taylor brand hygrometers to monitor the relative humidity (RH) of the environment (Figure 3-13). No other source of water was placed in the chambers, as the moisture given off by the curing mortar samples was enough to maintain >90% RH. Twice a day the chambers were opened to expose the mortar samples to carbon dioxide in the air, so that both water and carbon dioxide were present to aid in the carbonation process (see lime cycle, Chapter 1).

Samples were then removed from the chambers and allowed to dry in open air for several days. For two additional weeks, the samples were saturated with DI water once a day while remaining in open air at ~20% RH. A squeeze bottle was used to disperse the water on top of the samples, and the saturation of the entire sample was ensured by observing the uniform darkening of the mortar throughout (Figure 3-14).

Figure 3-13. Samples stored in sealed chambers to ensure high relative humidity.

Figure 3-14. Saturating of samples in open air with DI water.

Examination of Carbonation Using Chemical Indicator

Once the samples made from each of the commercial limes had undergone the described curing regimen, rainbow indicator was used to explore the level of carbonation. Rainbow indicator is a spray that changes color according to the pH of the material (see color scale in Figure 3-15). Presumably, the pH of a mortar sample should reflect the level of carbonation. As the basic hydroxides transform into carbonates, the pH should lower and the color of the rainbow indicator spray should shift from the basic dark blue toward orange, which is indicative of a lower pH.

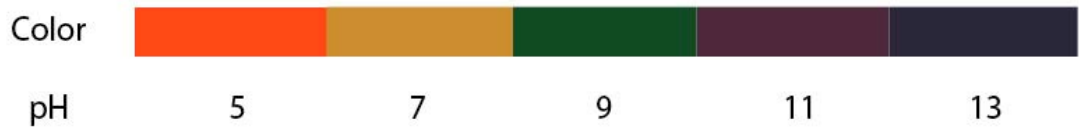

Figure 3-15. Rainbow indicator color scale and pH association.

To more accurately attribute the observed colors to particular compounds, chemical grade reagents (as described in Chapter 2) were combined with one spray of rainbow indicator. The chemical grade calcite combined with rainbow indicator turned an orange color, indicating a more neutral and even slightly acidic pH. Similarly, rainbow indicator sprayed on a piece of limestone resulted in an orange color (Figure 3-16).

Figure 3-16. Combination of rainbow indicator with limestone (L) and calcite (R).

Both the chemical grade hydromagnesite and brucite yielded a green color upon combination with the rainbow indicator (Figure 3-17). Therefore, even the carbonate and hydroxide of magnesium did not result in particularly different coloring in the presence of rainbow indicator as expected.

Figure 3-17. Combination of rainbow indicator with hydromagnesite (L) and brucite (R).

When either of these magnesium compounds was combined with calcite, the nature of the magnesium compound took over, as evidenced by the resulting green color of the solids upon mixing with rainbow indicator (Figure 3-18). This lack of differentiation using chemical indicator only adds to the confusion about the carbonation of dolomitic lime mortars.

Figure 3-18. Combination of rainbow indicator with calcite/brucite (L) and calcite/hydromagnesite (R).

When a sample was broken open and sprayed with rainbow indicator, the high-calcium lime mortar (Figure 3-19) exhibited a clear distinction between the portlandite (blue) and the calcite (red).

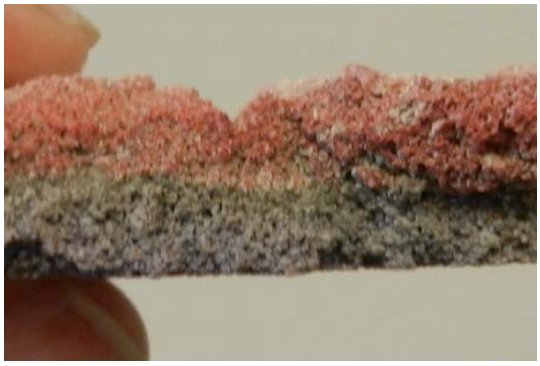

Figure 3-19. Mercer high-calcium lime mortar sample after application of rainbow indicator.

However, the separation between the carbonated and uncarbonated portions was less distinct in the dolomitic lime mortar samples (Figure 3-20). Upon spraying with rainbow indicator, the bottom of the mortar disc (encased in the Petri dish) transitioned from a blue-green to an orange interspersed with parts of blue and green at the top of the sample that was more open to the air.

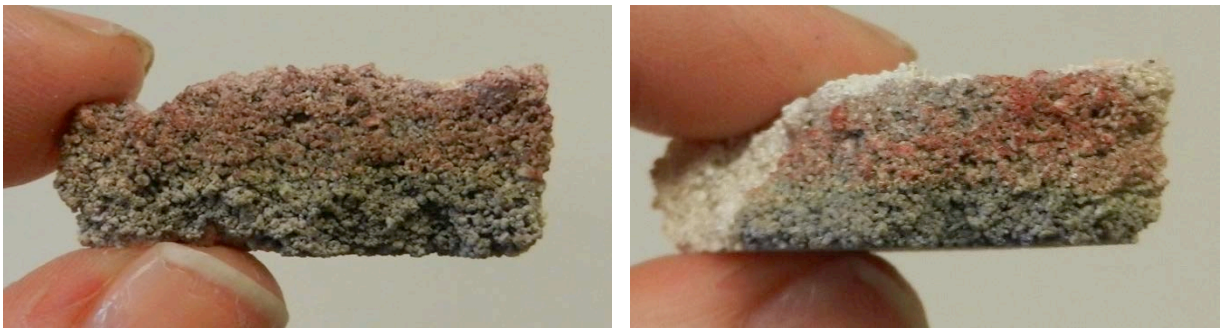

Figure 3-20. Graymont (L) and Western (R) dolomitic lime mortar sample after application of rainbow indicator.

Examination of Carbonation via X-Ray Diffraction

Next, the cured mortars were examined via XRD to identify the compounds present and determine the level of carbonation. Although XRD is a reliable method of analysis for determining chemical composition, the presence of sand created a strong pattern for quartz that diminished or masked the observation of the other minerals in the samples. To reduce the quartz pattern and enhance the detection of the other components, the mortars were gently ground, and the majority of the sand was removed until only particles less than 63 μm remained (passing No. 230 sieve). Smaller amounts of quartz were still present, but it will be omitted from the description of the chemical composition of each sample for the sake of clarity.

Dolomitic Mortars

Both of the cured dolomitic lime mortars (Figures 3-21 and 3-22) contained the same minerals: calcite, brucite, portlandite, and dolomite. The dolomite was most likely residual starting material. Although periclase was not detected in the cured model mortars, as it was in the commercial lime, it could be hidden under the pattern for calcite.

There appears to be more calcite than portlandite present in the sample, suggesting the more complete carbonation of the calcium component. The portlandite present was most likely from the back face of mortar (less exposed to air), which was observed to be less carbonated upon application of the rainbow indicator. The only magnesium component detected was brucite, suggesting that, at least at this stage in the curing process, no magnesite or hydroxycarbonates are formed. Since these mortars were subjected to an accelerated curing method, and tested after two months, it can be assumed that carbonation in the field occurs even more slowly. In fact, the magnesium component can remain uncarbonated in mortars for many years, as brucite has been petrographically observed in mortars as many as two centuries old.[6,7]

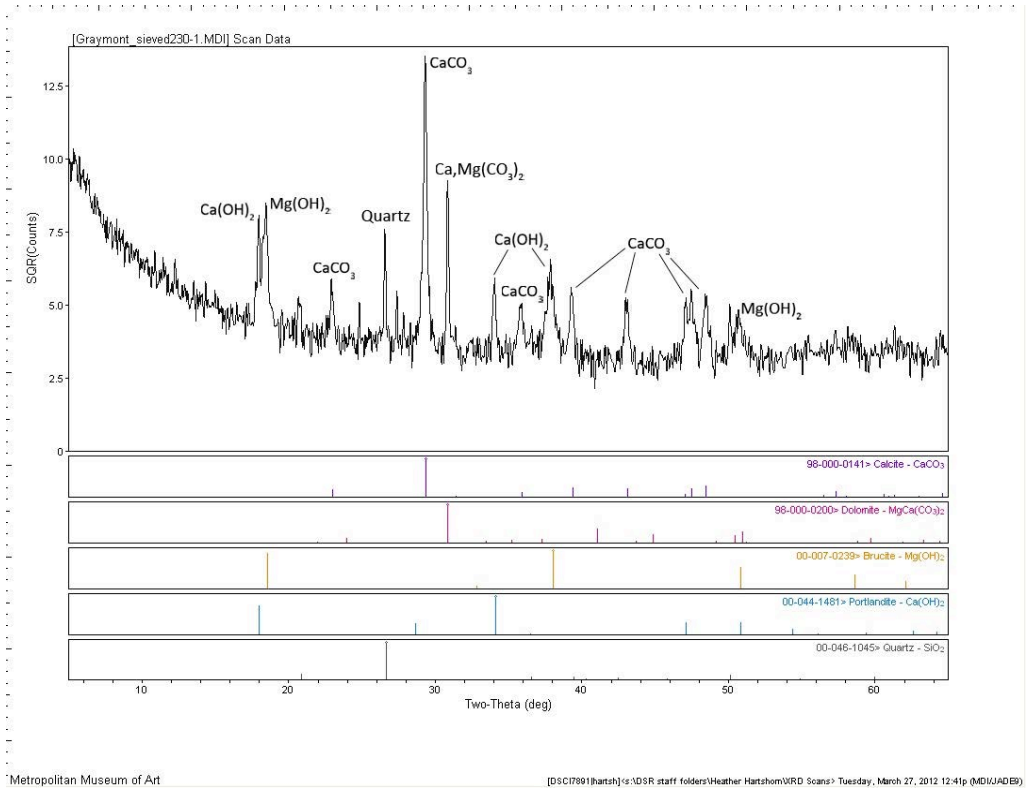

Figure 3-21. X-ray diffractogram of cured model mortar made with Graymont Dolime.

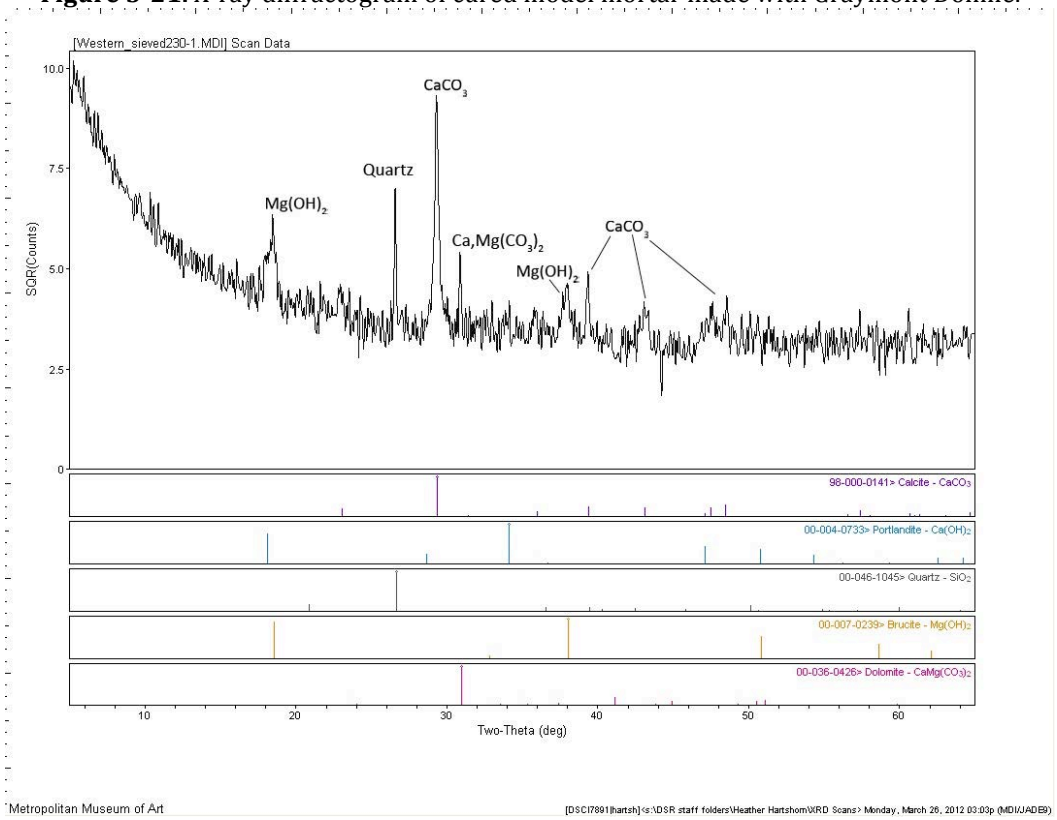

Figure 3-22. X-ray diffractogram of cured model mortar made with Western dolomitic limes.

High-Calcium Mortar

XRD patterns revealed that the Mercer high-calcium lime mortar sample (Figure 3-23) had partially carbonated to calcite, although some portlandite remained. This was most likely due to the change in carbonation level throughout the sample, observed using the rainbow indicator and discussed earlier in this chapter. The face of the mortar sample, which had greater exposure to carbon dioxide in the air, appeared to have fully carbonated while the back of the mortar disc was surrounded by the petri dish and only carbonated partially. The straightforward nature of the carbonation of portlandite alone is reinforced by these results, as is the complicated nature of carbonation of dolomitic lime mortars by comparison.

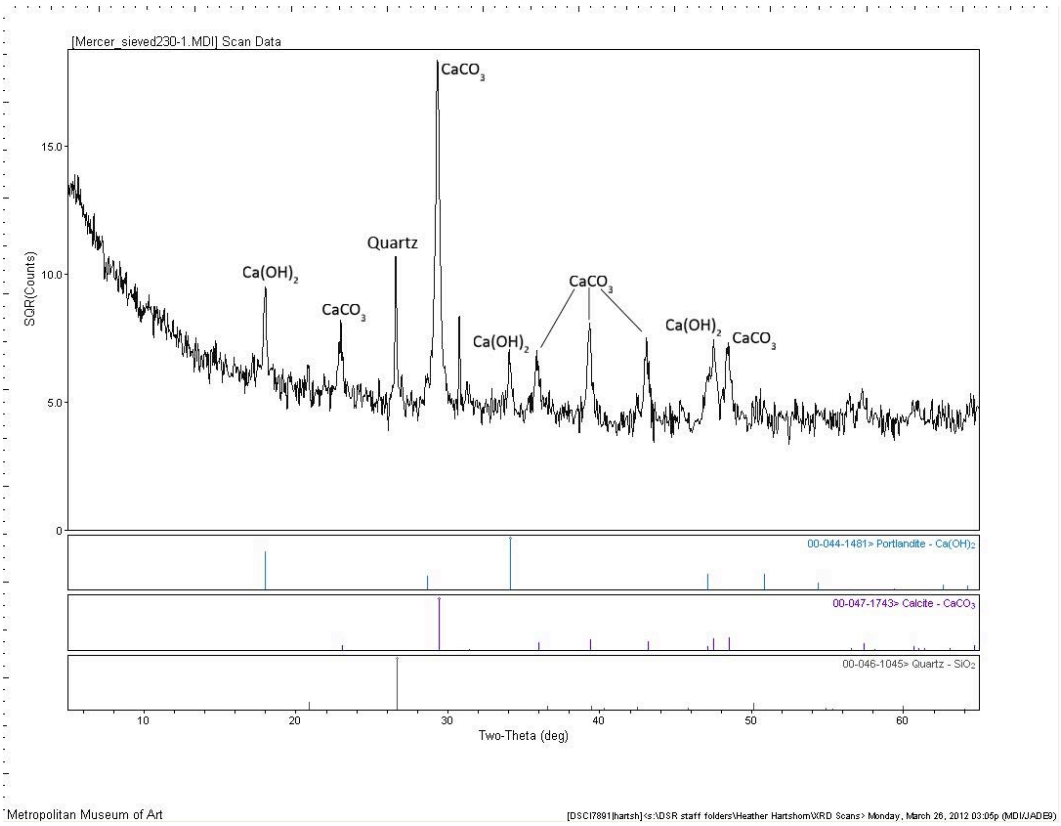

Figure 3-23. X-ray diffractogram of cured model mortar made with Mercer high-calcium lime.

Conclusions

Carbonation is a complicated process, especially in dolomitic lime mortars. As observed in these experiments, using both chemical indicator and x-ray diffraction to analyze the level of carbonation, high-calcium lime mortars undergo an uncomplicated carbonation process. When exposed to water and carbon dioxide, portlandite readily carbonates to calcite. The same holds true for the portlandite in dolomitic lime mortars. However, the carbonation of brucite is much more delayed, and a carbonation product from brucite was not observed in these experiments in any form -- either as magnesite or any of the hydroxycarbonates. Even with an accelerated curing process, only brucite and calcite were detected in the dolomitic model mortars after two months of curing. While this chapter offered greater insight into the carbonation of dolomitic lime and the compounds resulting in the mortar, Chapter 4 explores how these potential components of cured dolomitic lime mortar interact with acid rain.

[1] "Dolomitic Hydrate Type S," Graymont. http://www.graymont.com/prod_pressure_hydrate_S.shtml.
[2] "MSDS – Miracle Lime, Dolomitic Hydrated Lime," Western Lime. http://www.westernlime.com/pdfs/MSDSMiracle.pdf
[3] "Lime Products," Mercer Lime Co. http://www.mercerlime.com/lime-products.html
[4] Tate, Mike. Graymont Dolime, Inc. Phone interview, 1 March 2012.
[5] Westerman, Tom. Mercer Lime Co. E-mail correspondence, 14 February 2012.
[6] Coultrone, G.; Arizzi, A.; Rodriguez-Navarro, C; Sebastian, E. "Sulfation of Calcitic and Dolomitic Lime Mortars in the Presence of Diesel Particulate Matter." *Environmental Geology* Vol. 56, No. 3-4 (December 2008).
[7] Walsh, John. Highbridge Materials Consulting, Inc. E-mail correspondence, 28 March 2012.

Chapter 4:

Acidic Sulfate Interactions with Mortar Components

In this chapter, experiments examine the interactions of some potential dolomitic mortar components with acidic sulfate solutions in concentrations comparable to acid rain. Such solutions were combined with chemical grade calcite, brucite, and hydromagnesite individually as well as with combinations of calcite/brucite and calcite/hydromagnesite (in a 1:1 molar ratio). By exploring the interactions of these reagent combinations with acidic sulfate solutions, the reactivity of the individual components could be assessed along with any changes in the behavior of the magnesium and calcium components when in the presence of one another.

The solutions of varying acidic sulfate content included distilled water (H_2O), carbonated water (H_2O/CO_2), dilute sulfuric acid (H_2SO_4, pH = 4.0), dilute sulfurous acid (H_2SO_3, pH = 4.0), and an acid rain simulant (pH = 4.0, from a combination of carbonated water and dilute H_2SO_3). The chemical grade reagents of calcite, hydromagnesite, and brucite were acquired from the same scientific suppliers listed in Chapter 2. A commercial carbonated water (Vintage brand) was store bought while sulfuric and sulfurous acid, both certified ACS grade, were ordered from Fisher Scientific (catalog 7664-93-9 and 7782-99-2).

Solutions of both dilute sulfuric and sulfurous acids were used to note any differences in interactions of the two acids with the mortar components. However, the use of sulfuric acid to create solutions containing the sulfate ion (SO_4^{2-}) is a more accurate representation of acid rain, which is formed by the conversion of as the SO_2 emissions in the atmosphere to acidic sulfate that is incorporated into rainwater.[1] Carbonated water was employed as a representation of pollutant-free rain, which contains some carbonic acid as a result of the dissolution of carbon dioxide in the atmosphere.

Solution Preparation and Measurement of Ion Content

Each solid reagent (or equimolar combination of solid reagents) was added to each solution (1.0 g solid, 180 mL solution), and the resulting mixture was stirred for 15 minutes. This duration

was chosen after monitoring the addition of brucite in distilled water, in which the pH no longer increased after ~2.5 min. The stabilizing pH indicated the tapering of the reaction between the solid component and the solution. A much longer mixing time of 15 minutes was chosen to ensure a more complete reaction.

The solutions were then vacuum filtered, and the filtrate containing the dissociated magnesium (Mg^{2+}) and calcium (Ca^{2+}) ions was collected. Then the filtrate solution was brought to volume in a 250 mL volumetric flask (with 0.1 mL 50% (v/v) HNO_3 in order to maintain the ion content of the solution), and the resulting solution was transferred to Nalgene bottles for storage.

The following day, the amount of magnesium and calcium ions in each solution was quantified by Atomic Absorption Spectroscopy (AA) using a Perkin Elmer AAnalyst 200 Atomic Absorption Spectrometer. From the measured metal ion concentrations in the solution, the amount of their solid counterpart that had been dissolved (brucite, hydromagnesite, or calcite) was also calculated to examine the reactivity of the materials within each solution. Parameters and raw data for the AA can be found in Appendix D.

Susceptibility of Magnesium and Calcium Components

The metal ion concentration (Tables 4-1 and 4-2) was derived from the concentration detected in the diluted solutions analyzed with AA. The mass of solid dissolved was calculated from the corresponding ion content in solution and converted to a weight percentage (Tables 4-3 and 4-4) given the original mass introduced to the solution. It appears that all compounds, magnesium- and calcium-containing alike, were most reactive in the acid rain simulant, as evidenced by the metal ion concentration and corresponding amount of solid brought into that solution. However, higher concentrations of both metal ions were detected in carbonated water than in dilute sulfuric and sulfurous acid, and the lowest concentration were detected in distilled water.

Generally calcite was less susceptible to acidic sulfate attack than both hydromagnesite and brucite, as evidenced by the lower concentration of calcium ion brought into solution when calcite was individually exposed to the acidic sulfate solutions (Figure 4-1). When individually exposed to dilute acid solutions, hydromagnesite yielded higher amounts of magnesium ion than brucite. However, upon the exposure of these magnesium-containing solids to carbonated water and acid rain simulants, higher magnesium ion concentrations were detected in the solutions from brucite (Figure 4-2). As individual mortar components, it appears that brucite and hydromagnesite were more reactive with acidic sulfate solutions (in differing capacities) than calcite. However, the difference in reactivity between the calcium- and magnesium-containing compounds was observed to be greatest in the acid rain simulant.

	H_2O	H_2SO_4	H_2SO_3	H_2O/CO_2	Acid Rain
CaCO3	0.255	0.438	0.681	5.02	6.46
$CaCO_3$ /$Mg(OH)_2$	0.581	0.0750	0.079	0	0.022
$CaCO_3$ / $Mg_5(CO_3)_4(OH)_2{\cdot}4H_2O$	0.229	0.0656	0.050	0.621	0.545

Table 4-1. Concentration of calcium ion [Ca^{2+}] (mM) brought into solution as a result of exposure to attacking solution.

	H_2O	H_2SO_4	H_2SO_3	H_2O/CO_2	Acid Rain
Mg(OH)2	0.623	0.798	1.16	39.5	33.8
$Mg_5(CO_3)_4(OH)_2{\cdot}4H_2O$	1.74	2.14	2.49	33.6	31.3
$CaCO_3$ /$Mg(OH)_2$	0.539	0.544	0.706	28.3	31.3
$CaCO_3$ / $Mg_5(CO_3)_4(OH)_2{\cdot}4H_2O$	1.53	0.560	2.07	18.1	21.0

Table 4-2. Concentration of magnesium ion [Mg^{2+}] (mM) brought into solution as a result of exposure to attacking solution.

In the presence of hydromagnesite or brucite, calcite was observed to be less reactive with the acidic sulfate solutions (Figure 4-3) than it was on its own. The opposite was true for both hydromagnesite and brucite, which reacted with the solutions to a greater extent in the presence of calcite (Figure 4-4). This suggests that in dolomitic lime mortars, acid rain will have a greater interaction with the brucite and hydromagnesite to form magnesium sulfate salts than with the

calcite to form gypsum, which can act as a protective layer. Not only do these interactions result in higher concentrations of magnesium ions that can react with sulfates, large amounts of the original magnesium-containing components were dissolved (up to 88.3% of the $Mg(OH)_2$ in the combination of $CaCO_3/Mg(OH)_2$ with the acid rain simulant), which suggests there could be great material losses in the mortar itself.

	H_2O	H_2SO_4	H_2SO_3	H_2O/CO_2	Acid Rain
$CaCO_3$	0.462	0.781	1.23	8.84	11.4
$CaCO_3$ /$Mg(OH)_2$	0.165	0.215	0.227	0	0.625
$CaCO_3$ / $Mg_5(CO_3)_4(OH)_2{\cdot}4H_2O$	0.0751	0.213	0.165	2.03	1.66

Table 4-3. Amount of $CaCO_3$ dissolved (wt %) as a result of exposure to attacking solution.

	H_2O	H_2SO_4	H_2SO_3	H_2O/CO_2	Acid Rain
$Mg(OH)_2$	0.636	0.815	1.21	41.5	34.5
$Mg_5(CO_3)_4(OH)_2{\cdot}4H_2O$	2.63	3.19	3.71	50.5	47.2
$CaCO_3$ /$Mg(OH)_2$	1.51	1.51	2.01	78.8	88.3
$CaCO_3$ / $Mg_5(CO_3)_4(OH)_2{\cdot}4H_2O$	4.97	1.86	6.75	59.2	69.3

Table 4-4. Amount of Mg-containing solid dissolved (wt %) as a result of exposure to attacking solution.

It should be noted that the carbonated water (also used to make the acid rain simulant) already contained small amounts of Mg^{2+} (0.21 mM) and Ca^{2+} (0.50 mM). This could possibly lead to the common ion effect, in which greater amounts of the ion already in solution may be dissolved to achieve chemical equilibrium. However, it is not considered to be a factor here because the concentrations of ions already in solution are small compared to the much higher concentrations resulting from combination with the solid reagents.

Conclusions

In these preliminary experiments using chemical grade reagents to simulate acid sulfate attack on dolomitic lime mortar components, it was observed that calcite was less susceptible to attack, particularly in the presence of the brucite or hydromagnesite. The opposite was true for the

magnesium-containing compounds, which appear to be more susceptible to acidic sulfate solutions in the presence of calcite. This suggests that in dolomitic lime mortars, the magnesium components are more likely to react with acid rain, and could ultimately lead to the formation of magnesium sulfate salts and the loss of material in the mortar.

Although this chapter provided insight into the interactions of acidic sulfate solutions with individual compounds likely found in mortar, the experiments performed were simply exploratory and not reflective of field conditions. Chapter 5 will elaborate on these initial findings by examining the susceptibility of cured model mortars exposed to an acid rain simulation.

[1] Seinfeld, John H.; Pandis, Spyros N. *Atmospheric Chemistry and Physics – From Air Pollution to Climate Change, 2nd ed*. New York: John Wiley, 2006.

Chapter 5:

Acid Rain Simulation on Model Mortars

While Chapter 4 explored the interactions of acidic sulfate solutions with chemical grade representations of dolomitic lime mortar components, the experiments in this chapter expand that exploration to examine the effects of acid rain on actual mortar samples. Although the model mortars were subjected to an accelerated curing process, their carbonation was only partial (see Chapter 3). It was expected that the surface of the mortars contained mostly calcite and brucite, and that the acid rain simulants interacted primarily with these components of the mortar, as the sand was chemically inert.

Simulation of Acid Rain on Model Mortars

Although an ideal acid rain simulation would employ multiple cycles of wetting and drying, this thesis is limited by time constraints that did not permit such cyclical experiments. Rather, model mortars were exposed to various solutions and the runoff collected in multiple aliquots to give a preliminary study of the interactions. Livingston performed similar tests, in which runoff was analyzed to evaluate building deterioration by acid rain.[1] Note that no laboratory test can accurately simulate real acid rain, as field conditions are variable and dependent on many changing conditions.

In this experiment, the two dolomitic lime mortars (Graymont and Western) as well as one high-calcium lime mortar (Mercer) were exposed to three "attacking" solutions containing varied amounts of sulfate ion. These solutions included: deionized (DI) water, dilute sulfuric acid (pH = 3.5), and acid rain simulant (carbonated water with sulfuric acid, pH = 3.5). The sulfuric acid and carbonated water used in these solutions were acquired from the same sources described in Chapter 4.

Each model mortar disc was suspended below a 50 mL burette containing the attacking solution. Due to the absorbent nature of the mortar, the disc was saturated with water prior to exposure in order to direct the interaction of the solution along the grooved surface of the mortar. A

Nalgene collection bottle was placed below the mortar disc to collect runoff, and the burette was adjusted to release one drop of solution approximately every three seconds. The runoff was collected in five subsequent aliquots, replacing the Nalgene bottle following the exposure of the mortar to every 10 mL of solution from the burette.

The collected runoff was then analyzed with atomic absorption spectroscopy (AA) to determine the amount of magnesium and calcium ion that was brought into solution and dissolved from the mortar disc. Parameters and raw data for the AA can be found in Appendix D. The groove of the mortar disc exposed to the solution was then sampled and examined with x-ray diffraction (XRD) to determine the remaining mortar components. These runoff experiments do not examine all factors involved in the susceptibility of these mortars to acidic sulfate attack, and although kinetics are not explicitly discussed here, they may be kept in mind.

Analysis of Susceptibility Using Atomic Absorption Spectroscopy

The dolomitic lime mortars (Graymont and Western) generally exhibited high initial concentrations of magnesium ion in the runoff while the calcium ion content remained much lower throughout exposure to the attacking solutions. As expected, a much higher calcium ion concentration and minimal amounts of magnesium ion were detected in runoff from the high-calcium lime mortar (Mercer).

Although runoff from the exposure of the dolomitic lime mortars to both DI water and dilute sulfuric acid led to the detection of diminishing magnesium ion concentrations in each subsequent aliquot collected, the exposure of the same mortars to the acid rain simulant resulted in the maintenance of high magnesium ion concentrations in each aliquot (see Table 5-1). While the magnesium ion concentration of the acid rain runoff from the Graymont mortar did decrease, it did so to a much lesser extent – decreasing only from 8.64 mM to 7.25 mM, as opposed to the decrease from 7.25 mM to 1.57 mM upon exposure to dilute sulfuric acid. The acid rain runoff from the

Western mortar contained increasing amounts of magnesium ion in each subsequent aliquot (from 7.21 mM to 9.26 mM). There is no obvious explanation for the differences between the two dolomitic lime mortars – Graymont decreased in magnesium ion concentration while Western increased. However, the higher concentrations of both dolomitic lime mortars throughout all five aliquots suggest that the magnesium compounds in dolomitic lime mortar continue interacting with the acid rain simulant, as opposed to the rapidly diminishing concentrations observed upon exposure to the other attacking solutions.

The amount of magnesium ion present in runoff from the Mercer high-calcium lime mortar was also greatest upon exposure to the acid rain simulant. However, magnesium ion concentrations from the high-calcium lime mortar were always much less than those observed in the dolomitic lime mortars. It was surprising that any magnesium ion should be detected in the runoff from the high-calcium lime mortar, as no magnesium-containing compounds were detected in the commercial Mercer hydrate lime upon examination with XRD (see Chapter 3). Perhaps, the small amounts of magnesium present could have been below the detection limits of the XRD instrument. The higher concentrations of magnesium ion present in the runoff from the acid rain simulant and Mercer mortars may be attributed to the amount of magnesium already present in the carbonated water used to make the acid rain simulant.

		Aliquot				
Mortar	**Attacking Solution**	**1**	**2**	**3**	**4**	**5**
Graymont	Acid Rain	8.64	7.86	7.54	7.51	7.25
Western	Acid Rain	7.21	8.75	10.07	9.24	9.26
Mercer	Acid Rain	1.35	1.79	2.03	1.81	1.54
Graymont	Dilute Sulfuric Acid	7.52	3.54	2.56	1.96	1.57
Western	Dilute Sulfuric Acid	6.08	3.78	2.69	1.93	1.64
Mercer	Dilute Sulfuric Acid	0.74	0.28	0.15	0.11	0.07
Graymont	DI Water	9.57	4.60	3.03	2.20	1.75
Western	DI Water	6.39	3.91	2.74	2.84	1.44
Mercer	DI Water	0.65	0.29	0.13	0.11	0.1

Table 5-1. Concentration of Magnesium Ion [Mg^{2+}] (mM) detected in runoff solutions.

As expected, the highest concentration of calcium ion was detected in runoff from the Mercer high-calcium lime mortar (Table 5-2). Each aliquots maintained similar concentrations of calcium ion, regardless of attacking solution. However, runoff from the exposure of the high-calcium mortar to the acid rain simulant yielded lower concentrations of calcium ion than runoff from dilute sulfuric acid, which, in turn, had calcium ion concentrations lower than that detected in the runoff from DI water. Therefore, high-calcium lime mortars, containing calcite alone, appear to be less reactive with the acidic sulfate solutions.

Conversely, the dolomitic lime mortars had less calcium ion in the runoff solutions (Table 5-2). This could be due not only to the smaller amount of calcite in dolomitic lime mortars (as opposed to high-calcium lime mortars), but also to the presence of the magnesium components. Most of the runoff solutions from dolomitic lime mortars contained similar concentrations of calcium ion, regardless of the solution. However, runoff from the exposure of the Graymont mortar to the acid rain simulant yielded diminishing amounts of calcium ion in each subsequent aliquot.

		Aliquot				
Mortar	**Attacking Solution**	**1**	**2**	**3**	**4**	**5**
Graymont	Acid Rain	5.89	8.07	3.08	1.3	1.25
Western	Acid Rain	2.7	1.53	2.26	2.85	2.28
Mercer	Acid Rain	6.14	6.5	7.4	6.01	7.41
Graymont	Dilute Sulfuric Acid	5.92	7.47	7.8	8.7	7.81
Western	Dilute Sulfuric Acid	2.98	3.06	3.28	4.6	2.88
Mercer	Dilute Sulfuric Acid	7.64	8.76	9.25	8.62	8.95
Graymont	DI Water	4.08	3.09	6.69	4.97	5.15
Western	DI Water	3.76	2.75	5.15	8.67	3.96
Mercer	DI Water	10.86	10.53	10.23	10.32	9.98

Table 5-1. Concentration of Calcium Ion [Ca^{2+}] (mM) detected in runoff solutions.

Experiments outlined in Chapter 4, which explored the interactions of these attacking solutions with chemical grade calcite, brucite, and hydromagnesite, suggested that the reactivity of the calcite with acidic sulfate solutions decreased in the presence of magnesium compounds.

Perhaps the same phenomena can explain the lower concentrations of calcium ion in the runoff from the dolomitic (rather than high-calcium) lime mortars observed here.

Analysis of Susceptibility via X-Ray Diffraction

The groove of each mortar sample exposed to an attacking solution was then analyzed by x-ray diffraction (XRD). Mortar from the surface in and adjacent to the groove was scraped off, ground with mortar and pestle, and then sieved to remove unwanted sand particles that overwhelm the diffraction pattern (see "Examination of Carbonation via X-Ray Diffraction" in Chapter 3). Although residual quartz from the sand was observed, it will be omitted from the description of the following chemical compositions for the sake of clarity.

The mortar samples exposed to DI water were used as a basis of comparison to the effects of the acidic sulfate solutions. Upon exposure to DI water, the dolomitic lime mortar samples were found to contain mostly calcite and brucite. Like these mortars, the cured dolomitic lime mortar samples (discussed in Chapter 3, with material from the entire thickness of the mortar disc) contained large amounts of calcite and brucite, but also portlandite. The portlandite was most likely from the back face of the mortar, which was less open to air during the curing process. Therefore, it is reasonable to assume that the mortars exposed to DI water are indicative of the surface chemistry of the cured model mortars with which the attacking solutions interacted.

Surprisingly, the dolomitic lime mortars exposed to the acid rain simulant still contained calcite and brucite (Figure 5-1). However, when exposed to dilute sulfuric acid, only calcite (and residual dolomite) was detected in the dolomitic lime mortars (Figure 5-2). The brucite had been removed from the surface of the mortar by the dilute sulfuric acid. In the past, scholars have noted the trouble with using sulfuric acid to simulate sulfate solutions as sometimes acid rather than sulfate attack occurs.[2] Perhaps it was the acid rather than the reaction with the sulfate content that caused the removal of brucite from the mortar sample. This could also explain the continued

interaction of dolomitic lime mortars with the acid rain simulant, observed earlier by the maintenance of magnesium ion concentration in the runoff solutions, as opposed to the diminishing concentrations observed in runoff from dilute sulfuric acid.

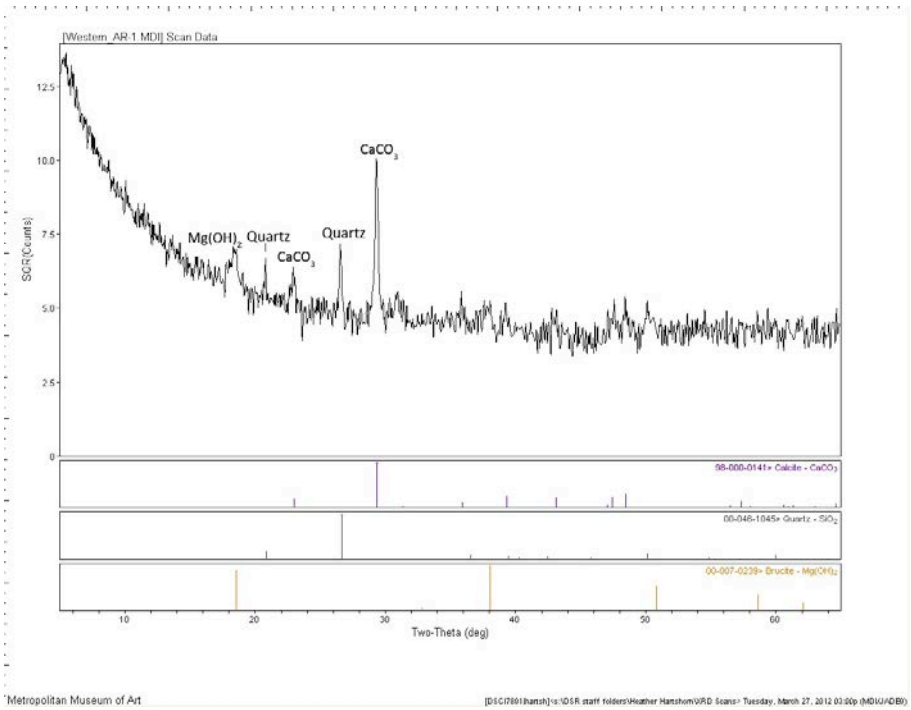

Figure 5-1. X-ray diffractogram of Western mortar exposed to acid rain simulant (pH=3.5).

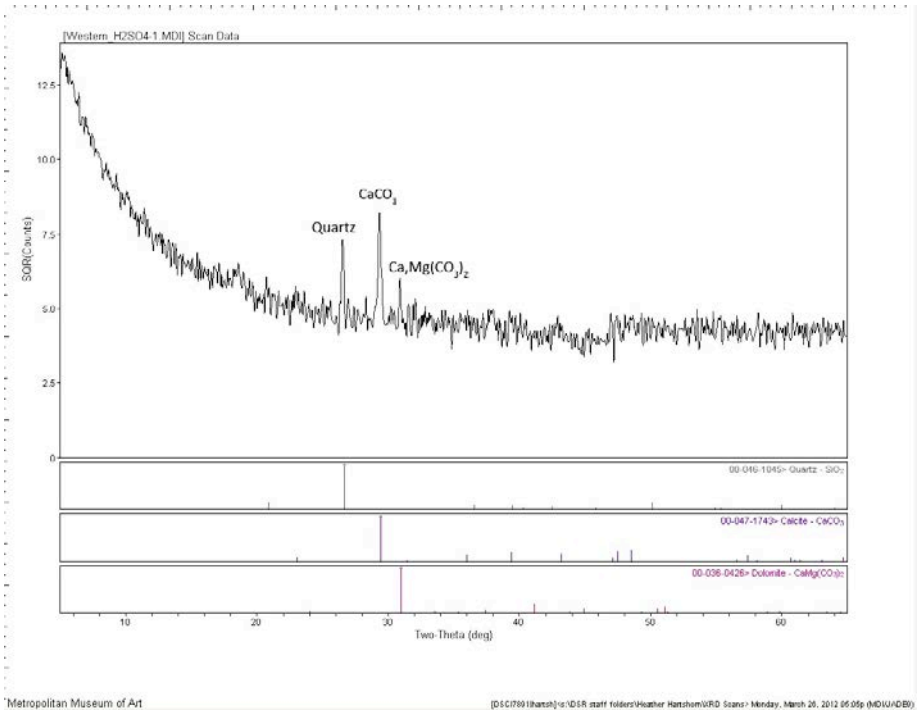

Figure 5-2. X-ray diffractogram of Western mortar exposed to dilute sulfuric acid (pH=3.5).

By comparison, the Mercer high-calcium lime mortars behaved rather simply. Although the cured mortar was found to contain calcite as well as portlandite in Chapter 3, the mortar exposed to DI water was comprised only of calcite. Again, the chemical composition observed here is most likely indicative of the chemistry of the mortar surface, which was exposed to the attacking solutions. Upon exposure to both acidic sulfate solutions (dilute sulfuric acid and acid rain), the Mercer high-calcium mortar was still found to contain calcite. This suggests that high-calcium lime mortars are less susceptible to material loss than dolomitic lime mortars when exposed to acidic sulfate solutions, particularly dilute sulfuric acid.

Conclusions

Most of the observations made here reflect the findings in Chapter 4, which studied the interactions of chemical grade representations of mortar components with acidic sulfate solutions. Chemical grade calcite on its own produced greater amounts of calcium ion in solution, which decreased greatly upon combination with brucite or hydromagnesite suggesting that acid rain reacts preferentially with the magnesium-containing compounds. Similar results occurred upon exposure of model mortars to sulfate solutions, as the high-calcium mortar yielded the highest concentration of calcium ion in the runoff. Although this would be expected given the greater amount of calcite available, the concentration of calcium ion more than doubles suggesting that calcite is less reactive in the presence of brucite in the model mortars - just as chemical grade calcite was less reactive in the presence of chemical grade brucite (see Chapter 4).

The inverse was true for brucite and hydromagnesite, which were more reactive in the presence of calcite. In fact, experiments from Chapter 4 demonstrated that brucite in the combination of chemical grade brucite and calcite (similar to the composition of the model mortars in this chapter) was most reactive with the acid rain simulant. Here, the acidic sulfate exposure of the dolomitic lime mortars displayed similar results, as the highest concentration of magnesium ion

occurred in the acid rain runoff. This runoff also contained a much higher cumulative magnesium ion content due to the fact that the subsequent aliquots continued to have high concentrations of magnesium ion, rather than diminishing concentrations as observed in runoff from the DI water or dilute sulfuric acid. The combination of brucite and calcite, whether chemical grade or in a model mortar, responds similarly, as acid rain yields the greatest amount of magnesium ion in solution.

However, the XRD analysis of the exposed model mortar surfaces suggests a more complicated situation. In every exposed mortar surface, calcite always remained. The surface of the dolomitic mortars also retained brucite upon exposure to DI water and acid rain. Although the greatest amount of magnesium ion was detected in the runoff from exposure of the dolomitic lime mortars to the acid rain simulant, the mortar itself still retained a significant amount of brucite on the surface. Alternatively, the concentration of magnesium ion was lower in the runoff from dilute sulfuric acid exposure, yet no brucite was detected on the surface of the exposed mortar.

It can be determined from these experiments that acid rain interacts to a greater extent with the components of dolomitic lime mortar than with high-calcium lime mortar. Experiments undertaken in Chapters 4 and 5 indicate that the interaction of acid rain with dolomitic lime mortars may lead to a large dissociation of magnesium ion, which could combine with sulfate ions in the acid rain to yield magnesium sulfate salts. However, it appears that such interactions do not necessarily lead to an extensive loss of material within the mortar itself -- at least in the early stages of interaction that were examined. This is particularly interesting when compared to the complete removal of brucite from the model dolomitic lime mortars upon exposure to dilute sulfuric acid, suggesting that acid attack (rather than dissociation and reaction with sulfate ions) is responsible for the rapid loss of material.

---

[1] Livingston, R. A. "Evaluation of Building Deterioration by Water Runoff," *Building Performance: Function, Preservation, and Rehabilitation. ASTM STP 901.* G. Davis, Ed., American Society for Testing and Materials, Philadelphia (1986): 181-188.

[2] Santhanam, Manu; Cohen, Menashi D.; Olek, Jan. "Sulfate Attack Research - Whither Now?," *Cement and Concrete Research* 31 (2001): 845-851.

Chapter 6:

Summary and Future Recommendations

Carbonation

Recreating the production process of dolomitic lime in the laboratory offered greater insight into the resulting material used to make dolomitic lime mortars (see Chapter 2). Although the magnesium components of dolomitic materials decompose at a lower temperature than the calcium components, the slaking of periclase to brucite is much slower than that of quicklime to portlandite. It was observed that the carbonation of portlandite to calcite was unhindered while the carbonation of brucite was quite delayed, as no magnesite or any hydroxycarbonates were observed in the cured model mortars studied here (see Chapter 3).

Petrographically, the carbonation of brucite has been observed to be sluggish as it can be identified in many historic mortars along with calcite. Studies on historic dolomitic lime mortars detected the presence of a variety of magnesium components including brucite, magnesite, hydromagnesite, and amorphous magnesium phases.[1,2] Although the mortars studied in this thesis were only allowed to cure (in an accelerated process) for two months, the continued presence of brucite in historic mortars indicates that the acidic sulfate exposure experiments on these model mortars may offer some insight into effects in the field.

Susceptibility to Acidic Sulfates

Experiments that studied the interactions acidic sulfate solutions with chemical grade representations of mortar components (see Chapter 4) suggested the greater susceptibility of the magnesium-containing compounds, particularly in the presence of calcite. The combination of reagent grade brucite and calcite was most reactive in the acid rain simulant.

The prepared model dolomitic lime, with brucite and calcite on the surface, behaved in a similar manner (see Chapter 5). Upon exposure of these mortars to acidic sulfate solutions, runoff from the acid rain simulant was found to contain the highest concentration of magnesium ion.

Although atomic absorption data showed that a greater concentration of magnesium ion was brought into solution by the acid rain simulant than by the dilute sulfuric acid, x-ray diffraction analysis of the exposed mortar samples revealed that the dilute sulfuric acid completely removed brucite from the sample surface while the acid rain simulant did not. This indicates that a greater loss of material in the mortar may be attributed to acid attack by the dilute sulfuric acid rather than to reaction with the acid rain simulant. Although brucite was observed to be susceptible to acidic sulfate attack, either by dissolution of the magnesium ion or observed material losses, calcite remained present in every exposed mortar surface. The concentration of calcium ion brought into solution from the dolomitic lime mortars was much less than that of magnesium ion in runoff from the dolomitic lime mortars. Runoff from the high-calcium mortars exhibited much high concentrations of calcium ion, suggesting the lower reactivity of calcite in the presence of the magnesium-containing compounds found in dolomitic lime mortars.

The experiments undertaken in this thesis suggest the favored reaction of acidic sulfates with the magnesium-containing compounds of dolomitic lime mortar. Although the dissolution of the magnesium ion was observed here along with some material loss of brucite, neither epsomite nor hexahydrite (magnesium sulfate salts) was detected in the model mortars. Similary, petrographers have not been able to detect epsomite in dolomitic lime mortars while gypsum surface crusts have been clearly evident.[3] However, other researchers have observed the presence of epsomite, hexahydrite, and gypsum in historic dolomitic lime mortars in Spain using techniques such as XRD.[4,5] It should be noted that the acid rain simulations performed in this thesis were limited, and further study is necessary to assess the role of dolomitic lime mortars in the formation of magnesium sulfate salts.

Future Recommendations

Many aspects of this thesis research may be continued to develop a more complete picture of the carbonation of dolomitic lime mortars and their susceptibility to acidic sulfate attack. It would be interesting to continue monitoring the carbonation of such model mortars as those described here. To simplify carbonation experiments, it would also be advantageous to analyze the cyclical wetting and drying of the commercial dolomitic limes alone to monitor their carbonation.

The experiments using chemical grade reagents to explore interactions between mortar component and acidic sulfate solutions could be expanded to include the testing of other potential compounds in dolomitic lime mortar, such as periclase, magnesite, nesquehonite, artinite, and dypingite. Additional acid rain simulations on model mortars could employ additional analysis methods, such as SEM and polarized light microscopy (PLM), to acquire more information on the mortar surfaces following exposure to the attacking solutions. The mobility and crystallization of magnesium sulfate salts could also be studied to elaborate on the implications of these salts and the common use of dolomitic lime mortars in buildings.

Lastly, all of the experiments performed for this thesis were conducted on laboratory prepared specimens, which are never identical to real world situations. The analysis of field samples would offer immense insight into the actual state of dolomitic lime mortars (and surrounding building materials) after years of environmental exposure.

---

[1] Diekamp, A., J. Konzett, W. Wertl, R. Tessadri, and P.W. Mirwald. "Dolomitic Lime Mortar – A Commonly Used Building Material for Medieval Buildings in Western Austria and Northern Italy." *Proceedings of the 11th International Congress on Deterioration and Conservation of Stone, 15-20 September 2008, Torun, Poland* 1. Eds. J. W. Lukaszewicz and P. Niemcewicz: (2008) 597–604.

[2] Montoya, C.; Lanas, J.; Arandigoyen, M.; Navarro, I.; García Casado, P.J.; Alvarez, J.I. "Study of Ancient Dolomitic Mortars of the Church of Santa María de Zamarce in Navarra (Spain): Comparison with Simulated Standards," *Thermochimica Acta* 398 (2003): 107-122.

[3] Walsh, John. Highbridge Materials Consulting, Inc. E-mail correspondence, 28 March 2012.

[4] Coultrone, G.; Arizzi, A.; Rodriguez-Navarro, C; Sebastian, E. "Sulfation of Calcitic and Dolomitic Lime Mortars in the Presence of Diesel Particulate Matter." *Environmental Geology* Vol. 56, No. 3-4 (December 2008).

[5] Lopez-Arce, P.; Garcia-Guinea, J.; Benavente, D.; Tormo, L.; Doehne, E. "Deterioration of Dolostone by Magnesium Sulphate Salt: An Example of Incompatible Building Materials at Bonaval Monastery, Spain," *Construction and Building Materials* 23 (2009): 846-855.

Bibliography

"BS 890: Specification for Building Limes," *British Standard*. London: BSI, 1995.

"The Venice Charter: International Charter for the Conservation and Restoration of Monuments and Sites," *Second International Congress of Architects and Technicians of Historic Monuments*. Venice: ICOMOS, 1964.

"U.S. & Canadian Lime Companies >> Interactive Map," National Lime Association, 2012, http://www.lime.org/about_nla/find_a_lime_plant/us_canadian_lime_companies/interactive-map.asp.

ASTM C1012/C1012M – 10, "Standard Test Method for Length Change of Hydraulic-Cement Mortars Exposed to Sulfate Solution." West Conshohocken, PA: American Society for Testing Materials International, 2011.

ASTM C207-06 "Standard Specification for Hydrated Lime for Masonry Purposes." West Conshohocken, PA: American Society for Testing Materials International, 2011.

ASTM C88-05, "Standard Test Method for Soundness of Aggregates by Use of Sodium Sulfate or Magnesium Sulfate." West Conshohocken, PA: American Society for Testing Materials International, 2005.

ASTM D5240 – 04, "Standard Test Method for Test Rock Slabs to Evaluate Soundness of Riprap by Use of Sodium Sulfate or Magnesium Sulfate." West Conshohocken, PA: American Society for Testing Materials International, 2004.

Berman, Scott, Frage, Debera F.; Tate, Michael J. "The Effect of Acid Rain on Magnesium Hydroxide Contained in Cement-Lime Mortar," *Masonry: Opportunities for the 21st Century, ASTM STP 1432,* ed. D. Throop and R.E. Klingner (West Conshohocken, PA: ASTM International, 2003).

Bläuer Böhm, C.; Jägers, E. "Analysis and Recognition of Dolomitic Lime Mortars," *International Workshop of Roman Wall Painting: Materials, Techniques, Analysis and Conservation*. Fribourg (1996).

Boynton, Robert S. *Chemistry and Technology of Lime and Limestone,* 2nd edition. New York: John Wiley, 1980.

Carello, Sandra A., Vilela, Antônio C.F. "Evaluation of the Reactivity of South Brazilian Limestones in Relation to Pure SO_2 through Thermoanalysis and Scanning Electron Microscopy," *Ind. Eng. Chem. Res.* 32 (1993): 3135-3142.

Carmona-Quiraga, Paula María; Panas, Itai; Svensson, Jan-Erik; Johansson, Lars-Gunnar; Blanco Varela, María Teresa; Martínez-Ramírez, Sagrario. "Protective Performaces of Two Anti-Graffiti Treatments Towards Sulfite and Sulfate Formation in SO_2 Polluted Model Environment," *Applied Surface Science* 257 (2010): 852-856.

Clark, George L.; Sprague, Robert S. "Analysis of Highly Hydrated Dolomitic Lime: Critical Comparison of Chemical and Instrumental Methods," *Analytical Chemistry* 24, 4 (1952): 688-701.

Coultrone, G.; Arizzi, A.; Rodriguez-Navarro, C; Sebastian, E. "Sulfation of Calcitic and Dolomitic Lime Mortars in the Presence of Diesel Particulate Matter." *Environmental Geology* Vol. 56, No. 3-4 (December 2008).

Diekamp, A.; Konzett, J.; Mirwald, P.W. "Magnesian Lime Mortars – Identification of Magnesium-Phases in Medieval Mortars and Plasters with Imaging Techniques," *12th Euroseminar on Microscopy Applied to Building Materials.* Dortmund, Germany (September 2009).

Diekamp, A., J. Konzett, W. Wertl, R. Tessadri, and P.W. Mirwald. "Dolomitic Lime Mortar – A Commonly Used Building Material for Medieval Buildings in Western Austria and Northern Italy." *Proceedings of the 11th International Congress on Deterioration and Conservation of Stone, 15-20 September 2008, Torun, Poland* 1. Eds. J. W. Lukaszewicz and P. Niemcewicz: (2008) 597–604.

Eckel, Edwin C. *Cements, Limes, and Plasters; Their Materials, Manufacture and Properties,* 3rd ed. New York: John Wiley, 1928.

Elert, Kerstin; Rodrigues-Navarro, Carlos; Pardo, Eduardo Sebastian; Hansen, Eric; Cazalla, Olga. "Lime Mortars for the Conservation of Historic Buildings." *Studies in Conservation* 47 (2002): 62-75.

Emley, Warren E. "Manufacture of Lime" in *Technologic Papers of the Bureau of Standards*, Department of Commerce. Washington: Government Printing Office, 1913.

GCI Lime Mortars and Plasters Bibliography, The Getty Conservation Institute (2003).

Klemm, Werner and Heiner Siedel. "Evaluation of the Origin of Sulphate Compounds in Building Stone by Sulphur Isotope Ratio," *Geological Society, London, Special Publications* 205 (2002): 419-429.

Knibbs, N.V.S. *Lime and Magnesia: The Chemistry, Manufacture and Uses of the Oxides, Hydroxides and Carbonates of Calcium and Magnesium*. London: Ernest Benn, 1924.

Livingston, R. A. "Evaluation of Building Deterioration by Water Runoff," *Building Performance: Function, Preservation, and Rehabilitation. ASTM STP 901.* G. Davis, Ed., American Society for Testing and Materials, Philadelphia (1986): 181-188.

Lopez-Arce, P.; Garcia-Guinea, J.; Benavente, D.; Tormo, L.; Doehne, E. "Deterioration of Dolostone by Magnesium Sulphate Salt: An Example of Incompatible Building Materials at Bonaval Monastery, Spain," *Construction and Building Materials* 23 (2009): 846-855.

Lucas, A. *Ancient Egyptian Materials and Industries*. Great Britain: Kessinger, 2003.

Mack, Robert C. and John P. Speweik. "Preservation Brief 2: Repointing Mortar Joints in Historic Masonry Buildings." Technical Preservation Service, National Park Service, U.S. Dept of the Interior (1998).

Martínez-Ramírez, S.; Puertas, F.; Blanco-Varela, M.T.; Thompson, G.E. "Studies on Degradation of Lime Mortars in Atmospheric Simulation Chambers," *Cement and Concrete Research* 27, 5 (1997): 777-784.

Maurenbrecher, A. H. Paul. "Mortars for Repair of Traditional Masonry," *Practice Periodical on Structural Design and Construction* (2004).

Maurenbrecher, A. H. Paul and Madeleine Rousseau. "Repointing Mortars for Older Masonry," *The Canadian Architect* 45 (2000): 44.

Montoya, C.; Lanas, J.; Arandigoyen, M.; Navarro, I.; García Casado, P.J.; Alvarez, J.I. "Study of Ancient Dolomitic Mortars of the Church of Santa María de Zamarce in Navarra (Spain): Comparison with Simulated Standards," *Thermochimica Acta* 398 (2003): 107-122.

Pemberton, Henry. "On the Evil Effects Arising From the Use of Dolomitic Lime in Building Brick Walls." *Journal of the Franklin Institute* Vol. 106 Nos. 631- 636, Third Series, Vol. 76 July-Dec. (1878).

Reeder, Richard J.; Markgraf, Steven A. "High-Temperature Crystal Chemistry of Dolomite," *American Mineralogist* 71 (1986): 795-804.

Santhanam, Manu; Cohen, Menashi D.; Olek, Jan. "Effects of gympsum formation on the performance of cement mortars during external sulfate attack," *Cement and Concrete Research* 33 (2003): 325-332.

Santhanam, Manu; Cohen, Menashi D.; Olek, Jan. "Sulfate Attack Research - Whither Now?," *Cement and Concrete Research* 31 (2001): 845-851.

Schork, Jennifer. "Evaluation of the Physical and Chemical Properties of Dolomitic Lime Mortar." Masters Thesis, Columbia University, 2009.

Seeley, Nigel. "Magnesian and Dolomitic Lime Mortars in Building Conservation." *Journal of Architectural Conservation* 2 (July 2000): 21-29.

Seinfeld, John H.; Pandis, Spyros N. *Atmospheric Chemistry and Physics – From Air Pollution to Climate Change, 2nd ed*. New York: John Wiley, 2006. Tate, Mike. Graymont Dolime, Inc. Phone interview, 1 March 2012.

Thomson, Margaret. "Why is Type S Hydrated Lime Special?" National Lime Association Building Lime Group, 2005.

Vicat, Louis-Joseph. *A Practical and Scientific Treatise on Calcareous Mortars and Cements*. London: John Weale, 1837.

Westerman, Tom. Mercer Lime Co. E-mail correspondence, 14 February 2012.

Walsh, John. Highbridge Materials Consulting, Inc. E-mail correspondence, 28 March 2012.

Appendix A:

Glossary of Mineralogical Terms

Mineral Name	Chemical Formula	Description
Aragonite	$CaCO_3$ (orthorhombic)	A mineral found, along with calcite, in chalk, coral rocks, and shells.
Artinite	$Mg_2(CO_3)(OH)_2 \cdot 3H_2O$	A possible hydroxycarbonate product of the carbonation of brucite in dolomitic lime mortar.
Brucite	$Mg(OH)_2$	The hydration product of slaking periclase. One component of dolomitic lime hydrate.
Calcite	$CaCO_3$ (rhombohedral)	The principal mineral in limestone and marble. The product of the carbonation of portlandite.
Dolomite	$Ca,Mg(CO_3)_2$	The principal mineral in dolostone; a secondary mineral in non-dolomitic limestone and marble.
Dypingite	$Mg_5(CO_3)_4(OH)_2 \cdot 5H_2O$	A possible hydroxycarbonate product of the carbonation of brucite in dolomitic lime mortar.
Epsomite	$MgSO_4 \cdot 7H_2O$	A magnesium sulfate salt, which appears as crusts and effloresces on buildings.
Gypsum	$CaSO_4 \cdot 2H_2O$	A salt, which appears as crusts and effloresces on buildings often forming a protective layer.
Hexahydrite	$MgSO_4 \cdot 6H_2O$	A magnesium sulfate salt, the dehydrated form of epsomite.
Hydromagnesite	$Mg_5(CO_3)_4(OH)_2 \cdot 4H_2O$	A possible hydroxycarbonate product of the carbonation of brucite in dolomitic lime mortar.
Magnesite	$MgCO_3$	A possible product of the carbonation of brucite in dolomitic lime mortar.
Muscovite	$KAl_2(AlSi_3O_{10})(OH)_2$	A common micaceous mineral found as a constituent of many rock types, including dolostone.
Nesquehonite	$Mg(HCO_3)(OH) \cdot 2H_2O$	A possible hydroxycarbonate product of the carbonation of brucite in dolomitic lime mortar.

Periclase	MgO	The partial product of burning dolomitic stone, found in raw dolomitic lime.
Portlandite	$Ca(OH)_2$	The hydration product of slaking quicklime. One component of dolomitic lime hydrate.
Quartz	SiO_2	The mineral composing grains of sand.
Quicklime	CaO	The product of burning calcite in high-calcium limestone, found in raw high-calcium lime. The partial product of burning dolomitic stone, found in raw dolomitic lime.

Appendix B:

Sieve Analysis

Sieve Analysis for the preparation of model mortars discussed in Chapter 3

Material: Common Brown Mason's Sand from Extech Building Materials

Sieve No.	Particle Size (mm)	Mass of Sieve (g)	Mass of Sieve + Sand (g)	Sand Retained (g)	Cumulative Sand Passed (g)	Cumulative Sand Retained (%)	Cumulative Sand Passed (%)
4	4.76	515.42	515.60	0.18	249.13	0.07	99.93
6	3.36	508.62	508.62	0.00	249.13	0.07	99.93
8	2.38	434.53	434.84	0.31	248.82	0.20	99.80
16	1.19	342.52	362.89	20.37	228.45	8.37	91.63
30	0.595	323.58	400.81	77.23	151.22	39.34	60.66
50	0.297	284.46	398.08	113.62	37.60	84.92	15.08
100	0.149	262.09	295.88	33.79	3.81	98.47	1.53
120	0.125	345.99	347.38	1.39	2.42	99.03	0.97
140	0.105	350.77	351.71	0.94	1.48	99.41	0.59
200	0.074	349.95	350.55	0.60	0.88	99.65	0.35
> 200	<0.074	383.66	383.92	0.26	0.62	99.75	0.25

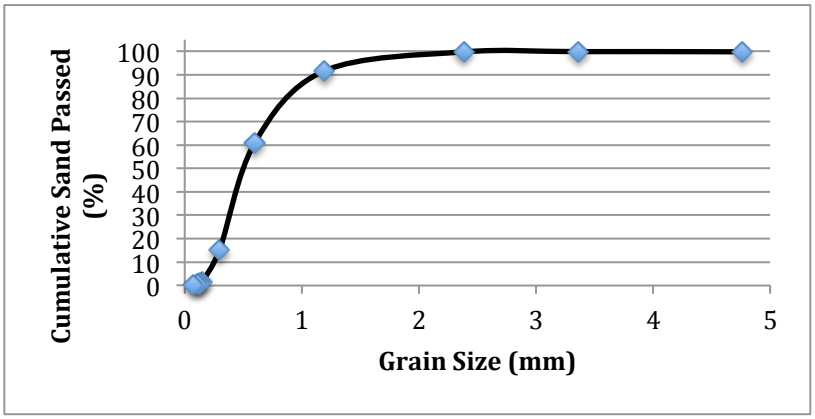

Appendix C:

X-Ray Diffractograms

Pure dolomite crystal

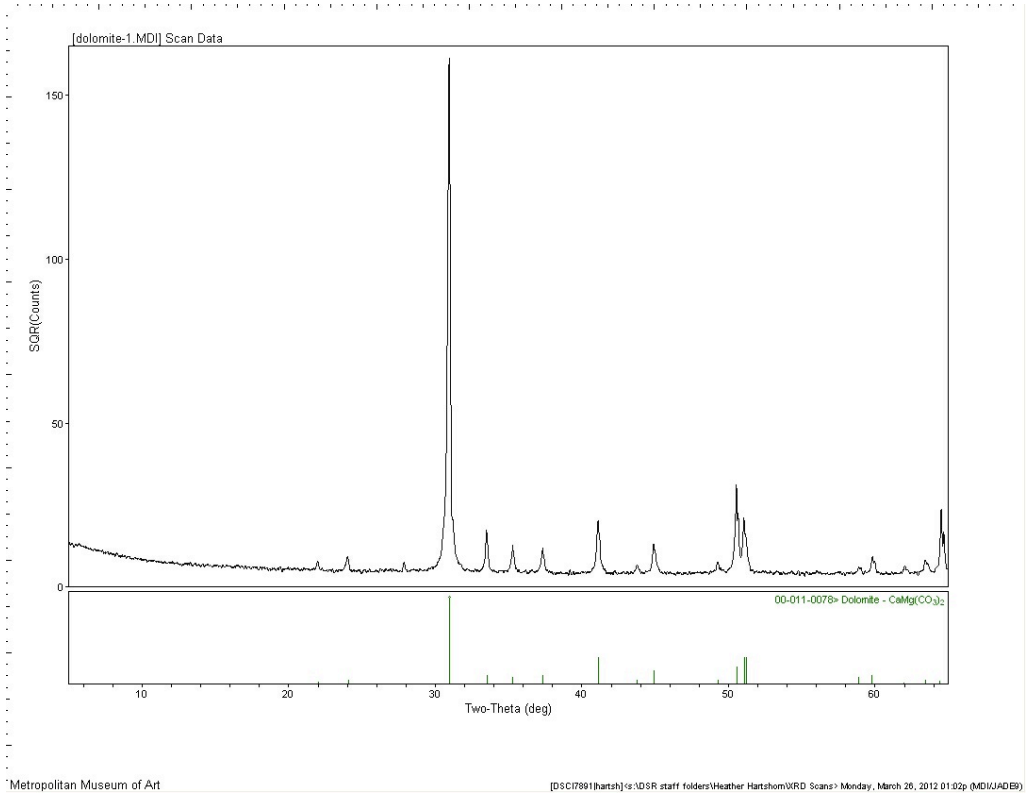

X-ray diffractogram of uncalcined dolomite crystal.

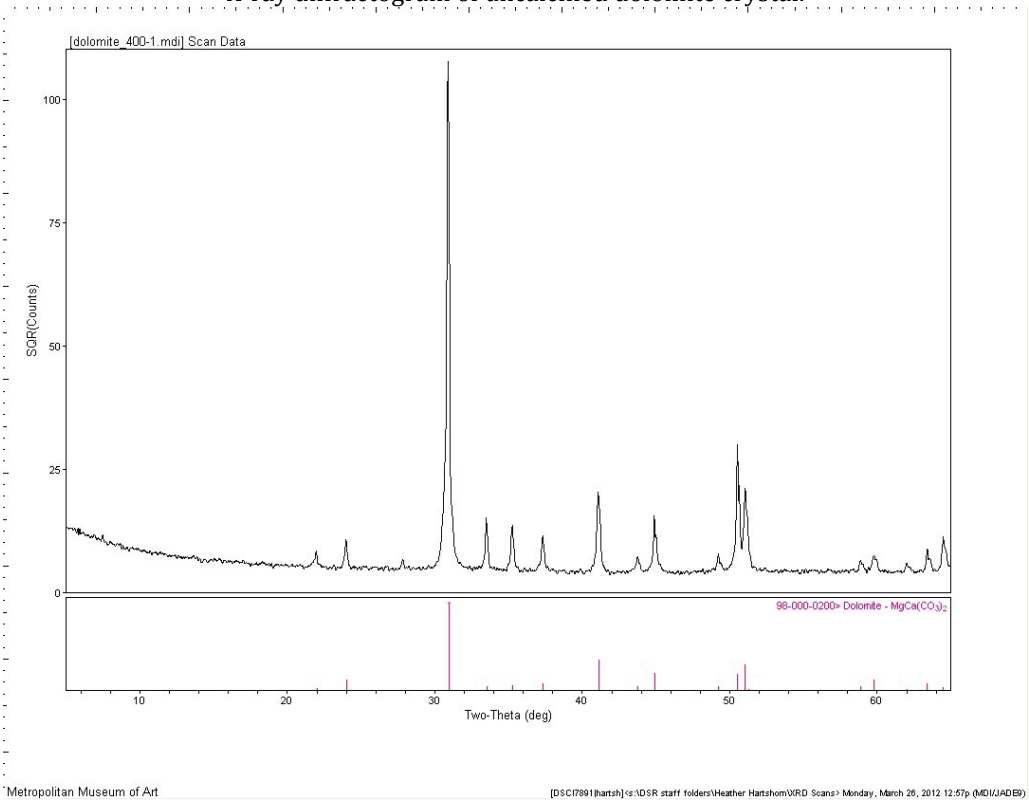

X-ray diffractogram of dolomite crystal calcined at 400°C.

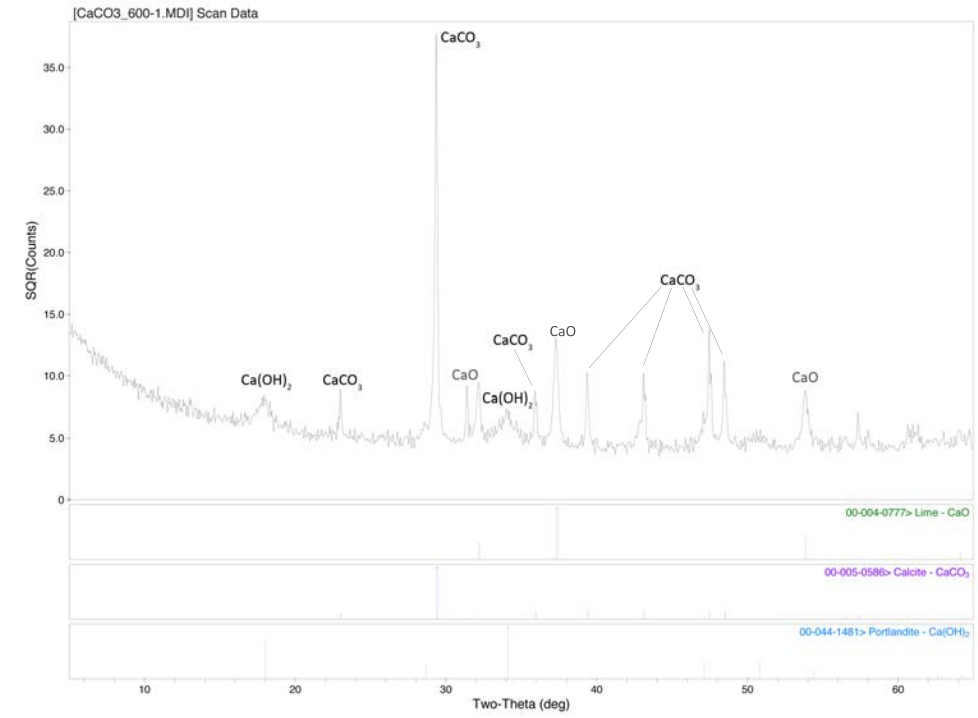

X-ray diffractogram of dolomite crystal calcined at 600°C.

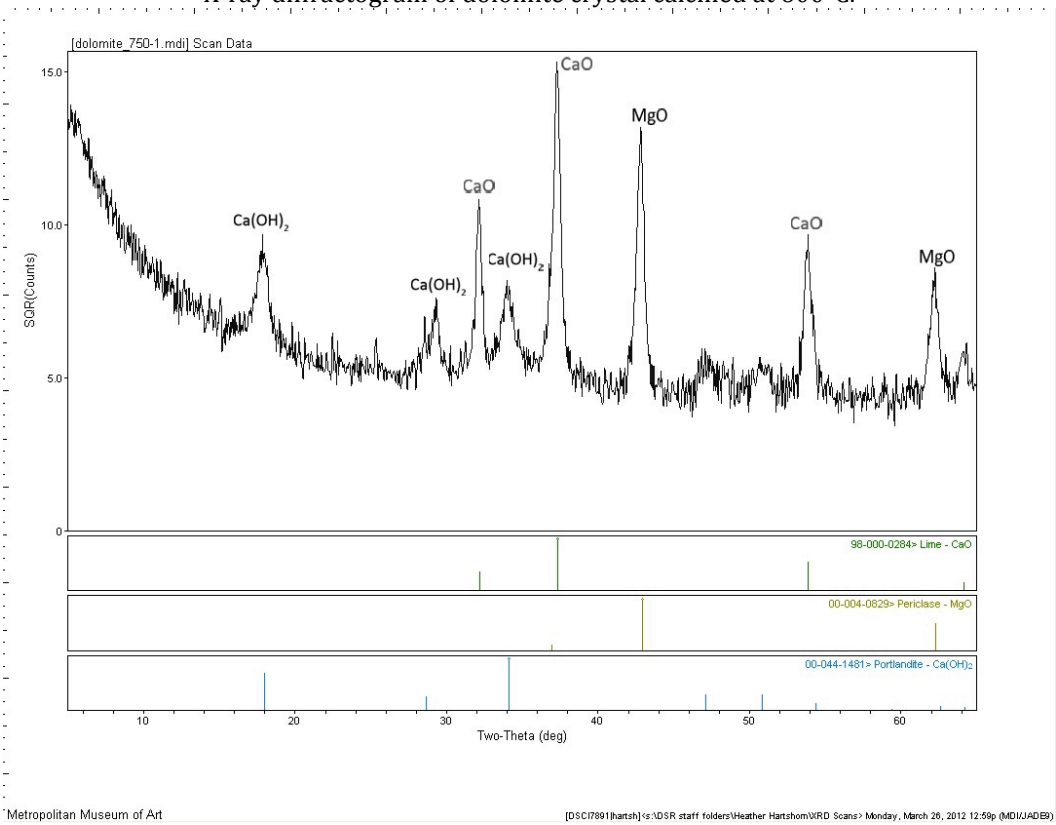

X-ray diffractogram of dolomite crystal calcined at 750°C.

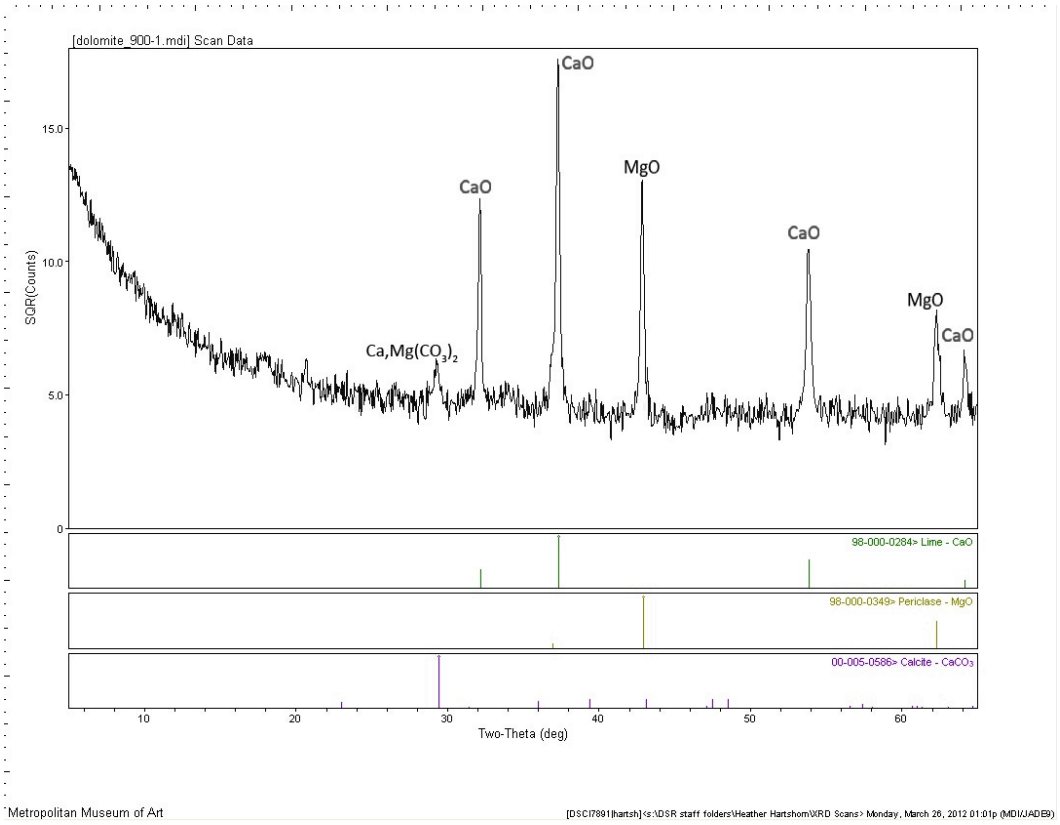

X-ray diffractogram of dolomite crystal calcined at 900°C.

Kasota Stone

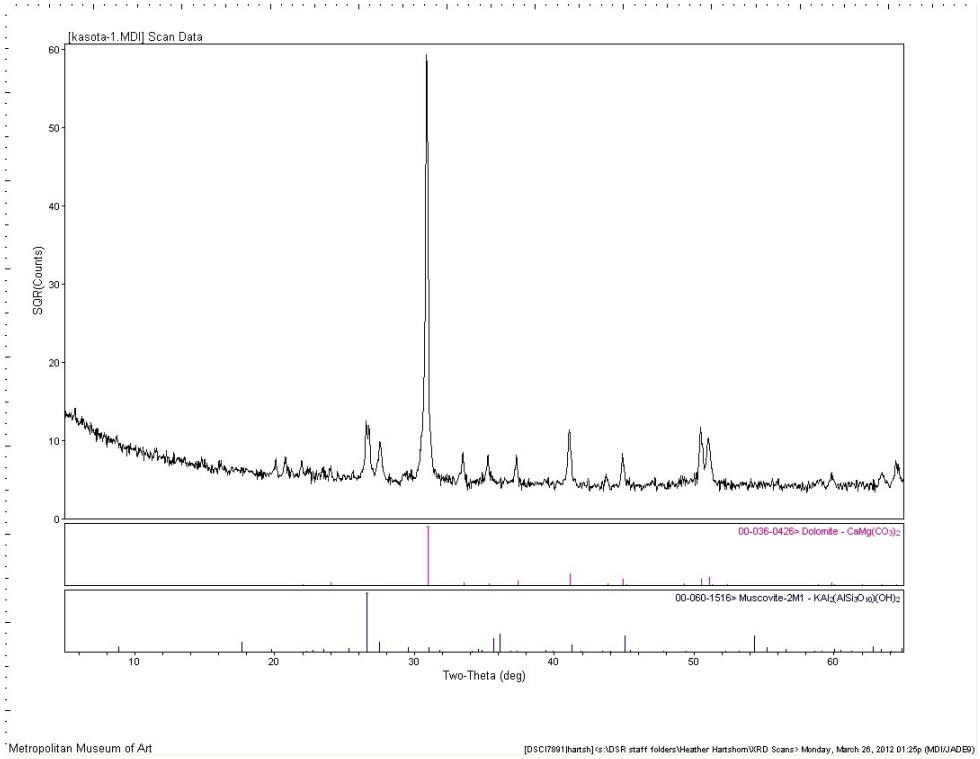

X-ray diffractogram of uncalcined Kasota stone.

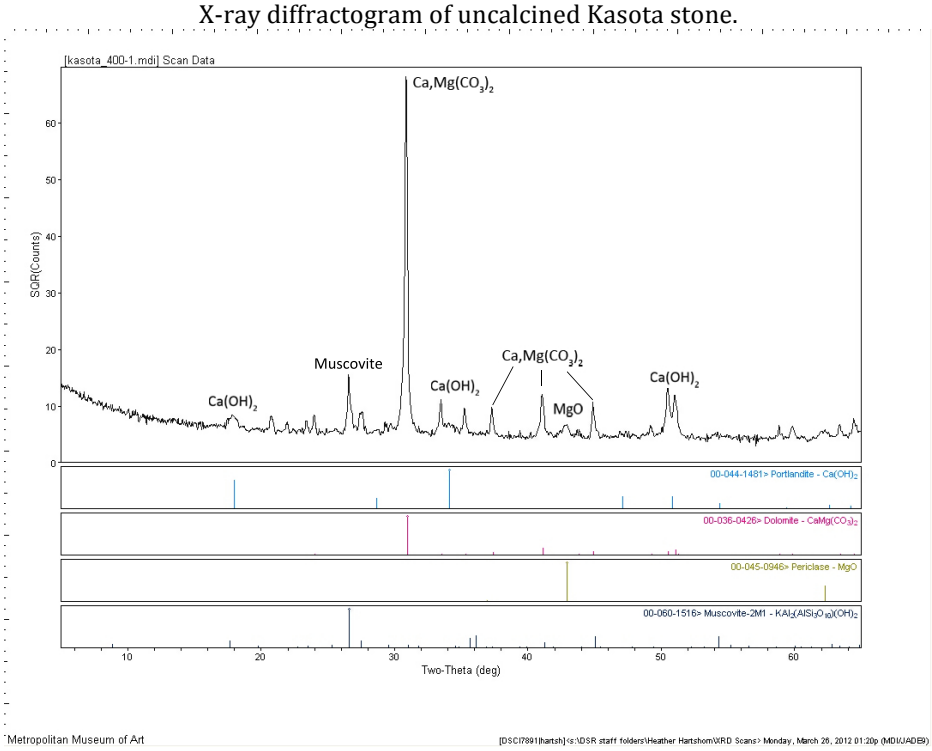

X-ray diffractogram of Kasota stone calcined at 400°C.

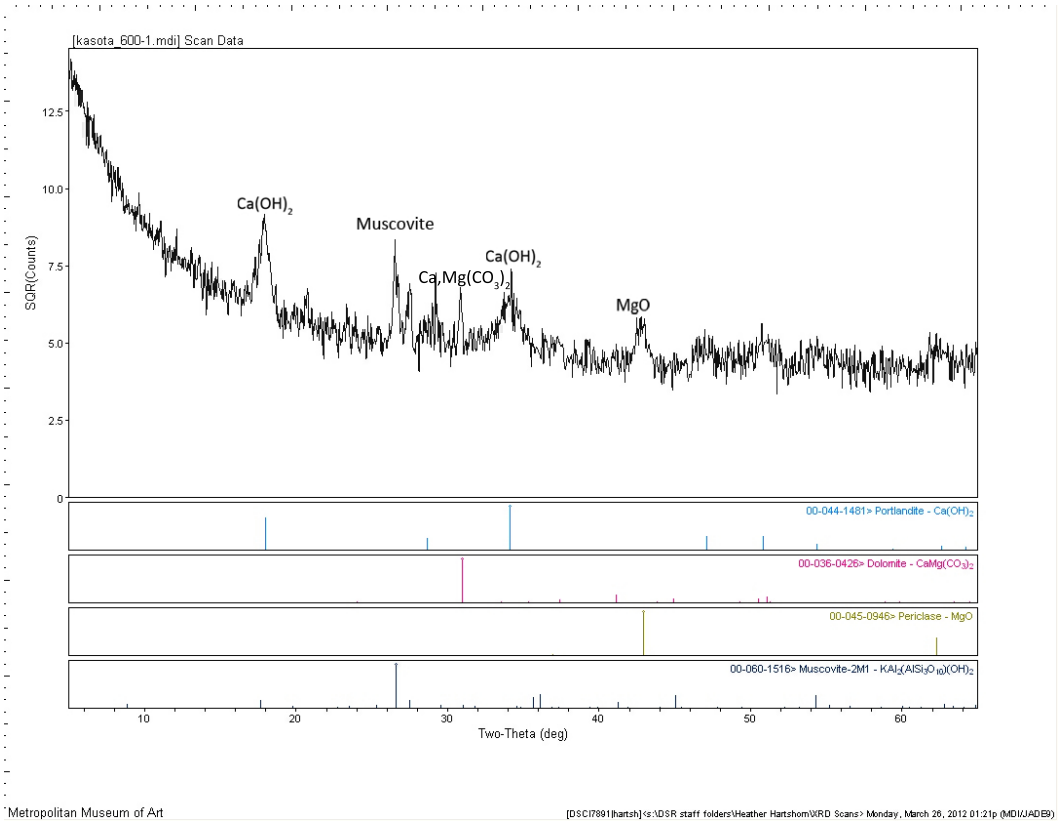

X-ray diffractogram of Kasota stone calcined at 600°C.

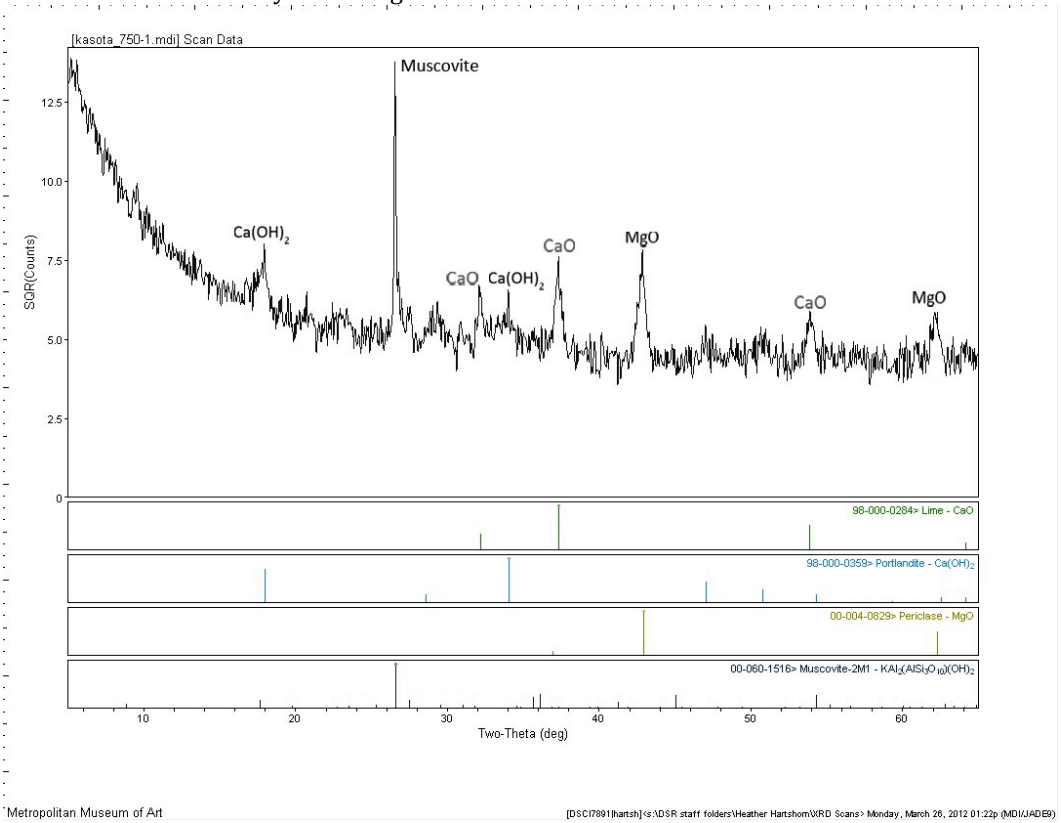

X-ray diffractogram of Kasota stone calcined at 750°C.

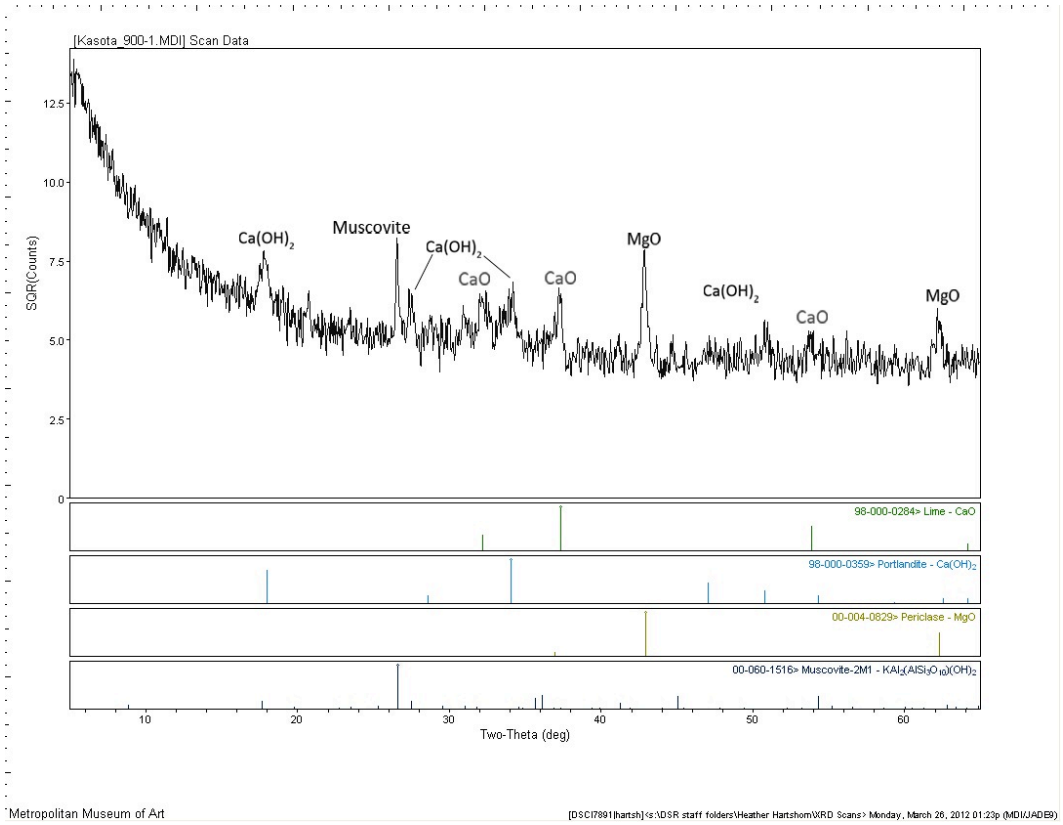

X-ray diffractogram of Kasota stone calcined at 900°C.

Tuckahoe marble

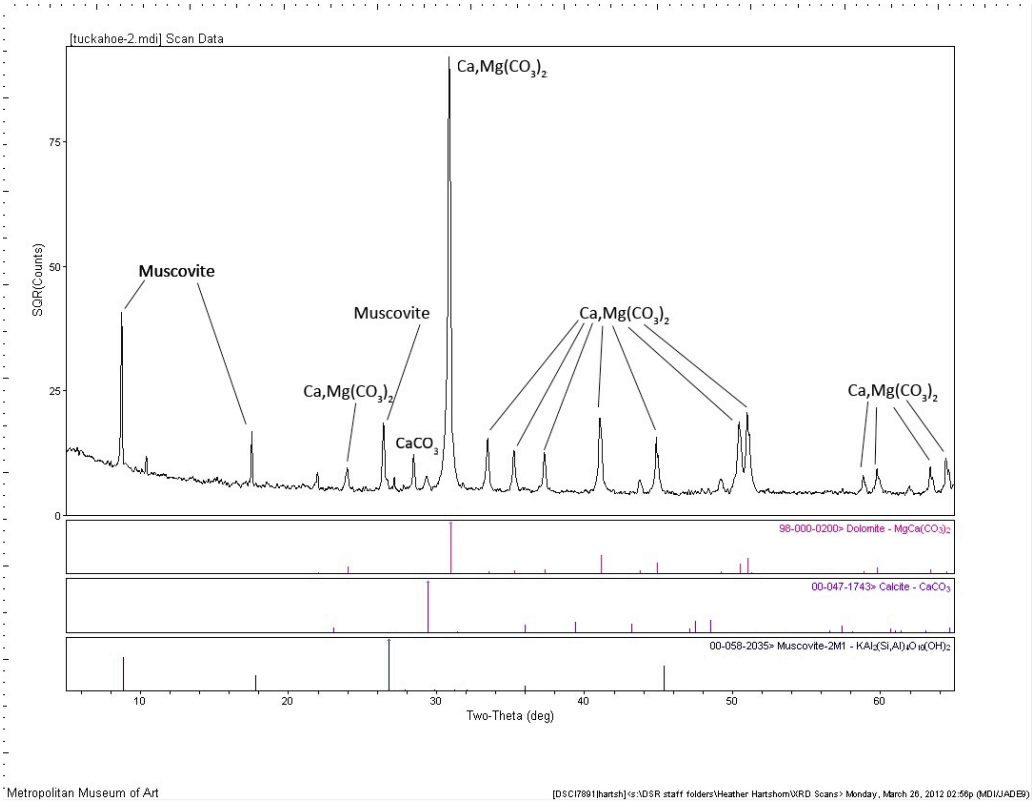

X-ray diffractogram of uncalcined Tuckahoe marble.

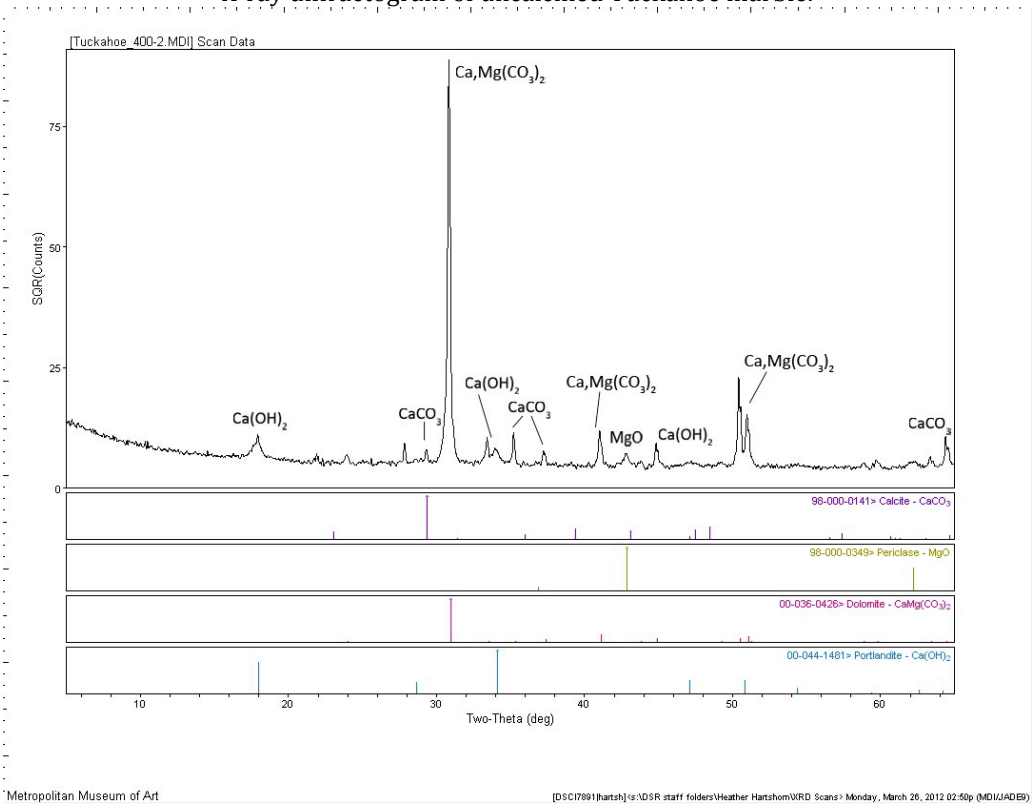

X-ray diffractogram of Tuckahoe marble calcined at 400°C.

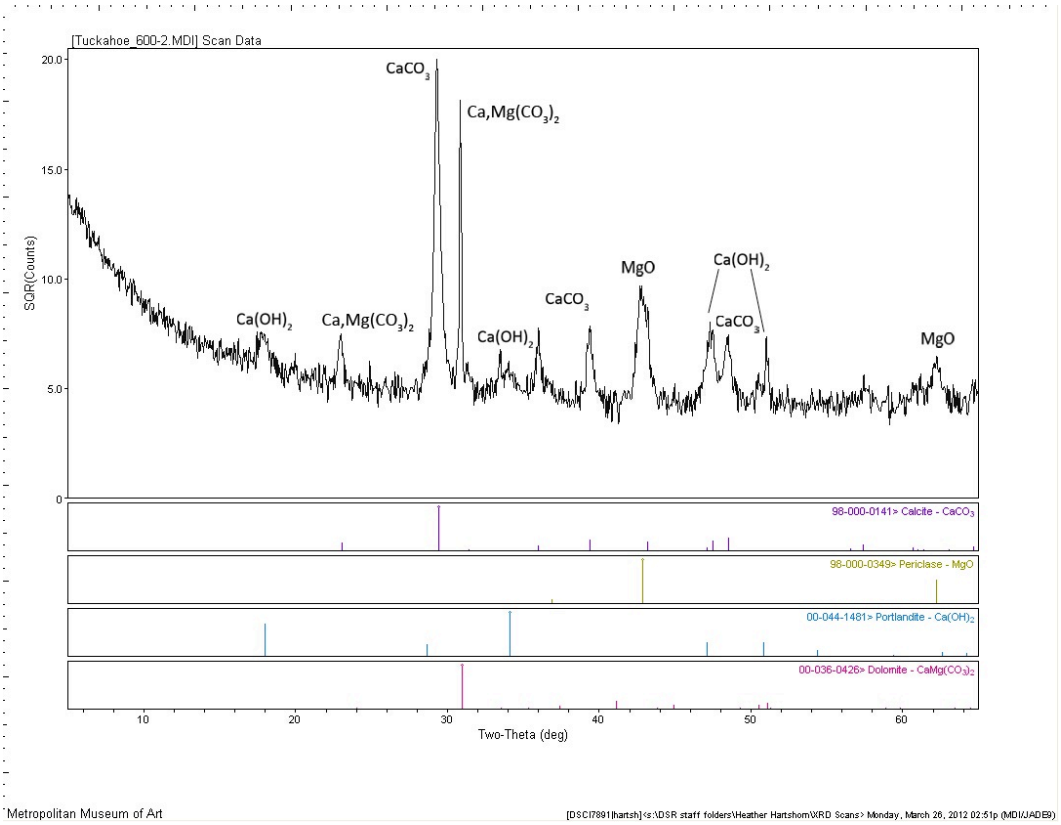

X-ray diffractogram of Tuckahoe marble calcined at 600°C.

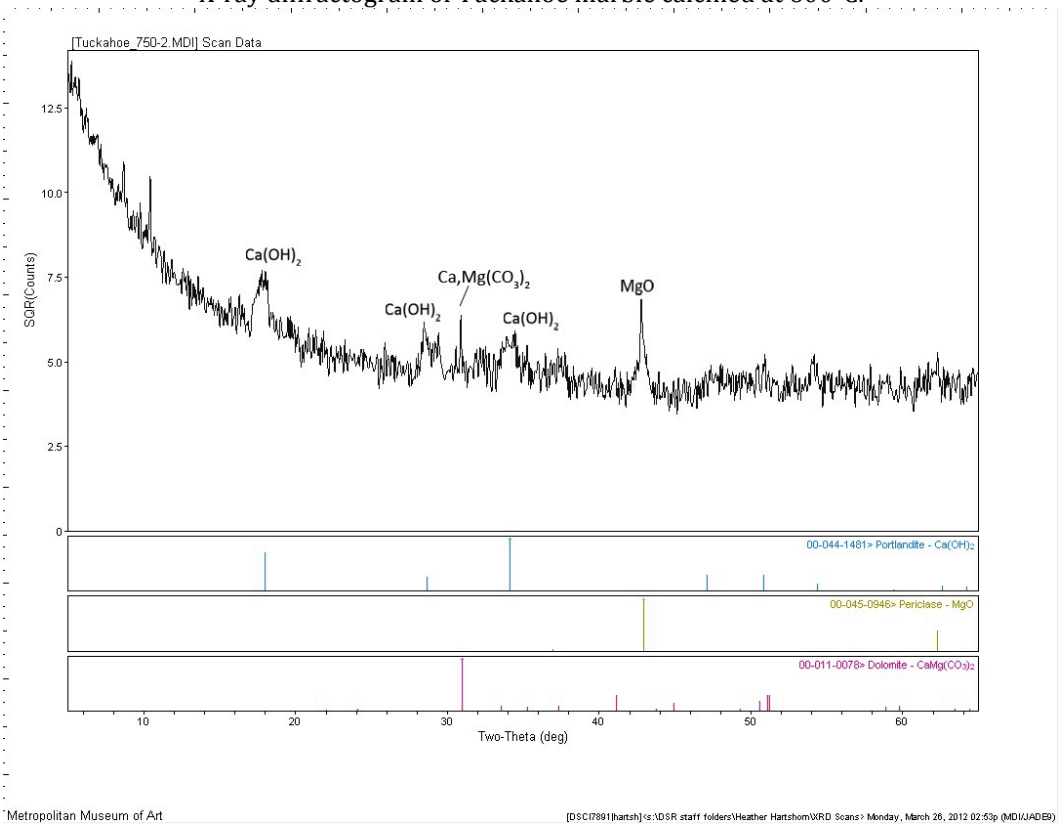

X-ray diffractogram of Tuckahoe marble calcined at 750°C.

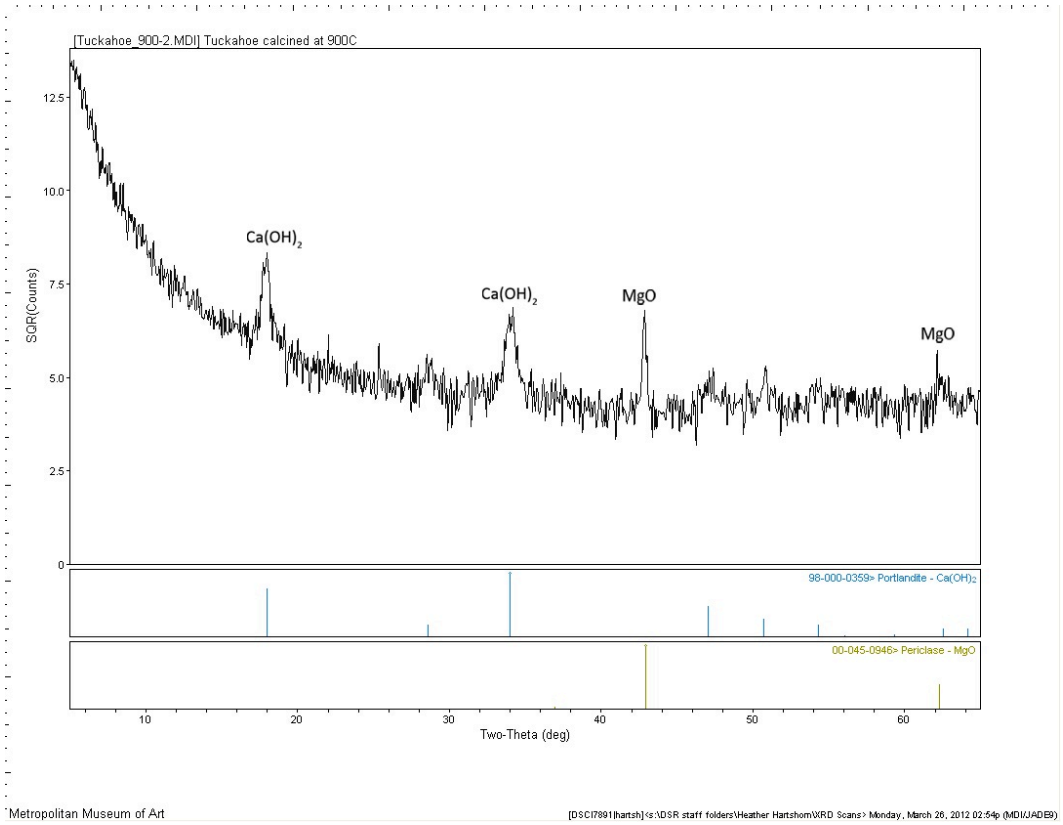

X-ray diffractogram of Tuckahoe marble calcined at 900°C.

Chemical Grade Calcite

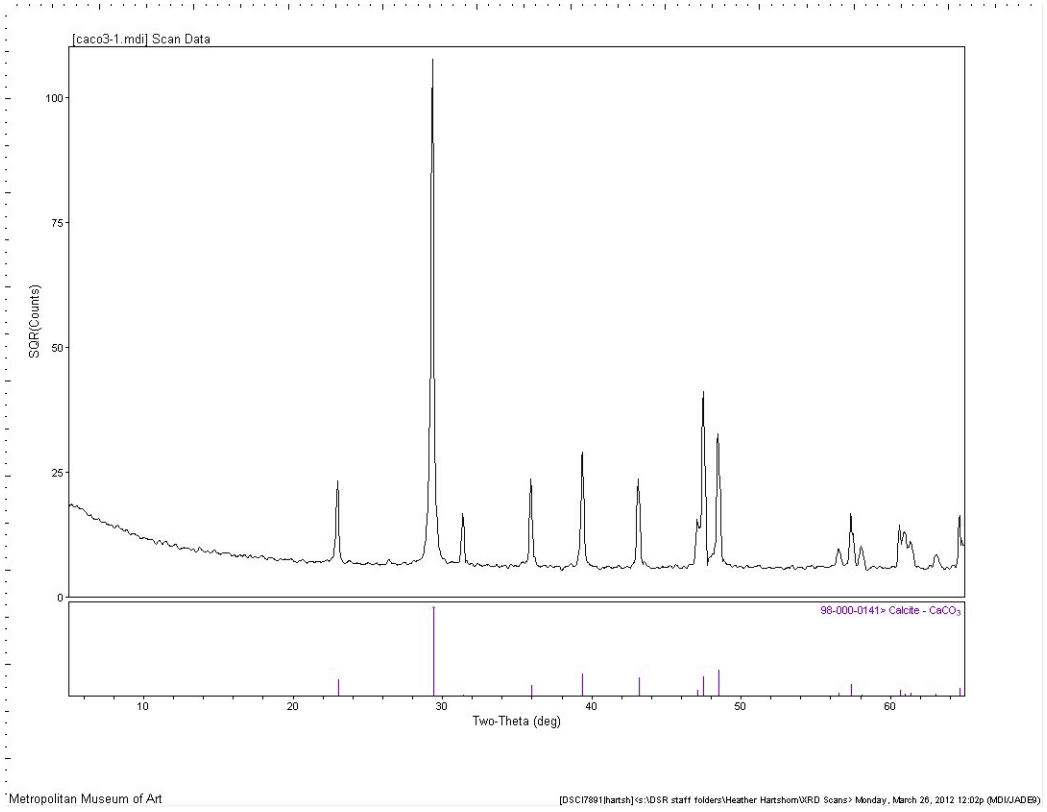

X-ray diffractogram of uncalcined chemical grade calcite.

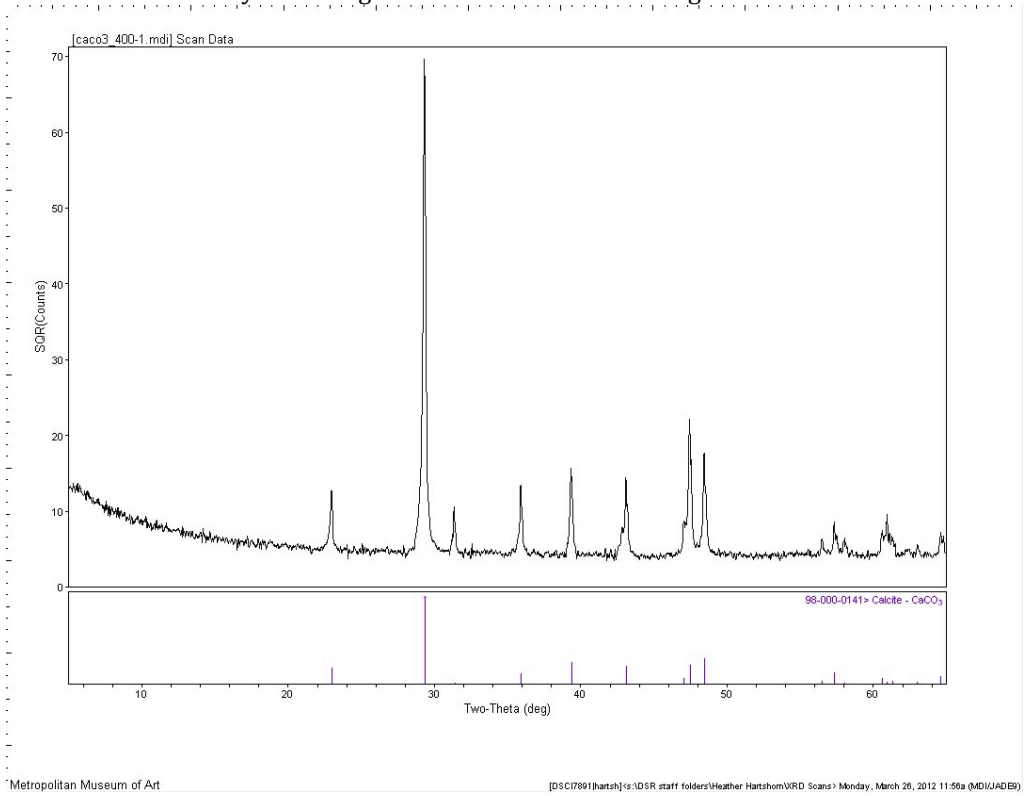

X-ray diffractogram of chemical grade calcite calcined at 400°C.

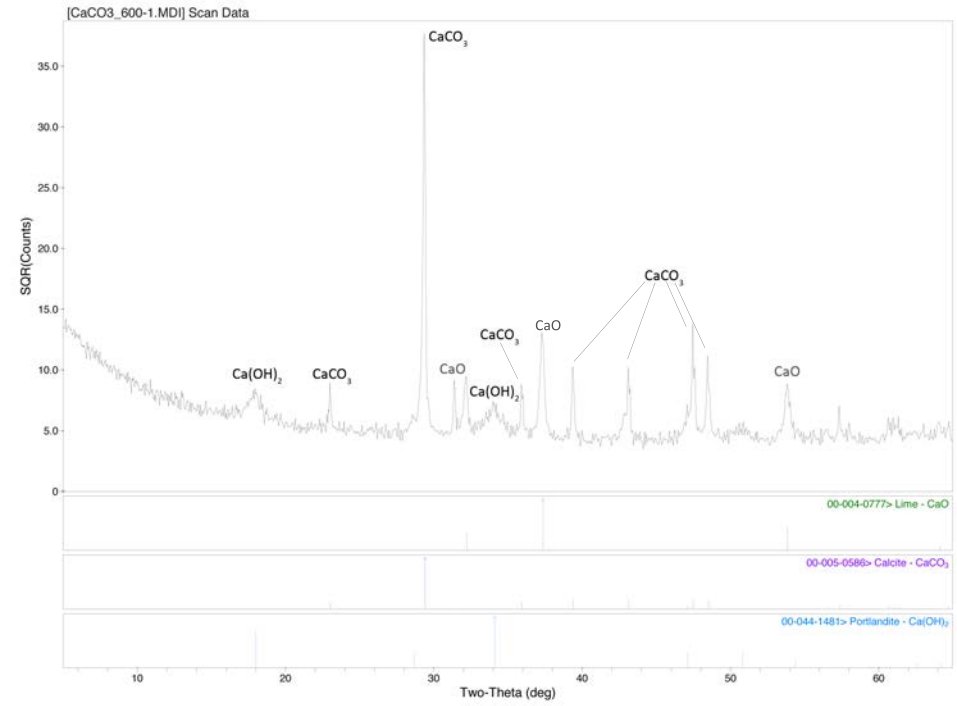

X-ray diffractogram of chemical grade calcite calcined at 600°C.

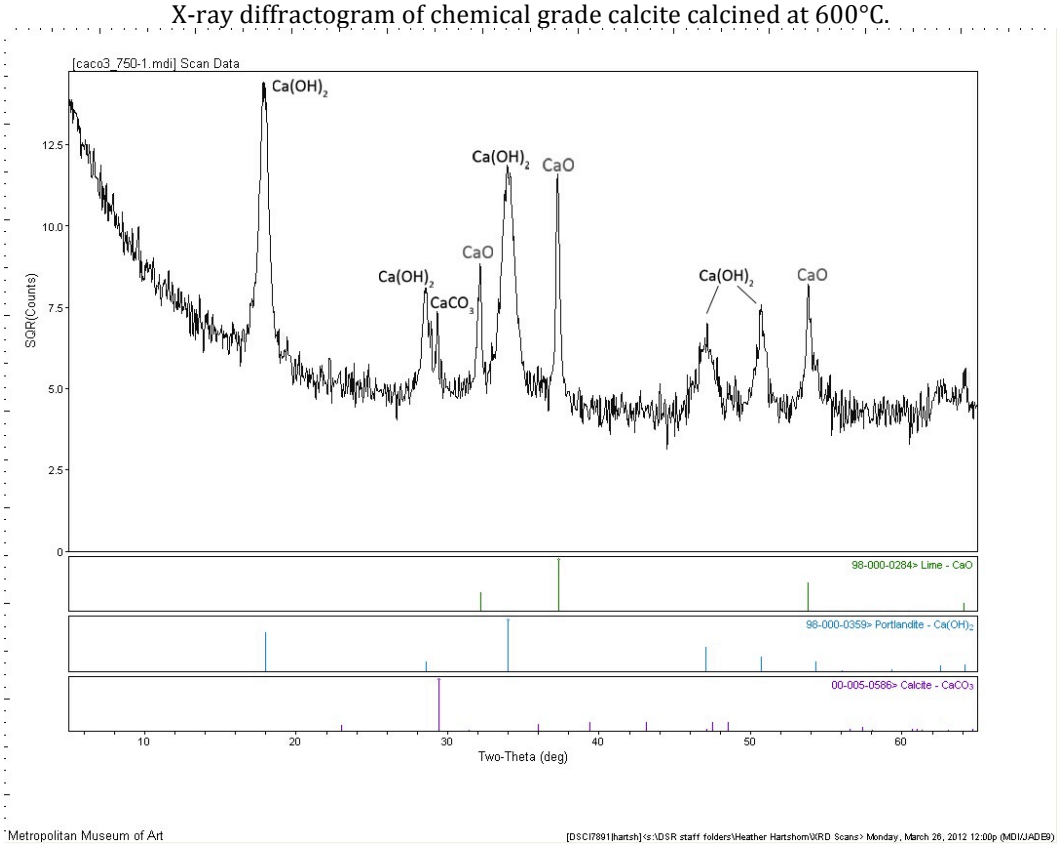

X-ray diffractogram of chemical grade calcite calcined at 750°C.

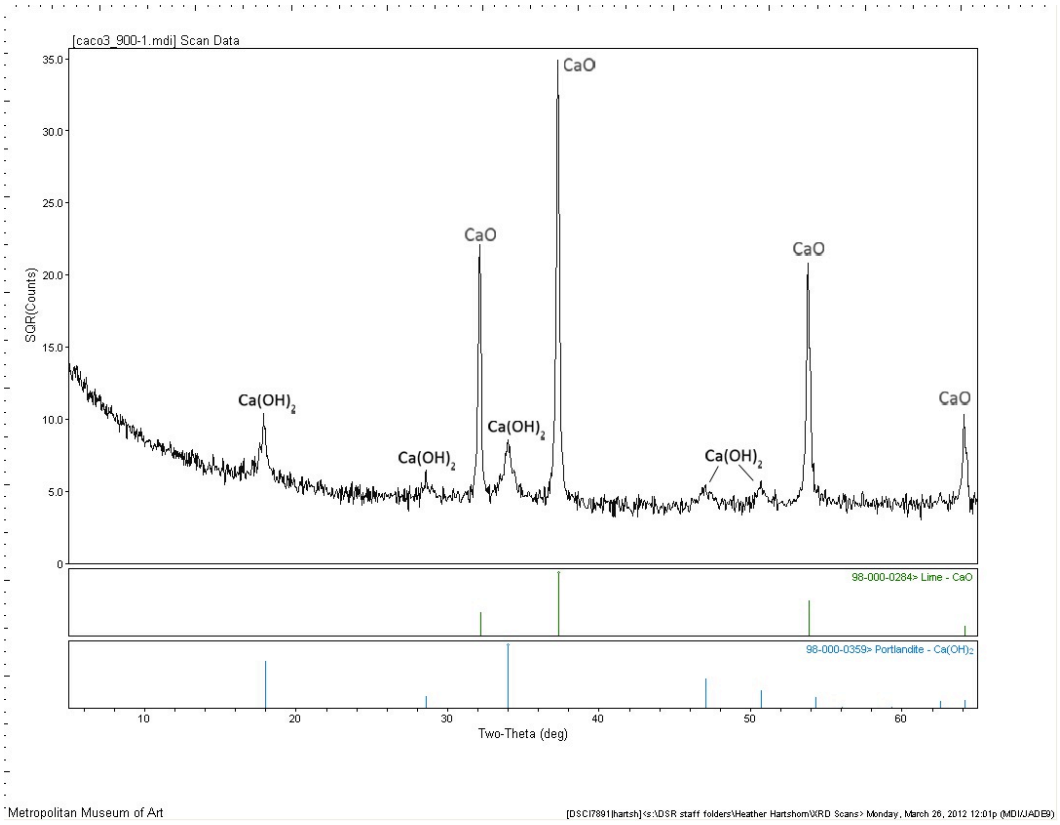

X-ray diffractogram of chemical grade calcite calcined at 900°C.

Chemical Grade Magnesite

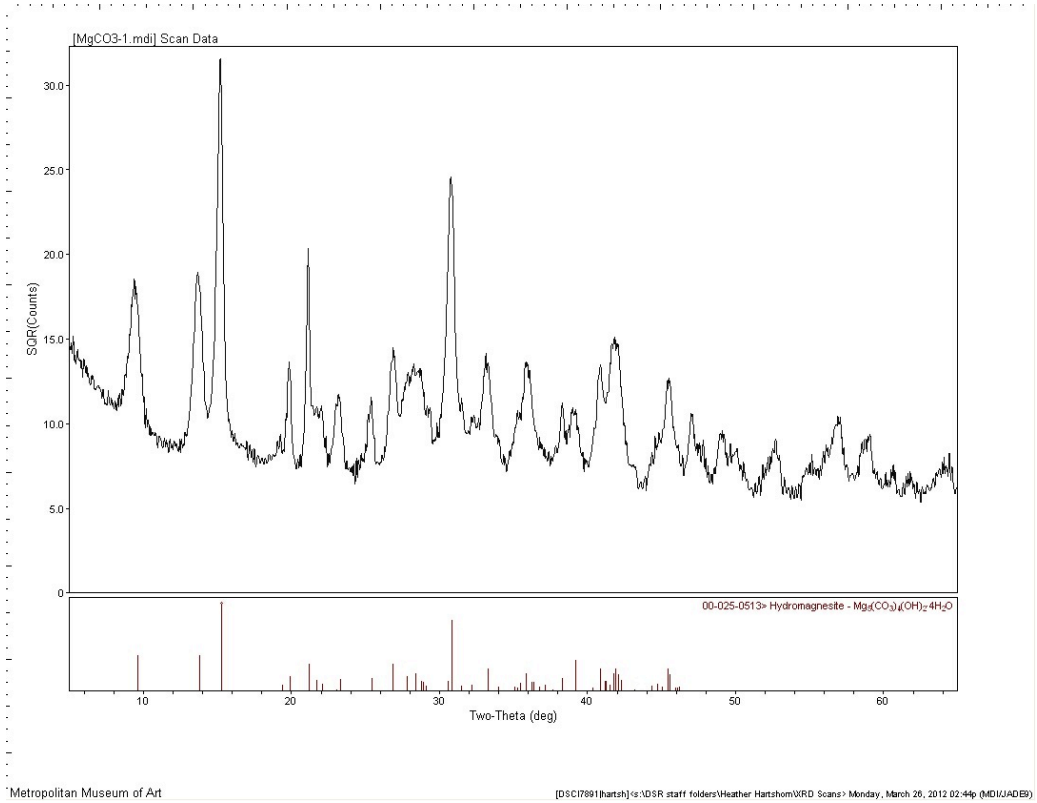

X-ray diffractogram of uncalcined chemical grade magnesite.

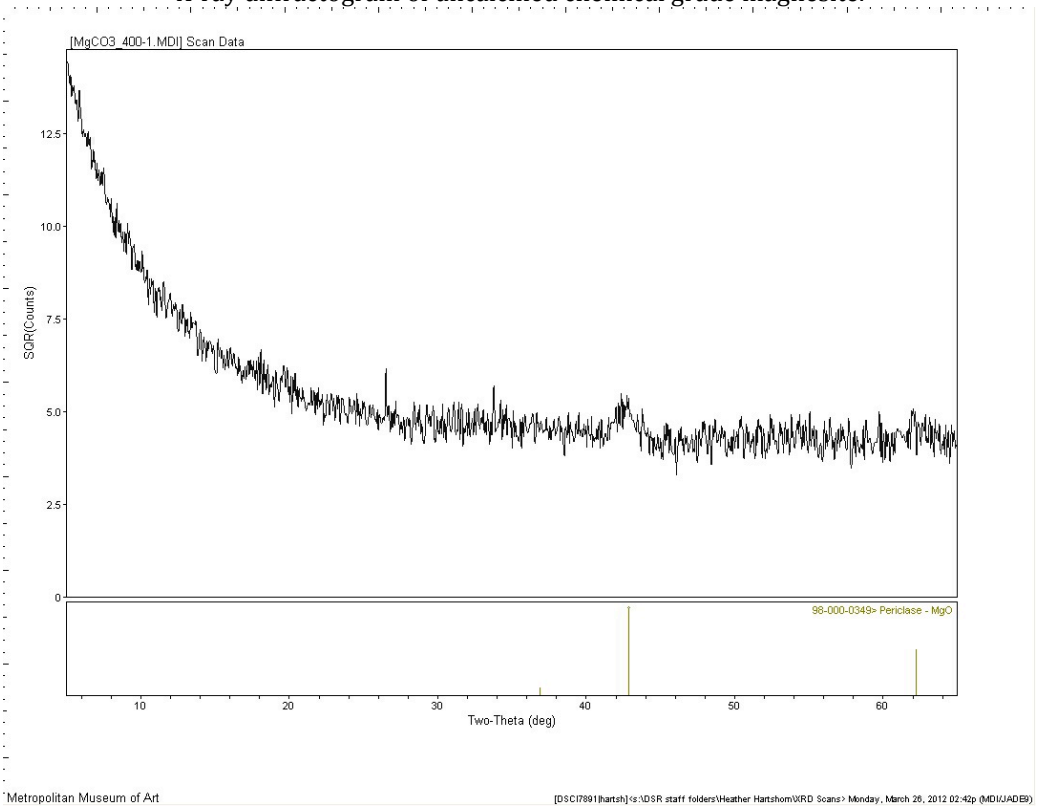

X-ray diffractogram of chemical grade magnesite calcined at 400°C.

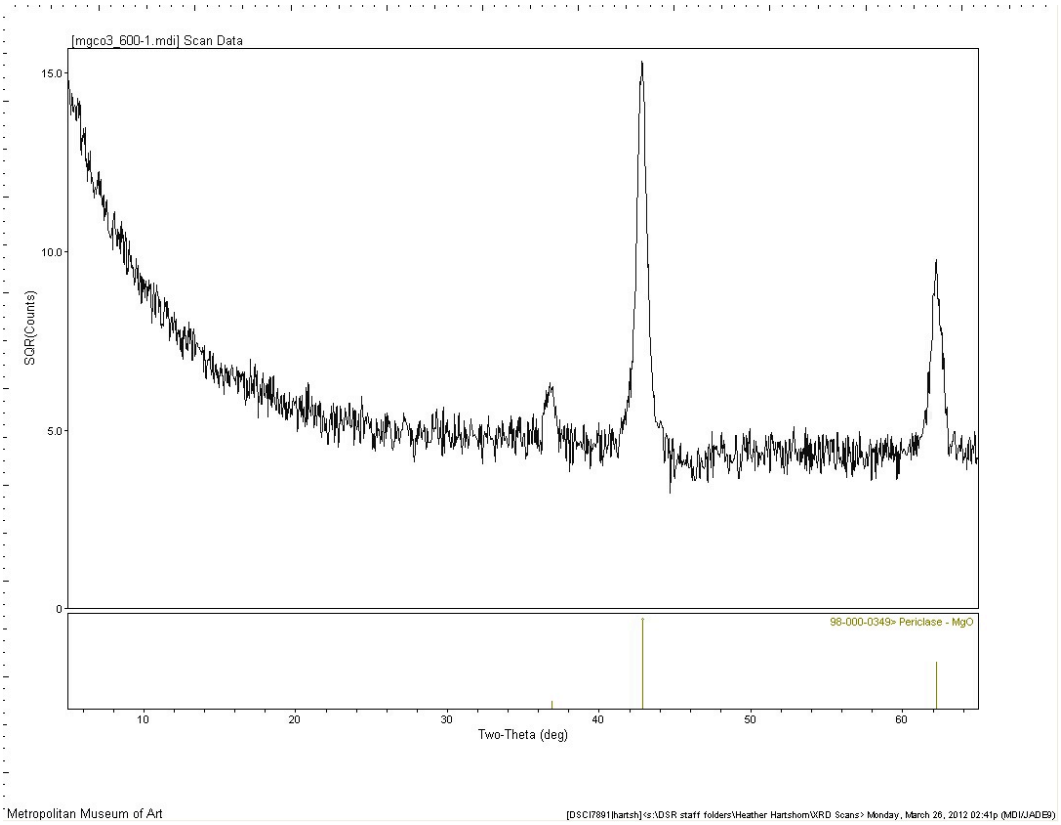

X-ray diffractogram of chemical grade magnesite calcined at 600°C.

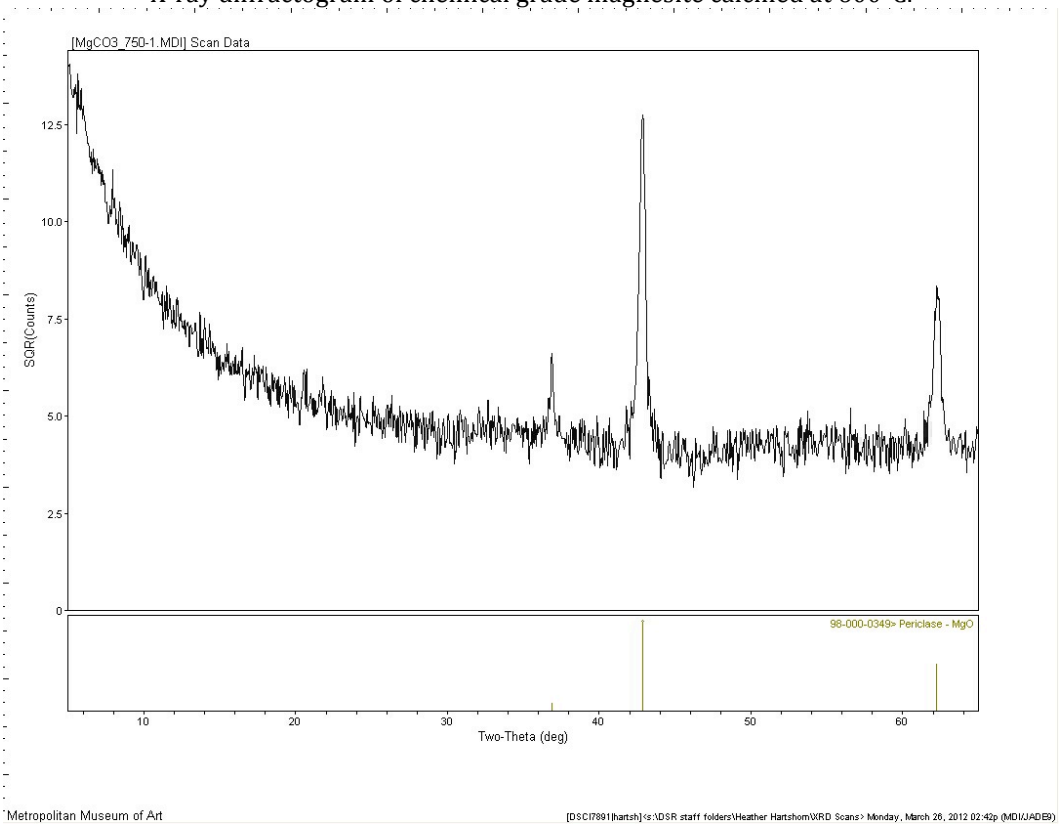

X-ray diffractogram of chemical grade magnesite calcined at 750°C.

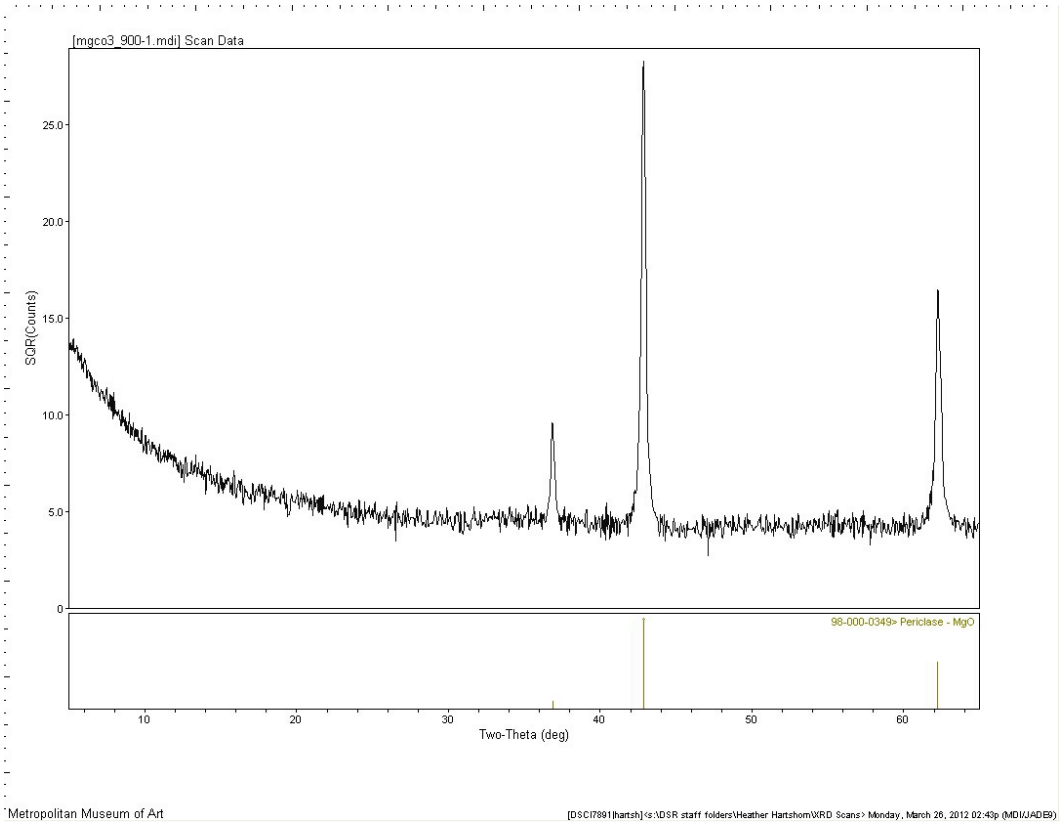

X-ray diffractogram of chemical grade magnesite calcined at 900°C.

Chemical Grade Magnesite/Calcite in a 25/75 Ratio

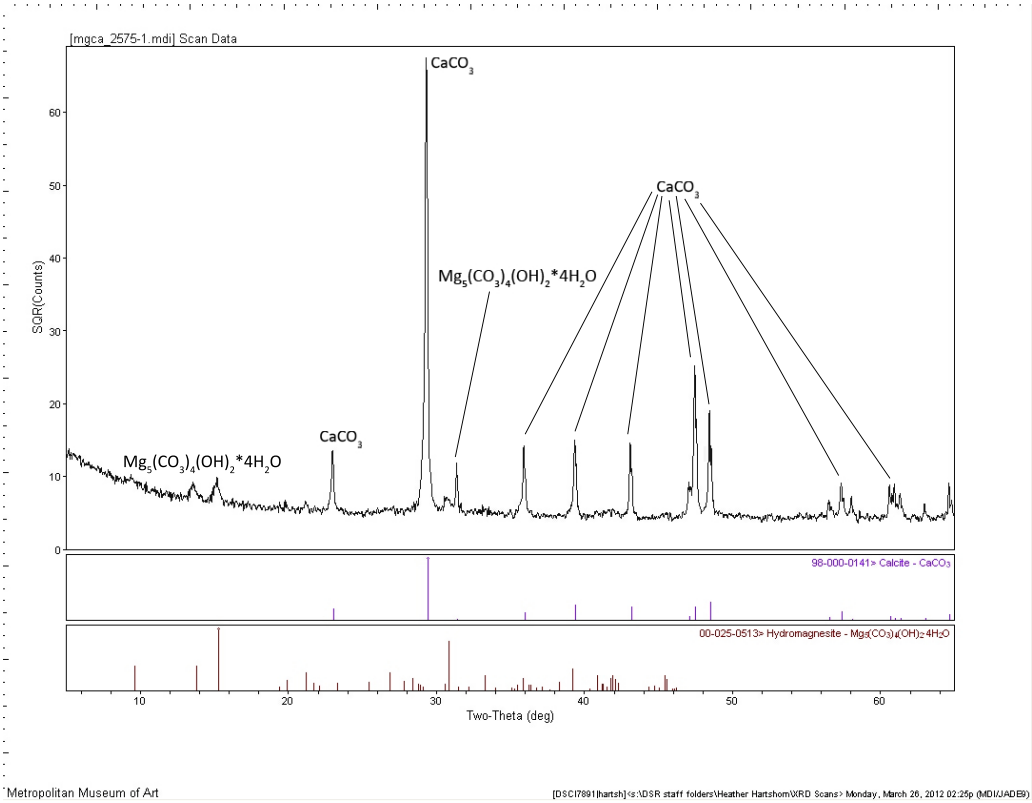

X-ray diffractogram of uncalcined 25/75 chemical grade calcite/magnesite.

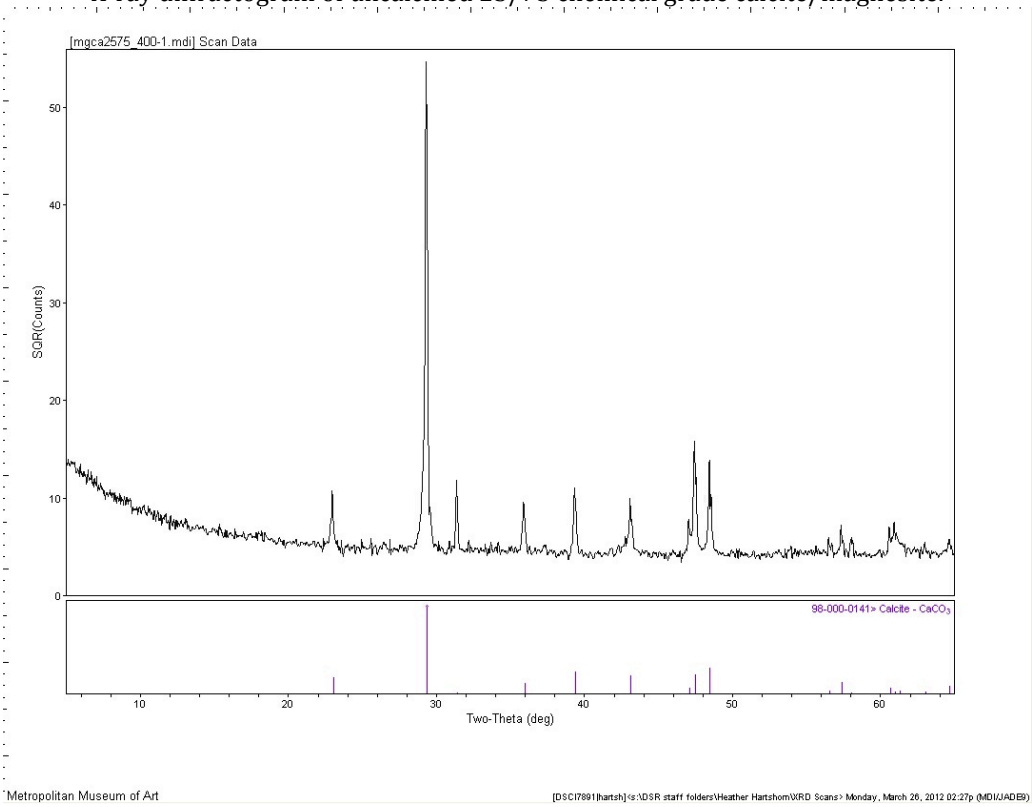

X-ray diffractogram of 25/75 chemical grade calcite/magnesite calcined at 400°C.

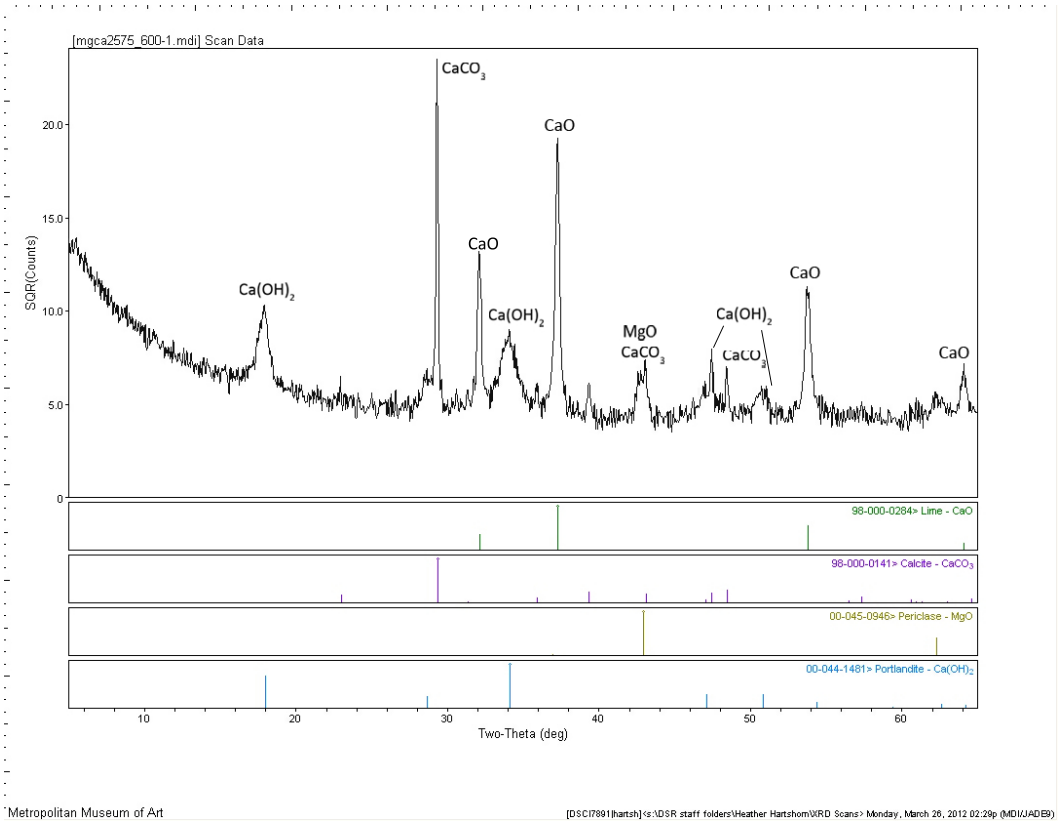

X-ray diffractogram of 25/75 chemical grade calcite/magnesite calcined at 600°C.

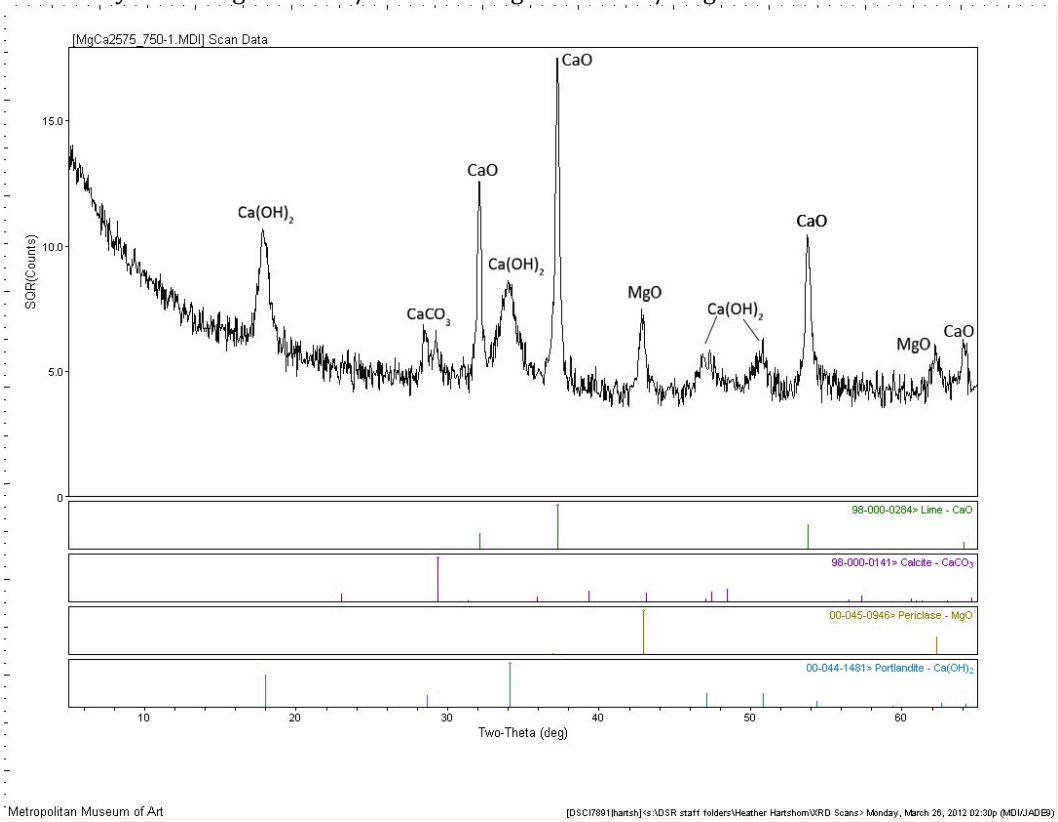

X-ray diffractogram of 25/75 chemical grade calcite/magnesite calcined at 750°C.

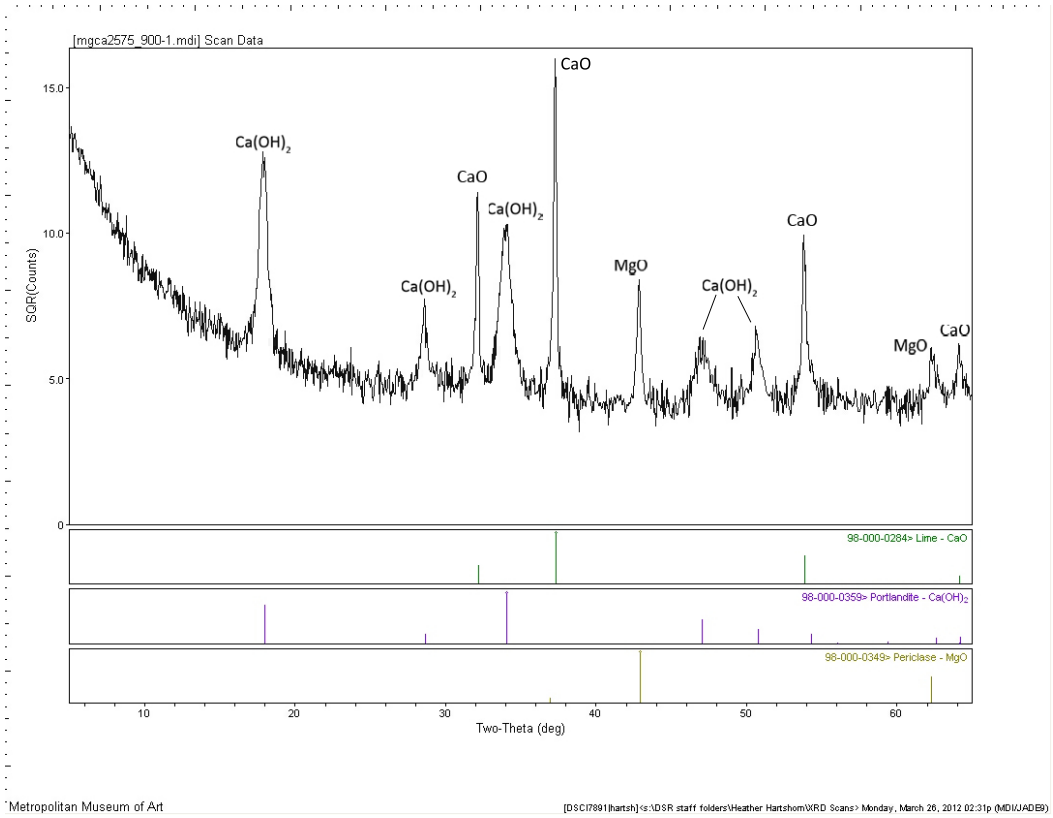

X-ray diffractogram of 25/75 chemical grade calcite/magnesite calcined at 900°C.

Chemical Grade Magnesite/Calcite in a 50/50 Ratio

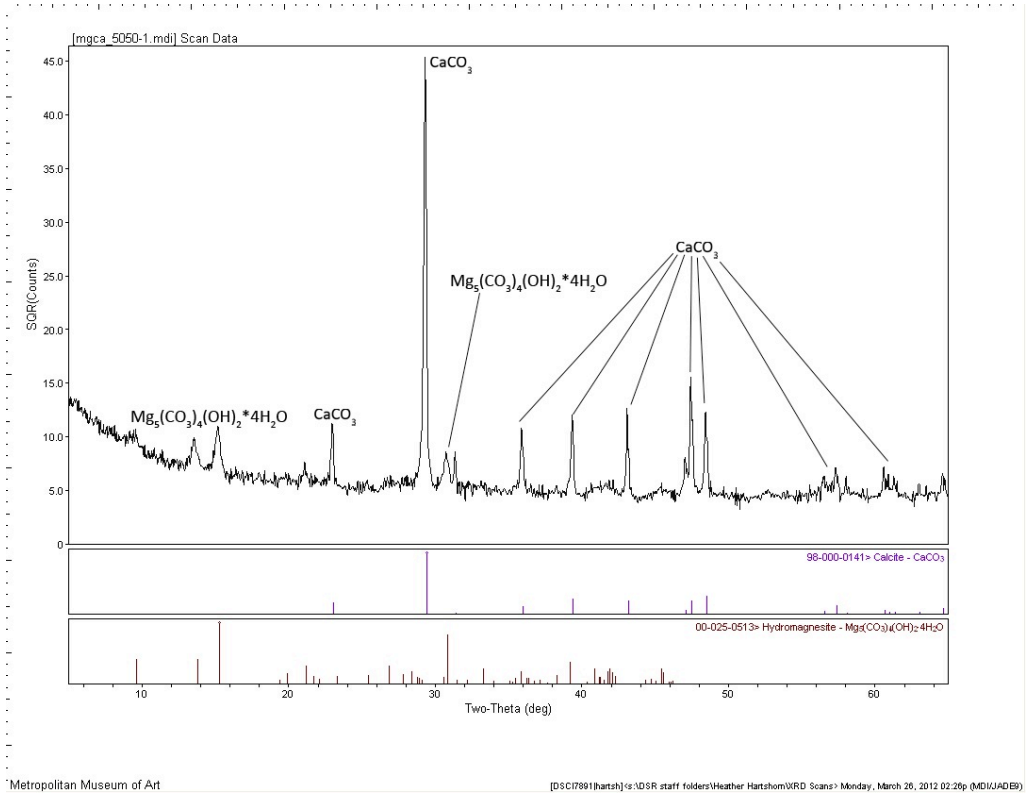

X-ray diffractogram of uncalcined 50/50 chemical grade calcite/magnesite.

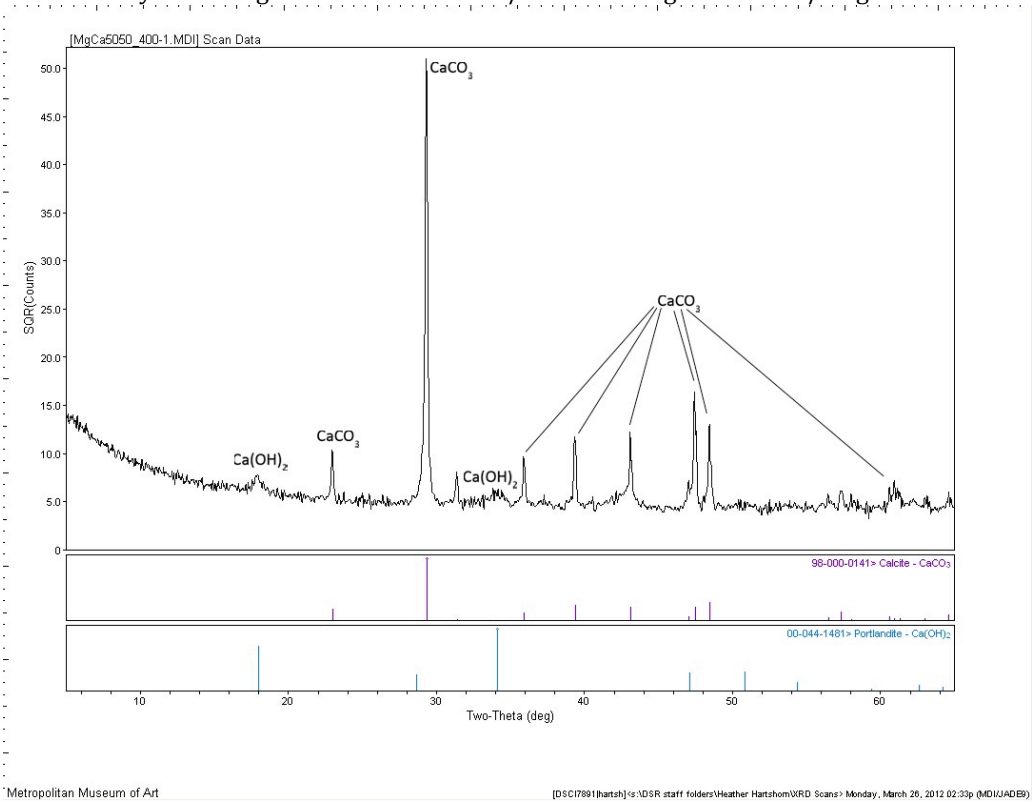

X-ray diffractogram of 50/50 chemical grade calcite/magnesite calcined at 400°C.

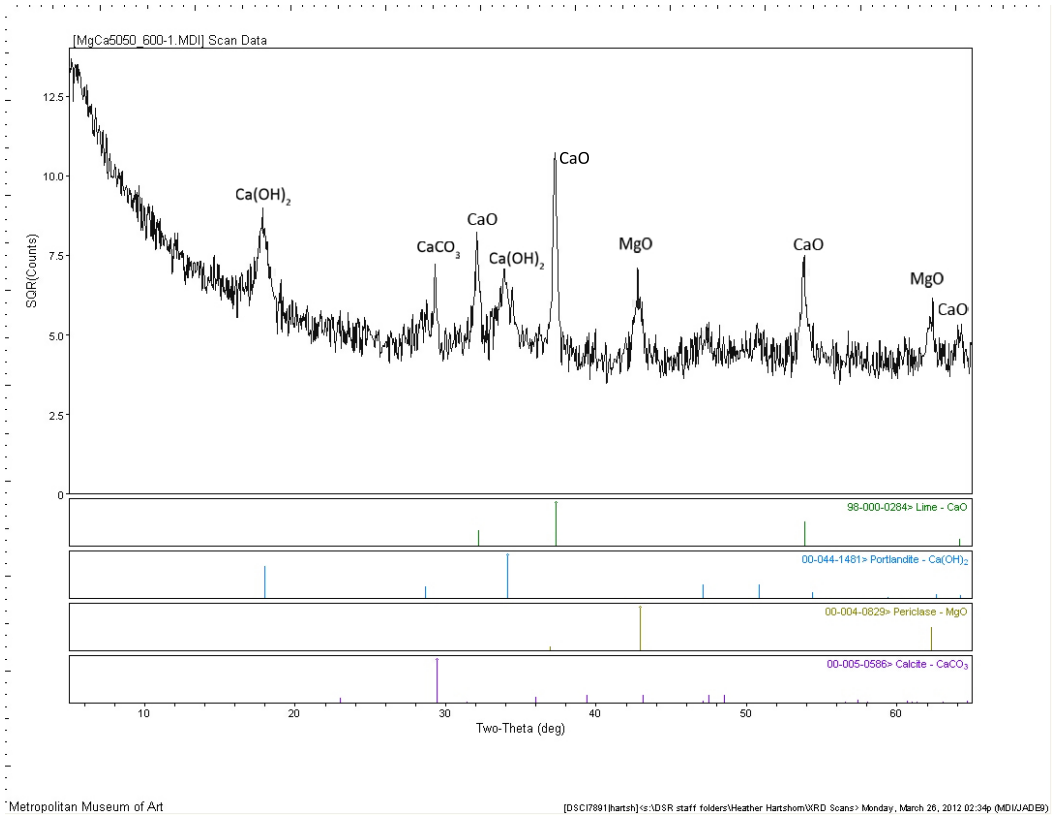

X-ray diffractogram of 50/50 chemical grade calcite/magnesite calcined at 600°C.

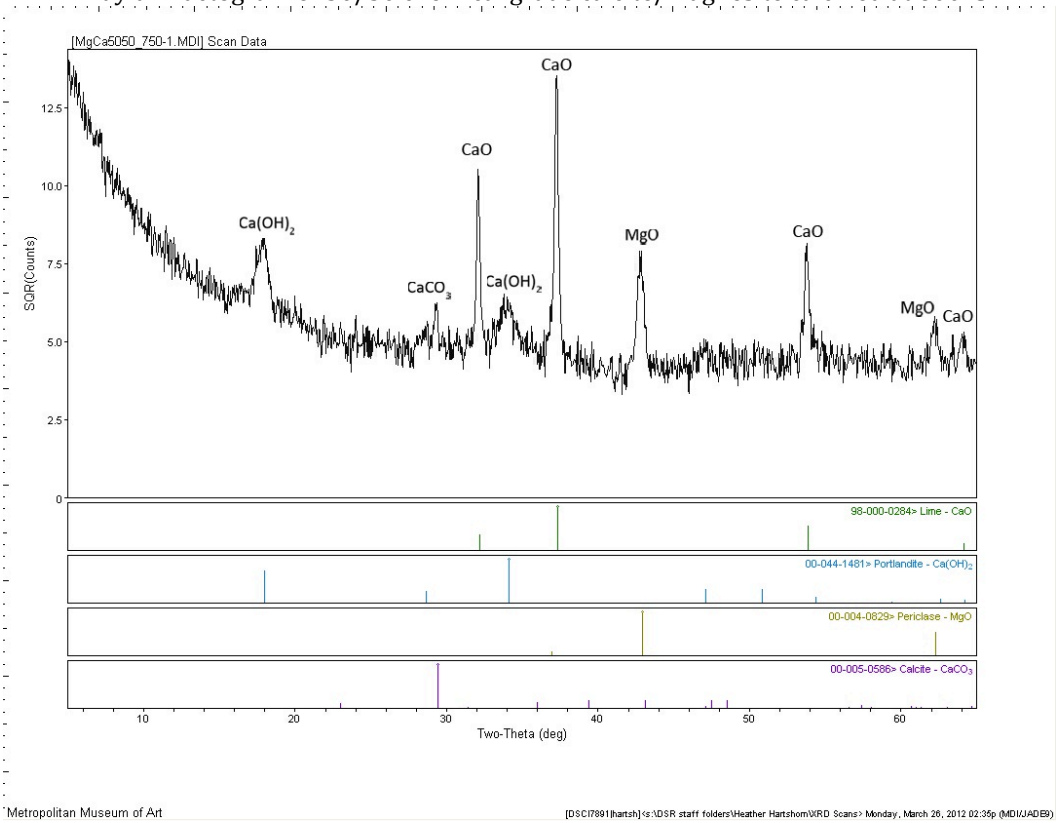

X-ray diffractogram of 50/50 chemical grade calcite/magnesite calcined at 750°C.

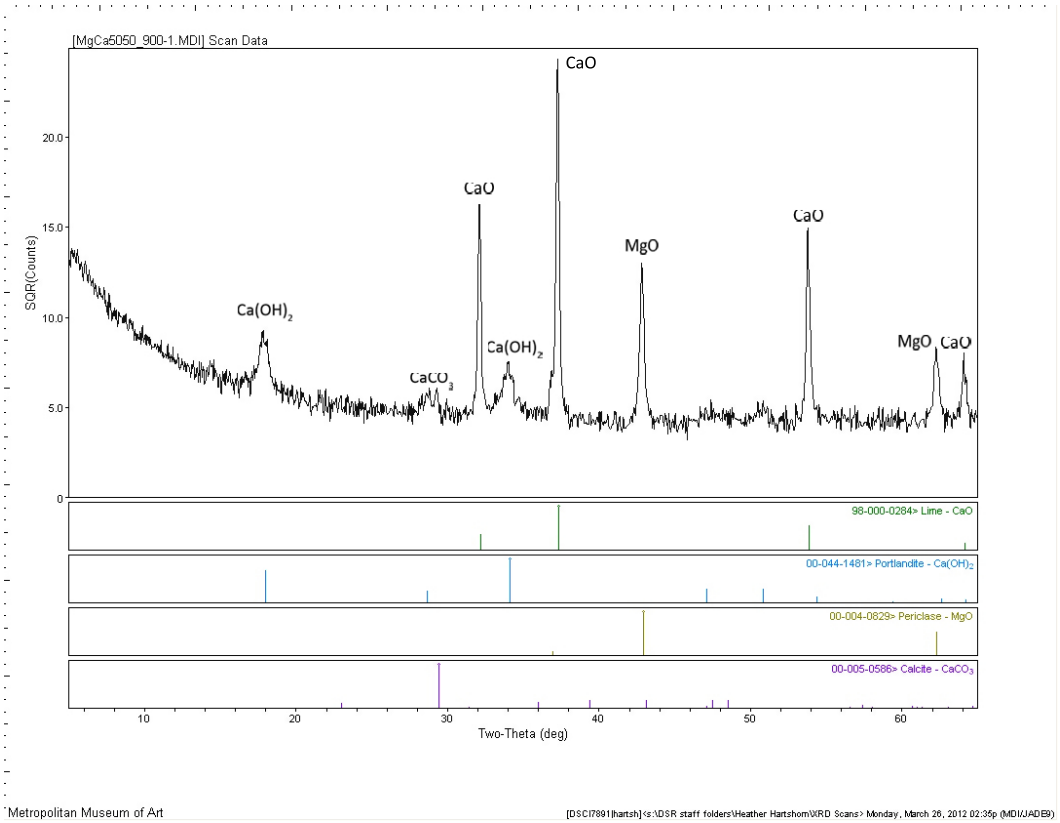

X-ray diffractogram of 50/50 chemical grade calcite/magnesite calcined at 900°C.

Chemical Grade Magnesite/Calcite in a 75/25 Ratio

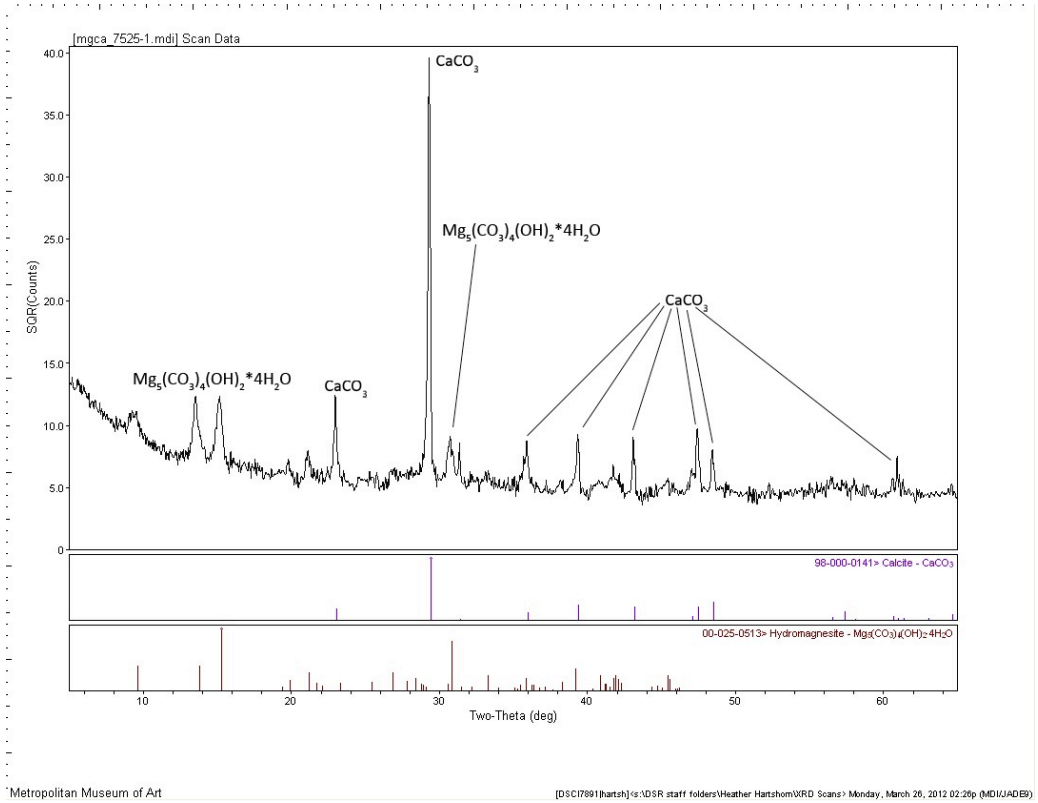

X-ray diffractogram of uncalcined 75/25 chemical grade calcite/magnesite.

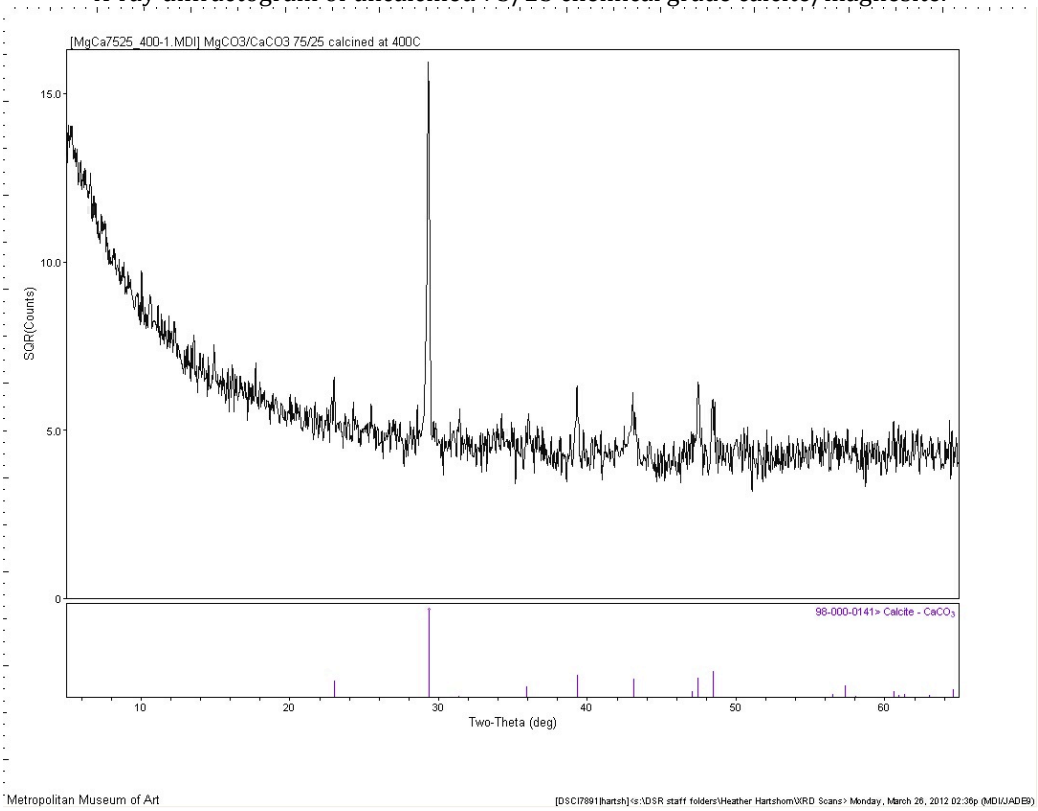

X-ray diffractogram of 75/25 chemical grade calcite/magnesite calcined at 400°C.

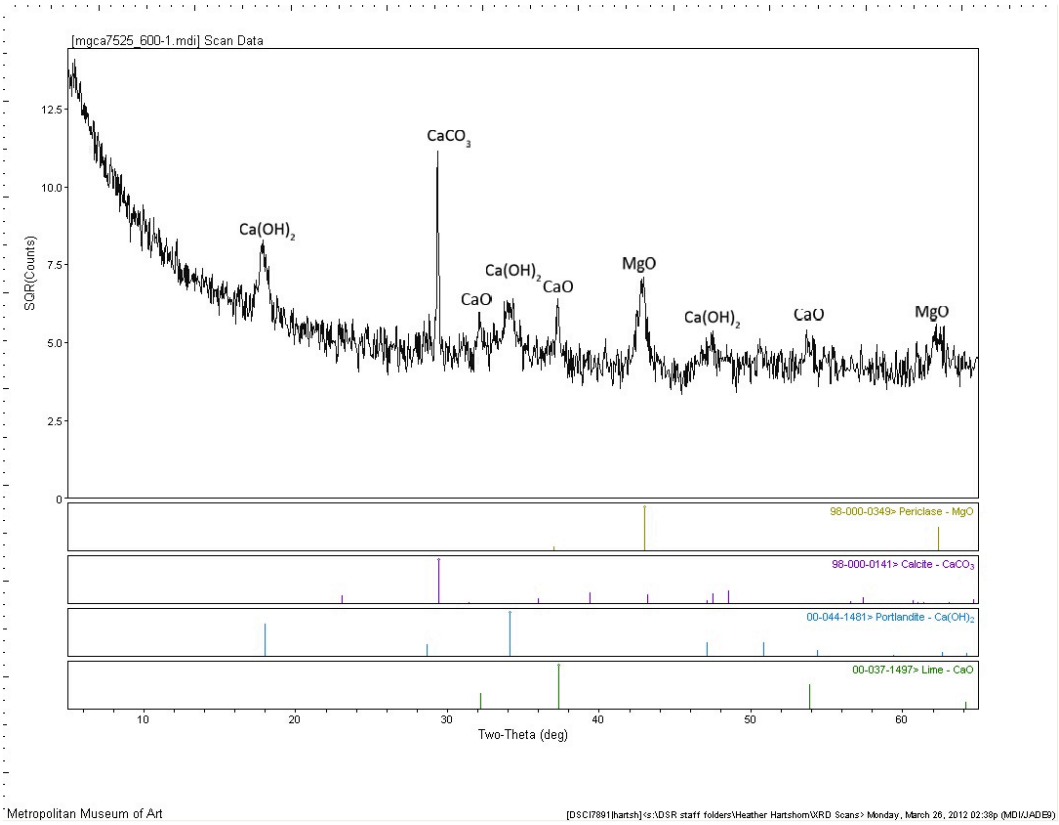

X-ray diffractogram of 75/25 chemical grade calcite/magnesite calcined at 600°C.

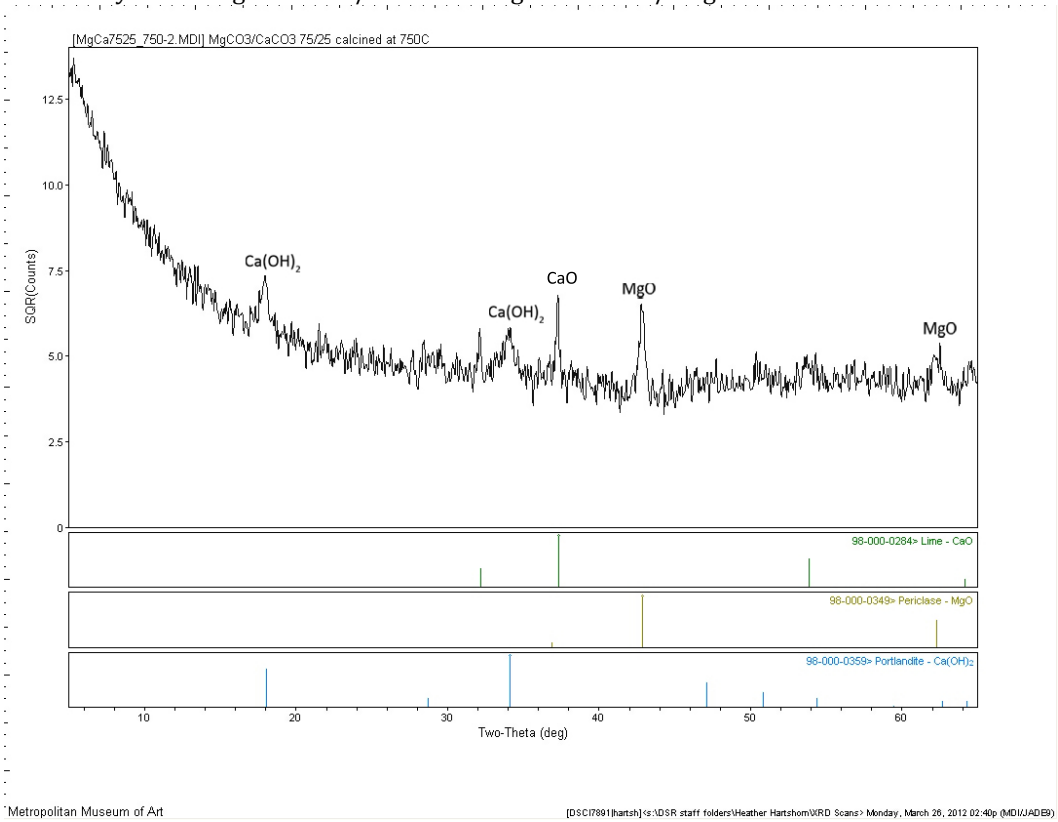

X-ray diffractogram of 75/25 chemical grade calcite/magnesite calcined at 750°C.

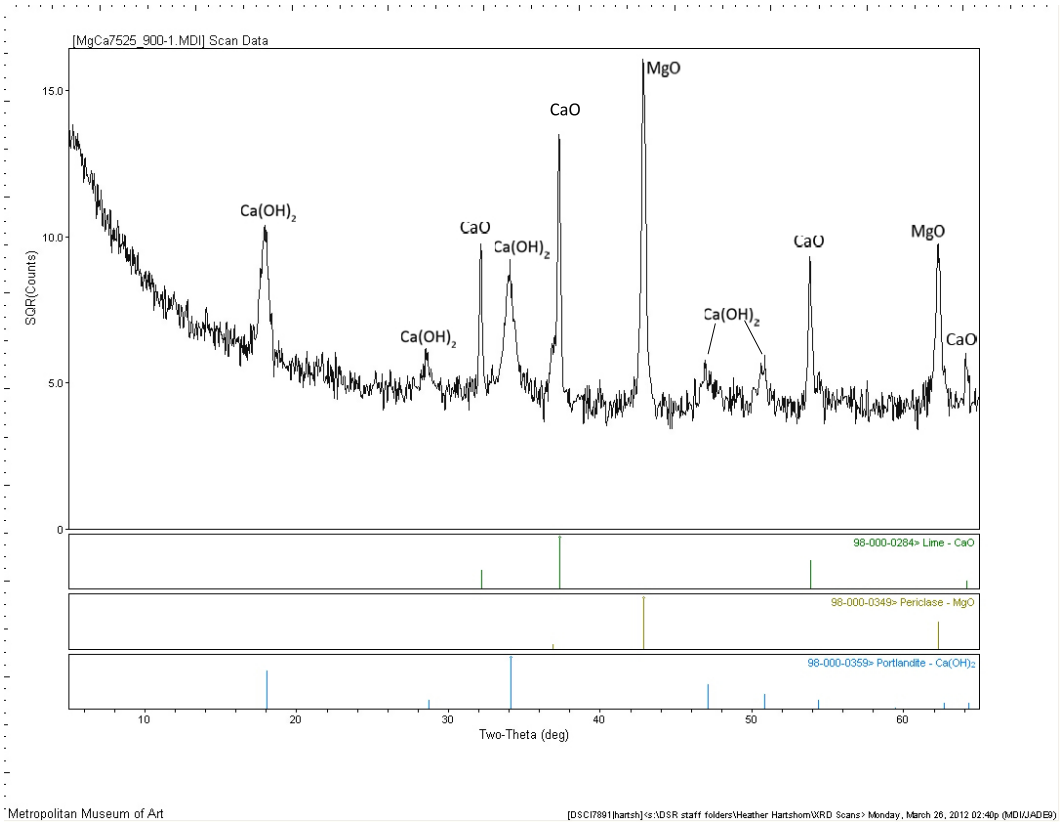

X-ray diffractogram of 75/25 chemical grade calcite/magnesite calcined at 900°C.

Chemical Grade Periclase

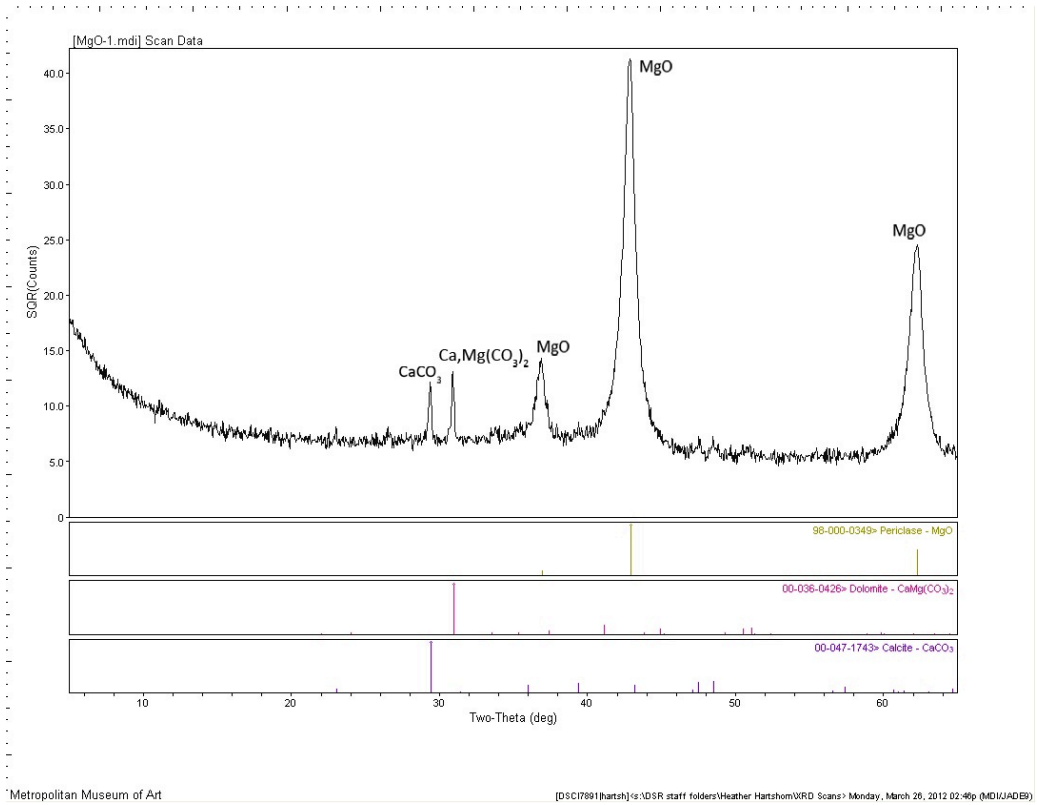

X-ray diffractogram of uncalcined chemical grade periclase.

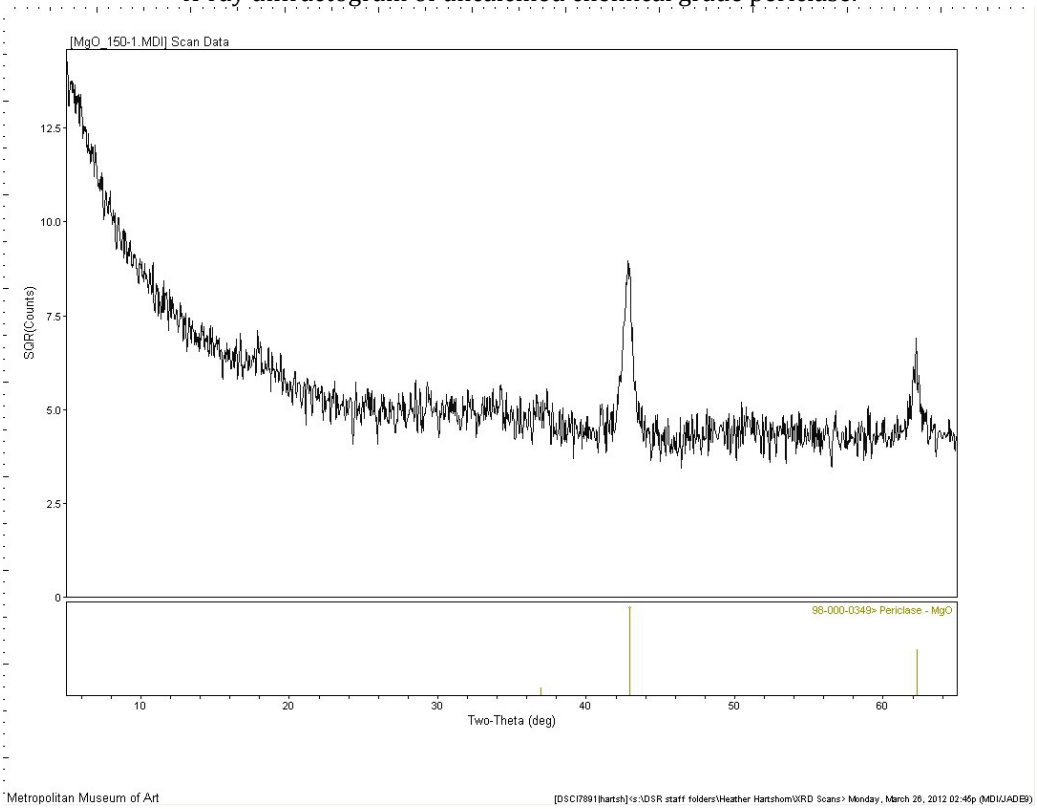

X-ray diffractogram of chemical grade periclase calcined at 150°C.

Chemical Grade Quicklime

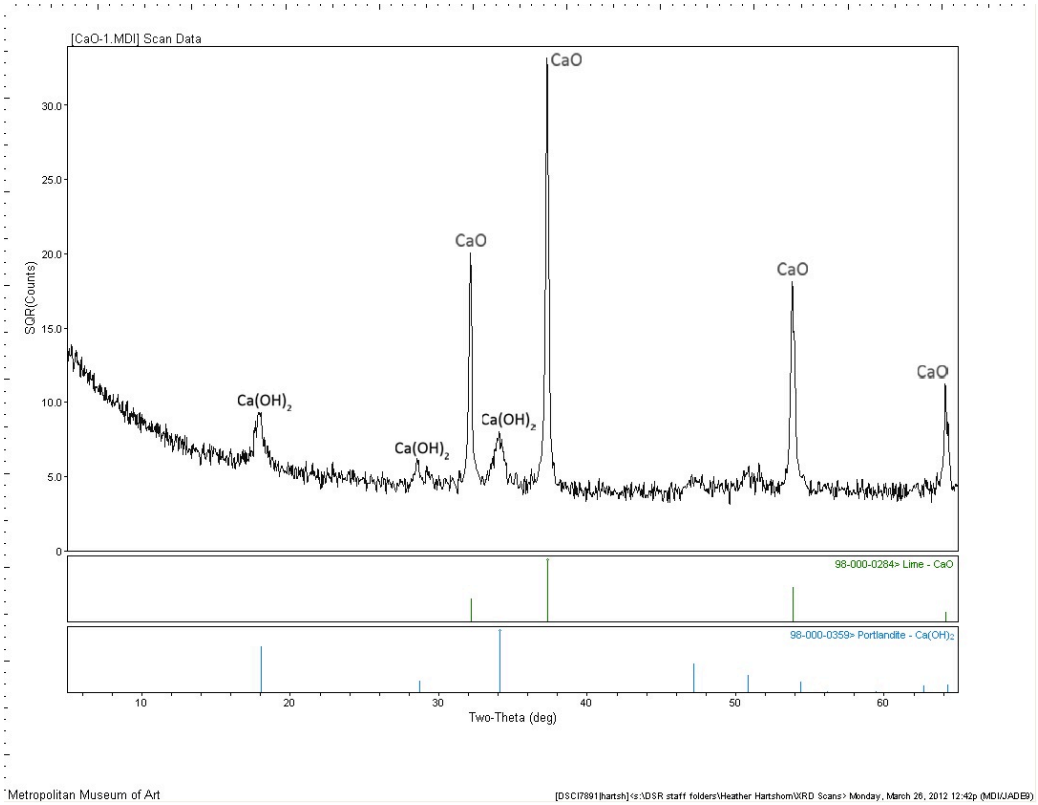

X-ray diffractogram of uncalcined chemical grade quicklime.

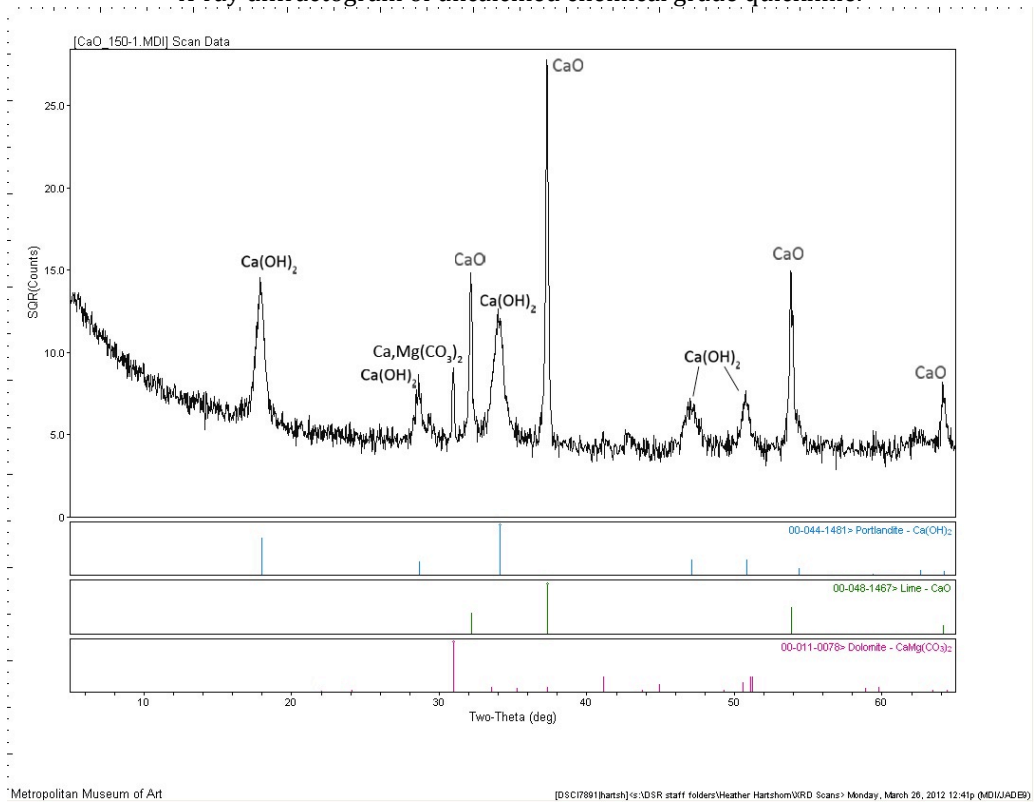

X-ray diffractogram of chemical grade quicklime calcined at 150°C.

Chemical Grade Brucite

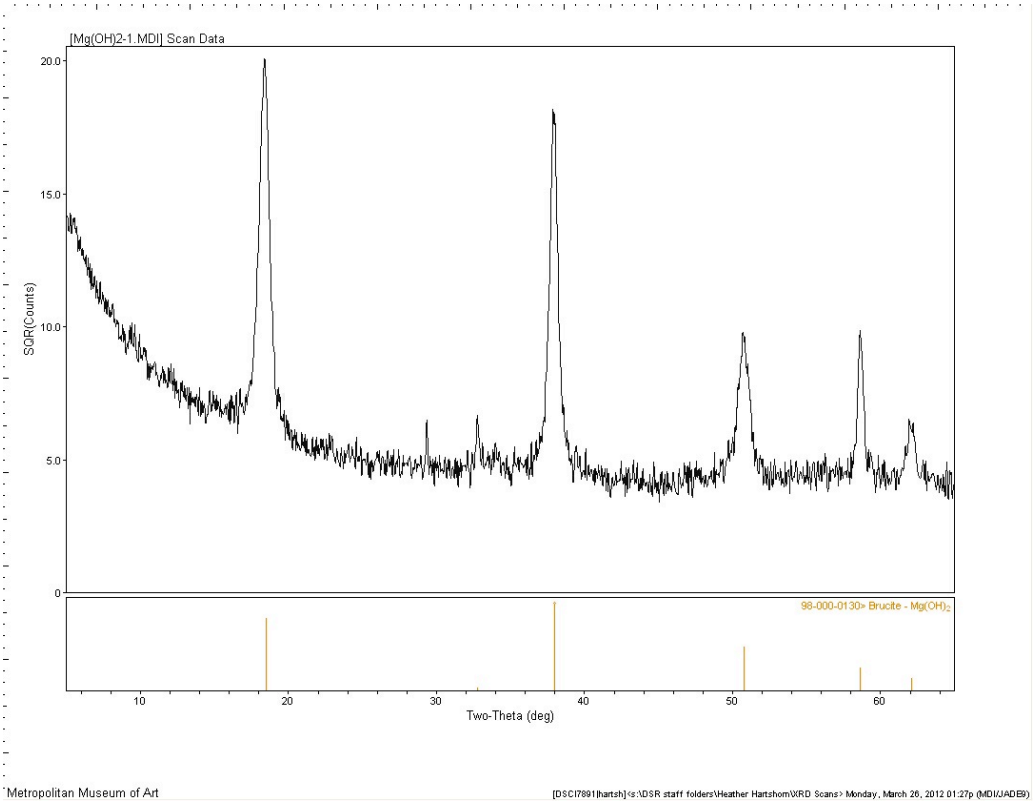

X-ray diffractogram of uncalcined chemical grade brucite.

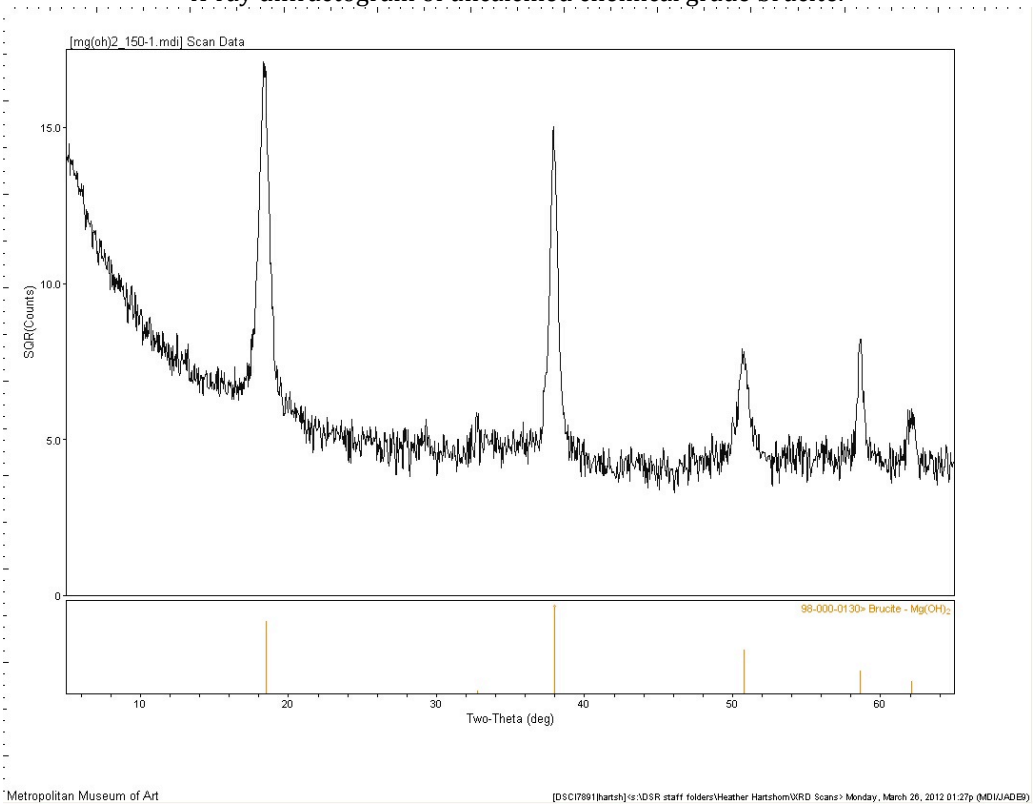

X-ray diffractogram of chemical grade brucite calcined at 150°C.

Chemical Grade Portlandite

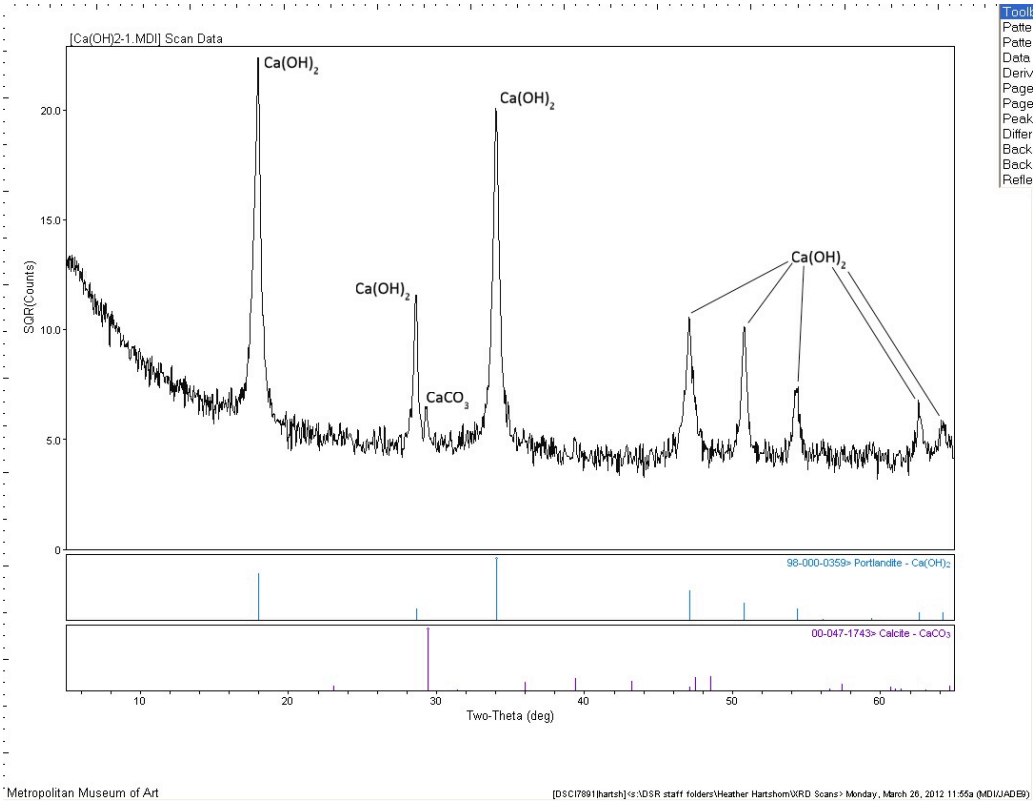

X-ray diffractogram of uncalcined chemical grade portlandite.

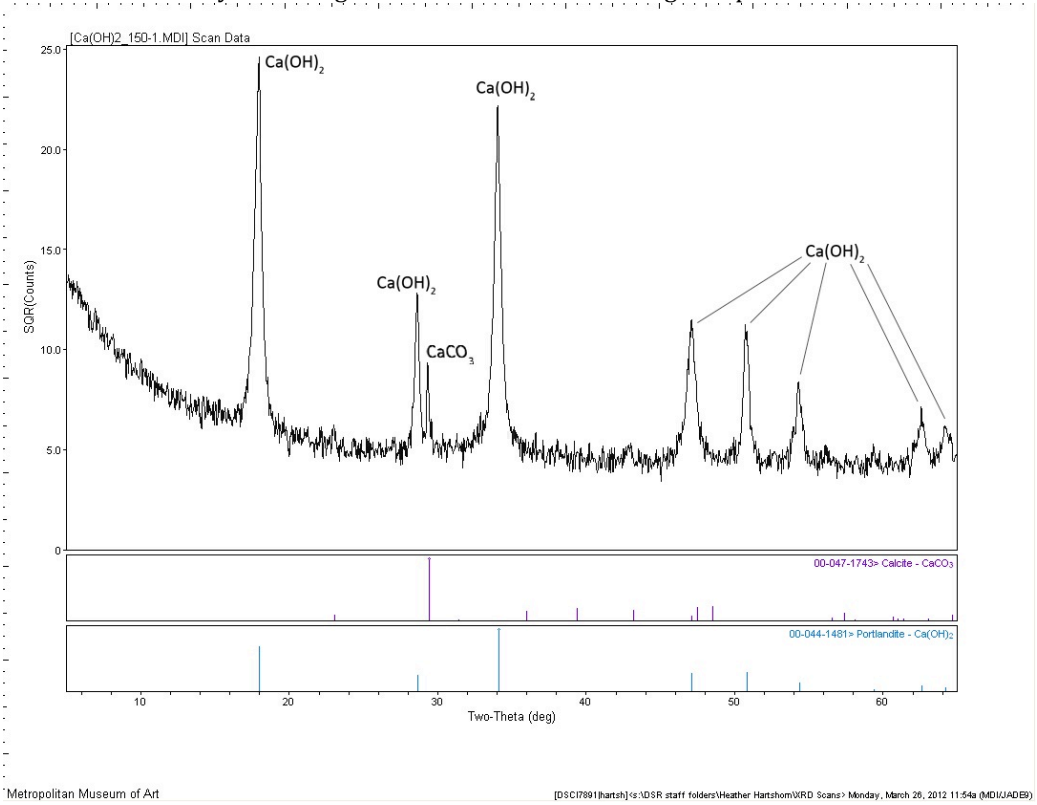

X-ray diffractogram of chemical grade portlandite calcined at 150°C.

Chemical Grade Epsomite

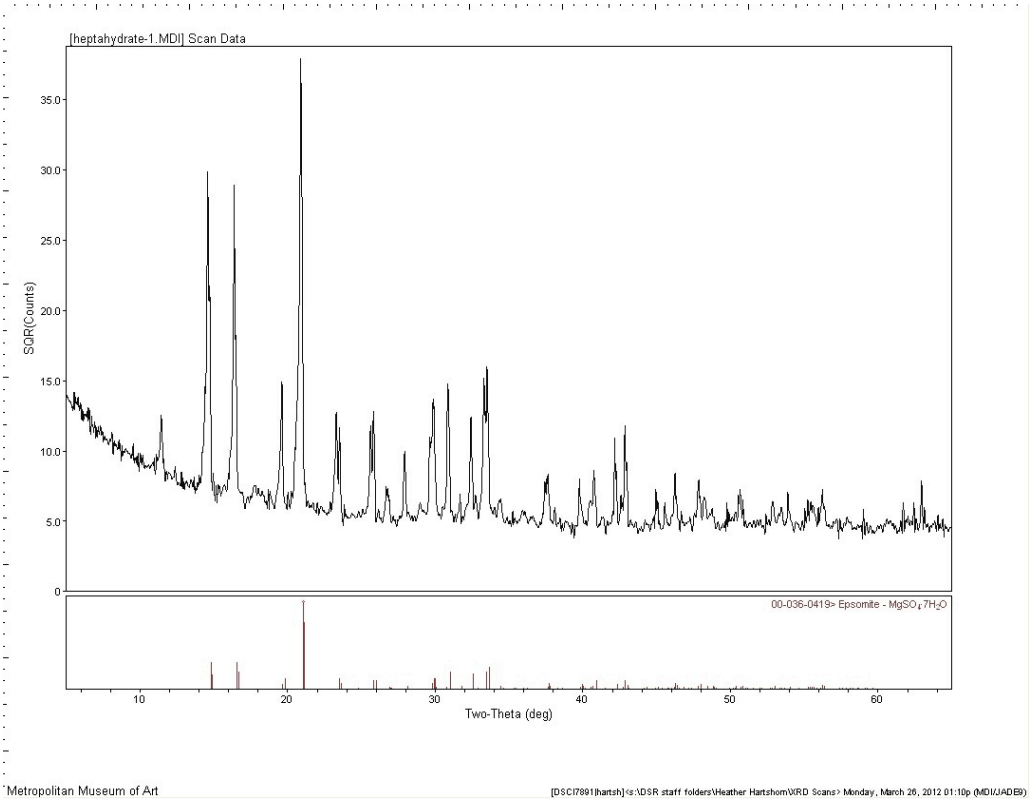

X-ray diffractogram of uncalcined chemical grade epsomite.

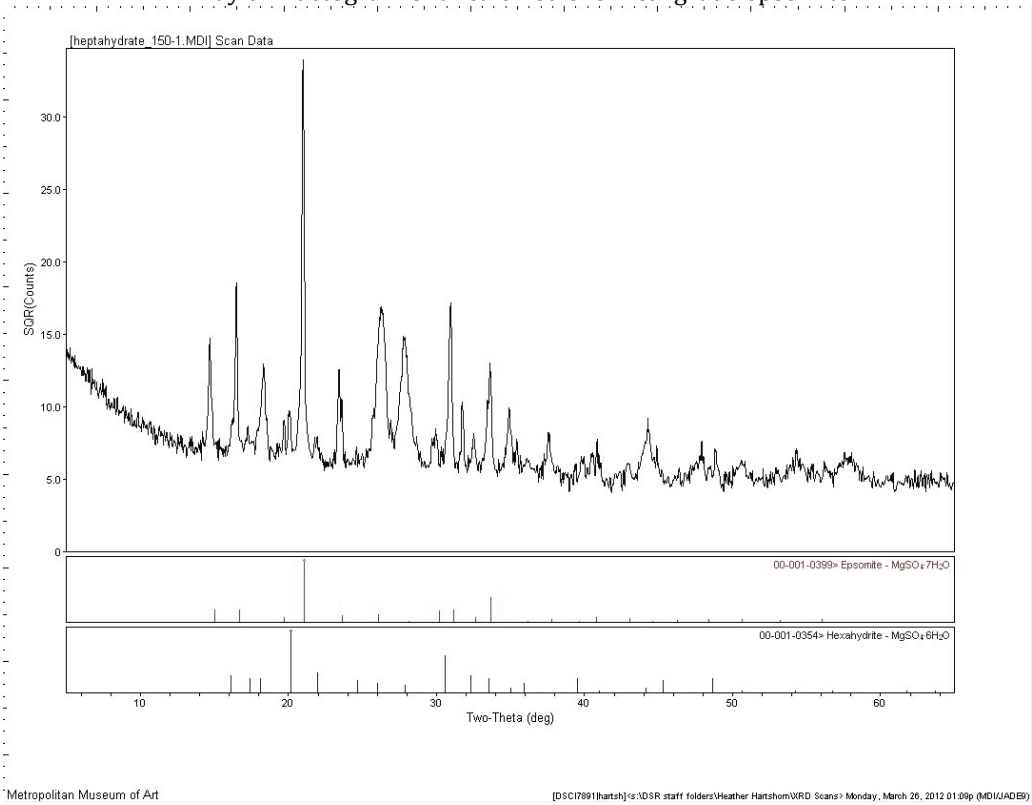

X-ray diffractogram of chemical grade epsomite calcined at 150°C.

Commercial Limes

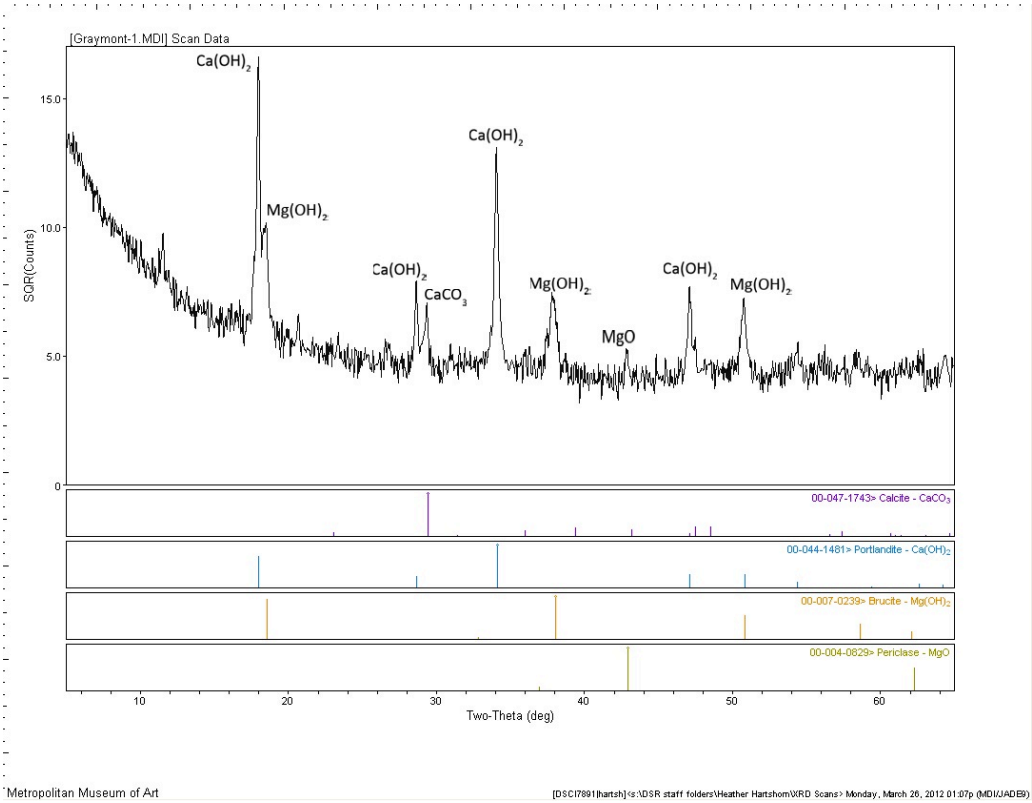

X-ray diffractogram of Graymont Dolime.

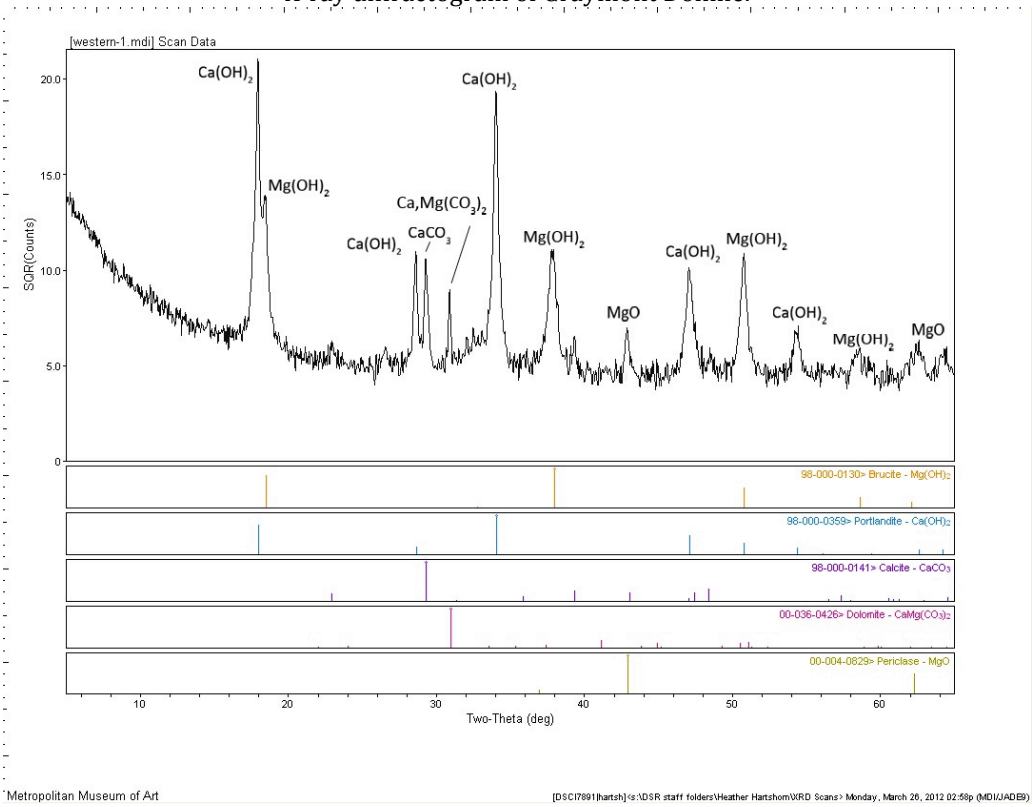

X-ray diffractogram of Western dolomitic lime.

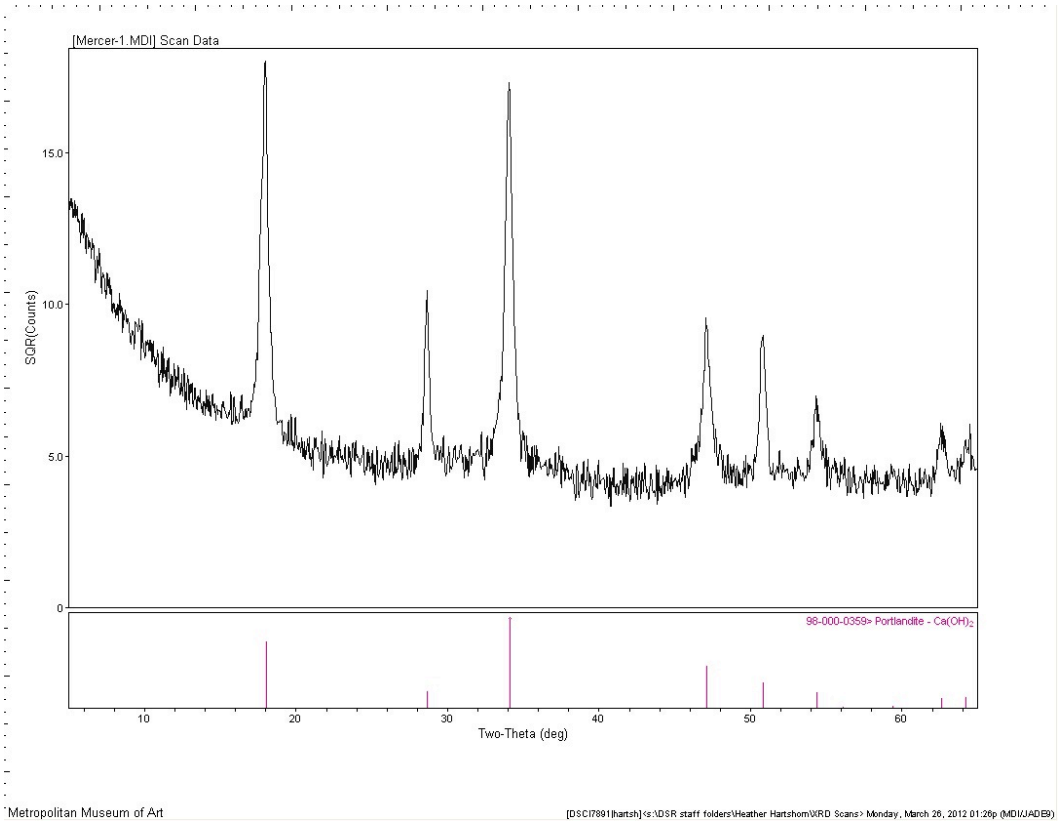

X-ray diffractogram of Mercer high-calcium lime.

Cured Model Mortars

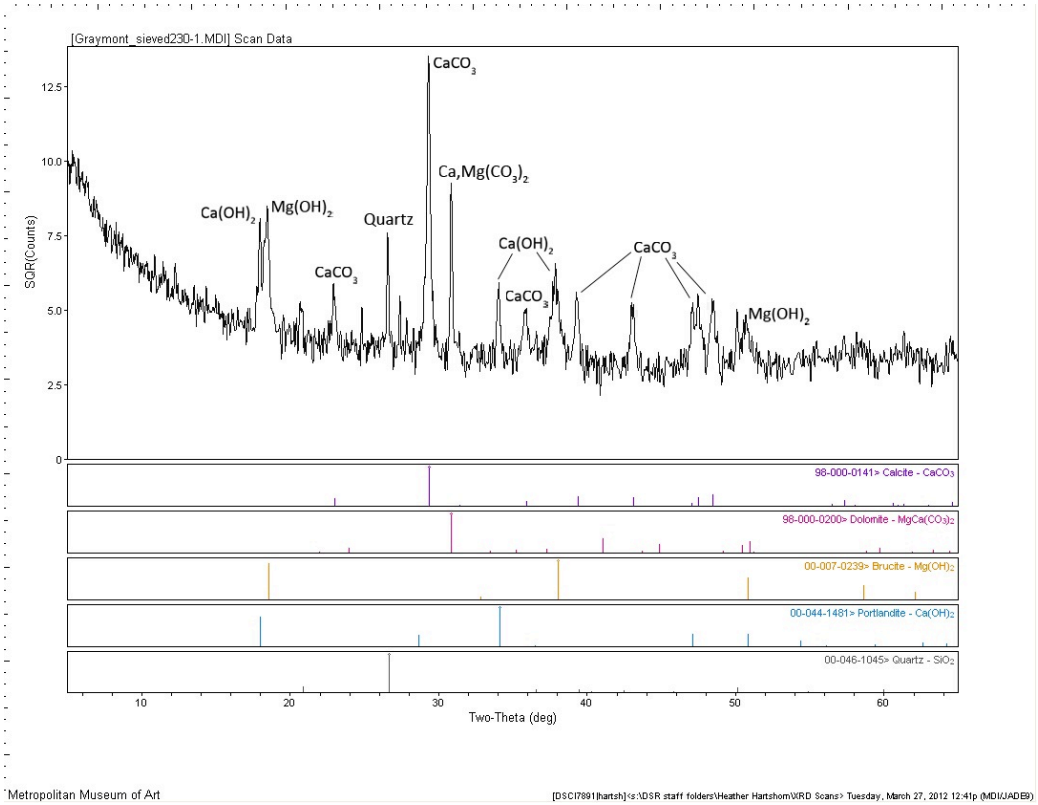

X-ray diffractogram of cured Graymont mortar.

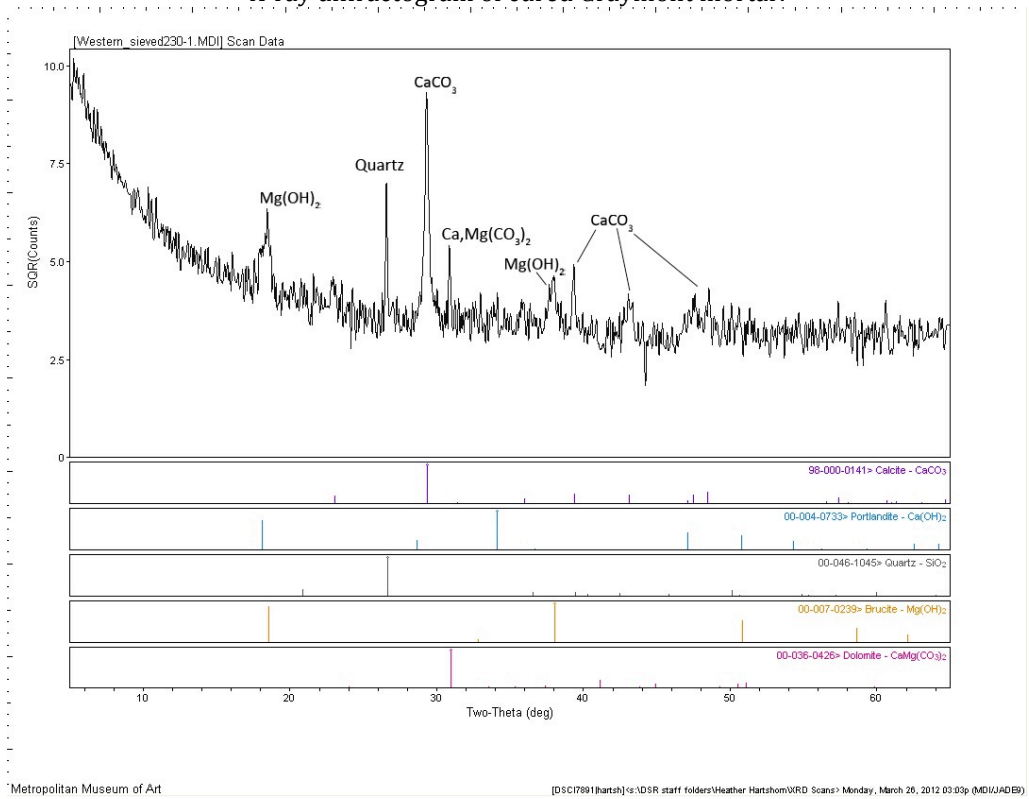

X-ray diffractogram of cured Western mortar.

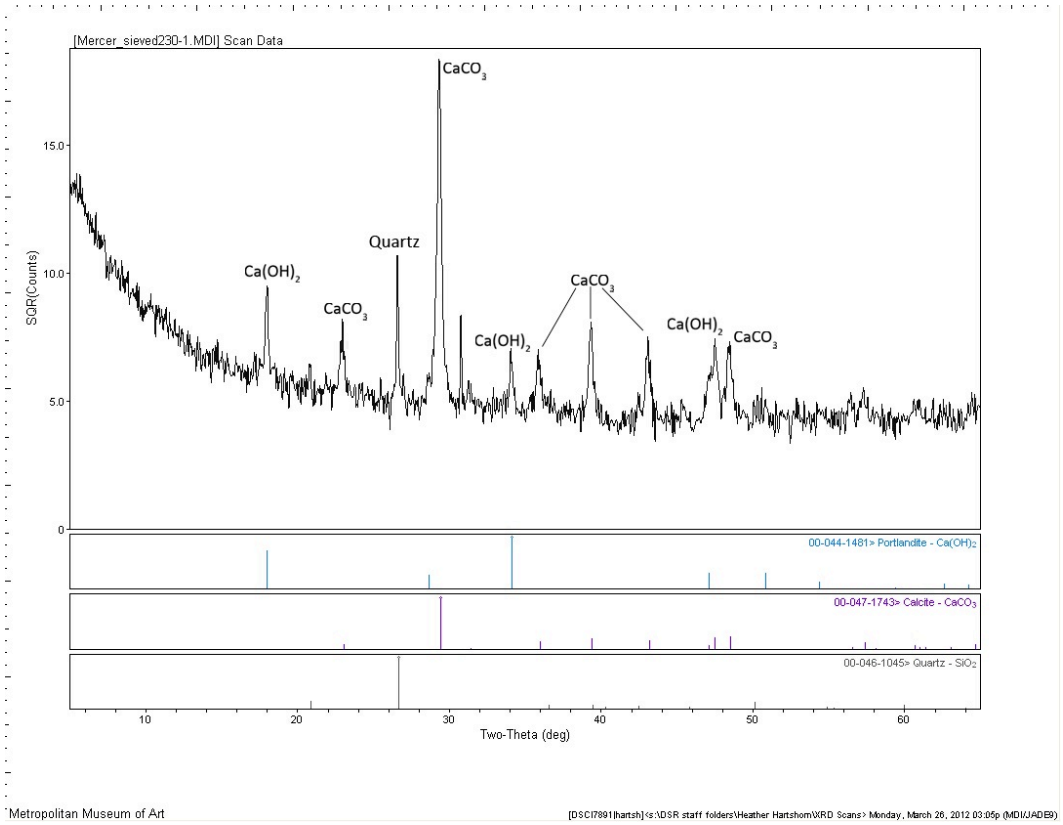

X-ray diffractogram of cured Mercer mortar.

Model Mortars Exposed to Acidic Sulfate Solutions

Graymont Mortar

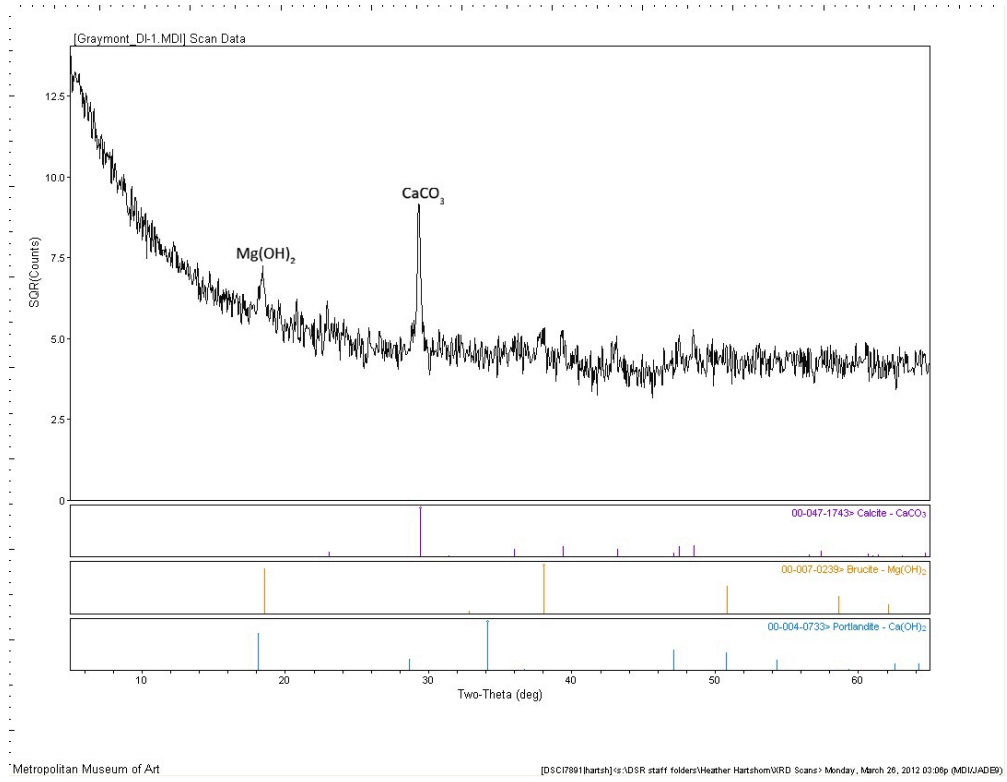

X-ray diffractogram of Graymont mortar exposed to DI water.

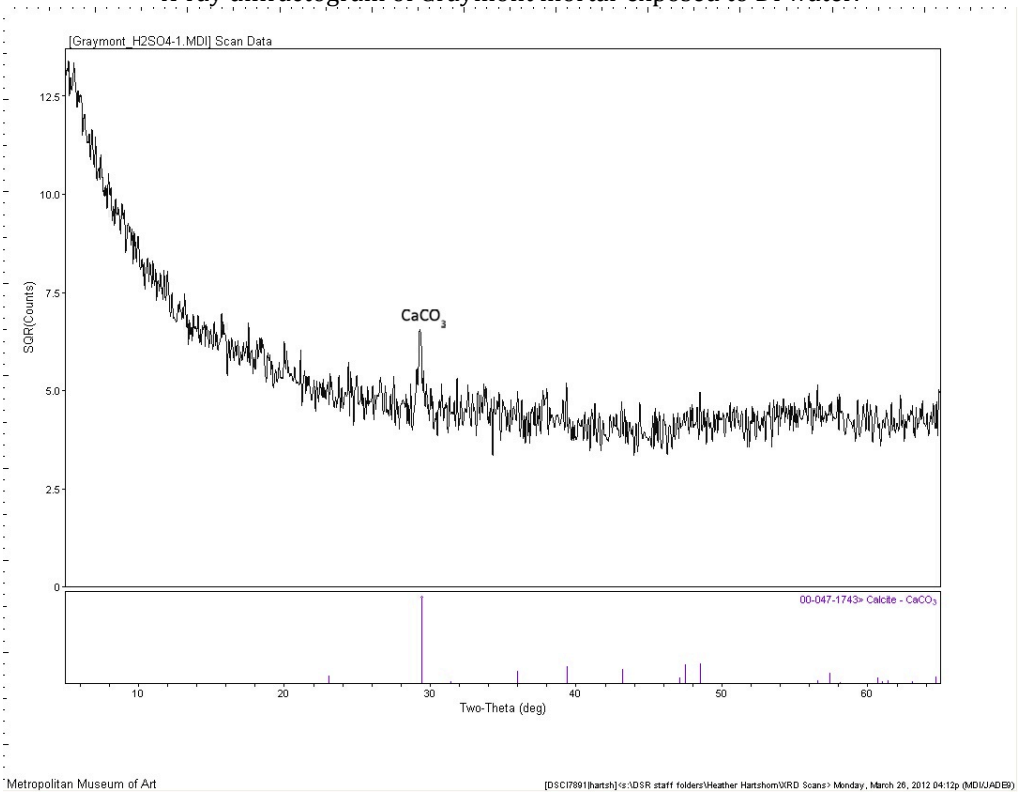

X-ray diffractogram of Graymont mortar exposed to dilute sulfuric acid (pH=3.50).

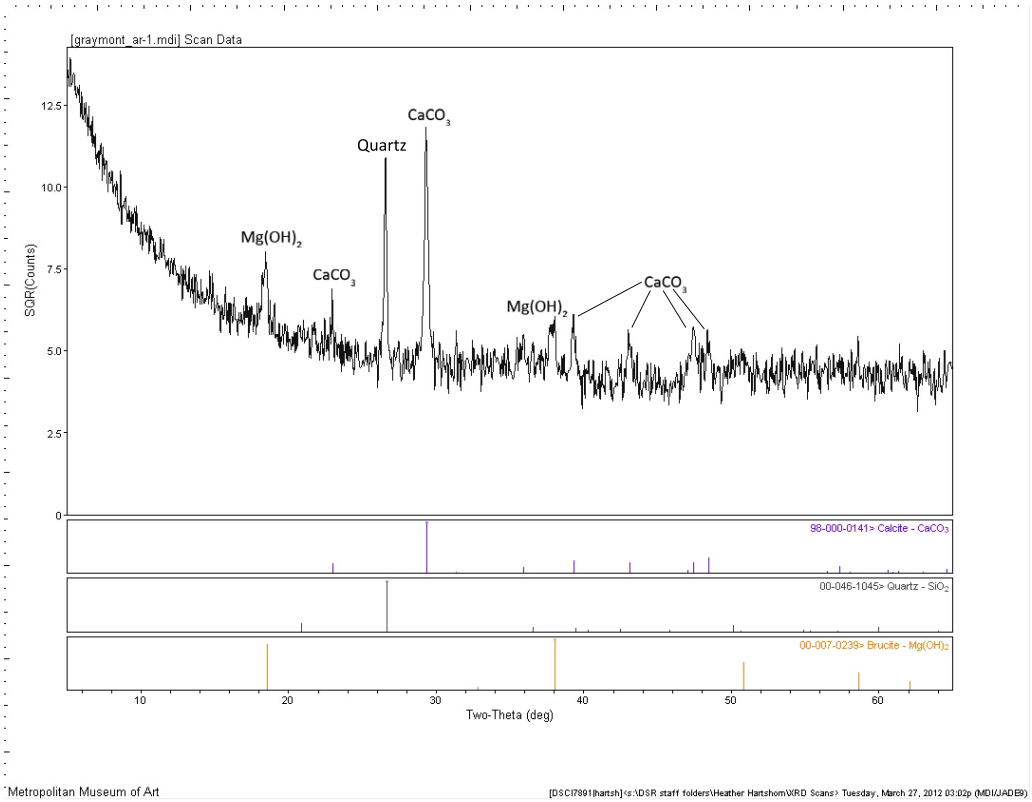

X-ray diffractogram of Graymont mortar exposed to acid rain simulant (pH=3.50).

Western Mortar

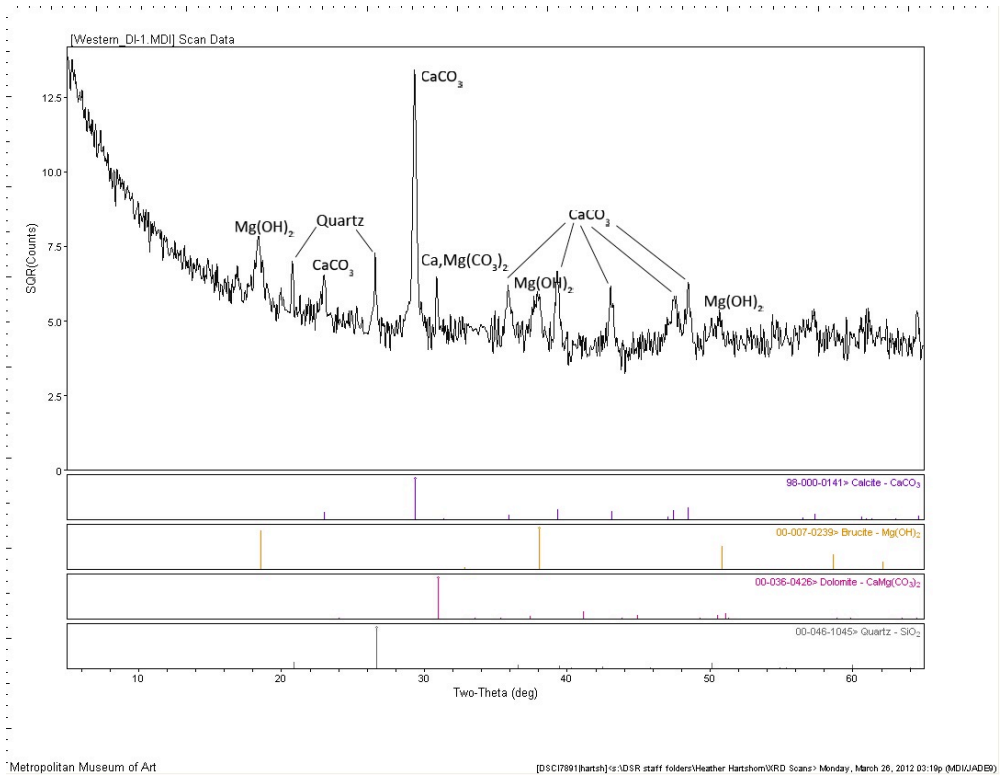

X-ray diffractogram of Western mortar exposed to DI water.

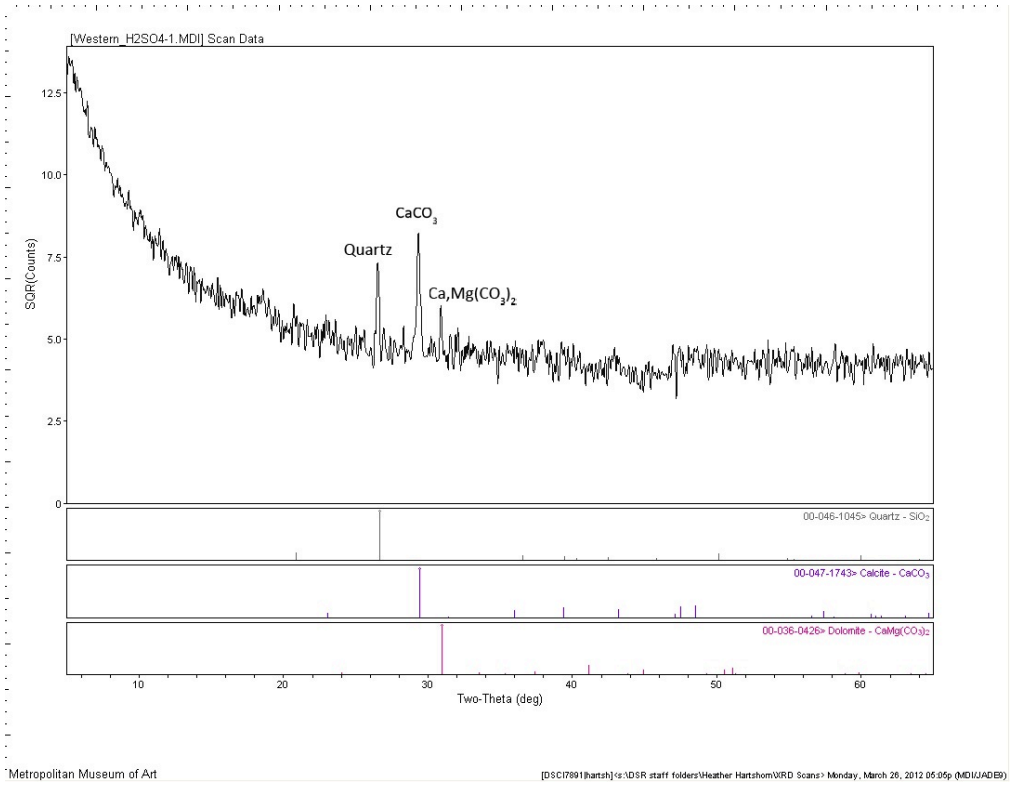

X-ray diffractogram of Western mortar exposed to dilute sulfuric acid (pH=3.50).

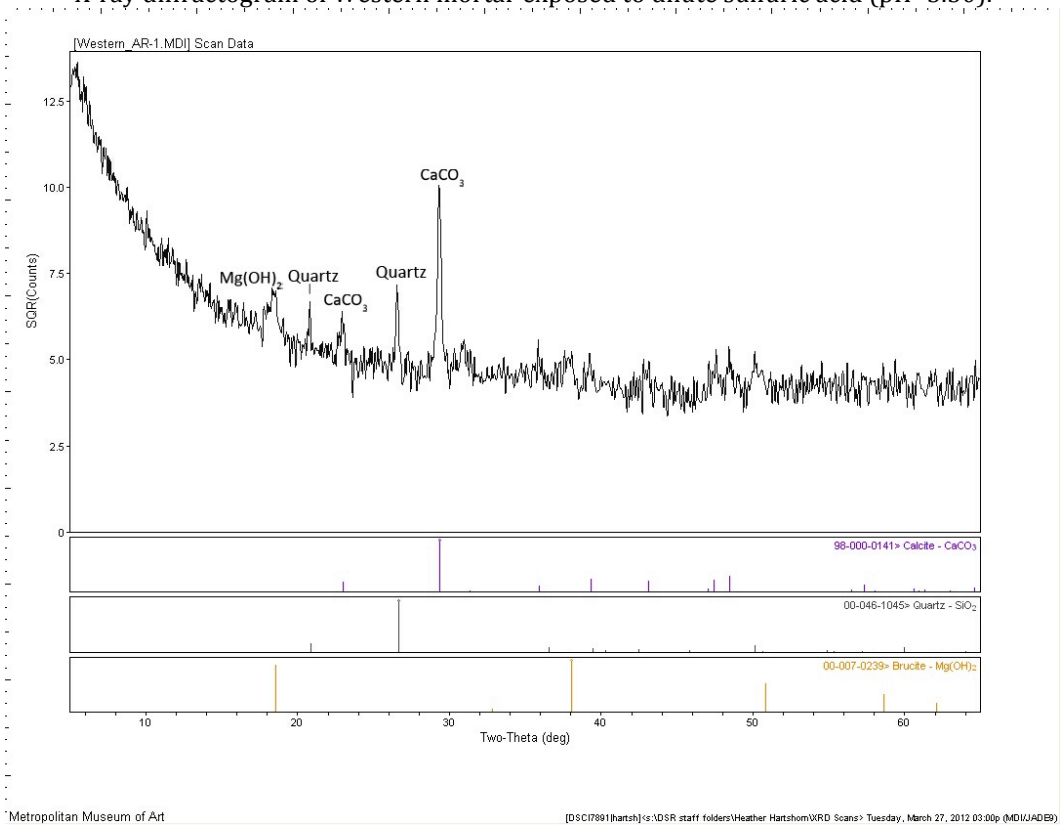

X-ray diffractogram of Western mortar exposed to acid rain simulant (pH=3.50).

Mercer Mortar

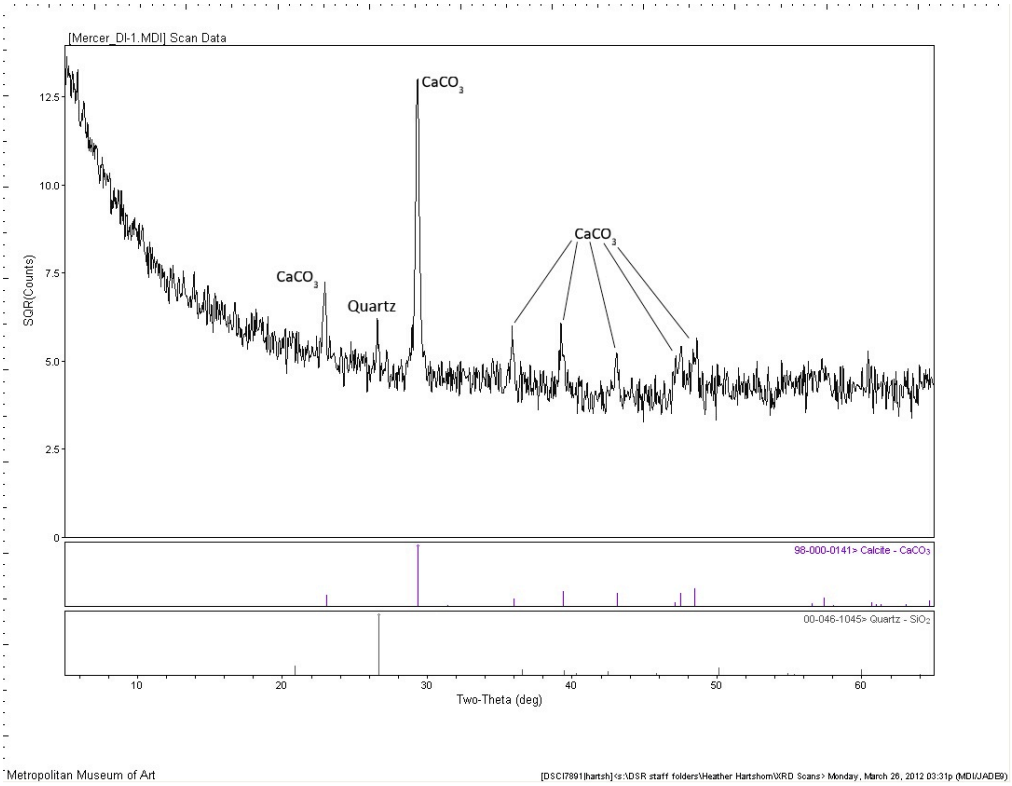

X-ray diffractogram of Mercer mortar exposed to DI water.

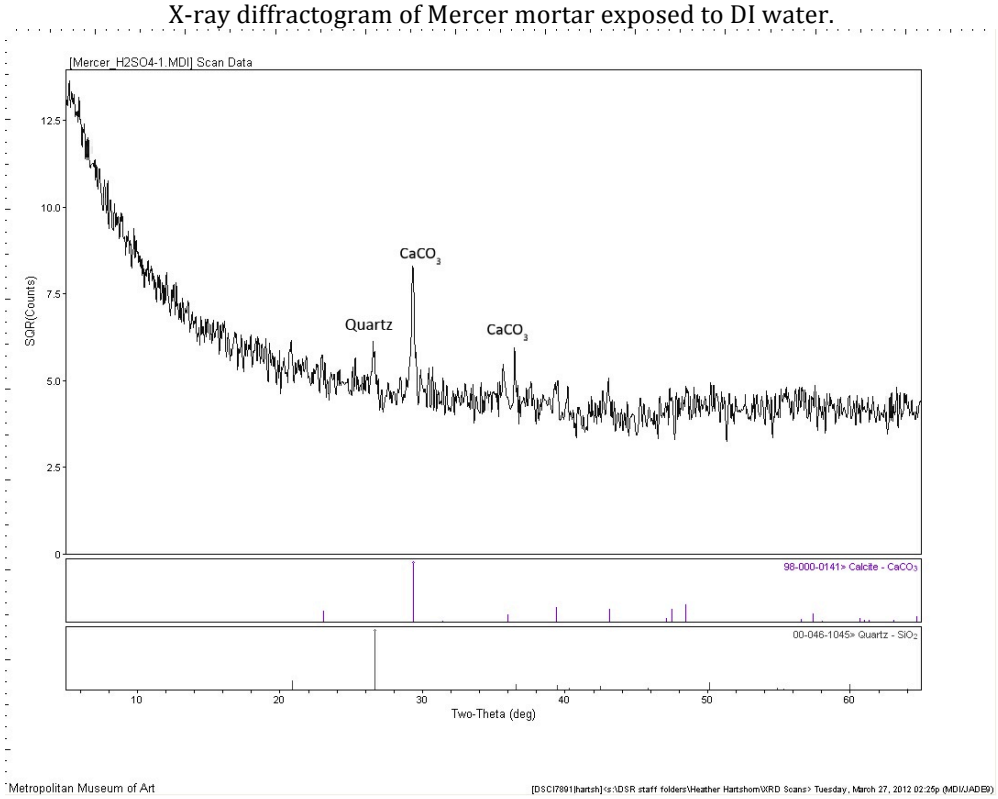

X-ray diffractogram of Mercer mortar exposed to dilute sulfuric acid (pH=3.50).

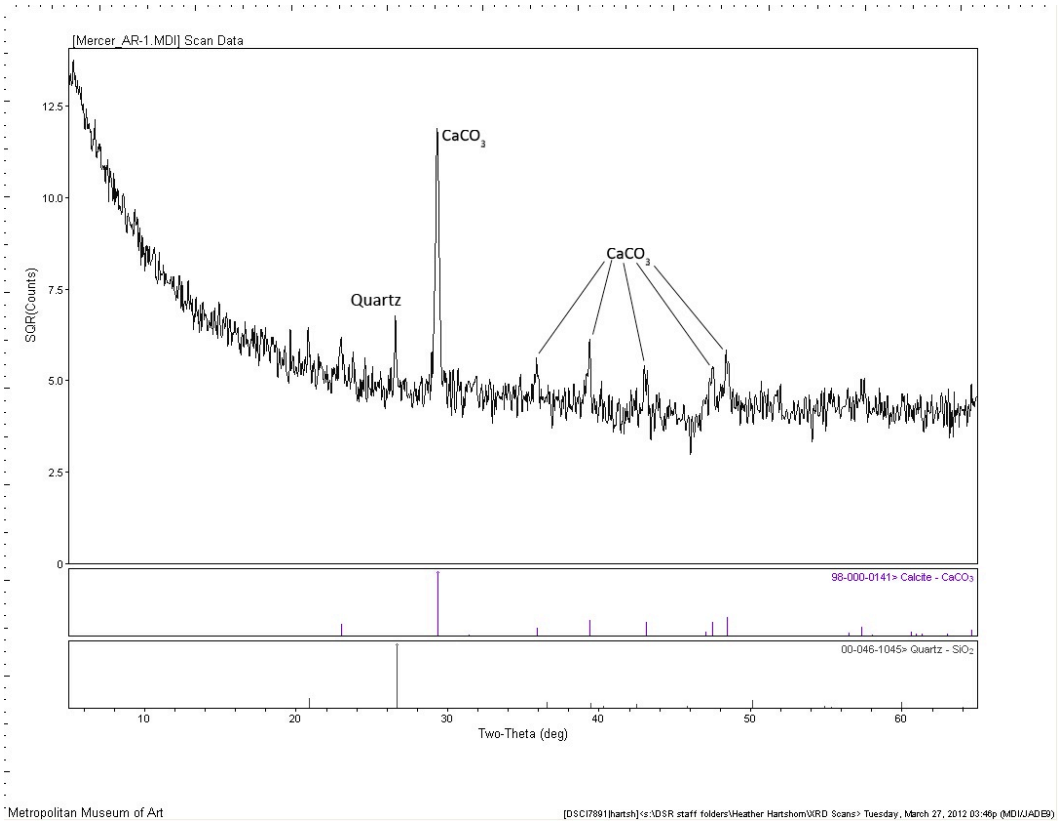

X-ray diffractogram of Mercer mortar exposed to acid rain simulant (pH=3.50).

Appendix D:

Atomic Absorption Data

Chapter 4 Data: Acidic Sulfate Interactions with Mortar Components

Magnesium Ion [Mg^{2+}] Content:

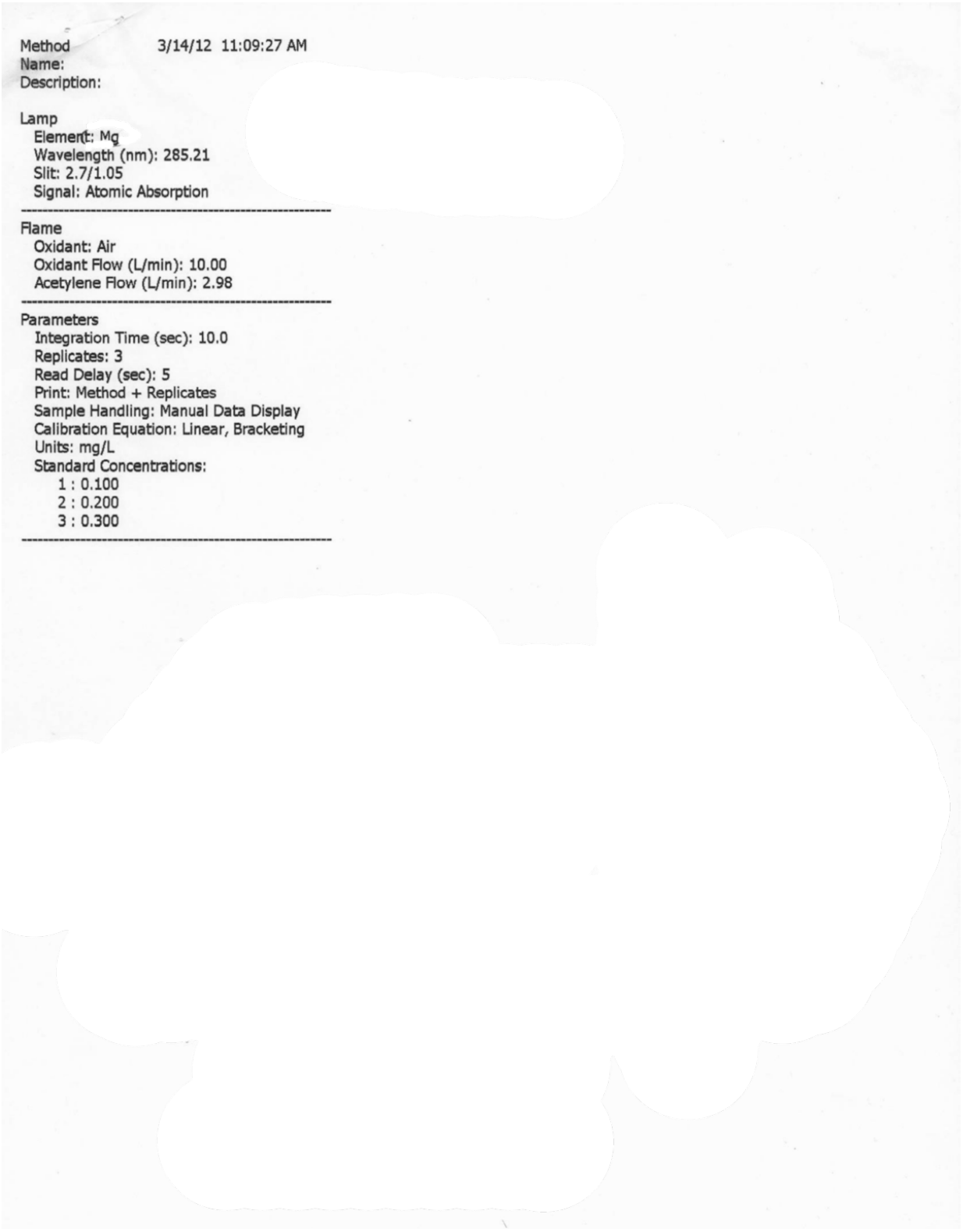

Method 3/14/12 11:09:27 AM
Name:
Description:

Lamp
Element: Mg
Wavelength (nm): 285.21
Slit: 2.7/1.05
Signal: Atomic Absorption

Flame
Oxidant: Air
Oxidant Flow (L/min): 10.00
Acetylene Flow (L/min): 2.98

Parameters
Integration Time (sec): 10.0
Replicates: 3
Read Delay (sec): 5
Print: Method + Replicates
Sample Handling: Manual Data Display
Calibration Equation: Linear, Bracketing
Units: mg/L
Standard Concentrations:
1 : 0.100
2 : 0.200
3 : 0.300

Mean: 0.296 SD: 0.0006 RSD(%): 0.2
No calibration because absorbance and concentration values are not in the same order
---
Standard 1 3/14/12 11:25:20 AM
Absorbance
0.165 0.164 0.163
Mean: 0.164 SD: 0.0010 RSD(%): 0.6

Standard 2 3/14/12 11:26:14 AM
Absorbance
0.295 0.293 0.293
Mean: 0.294 SD: 0.0009 RSD(%): 0.3
Standard 2 Applied

Standard 3 3/14/12 11:27:11 AM
Absorbance
0.432 0.433 0.432
Mean: 0.432 SD: 0.0005 RSD(%): 0.1
Standard 3 Applied
Corr. Coef.: 0.999827 Slope: 1.34122 Intercept: 0.02840

0.2 PPM 3/14/12 11:28:08 AM
Concentration (mg/L) Factor: 1.000
0.195 0.198 0.195
Mean: 0.196 SD: 0.0018 RSD(%): 0.9

DI WATER 1 3/14/12 11:29:07 AM
Concentration (mg/L) Factor: 1000.000
233.199 233.633 230.967
Mean: 232.600 SD: 1.431 RSD(%): 0.6

DI WATER2 3/14/12 11:30:04 AM
Concentration (mg/L) Factor: 500.000
110.155 112.799 112.621
Mean: 111.858 SD: 1.478 RSD(%): 1.3

DI WATER3 3/14/12 11:31:14 AM
Concentration (mg/L) Factor: 333.333
73.628 73.429 73.837
Mean: 73.631 SD: 0.2038 RSD(%): 0.3

DI WATER4 3/14/12 11:32:11 AM
Concentration (mg/L) Factor: 200.000
53.565 53.644 53.337
Mean: 53.515 SD: 0.1589 RSD(%): 0.3

DI WATER 5 3/14/12 11:33:13 AM
Concentration (mg/L) Factor: 200.000
42.520 42.327 42.421
Mean: 42.423 SD: 0.0965 RSD(%): 0.2

0.2 PPM 3/14/12 11:34:15 AM
Concentration (mg/L) Factor: 1.000
0.195 0.194 0.193
Mean: 0.194 SD: 0.0009 RSD(%): 0.4

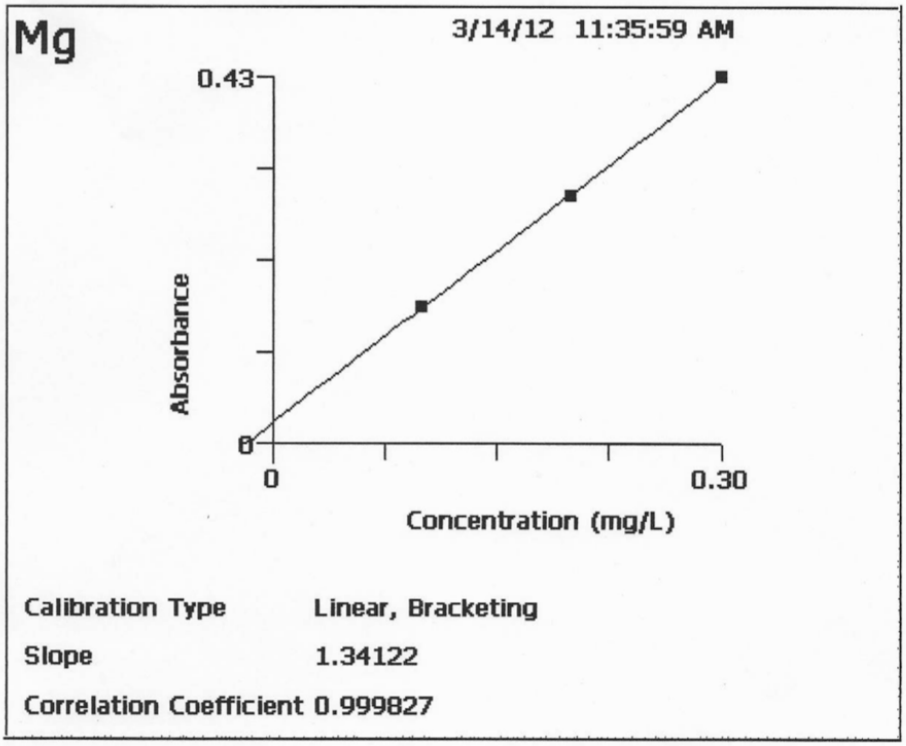
Mg
3/14/12 11:35:59 AM
0.43
0
Absorbance
0
0.30
Concentration (mg/L)
Calibration Type Linear, Bracketing
Slope 1.34122
Correlation Coefficient 0.999827

Solution	Solid	[Mg2+] in 180 mL solution (M)	Amount Mg dissolved (g)	Amount Mg-bearing solid dissolved (g)	Original amount of Mg-bearing solid (g)	% dissolved
H2O	CaCO3/Mg(OH)2	0.000539	0.00236	0.00566	0.3740	1.514
H2SO3	CaCO3/Mg(OH)2	0.000706	0.00309	0.00741	0.3677	2.015
H2SO4	CaCO3/Mg(OH)2	0.000544	0.00238	0.00571	0.3787	1.508
H20/CO2	CaCO3/Mg(OH)2	0.0283	0.124	0.298	0.3783	78.776
Acid Rain	CaCO3/Mg(OH)2	0.0313	0.137	0.329	0.3728	88.257
H2O	CaCO3/MgCO3	0.00153	0.00668	0.0232	0.4670	4.967
H2SO3	CaCO3/MgCO3	0.00207	0.00906	0.0314	0.4654	6.746
H2SO4	CaCO3/MgCO3	0.00056	0.00245	0.0085	0.4581	1.856
H20/CO2	CaCO3/MgCO3	0.0181	0.0791	0.274	0.4625	59.245
Acid Rain	CaCO3/MgCO3	0.021	0.0921	0.319	0.4605	69.272
H2O	Mg(OH)2	0.000623	0.00273	0.00654	1.0291	0.636
H2SO3	Mg(OH)2	0.00116	0.00509	0.0122	1.0103	1.208
H2SO4	Mg(OH)2	0.000798	0.00349	0.00837	1.0271	0.815
H20/CO2	Mg(OH)2	0.0395	0.173	0.415	1.0010	41.459
Acid Rain	Mg(OH)2	0.0338	0.148	0.355	1.0297	34.476
H2O	MgCO3	0.00174	0.0076	0.0264	1.0025	2.633
H2SO3	MgCO3	0.00249	0.0109	0.0378	1.0182	3.712
H2SO4	MgCO3	0.00214	0.00935	0.0324	1.0158	3.190
H20/CO2	MgCO3	0.0336	0.147	0.51	1.0093	50.530
Acid Rain	MgCO3	0.0313	0.137	0.475	1.0060	47.217

Table D-1. Data Table on Magnesium Ion Concentration [Mg^{2+}]

Calcium Ion [Ca^{2+}] Content:

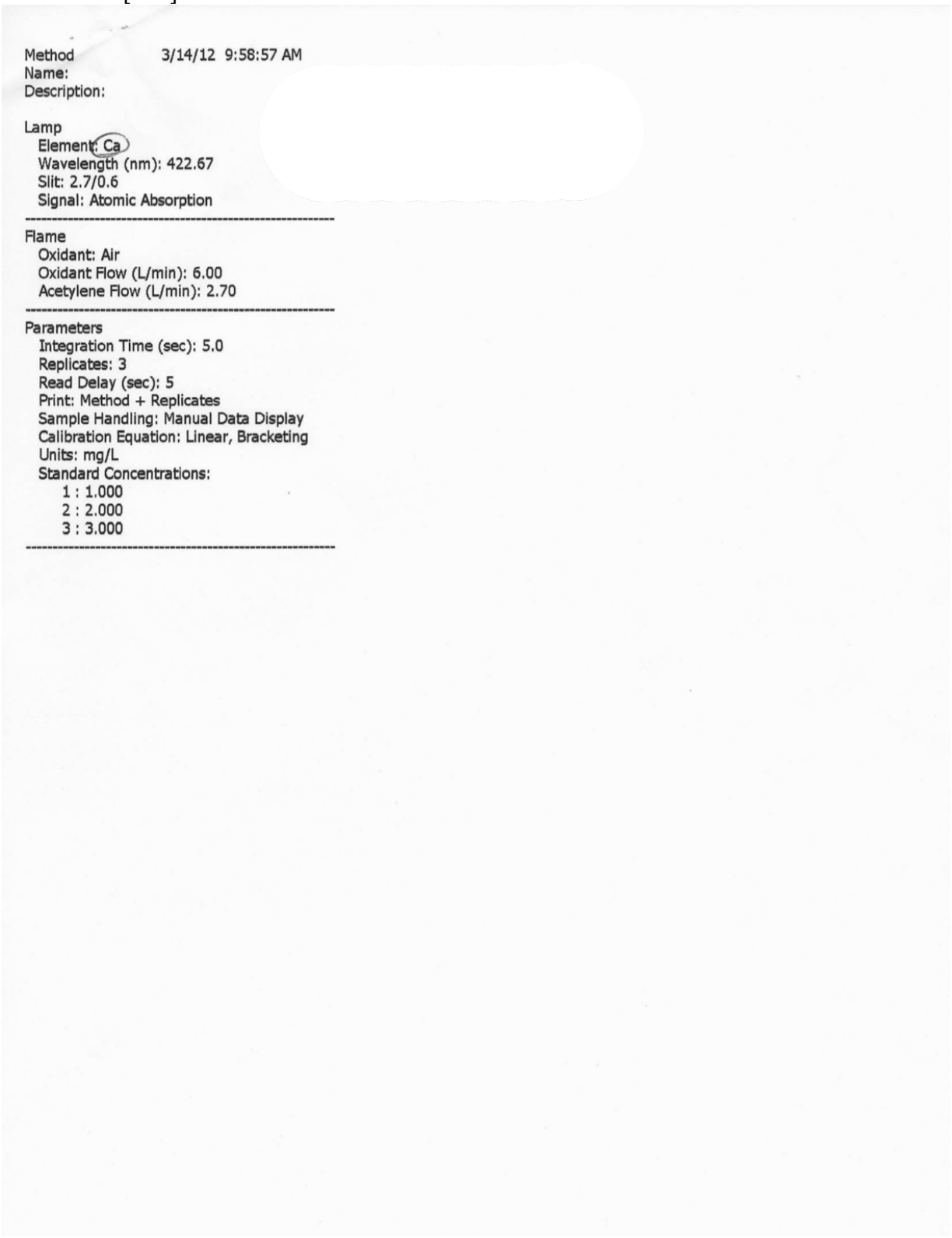

Method 3/14/12 9:58:57 AM
Name:
Description:

Lamp
Element: Ca
Wavelength (nm): 422.67
Slit: 2.7/0.6
Signal: Atomic Absorption

Flame
Oxidant: Air
Oxidant Flow (L/min): 6.00
Acetylene Flow (L/min): 2.70

Parameters
Integration Time (sec): 5.0
Replicates: 3
Read Delay (sec): 5
Print: Method + Replicates
Sample Handling: Manual Data Display
Calibration Equation: Linear, Bracketing
Units: mg/L
Standard Concentrations:
1 : 1.000
2 : 2.000
3 : 3.000

---

2 PPM 3/14/12 10:08:32 AM
Concentration (mg/L) Factor: 1.000
1.878 1.855 1.818
Mean: 1.850 SD: 0.0305 RSD(%): 1.6

Standard 1 3/14/12 10:14:40 AM
Absorbance
0.070 0.071 0.071
Mean: 0.070 SD: 0.0004 RSD(%): 0.5
Standard 1 Applied

Standard 2 3/14/12 10:15:24 AM
Absorbance
0.142 0.142 0.143
Mean: 0.142 SD: 0.0008 RSD(%): 0.6
Standard 2 Applied

Standard 3 3/14/12 10:16:22 AM
Absorbance
0.207 0.209 0.208
Mean: 0.208 SD: 0.0011 RSD(%): 0.5
Standard 3 Applied
Corr. Coef.: 0.999659 Slope: 0.06882 Intercept: 0.00270
---
2 PPM 3/14/12 10:17:02 AM
Concentration (mg/L) Factor: 1.000
2.119 2.117 2.103
Mean: 2.113 SD: 0.0086 RSD(%): 0.4

DI WATER 1 3/14/12 10:17:42 AM
Concentration (mg/L) Factor: 50.000
163.093 164.203 162.761
Mean: 163.352 SD: 0.7549 RSD(%): 0.5

DI WATER2 3/14/12 10:18:27 AM
Concentration (mg/L) Factor: 50.000
123.048 123.652 124.327
Mean: 123.676 SD: 0.6397 RSD(%): 0.5

DI WATER3 3/14/12 10:19:17 AM
Concentration (mg/L) Factor: 50.000 x 2 268.214
135.332 133.377 133.613
Mean: 134.107 SD: 1.067 RSD(%): 0.8

DI WATER4 3/14/12 10:20:07 AM
Concentration (mg/L) Factor: 50.000 x 4 199.208
50.159 49.640 49.608
Mean: 49.802 SD: 0.3094 RSD(%): 0.6

DI WATER 5 3/14/12 10:20:49 AM
Concentration (mg/L) Factor: 100.000
201.474 205.952 211.858
Mean: 206.428 SD: 5.208 RSD(%): 2.5
---
2 PPM 3/14/12 10:21:35 AM
Concentration (mg/L) Factor: 1.000
2.002 2.025 2.033
Mean: 2.020 SD: 0.0164 RSD(%): 0.8

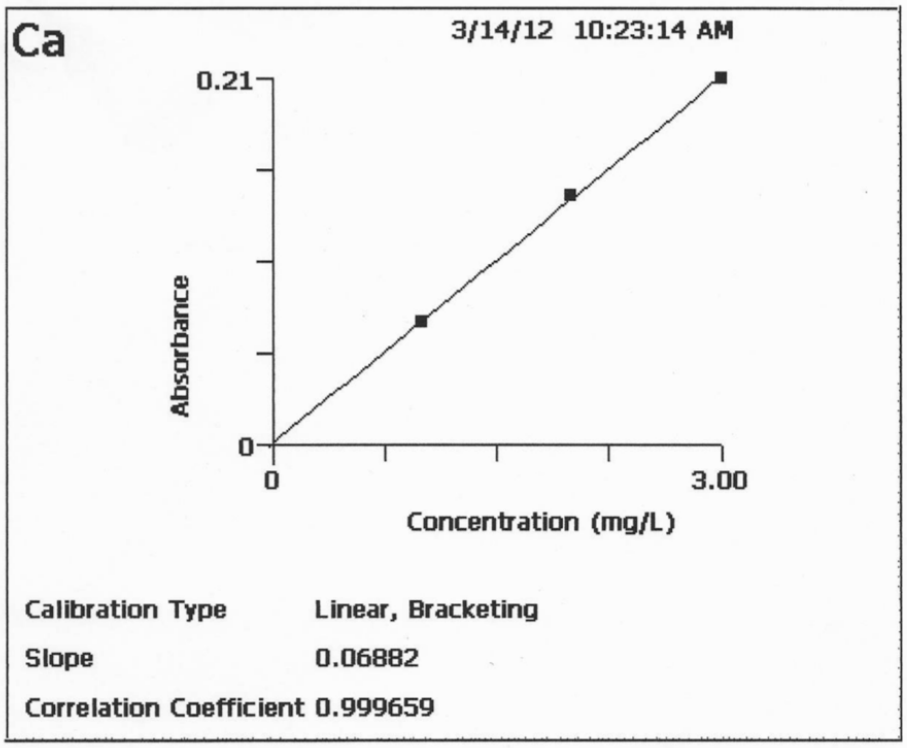
Ca
3/14/12 10:23:14 AM
0.21
0
Absorbance
0
3.00
Concentration (mg/L)
Calibration Type Linear, Bracketing
Slope 0.06882
Correlation Coefficient 0.999659

Solution	Solid	[Ca2+] in 180 mL solution (M)	Amount Ca dissolved (g)	Amount CaCO3 dissolved (g)	Original amount of CaCO3 (g)	% dissolved
H20	CaCO3	0.000255	0.00184	0.00459	0.9933	0.462
H2SO3	CaCO3	0.000681	0.00491	0.0123	0.9998	1.230
H2SO4	CaCO3	0.000438	0.00316	0.00789	1.0104	0.781
H20/CO2	CaCO3	0.00502	0.0362	0.0904	1.0229	8.838
Acid Rain	CaCO3	0.00646	0.0466	0.116	1.017	11.406
H20	CaCO3/Mg(OH)2	0.000581	0.000419	0.00105	0.636741	0.165
H2SO3	CaCO3/Mg(OH)2	0.000079	0.00057	0.00142	0.626157	0.227
H2SO4	CaCO3/Mg(OH)2	0.000075	0.000541	0.00135	0.627354	0.215
H20/CO2	CaCO3/Mg(OH)2	0	0	0	0	0.000
Acid Rain	CaCO3/Mg(OH)2	0.000022	0.000159	0.00397	0.634725	0.625
H20	CaCO3/MgCO3	0.000229	0.000165	0.000412	0.548262	0.075
H2SO3	CaCO3/MgCO3	0.00005	0.00036	0.000902	0.546372	0.165
H2SO4	CaCO3/MgCO3	0.0000656	0.000473	0.00118	0.552744	0.213
H20/CO2	CaCO3/MgCO3	0.000621	0.00448	0.0112	0.552096	2.029
Acid Rain	CaCO3/MgCO3	0.000545	0.00359	0.00897	0.540594	1.659

Table D-2. Data Table on Calcium Ion Concentration [Ca^{2+}]

Chapter 5 Data: Acid Rain Simulation on Model Mortars

Magnesium Ion [Mg^{2+}] Content:

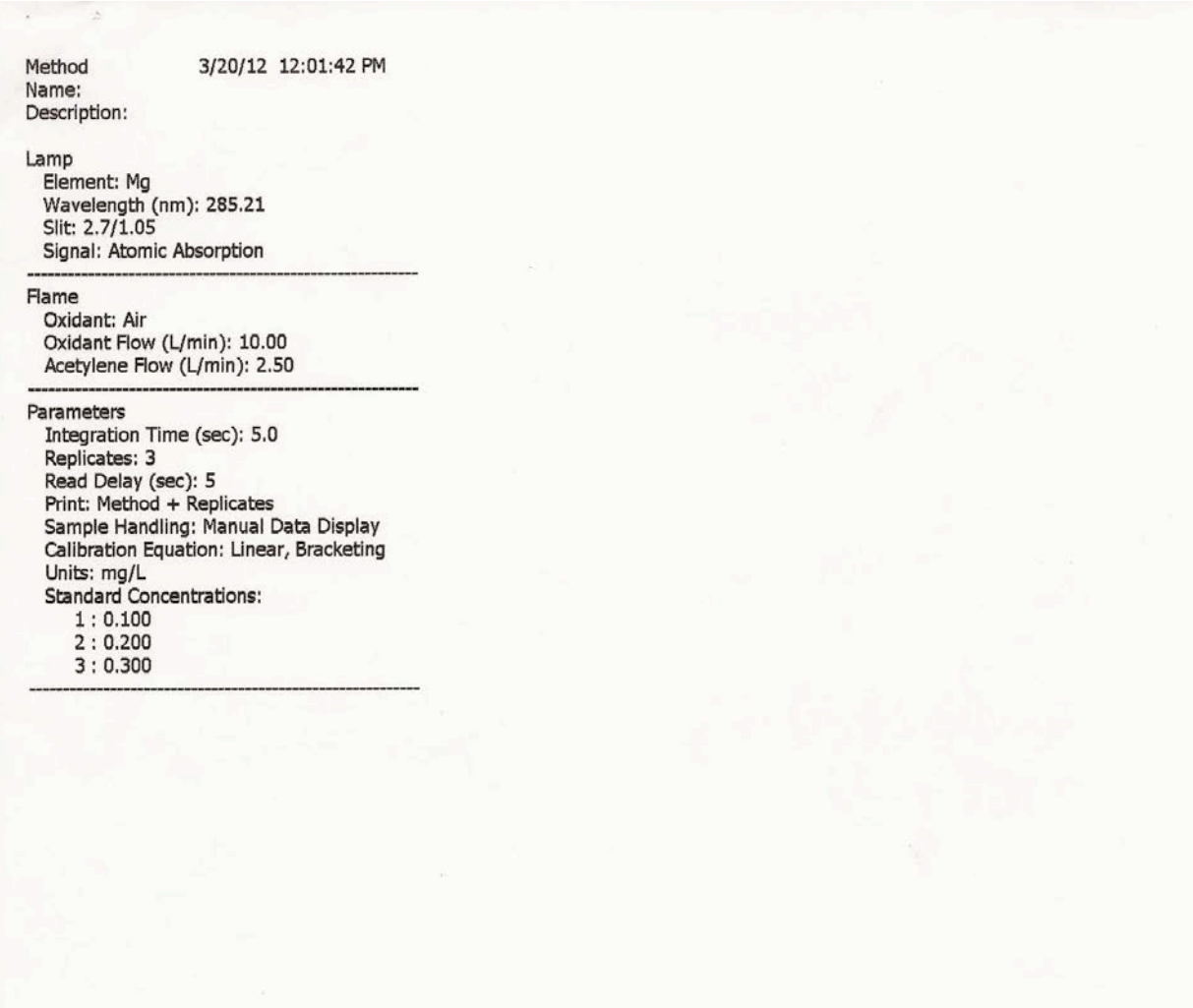

Method 3/20/12 12:01:42 PM
Name:
Description:

Lamp
Element: Mg
Wavelength (nm): 285.21
Slit: 2.7/1.05
Signal: Atomic Absorption

Flame
Oxidant: Air
Oxidant Flow (L/min): 10.00
Acetylene Flow (L/min): 2.50

Parameters
Integration Time (sec): 5.0
Replicates: 3
Read Delay (sec): 5
Print: Method + Replicates
Sample Handling: Manual Data Display
Calibration Equation: Linear, Bracketing
Units: mg/L
Standard Concentrations:
1 : 0.100
2 : 0.200
3 : 0.300

```
==================================================
Element: Mg   Date: 3/20/12   Time: 12:02:08 PM
--------------------------------------------------
Standard 1  3/20/12  12:02:08 PM
Absorbance
0.235  0.234  0.234
Mean: 0.235  SD: 0.0005  RSD(%): 0.2
--------------------------------------------------
Standard 2  3/20/12  12:02:50 PM
Absorbance
0.353  0.351  0.349
Mean: 0.351  SD: 0.0022  RSD(%): 0.6
Standard 2 Applied
--------------------------------------------------
Standard 3  3/20/12  12:03:28 PM
Absorbance
0.489  0.487  0.490
Mean: 0.489  SD: 0.0017  RSD(%): 0.3
Standard 3 Applied
Corr. Coef.: 0.998804   Slope: 1.27098   Intercept: 0.10402
--------------------------------------------------
0.2 PPM  3/20/12  12:04:15 PM
Concentration (mg/L)   Factor: 1.000
0.194  0.195  0.194
Mean: 0.194  SD: 0.0008  RSD(%): 0.4
--------------------------------------------------
Standard 1  3/20/12  12:11:47 PM
Absorbance
0.223  0.223  0.222
Mean: 0.222  SD: 0.0007  RSD(%): 0.3
Standard 1 Applied
--------------------------------------------------
Standard 2  3/20/12  12:12:28 PM
Absorbance
0.352  0.348  0.349
Mean: 0.350  SD: 0.0022  RSD(%): 0.6
Standard 2 Applied
--------------------------------------------------
0.2 PPM  3/20/12  12:13:05 PM
Concentration (mg/L)   Factor: 1.000
0.300  0.302  0.300
Mean: 0.301  SD: 0.0008  RSD(%): 0.3
--------------------------------------------------
Standard 3  3/20/12  12:13:35 PM
Absorbance
0.489  0.490  0.484
Mean: 0.488  SD: 0.0034  RSD(%): 0.7
Standard 3 Applied
Corr. Coef.: 0.999747   Slope: 1.32613   Intercept: 0.08807
--------------------------------------------------
0.2 PPM  3/20/12  12:14:20 PM
Concentration (mg/L)   Factor: 1.000
0.201  0.202  0.201
Mean: 0.201  SD: 0.0006  RSD(%): 0.3
--------------------------------------------------
W DI 1  3/20/12  12:15:18 PM
Concentration (mg/L)   Factor: 500.000
155.766  155.820  154.555
Mean: 155.380  SD: 0.7151  RSD(%): 0.5
```

W DI 2 3/20/12 12:16:05 PM
Concentration (mg/L) Factor: 500.000
94.674 95.215 94.987
Mean: 94.959 SD: 0.2718 RSD(%): 0.3

W DI 3 3/20/12 12:16:48 PM
Concentration (mg/L) Factor: 250.000
65.998 66.869 66.929
Mean: 66.599 SD: 0.5209 RSD(%): 0.8

W DI 4 3/20/12 12:17:33 PM
Concentration (mg/L) Factor: 333.000
68.875 69.165 68.730
Mean: 68.923 SD: 0.2217 RSD(%): 0.3

W DI 5 3/20/12 12:18:16 PM
Concentration (mg/L) Factor: 200.000
35.571 34.936 34.829
Mean: 35.112 SD: 0.4010 RSD(%): 1.1

0.2 PPM 3/20/12 12:19:02 PM
Concentration (mg/L) Factor: 1.000
0.202 0.200 0.199
Mean: 0.200 SD: 0.0015 RSD(%): 0.7

ME DI 1 3/20/12 12:19:46 PM
Concentration (mg/L) Factor: 100.000
15.740 15.773 15.982
Mean: 15.832 SD: 0.1312 RSD(%): 0.8

ME DI 2 3/20/12 12:20:30 PM
Concentration (mg/L) Factor: 100.000
6.930 6.931 6.979
Mean: 6.947 SD: 0.0281 RSD(%): 0.4
Sample signal is less than that of the lowest standard

ME DI 3 3/20/12 12:21:15 PM
Concentration (mg/L) Factor: 33.000
3.293 3.285 3.253
Mean: 3.277 SD: 0.0210 RSD(%): 0.6

ME DI 4 3/20/12 12:22:09 PM
Concentration (mg/L) Factor: 33.000
2.771 2.750 2.726
Mean: 2.749 SD: 0.0224 RSD(%): 0.8
Sample signal is less than that of the lowest standard

ME DI 5 3/20/12 12:22:59 PM
Concentration (mg/L) Factor: 33.000
2.513 2.515 2.514
Mean: 2.514 SD: 0.0012 RSD(%): 0.0
Sample signal is less than that of the lowest standard

0.2 PPM 3/20/12 12:23:42 PM
Concentration (mg/L) Factor: 1.000
0.201 0.200 0.199
Mean: 0.200 SD: 0.0009 RSD(%): 0.4

G H2SO4 1 3/20/12 12:24:58 PM
Concentration (mg/L) Factor: 500.000
169.033 167.665 167.844
Mean: 168.180 SD: 0.7435 RSD(%): 0.4
Sample concentration is greater than that of the highest standard
---
G H2SO4 2 3/20/12 12:25:42 PM
Concentration (mg/L) Factor: 500.000
86.619 85.539 86.370
Mean: 86.176 SD: 0.5655 RSD(%): 0.7

G H2SO4 3 3/20/12 12:26:25 PM
Concentration (mg/L) Factor: 333.000
62.664 62.336 61.696
Mean: 62.232 SD: 0.4926 RSD(%): 0.8

G H2SO4 4 3/20/12 12:27:09 PM
Concentration (mg/L) Factor: 200.000
48.040 47.539 47.683
Mean: 47.754 SD: 0.2582 RSD(%): 0.5

G H2SO4 5 3/20/12 12:27:51 PM
Concentration (mg/L) Factor: 200.000
38.264 38.112 38.068
Mean: 38.148 SD: 0.1031 RSD(%): 0.3

0.2 PPM 3/20/12 12:28:33 PM
Concentration (mg/L) Factor: 1.000
0.202 0.201 0.203
Mean: 0.202 SD: 0.0010 RSD(%): 0.5

W H2SO4 1 3/20/12 12:29:14 PM
Concentration (mg/L) Factor: 500.000
148.371 147.670 147.105
Mean: 147.715 SD: 0.6339 RSD(%): 0.4

WH2SO4 2 3/20/12 12:30:00 PM
Concentration (mg/L) Factor: 500.000
91.855 91.634 91.854
Mean: 91.781 SD: 0.1274 RSD(%): 0.1

W H2SO4 3 3/20/12 12:30:47 PM
Concentration (mg/L) Factor: 333.000
65.672 65.211 65.263
Mean: 65.382 SD: 0.2525 RSD(%): 0.4

W H2SO4 4 3/20/12 12:31:31 PM
Concentration (mg/L) Factor: 200.000
46.843 46.996 46.784
Mean: 46.875 SD: 0.1096 RSD(%): 0.2

W H2SO4 5 3/20/12 12:32:16 PM
Concentration (mg/L) Factor: 200.000
39.898 39.870 39.871
Mean: 39.880 SD: 0.0160 RSD(%): 0.0

0.2 PPM 3/20/12 12:32:58 PM
Concentration (mg/L) Factor: 1.000
0.202 0.201 0.201

Mean: 0.201 SD: 0.0003 RSD(%): 0.1

G H2SO4 1 3/20/12 12:36:32 PM
Concentration (mg/L) Factor: 1000.000
181.281 183.589 183.454
Mean: 182.775 SD: 1.296 RSD(%): 0.7

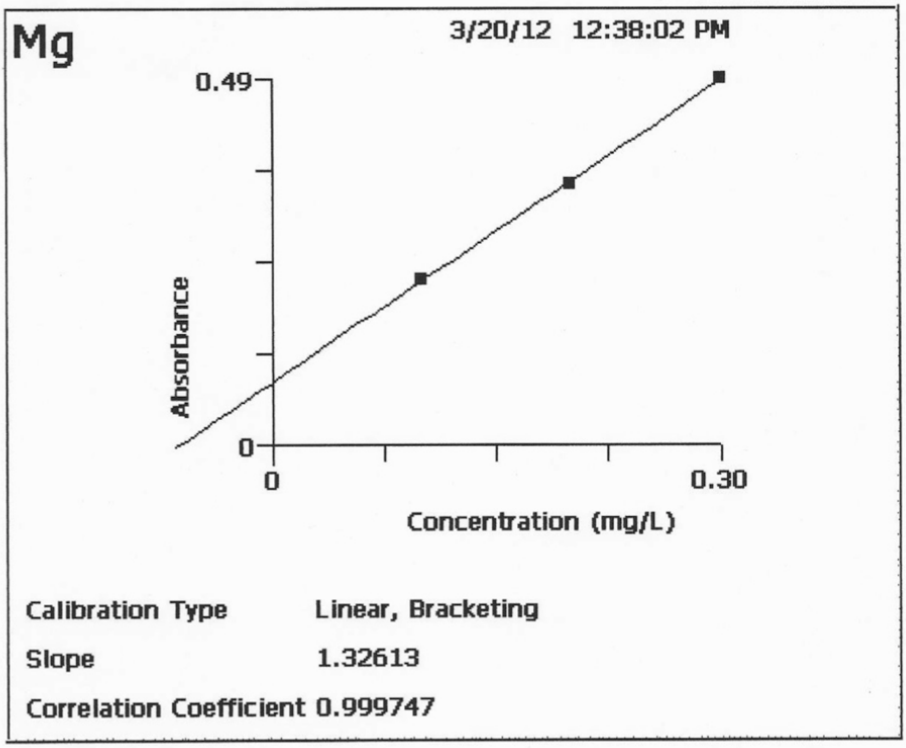
Mg
3/20/12 12:38:02 PM
0.49
0
Absorbance
0
0.30
Concentration (mg/L)
Calibration Type Linear, Bracketing
Slope 1.32613
Correlation Coefficient 0.999747

0.2 PPM 3/20/12 1:38:36 PM
Concentration (mg/L) Factor: 1.000
0.208 0.210 0.209
Mean: 0.209 SD: 0.0009 RSD(%): 0.4

ME H2SO4 1 3/20/12 1:39:30 PM
Concentration (mg/L) Factor: 100.000
18.109 18.021 17.961
Mean: 18.030 SD: 0.0748 RSD(%): 0.4

ME H2SO4 2 3/20/12 1:40:18 PM
Concentration (mg/L) Factor: 50.000
6.920 6.860 6.886
Mean: 6.889 SD: 0.0302 RSD(%): 0.4

ME H2SO4 3 3/20/12 1:41:06 PM
Concentration (mg/L) Factor: 33.000
3.755 3.793 3.753
Mean: 3.767 SD: 0.0228 RSD(%): 0.6

ME H2SO4 4 3/20/12 1:41:51 PM
Concentration (mg/L) Factor: 33.000
2.654 2.653 2.667
Mean: 2.658 SD: 0.0077 RSD(%): 0.3
Sample signal is less than that of the lowest standard

ME H3SO4 5 3/20/12 1:42:39 PM
Concentration (mg/L) Factor: 33.000
1.757 1.747 1.745
Mean: 1.750 SD: 0.0062 RSD(%): 0.4
Sample signal is less than that of the lowest standard

0.2 PPM 3/20/12 1:43:42 PM
Concentration (mg/L) Factor: 1.000
0.207 0.204 0.204
Mean: 0.205 SD: 0.0015 RSD(%): 0.7

G AR 1 3/20/12 1:44:26 PM
Concentration (mg/L) Factor: 1000.000
213.939 211.350 208.577
Mean: 211.289 SD: 2.682 RSD(%): 1.3

G AR 2 3/20/12 1:45:12 PM
Concentration (mg/L) Factor: 500.000
185.736 187.148 188.150
Mean: 187.011 SD: 1.213 RSD(%): 0.6
Sample concentration is greater than that of the highest standard
---
G AR 3 3/20/12 1:45:57 PM
Concentration (mg/L) Factor: 500.000
181.868 180.671 181.773
Mean: 181.437 SD: 0.6650 RSD(%): 0.4
Sample concentration is greater than that of the highest standard
---
G AR 4 3/20/12 1:46:42 PM
Concentration (mg/L) Factor: 500.000
179.858 180.472 181.946
Mean: 180.759 SD: 1.073 RSD(%): 0.6

Sample concentration is greater than that of the highest standard
---
G AR 5 3/20/12 1:47:25 PM
Concentration (mg/L) Factor: 500.000
172.063 171.295 170.795
Mean: 171.384 SD: 0.6389 RSD(%): 0.4
Sample concentration is greater than that of the highest standard
---
2 PPM 3/20/12 1:48:04 PM
Concentration (mg/L) Factor: 1.000
0.204 0.202 0.201
Mean: 0.202 SD: 0.0014 RSD(%): 0.7

W AR 1 3/20/12 1:48:46 PM
Concentration (mg/L) Factor: 500.000
172.083 171.843 171.572
Mean: 171.832 SD: 0.2555 RSD(%): 0.1
Sample concentration is greater than that of the highest standard
---
W AR 2 3/20/12 1:49:35 PM
Concentration (mg/L) Factor: 500.000
207.921 206.547 206.020
Mean: 206.829 SD: 0.9817 RSD(%): 0.5
Sample concentration is greater than that of the highest standard
---
W AR 3 3/20/12 1:50:18 PM
Concentration (mg/L) Factor: 500.000
231.639 231.078 230.243
Mean: 230.987 SD: 0.7027 RSD(%): 0.3
Sample concentration is greater than that of the highest standard
---
W AR 4 3/20/12 1:50:57 PM
Concentration (mg/L) Factor: 500.000
215.715 216.034 216.929
Mean: 216.226 SD: 0.6293 RSD(%): 0.3
Sample concentration is greater than that of the highest standard
---
W AR 5 3/20/12 1:51:50 PM
Concentration (mg/L) Factor: 500.000
215.786 214.553 215.854
Mean: 215.397 SD: 0.7324 RSD(%): 0.3
Sample concentration is greater than that of the highest standard
---
0.2 PPM 3/20/12 1:52:32 PM
Concentration (mg/L) Factor: 1.000
0.203 0.205 0.205
Mean: 0.205 SD: 0.0012 RSD(%): 0.6

ME AR1 3/20/12 1:53:14 PM
Concentration (mg/L) Factor: 200.000
34.050 33.953 34.049
Mean: 34.017 SD: 0.0554 RSD(%): 0.2

ME AR 2 3/20/12 1:53:55 PM
Concentration (mg/L) Factor: 200.000
44.460 44.938 44.558
Mean: 44.652 SD: 0.2522 RSD(%): 0.6

ME AR 3 3/20/12 1:54:37 PM

Concentration (mg/L) Factor: 200.000
50.358 50.855 50.800
Mean: 50.671 SD: 0.2725 RSD(%): 0.5

ME AR 4 3/20/12 1:55:23 PM
Concentration (mg/L) Factor: 200.000
45.064 45.348 45.418
Mean: 45.277 SD: 0.1873 RSD(%): 0.4

ME AR 5 3/20/12 1:56:05 PM
Concentration (mg/L) Factor: 200.000
38.499 38.825 38.590
Mean: 38.638 SD: 0.1681 RSD(%): 0.4

0.2 PPM 3/20/12 1:56:46 PM
Concentration (mg/L) Factor: 1.000
0.201 0.203 0.204
Mean: 0.203 SD: 0.0014 RSD(%): 0.7

H2SO4 3/20/12 1:57:32 PM
Concentration (mg/L) Factor: 1.000
-0.007 -0.007 -0.008
Mean: -0.007 SD: 0.0003 RSD(%): 3.4
Sample signal is less than that of the lowest standard

AR 3/20/12 1:58:12 PM
Concentration (mg/L) Factor: 5.000
1.218 1.218 1.220
Mean: 1.219 SD: 0.0012 RSD(%): 0.1

0.2 PPM 3/20/12 2:17:41 PM
Concentration (mg/L) Factor: 1.000
0.203 0.204 0.204
Mean: 0.203 SD: 0.0003 RSD(%): 0.2

G AR 2 3/20/12 2:18:35 PM
Concentration (mg/L) Factor: 1000.000
191.768 192.848 192.142
Mean: 192.253 SD: 0.5482 RSD(%): 0.3

G AR 3 3/20/12 2:19:22 PM
Concentration (mg/L) Factor: 1000.000
184.658 185.068 184.121
Mean: 184.616 SD: 0.4749 RSD(%): 0.3

G AR 4 3/20/12 2:20:08 PM
Concentration (mg/L) Factor: 1000.000
182.798 185.248 183.338
Mean: 183.795 SD: 1.288 RSD(%): 0.7

G AR 5 3/20/12 2:21:07 PM
Concentration (mg/L) Factor: 1000.000
177.219 177.568 177.264
Mean: 177.350 SD: 0.1894 RSD(%): 0.1
---
2 PPM 3/20/12 2:21:50 PM
Concentration (mg/L) Factor: 1.000
0.197 0.199 0.198
Mean: 0.198 SD: 0.0014 RSD(%): 0.7

W AR 1 3/20/12 2:22:37 PM
Concentration (mg/L) Factor: 1000.000
177.089 176.646 176.061
Mean: 176.599 SD: 0.5155 RSD(%): 0.3

W AR 2 3/20/12 2:23:21 PM
Concentration (mg/L) Factor: 1000.000
214.203 214.050 213.889
Mean: 214.047 SD: 0.1566 RSD(%): 0.1

W AR 3 3/20/12 2:24:15 PM
Concentration (mg/L) Factor: 1000.000
248.264 245.365 244.482
Mean: 246.037 SD: 1.978 RSD(%): 0.8

W AR 4 3/20/12 2:25:04 PM
Concentration (mg/L) Factor: 1000.000
225.324 225.862 226.188
Mean: 225.792 SD: 0.4363 RSD(%): 0.2

W AR 5 3/20/12 2:25:52 PM
Concentration (mg/L) Factor: 1000.000
226.100 226.619 226.327
Mean: 226.349 SD: 0.2604 RSD(%): 0.1

0.2 PPM 3/20/12 2:26:34 PM
Concentration (mg/L) Factor: 1.000
0.199 0.200 0.200
Mean: 0.200 SD: 0.0005 RSD(%): 0.2

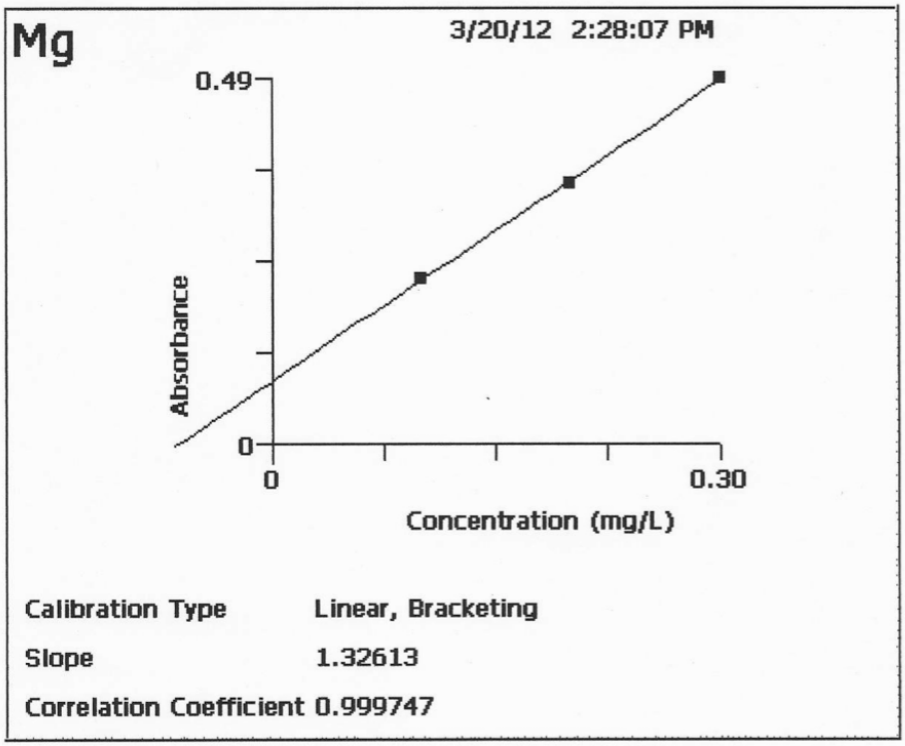
Mg
3/20/12 2:28:07 PM
0.49
Absorbance
0
0
0.30
Concentration (mg/L)
Calibration Type Linear, Bracketing
Slope 1.32613
Correlation Coefficient 0.999747

Calcium Ion [Ca^{2+}] Content:

Method 3/19/12 3:08:26 PM
Name:
Description:

Lamp
Element: Ca
Wavelength (nm): 422.67
Slit: 2.7/0.6
Signal: Atomic Absorption

Flame
Oxidant: Air
Oxidant Flow (L/min): 10.00
Acetylene Flow (L/min): 3.00

Parameters
Integration Time (sec): 5.0
Replicates: 3
Read Delay (sec): 5
Print: Method + Replicates
Sample Handling: Manual Data Display
Calibration Equation: Linear, Bracketing
Units: mg/L
Standard Concentrations:
1 : 1.000
2 : 2.000
3 : 3.000

==========
Element: Ca Date: 3/19/12 Time: 3:08:51 PM

Standard 1 3/19/12 3:08:51 PM
Absorbance
0.157 0.157 0.156
Mean: 0.157 SD: 0.0002 RSD(%): 0.1

Standard 2 3/19/12 3:09:39 PM
Absorbance
0.235 0.234 0.234
Mean: 0.234 SD: 0.0005 RSD(%): 0.2
Standard 2 Applied

Standard 3 3/19/12 3:10:26 PM
Absorbance
0.306 0.307 0.304
Mean: 0.306 SD: 0.0013 RSD(%): 0.4
Standard 3 Applied
Corr. Coef.: 0.999735 Slope: 0.07454 Intercept: 0.08297
---
2 PPM 3/19/12 3:11:17 PM
Concentration (mg/L) Factor: 1.000
2.021 2.023 1.985
Mean: 2.010 SD: 0.0213 RSD(%): 1.1

W DI 1 3/19/12 3:12:30 PM
Concentration (mg/L) Factor: 50.000
150.252 151.786 150.234
Mean: 150.758 SD: 0.8911 RSD(%): 0.6

W DI 2 3/19/12 3:13:19 PM
Concentration (mg/L) Factor: 50.000
111.224 109.883 109.441
Mean: 110.182 SD: 0.9284 RSD(%): 0.8

W DI 3 3/19/12 3:14:07 PM
Concentration (mg/L) Factor: 100.000
205.515 206.625 206.558
Mean: 206.233 SD: 0.6226 RSD(%): 0.3

W DI 4 3/19/12 3:14:53 PM
Concentration (mg/L) Factor: 100.000
480.411 482.507 480.683
Mean: 481.200 SD: 1.140 RSD(%): 0.2
Sample concentration is greater than that of the highest standard
---
W DI 5 3/19/12 3:15:52 PM
Concentration (mg/L) Factor: 100.000
349.799 352.807 352.959
Mean: 351.855 SD: 1.782 RSD(%): 0.5
Sample concentration is greater than that of the highest standard
---
2PPM 3/19/12 3:16:48 PM
Concentration (mg/L) Factor: 1.000
1.990 1.995 2.018
Mean: 2.001 SD: 0.0149 RSD(%): 0.7

ME DI 1 3/19/12 3:17:51 PM

Concentration (mg/L) Factor: 200.000
433.343 438.035 434.661
Mean: 435.346 SD: 2.420 RSD(%): 0.6

ME DI 2 3/19/12 3:18:39 PM
Concentration (mg/L) Factor: 200.000
422.748 421.573 422.258
Mean: 422.193 SD: 0.5903 RSD(%): 0.1

ME DI 3 3/19/12 3:19:19 PM
Concentration (mg/L) Factor: 200.000
411.509 406.816 411.504
Mean: 409.943 SD: 2.708 RSD(%): 0.7

ME DI 4 3/19/12 3:20:02 PM
Concentration (mg/L) Factor: 200.000
414.428 411.780 414.276
Mean: 413.495 SD: 1.487 RSD(%): 0.4

ME DI 5 3/19/12 3:20:46 PM
Concentration (mg/L) Factor: 200.000
400.129 400.224 399.916
Mean: 400.089 SD: 0.1580 RSD(%): 0.0
---
2 PPM 3/19/12 3:21:33 PM
Concentration (mg/L) Factor: 1.000
2.027 2.010 1.994
Mean: 2.010 SD: 0.0167 RSD(%): 0.8

W DI 4 3/19/12 3:22:43 PM
Concentration (mg/L) Factor: 200.000
346.659 348.793 346.881
Mean: 347.445 SD: 1.173 RSD(%): 0.3

W DI 5 3/19/12 3:23:34 PM
Concentration (mg/L) Factor: 200.000
158.627 159.277 158.582
Mean: 158.829 SD: 0.3888 RSD(%): 0.2

2PPM 3/19/12 3:25:32 PM
Concentration (mg/L) Factor: 1.000
2.023 2.009 2.004
Mean: 2.012 SD: 0.0098 RSD(%): 0.5

G H2SO4 1 3/19/12 3:26:29 PM
Concentration (mg/L) Factor: 100.000
235.329 238.640 237.895
Mean: 237.288 SD: 1.737 RSD(%): 0.7

G H2SO4 2 3/19/12 3:27:13 PM
Concentration (mg/L) Factor: 100.000
298.584 299.889 299.543
Mean: 299.339 SD: 0.6760 RSD(%): 0.2

G H2SO4 3 3/19/12 3:27:56 PM
Concentration (mg/L) Factor: 200.000
308.260 315.049 314.112
Mean: 312.474 SD: 3.679 RSD(%): 1.2

G H2SO4 4 3/19/12 3:28:38 PM
Concentration (mg/L) Factor: 200.000
346.307 348.099 351.104
Mean: 348.503 SD: 2.424 RSD(%): 0.7

G H2SO4 5 3/19/12 3:29:22 PM
Concentration (mg/L) Factor: 200.000
311.899 313.689 313.966
Mean: 313.185 SD: 1.122 RSD(%): 0.4
---
2 PPM 3/19/12 3:30:02 PM
Concentration (mg/L) Factor: 1.000
2.016 2.039 2.027
Mean: 2.027 SD: 0.0114 RSD(%): 0.6

W H2SO4 1 3/19/12 3:31:21 PM
Concentration (mg/L) Factor: 50.000
118.597 120.216 119.733
Mean: 119.515 SD: 0.8314 RSD(%): 0.7

W H2SO4 2 3/19/12 3:32:12 PM
Concentration (mg/L) Factor: 100.000
122.756 123.669 121.273
Mean: 122.566 SD: 1.209 RSD(%): 1.0

W H2SO4 3 3/19/12 3:32:55 PM
Concentration (mg/L) Factor: 100.000
130.933 132.485 130.733
Mean: 131.383 SD: 0.9590 RSD(%): 0.7

W H2SO4 4 3/19/12 3:33:45 PM
Concentration (mg/L) Factor: 100.000
182.515 185.203 185.668
Mean: 184.462 SD: 1.702 RSD(%): 0.9

W H2SO4 5 3/19/12 3:34:28 PM
Concentration (mg/L) Factor: 100.000
115.391 115.102 115.446
Mean: 115.313 SD: 0.1846 RSD(%): 0.2
---
2 PPM 3/19/12 3:35:07 PM
Concentration (mg/L) Factor: 1.000
2.017 2.002 2.029
Mean: 2.016 SD: 0.0135 RSD(%): 0.7

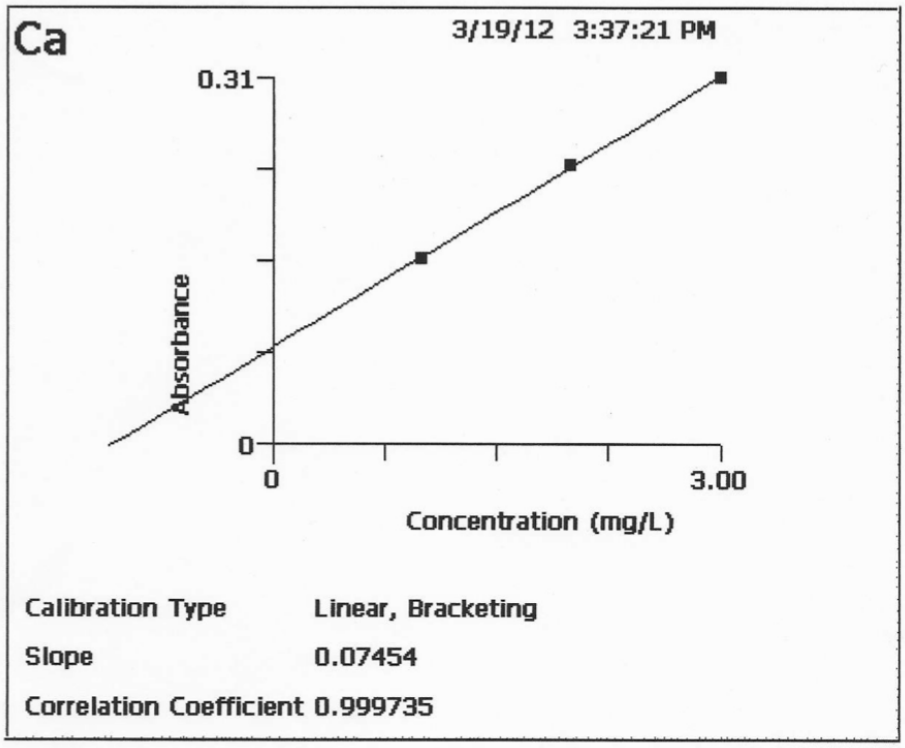
Ca
3/19/12 3:37:21 PM
0.31
0
Absorbance
0
3.00
Concentration (mg/L)
Calibration Type Linear, Bracketing
Slope 0.07454
Correlation Coefficient 0.999735

---
2 PPM 3/19/12 4:32:34 PM
Concentration (mg/L) Factor: 1.000
1.890 1.893 1.895
Mean: 1.893 SD: 0.0023 RSD(%): 0.1

Standard 1 3/19/12 4:34:03 PM
Absorbance
0.152 0.152 0.153
Mean: 0.152 SD: 0.0004 RSD(%): 0.3
Standard 1 Applied

Standard 2 3/19/12 4:34:43 PM
Absorbance
0.227 0.229 0.227
Mean: 0.228 SD: 0.0008 RSD(%): 0.4
Standard 2 Applied

Standard 3 3/19/12 4:35:22 PM
Absorbance
0.298 0.300 0.299
Mean: 0.299 SD: 0.0007 RSD(%): 0.2
Standard 3 Applied
Corr. Coef.: 0.999873 Slope: 0.07329 Intercept: 0.07975
---
2 PPM 3/19/12 4:36:04 PM
Concentration (mg/L) Factor: 1.000
2.026 2.037 2.042
Mean: 2.035 SD: 0.0083 RSD(%): 0.4

ME H2SO4 1 3/19/12 4:36:44 PM
Concentration (mg/L) Factor: 200.000
306.938 305.336 306.432
Mean: 306.235 SD: 0.8191 RSD(%): 0.3

ME H2SO4 2 3/19/12 4:37:19 PM
Concentration (mg/L) Factor: 200.000
349.764 350.929 353.113
Mean: 351.269 SD: 1.700 RSD(%): 0.5

ME H2SO4 3 3/19/12 4:37:55 PM
Concentration (mg/L) Factor: 200.000
368.879 371.007 373.205
Mean: 371.030 SD: 2.163 RSD(%): 0.6

ME H2SO4 4 3/19/12 4:38:34 PM
Concentration (mg/L) Factor: 200.000
344.131 344.521 347.684
Mean: 345.445 SD: 1.948 RSD(%): 0.6

ME H2SO4 5 3/19/12 4:39:14 PM
Concentration (mg/L) Factor: 200.000
356.219 359.686 359.974
Mean: 358.626 SD: 2.090 RSD(%): 0.6
---
2 PPM 3/19/12 4:39:56 PM
Concentration (mg/L) Factor: 1.000
2.047 2.036 2.040
Mean: 2.041 SD: 0.0054 RSD(%): 0.3

G AR 1 3/19/12 4:40:54 PM
Concentration (mg/L) Factor: 100.000
240.613 242.423 240.777
Mean: 241.271 SD: 1.001 RSD(%): 0.4

G AR 2 3/19/12 4:41:36 PM
Concentration (mg/L) Factor: 50.000
182.962 184.194 184.391
Mean: 183.849 SD: 0.7743 RSD(%): 0.4
Sample concentration is greater than that of the highest standard
---
G AR 3 3/19/12 4:42:16 PM
Concentration (mg/L) Factor: 66.667
128.395 128.865 128.731
Mean: 128.664 SD: 0.2421 RSD(%): 0.2

G AR 4 3/19/12 4:42:59 PM
Concentration (mg/L) Factor: 33.000
56.998 57.139 57.356
Mean: 57.164 SD: 0.1804 RSD(%): 0.3

G AR 5 3/19/12 4:43:47 PM
Concentration (mg/L) Factor: 40.000
54.846 55.225 55.097
Mean: 55.056 SD: 0.1929 RSD(%): 0.4
---
2 PPM 3/19/12 4:44:26 PM
Concentration (mg/L) Factor: 1.000
2.045 2.050 2.069
Mean: 2.055 SD: 0.0126 RSD(%): 0.6

W AR 1 3/19/12 4:45:08 PM
Concentration (mg/L) Factor: 66.667
112.448 113.251 113.797
Mean: 113.165 SD: 0.6787 RSD(%): 0.6

W AR 2 3/19/12 4:45:47 PM
Concentration (mg/L) Factor: 66.667
66.084 66.148 66.382
Mean: 66.204 SD: 0.1567 RSD(%): 0.2

W AR 3 3/19/12 4:46:28 PM
Concentration (mg/L) Factor: 66.667
95.475 95.867 95.955
Mean: 95.766 SD: 0.2557 RSD(%): 0.3

W AR 4 3/19/12 4:47:07 PM
Concentration (mg/L) Factor: 66.667
118.961 119.359 119.624
Mean: 119.315 SD: 0.3339 RSD(%): 0.3

W AR 5 3/19/12 4:47:51 PM
Concentration (mg/L) Factor: 66.667
96.315 96.671 96.867
Mean: 96.618 SD: 0.2799 RSD(%): 0.3
---
2 PPM 3/19/12 4:48:36 PM
Concentration (mg/L) Factor: 1.000

2.037 2.059 2.063
Mean: 2.053 SD: 0.0142 RSD(%): 0.7

ME AR 1 3/19/12 4:49:27 PM
Concentration (mg/L) Factor: 200.000
248.016 252.362 253.096
Mean: 251.158 SD: 2.746 RSD(%): 1.1

ME AR 2 3/19/12 4:50:12 PM
Concentration (mg/L) Factor: 100.000
264.612 265.637 266.169
Mean: 265.473 SD: 0.7916 RSD(%): 0.3

ME AR 3 3/19/12 4:50:55 PM
Concentration (mg/L) Factor: 100.000
300.814 302.785 300.777
Mean: 301.458 SD: 1.149 RSD(%): 0.4

ME AR 4 3/19/12 4:51:38 PM
Concentration (mg/L) Factor: 100.000
245.462 245.146 247.107
Mean: 245.905 SD: 1.053 RSD(%): 0.4

ME AR 5 3/19/12 4:52:24 PM
Concentration (mg/L) Factor: 100.000
302.803 301.171 301.890
Mean: 301.954 SD: 0.8181 RSD(%): 0.3
---
2 PPM 3/19/12 4:53:07 PM
Concentration (mg/L) Factor: 1.000
2.051 2.071 2.072
Mean: 2.065 SD: 0.0117 RSD(%): 0.6

G AR 2 3/19/12 4:57:49 PM
Concentration (mg/L) Factor: 100.000
325.569 329.052 330.370
Mean: 328.330 SD: 2.480 RSD(%): 0.8

H2SO4 3/19/12 5:01:02 PM
Concentration (mg/L) Factor: 1.000
-0.276 -0.279 -0.274
Mean: -0.276 SD: 0.0028 RSD(%): 1.0
Sample signal is less than that of the lowest standard

AR 3/19/12 5:01:46 PM
Concentration (mg/L) Factor: 5.000
5.045 5.097 5.042
Mean: 5.061 SD: 0.0309 RSD(%): 0.6

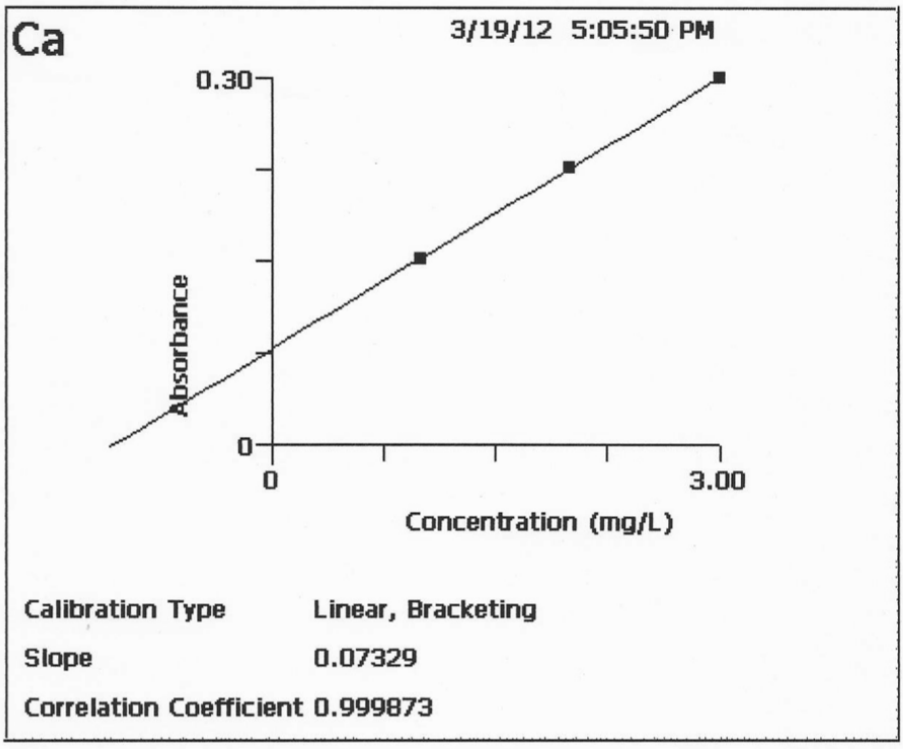
Ca
3/19/12 5:05:50 PM
0.30
Absorbance
0
0
3.00
Concentration (mg/L)
Calibration Type Linear, Bracketing
Slope 0.07329
Correlation Coefficient 0.999873

Graymont Mortar Exposed to DI Water

Solution Added (mL)	[Mg2+] in Runoff (ppm)	[Mg2+] in Runoff (mM)	Brucite dissolved (mg)
10	232.6	9.57	5.58
20	111.858	4.60	2.68
30	73.61	3.03	1.77
40	53.515	2.20	1.28
50	42.423	1.75	1.02

Table D-3. Magnesium Ion Concentration [Mg^{2+}] in DI water runoff from Graymont mortar.

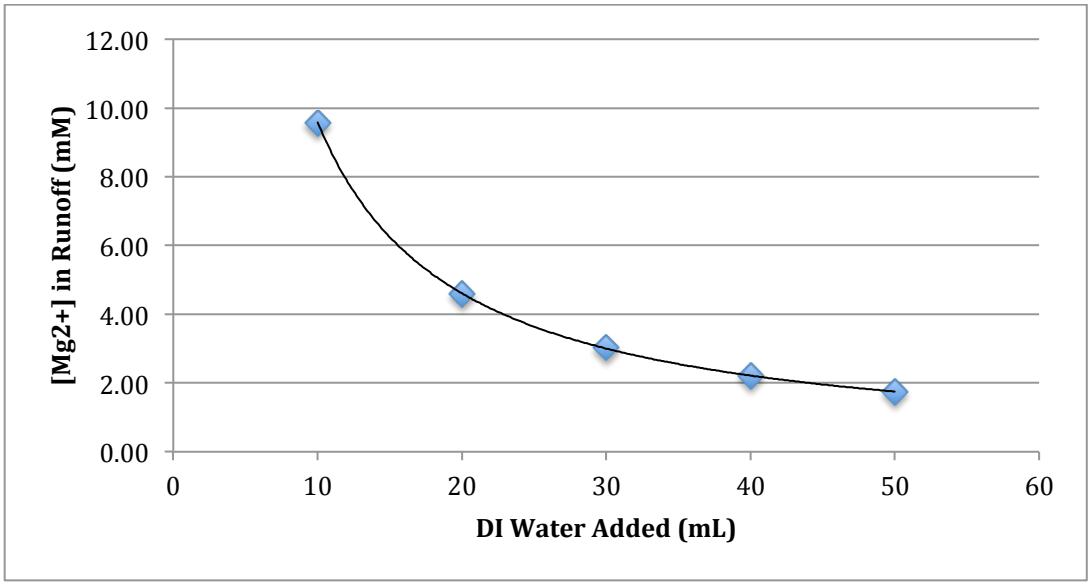

Figure D-1. Magnesium Ion Concentration [Mg^{2+}] in DI water runoff from Graymont mortar.

Solution Added (mL)	[Ca2+] in Runoff (ppm)	[Ca2+] in Runoff (mM)
10	163.352	4.08
20	123.676	3.09
30	268.107	6.69
40	199.208	4.97
50	206.428	5.15

Table D-4. Calcium Ion Concentration [Ca^{2+}] in DI water runoff from Graymont mortar.

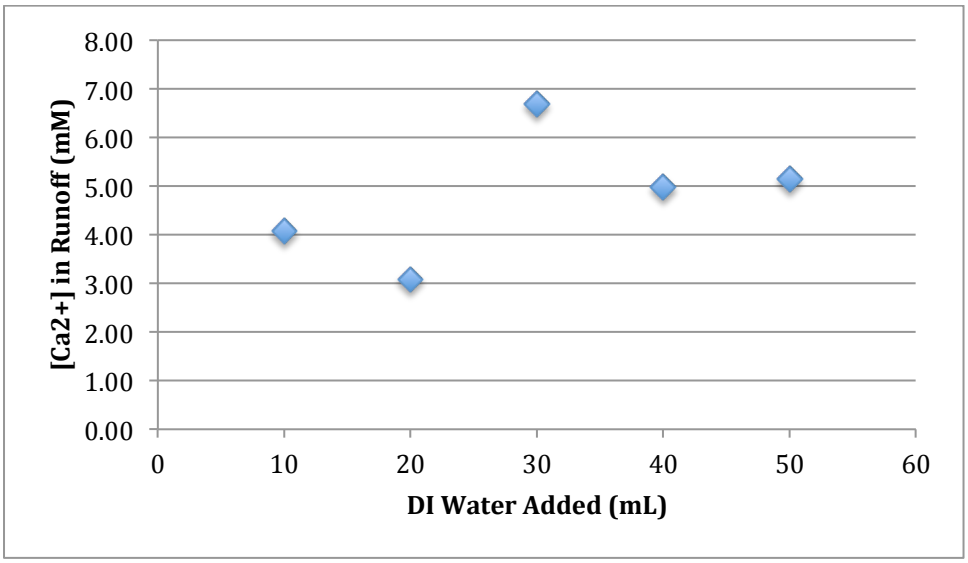

Figure D-2. Calcium Ion Concentration [Ca^{2+}] in DI water runoff from Graymont mortar.

Graymont Mortar Exposed to Dilute Sulfuric Acid

Solution Added (mL)	[Mg2+] in Runoff (ppm)	[Mg2+] in Runoff (mM)	Brucite dissolved (mg)
10	182.775	7.52	4.38
20	86.176	3.54	2.07
30	62.232	2.56	1.49
40	47.754	1.96	1.15
50	38.148	1.57	0.92

Table D-5. Magnesium Ion Concentration [Mg^{2+}] in dilute sulfuric acid runoff from Graymont mortar.

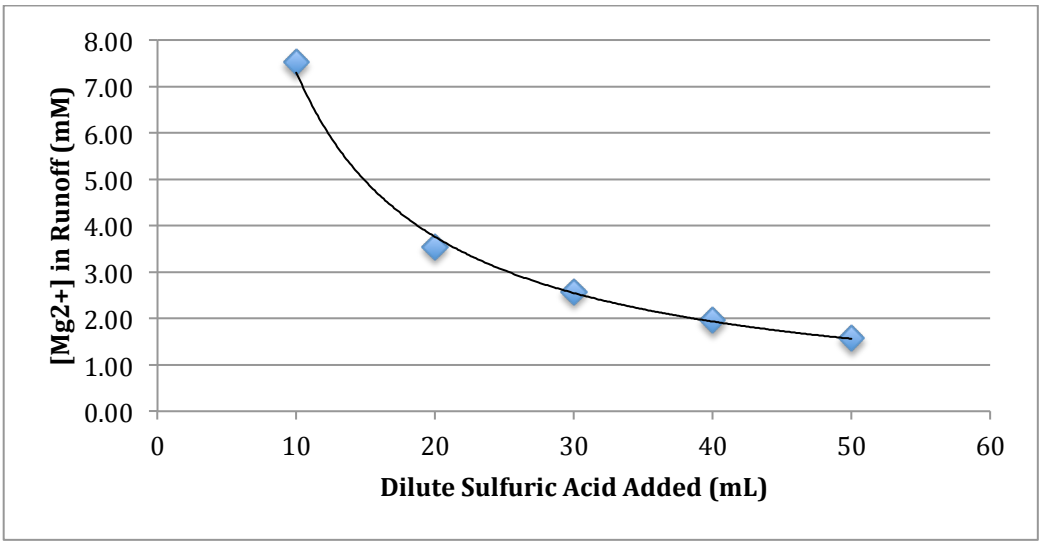

Figure D-3. Magnesium Ion Concentration [Mg^{2+}] in dilute sulfuric acid runoff from Graymont mortar.

Solution Added (mL)	[Ca2+] in Runoff (ppm)	[Ca2+] in Runoff (mM)
10	237.288	5.92
20	299.339	7.47
30	312.474	7.80
40	348.503	8.70
50	313.185	7.81

Table D-6. Calcium Ion Concentration [Ca^{2+}] in dilute sulfuric acid runoff from Graymont mortar.

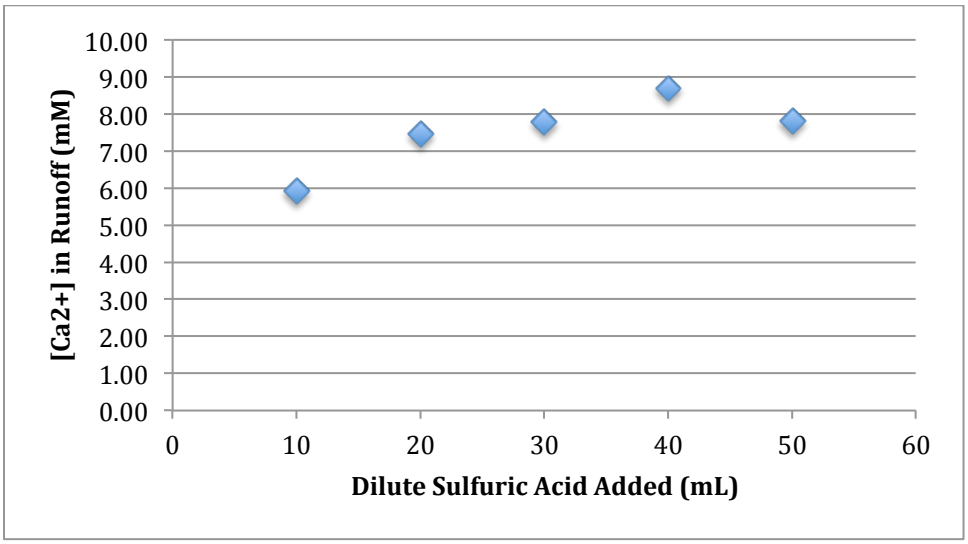

Figure D-4. Calcium Ion Concentration [Ca^{2+}] in dilute sulfuric acid runoff from Graymont mortar.

Graymont Mortar Exposed to Acid Rain Simulant

Solution Added (mL)	[Mg2+] in Runoff (ppm)	[Mg2+] Runoff-[Mg2+] Soln	[Mg2+] in Runoff (mM)	Brucite dissolved (mg)
10	211.289	210.07	8.64	5.04
20	192.253	191.03	7.86	4.58
30	184.616	183.40	7.54	4.40
40	183.795	182.58	7.51	4.38
50	177.35	176.13	7.25	4.23

Table D-7. Magnesium Ion Concentration [Mg^{2+}] in acid rain runoff from Graymont mortar.

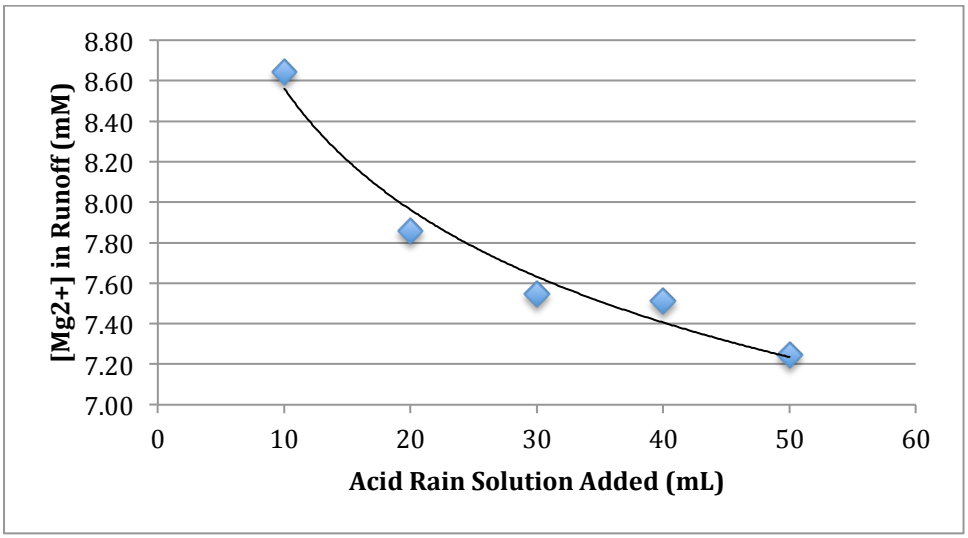

Figure D-5. Magnesium Ion Concentration [Mg^{2+}] in acid rain runoff from Graymont mortar.

Solution Added (mL)	[Ca2+] in Runoff (ppm)	[Ca2+] Runoff-[Ca2+] Soln	[Ca2+] in Runoff (mM)
10	241.271	236.21	5.893463074
20	328.33	323.27	8.065593812
30	128.664	123.60	3.083907186
40	57.164	52.10	1.29997505
50	55.056	50.00	1.24738024

Table D-8. Calcium Ion Concentration [Ca^{2+}] in acid rain runoff from Graymont mortar.

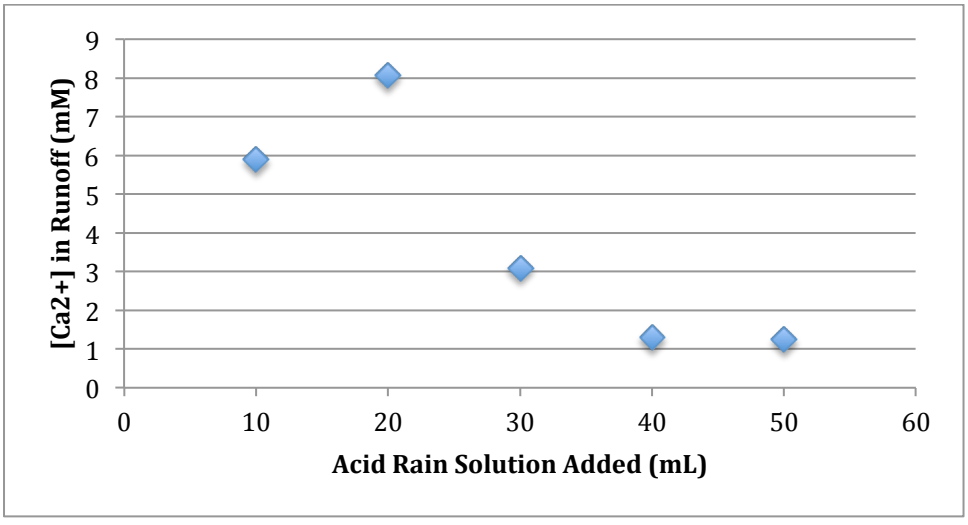

Figure D-6. Calcium Ion Concentration [Ca^{2+}] in acid rain runoff from Graymont mortar.

Western Mortar Exposed to DI Water

Solution Added (mL)	[Mg2+] in Runoff (ppm)	[Mg2+] in Runoff (mM)	Brucite dissolved (mg)
10	155.38	6.39	3.73
20	94.959	3.91	2.28
30	66.599	2.74	1.60
40	68.923	2.84	1.65
50	35.112	1.44	0.84

Table D-9. Magnesium Ion Concentration [Mg^{2+}] in DI water runoff from Western mortar.

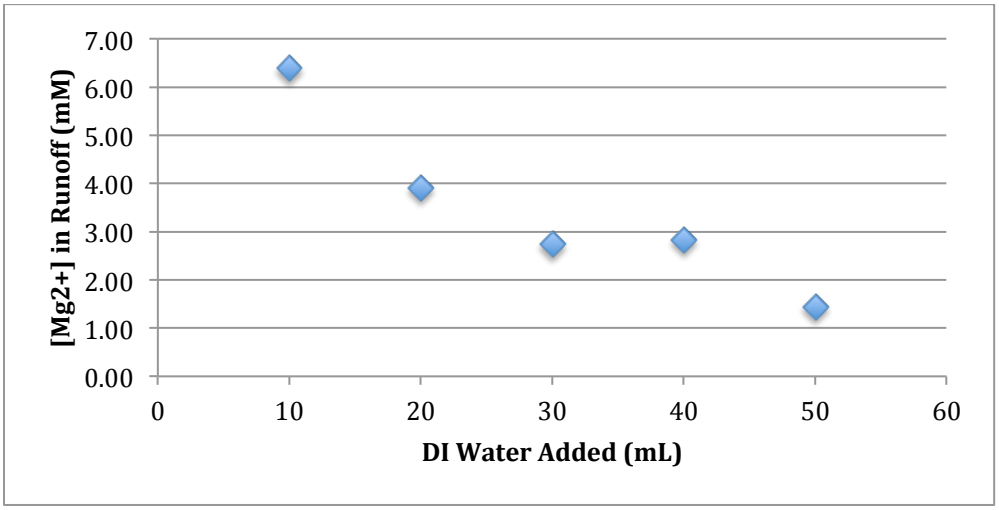

Figure D-7. Magnesium Ion Concentration [Mg^{2+}] in DI water runoff from Western mortar.

Solution Added (mL)	[Ca2+] in Runoff (ppm)	[Ca2+] in Runoff (mM)
10	150.786	3.76
20	110.182	2.75
30	206.233	5.15
40	347.445	8.67
50	158.829	3.96

Table D-10. Calcium Ion Concentration [Ca^{2+}] in DI water runoff from Western mortar.

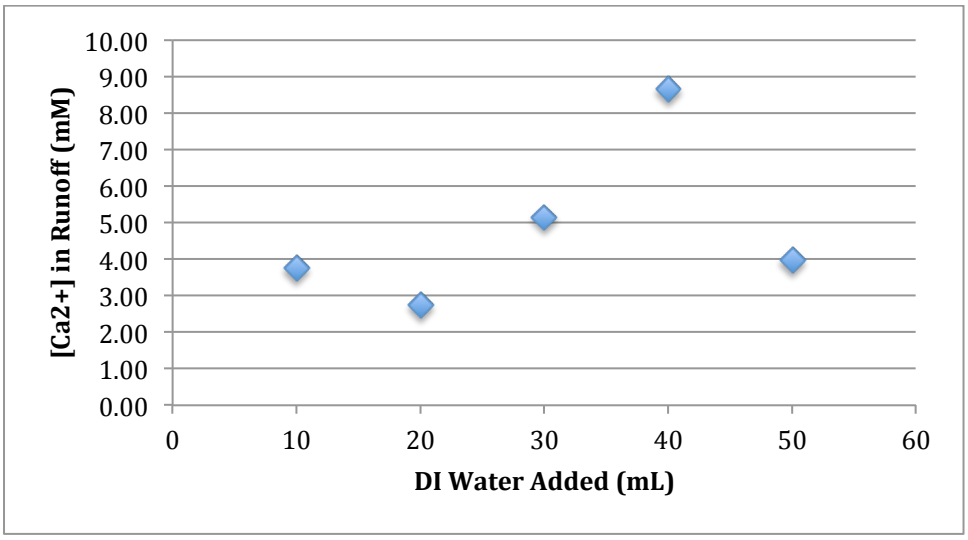

Figure D-8. Calcium Ion Concentration [Ca^{2+}] in DI water runoff from Western mortar.

Western Mortar Exposed to Dilute Sulfuric Acid

Solution Added (mL)	[Mg2+] in Runoff (ppm)	[Mg2+] in Runoff (mM)	Brucite dissolved (mg)
10	147.715	6.08	3.54
20	91.781	3.78	2.20
30	65.382	2.69	1.57
40	46.875	1.93	1.12
50	39.88	1.64	0.96

Table D-11. Magnesium Ion Concentration [Mg^{2+}] in dilute sulfuric acid runoff from Western mortar.

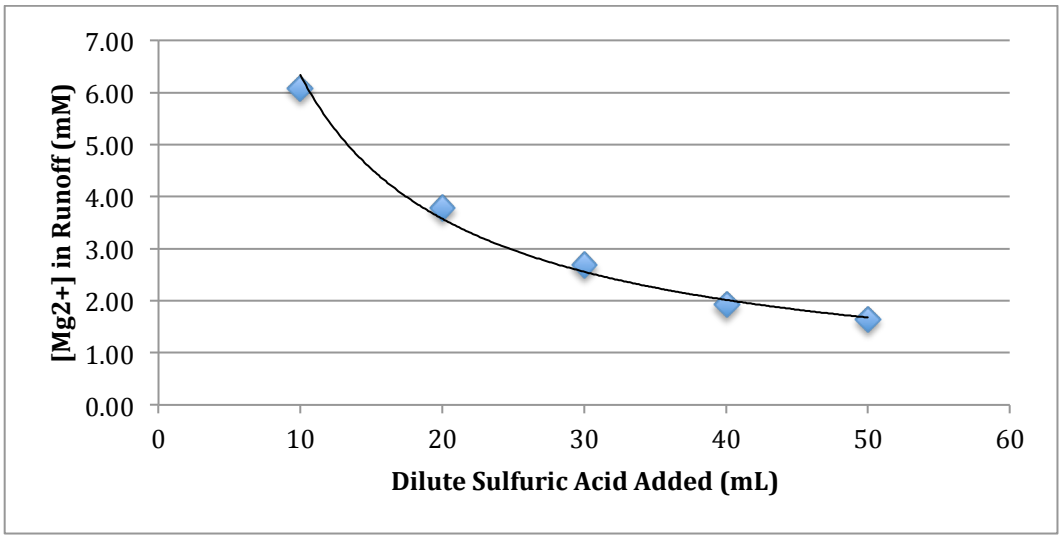

Figure D-9. Magnesium Ion Concentration [Mg^{2+}] in dilute sulfuric acid runoff from Western mortar.

Solution Added (mL)	[Ca2+] in Runoff (ppm)	[Ca2+] in Runoff (mM)
10	119.515	2.98
20	122.566	3.06
30	131.383	3.28
40	184.462	4.60
50	115.313	2.88

Table D-12. Calcium Ion Concentration [Ca^{2+}] in dilute sulfuric acid runoff from Western mortar.

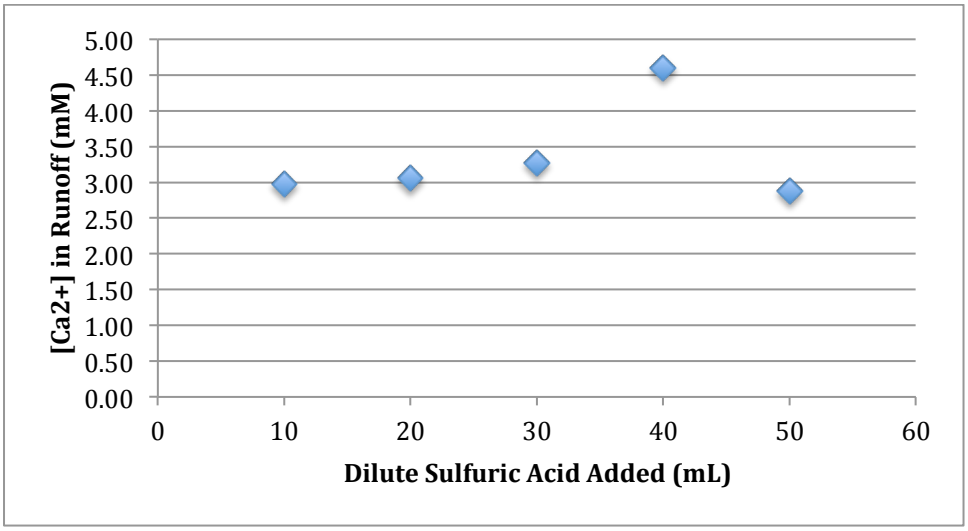

Figure D-10. Calcium Ion Concentration [Ca^{2+}] in dilute sulfuric acid runoff from Western mortar.

Western Mortar Exposed to Acid Rain Simulant

Solution Added (mL)	[Mg2+] in Runoff (ppm)	[Mg2+] Runoff-[Mg2+] Soln	[Mg2+] in Runoff (mM)	Brucite dissolved (mg)
10	176.599	175.38	7.21	4.21
20	214.047	212.83	8.75	5.11
30	246.037	244.82	10.07	5.87
40	225.792	224.57	9.24	5.39
50	226.349	225.13	9.26	5.40

Table D-13. Magnesium Ion Concentration [Mg^{2+}] in acid rain runoff from Western mortar.

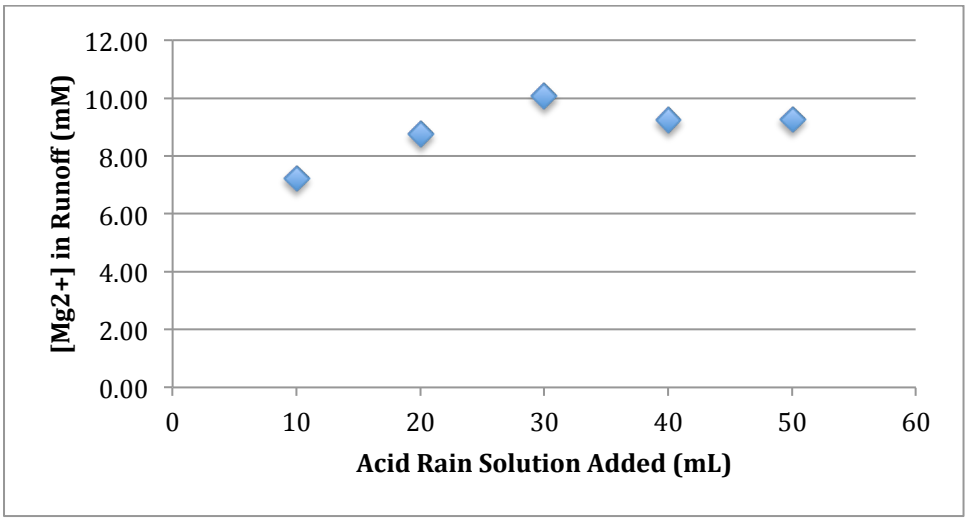

Figure D-11. Magnesium Ion Concentration [Mg^{2+}] in acid rain runoff from Western mortar.

Solution Added (mL)	[Ca2+] in Runoff (ppm)	[Ca2+] Runoff-[Ca2+] Soln	[Ca2+] in Runoff (mM)
10	113.165	108.10	2.697205589
20	66.204	61.14	1.525523952
30	95.766	90.71	2.263098802
40	119.315	114.25	2.850648703
50	96.618	91.56	2.284356287

Table D-14. Calcium Ion Concentration [Ca^{2+}] in acid rain runoff from Western mortar.

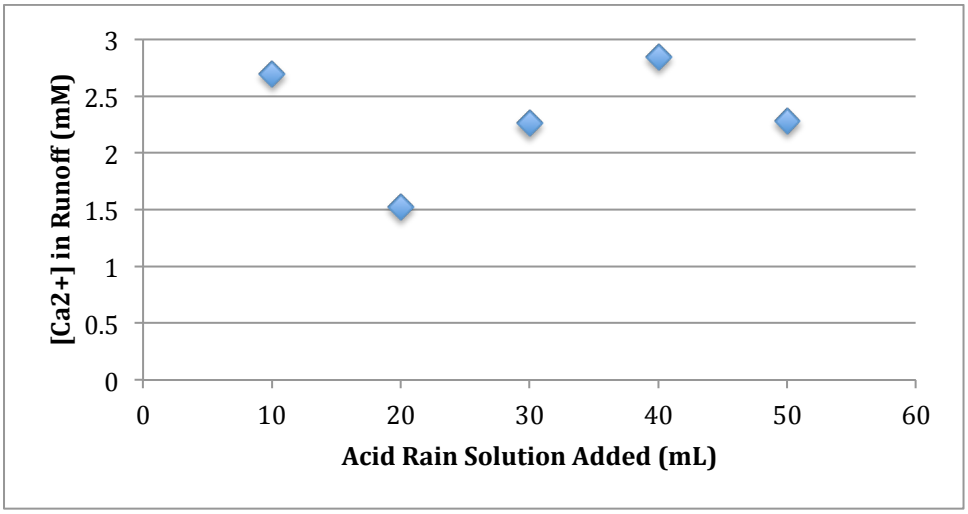

Figure D-12. Calcium Ion Concentration [Ca^{2+}] in acid rain runoff from Western mortar.

Mercer Mortar Exposed to DI Water

Solution Added (mL)	[Mg2+] in Runoff (ppm)	[Mg2+] in Runoff (mM)
10	15.832	0.65
20	6.947	0.29
30	3.277	0.13
40	2.749	0.11
50	2.514	0.10

Table D-15. Magnesium Ion Concentration [Mg^{2+}] in DI water runoff from Mercer mortar.

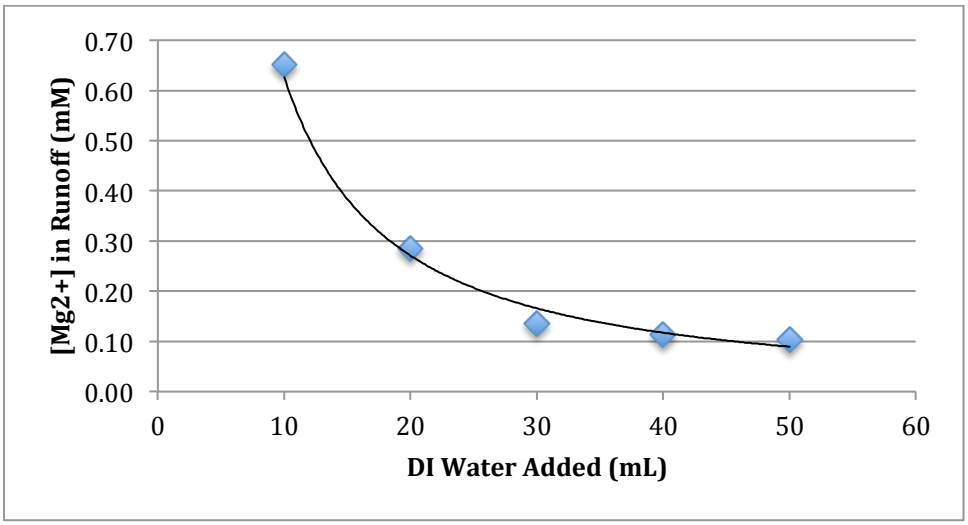

Figure D-13. Magnesium Ion Concentration [Mg^{2+}] in DI water runoff from Mercer mortar.

Solution Added (mL)	[Ca2+] in Runoff (ppm)	[Ca2+] in Runoff (mM)
10	435.346	10.86
20	422.193	10.53
30	409.943	10.23
40	413.495	10.32
50	400.089	9.98

Table D-16. Calcium Ion Concentration [Ca^{2+}] in DI water runoff from Mercer mortar.

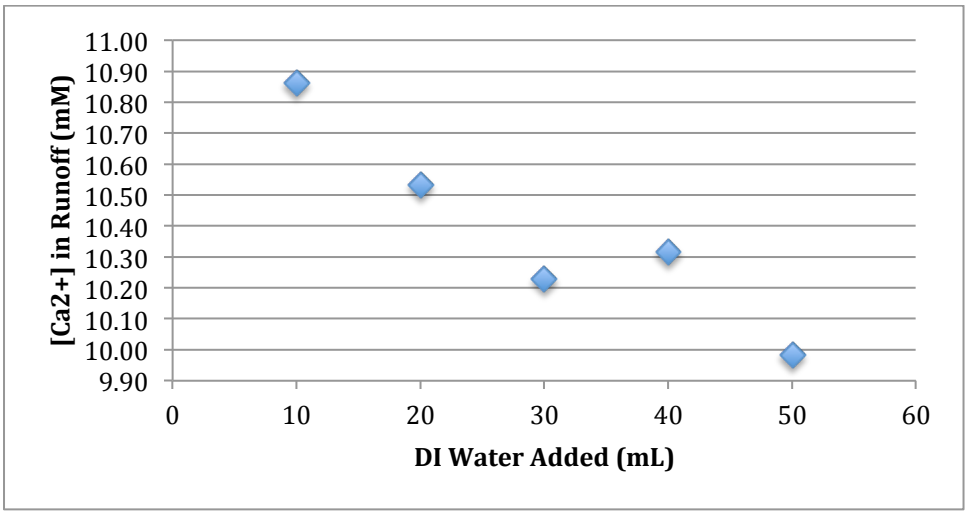

Figure D-14. Calcium Ion Concentration [Ca^{2+}] in DI water runoff from Mercer mortar.

Mercer Mortar Exposed to Dilute Sulfuric Acid

Solution Added (mL)	[Mg2+] in Runoff (ppm)	[Mg2+] in Runoff (mM)
10	18.03	0.74
20	6.889	0.28
30	3.767	0.15
40	2.658	0.11
50	1.75	0.07

Table D-17. Magnesium Ion Concentration [Mg^{2+}] in dilute sulfuric acid runoff from Mercer mortar.

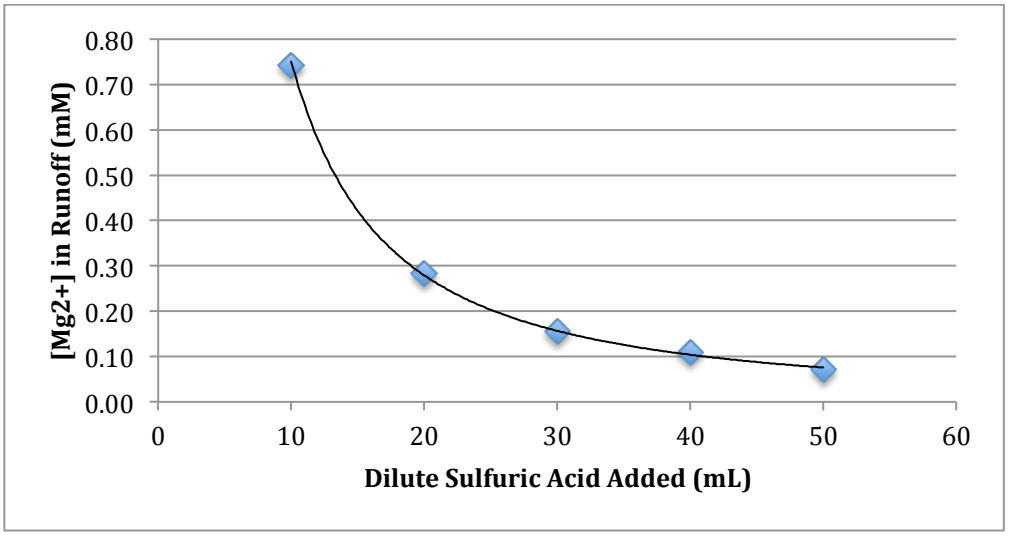

Figure D-15. Magnesium Ion Concentration [Mg^{2+}] in dilute sulfuric acid runoff from Mercer mortar.

Solution Added (mL)	[Ca2+] in Runoff (ppm)	[Ca2+] in Runoff (mM)
10	306.325	7.64
20	351.269	8.76
30	371.03	9.26
40	345.445	8.62
50	358.626	8.95

Table D-18. Calcium Ion Concentration [Ca^{2+}] in dilute sulfuric acid runoff from Mercer mortar.

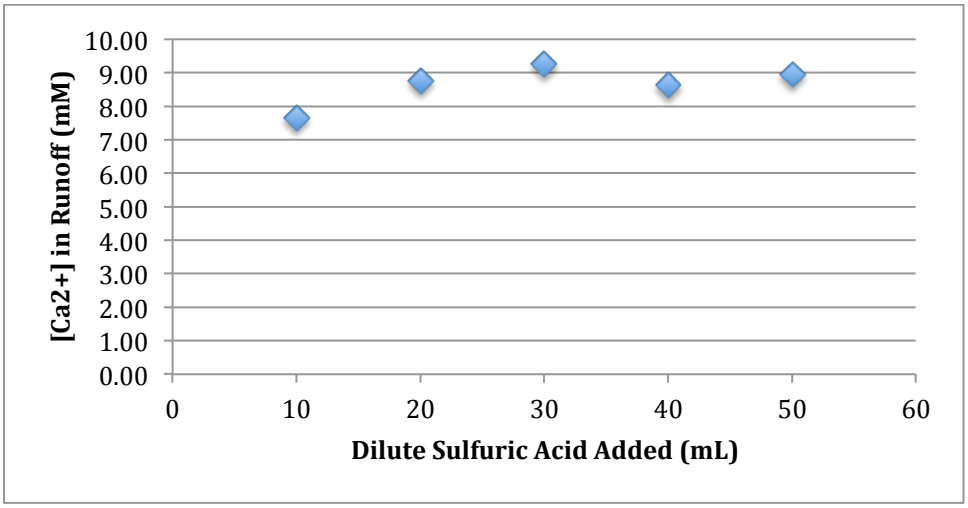

Figure D-16. Calcium Ion Concentration [Ca^{2+}] in dilute sulfuric acid runoff from Mercer mortar.

Mercer Mortar Exposed to Acid Rain Simulant

Solution Added (mL)	[Mg2+] in Runoff (ppm)	[Mg2+] Runoff-[Mg2+] Soln	[Mg2+] in Runoff (mM)
10	34.017	32.80	1.35
20	44.652	43.43	1.79
30	50.671	49.45	2.03
40	45.277	44.06	1.81
50	38.638	37.42	1.54

Table D-19. Magnesium Ion Concentration [Mg^{2+}] in acid rain runoff from Mercer mortar.

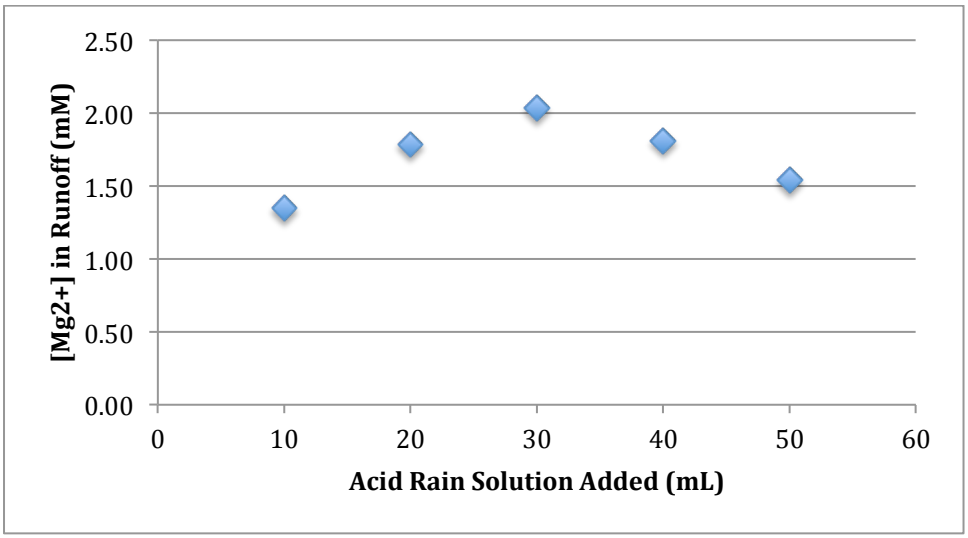

Figure D-17. Magnesium Ion Concentration [Mg^{2+}] in acid rain runoff from Mercer mortar.

Solution Added (mL)	[Ca2+] in Runoff (ppm)	[Ca2+] Runoff-[Ca2+] Soln	[Ca2+] in Runoff (mM)
10	251.158	246.10	6.140144711
20	265.473	260.41	6.497305389
30	301.458	296.40	7.395134731
40	245.905	240.84	6.009081836
50	301.954	296.89	7.40750998

Table D-20. Calcium Ion Concentration [Ca^{2+}] in acid rain runoff from Mercer mortar.

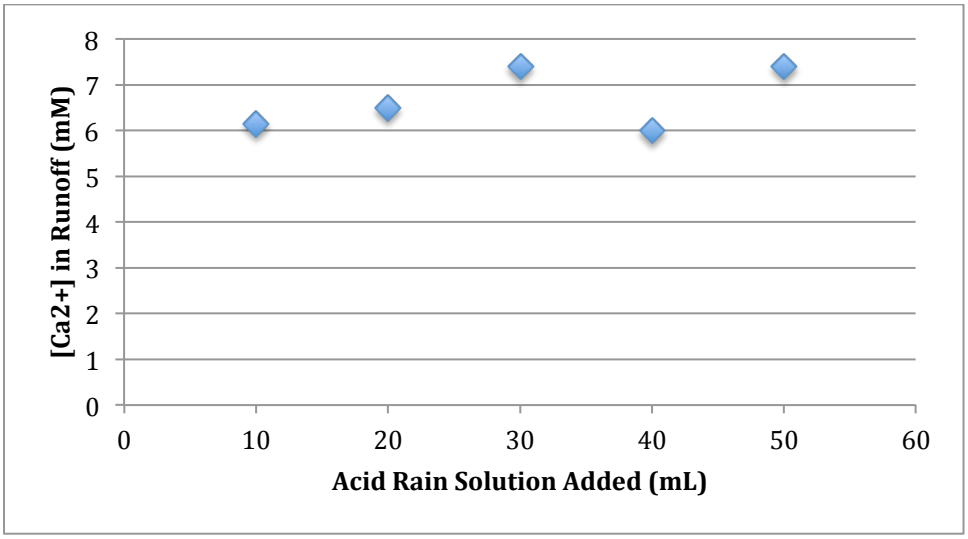

Figure D-18. Calcium Ion Concentration [Ca^{2+}] in acid rain runoff from Mercer mortar.

Appendix E:

Scanning Electron Micrographs

Dolomite Crystal

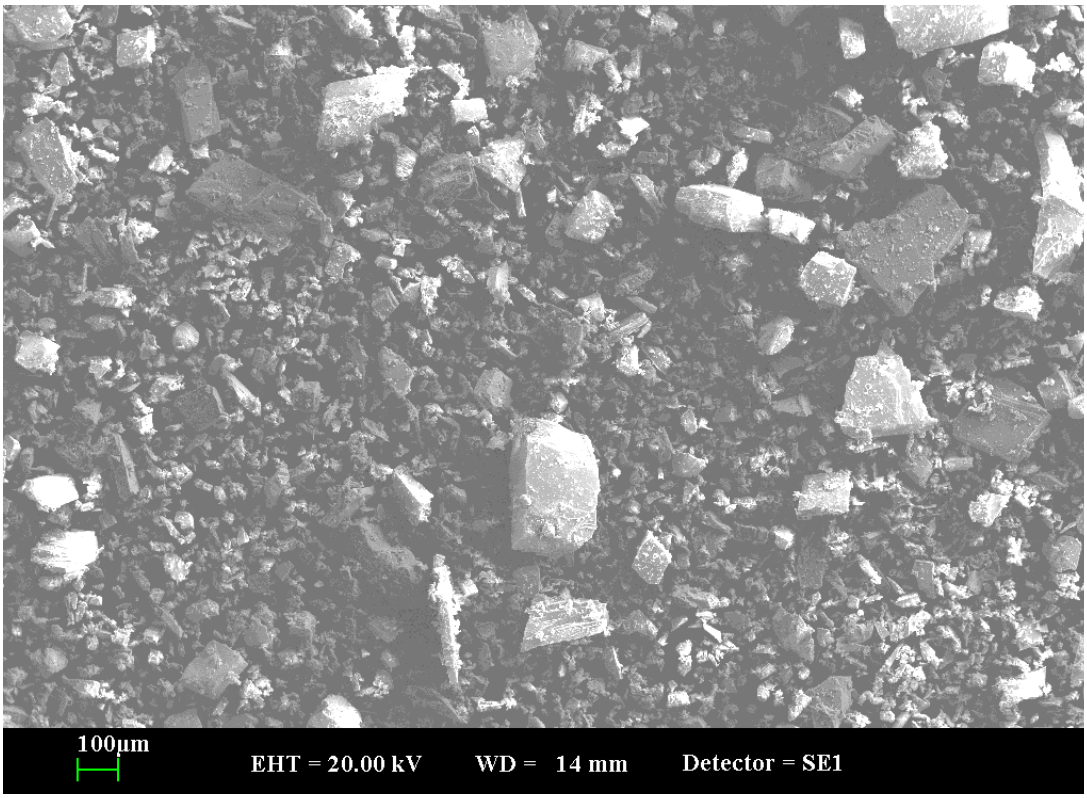

Crushed dolomite crystal, uncalcined, at 100X magnification.

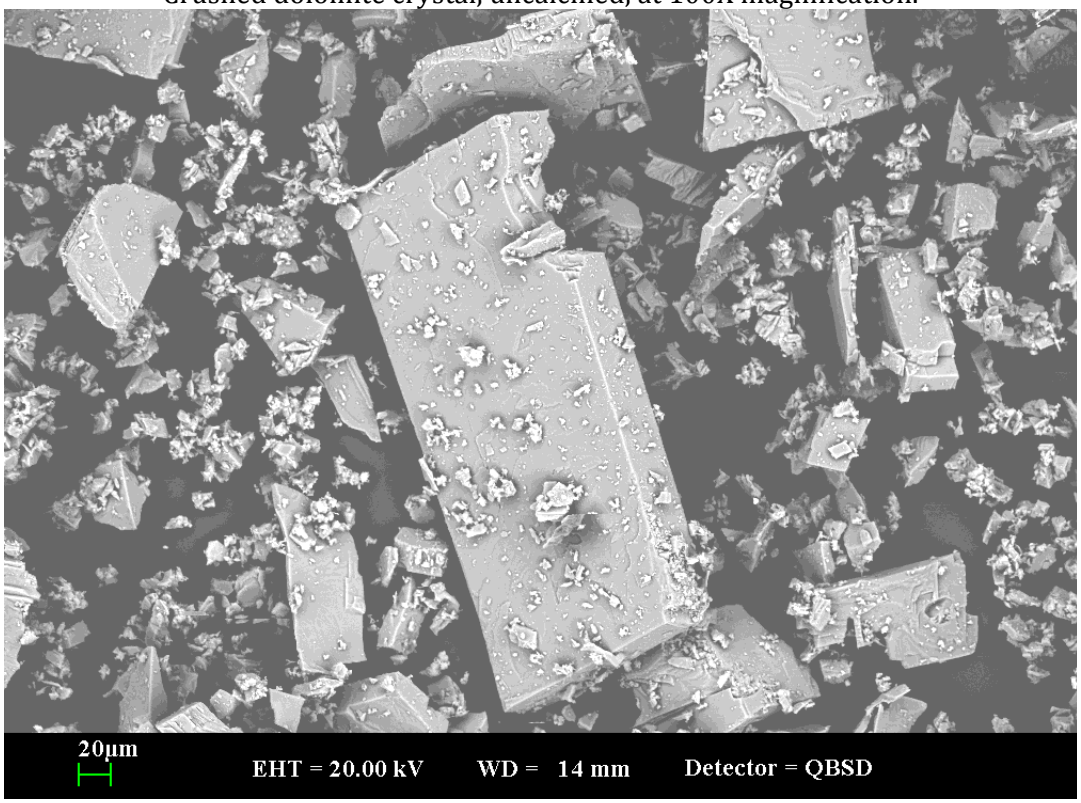

Crushed dolomite crystal, uncalcined, at 362X magnification.

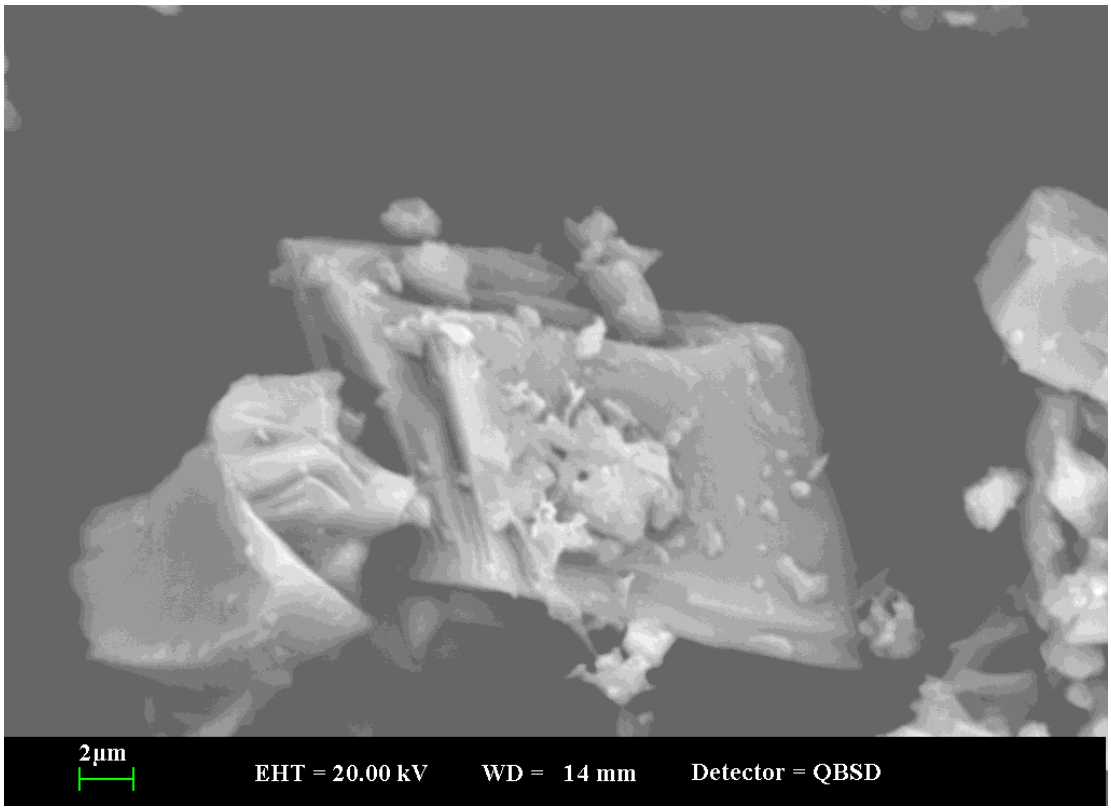

Crushed dolomite crystal, uncalcined, at 6500X magnification.

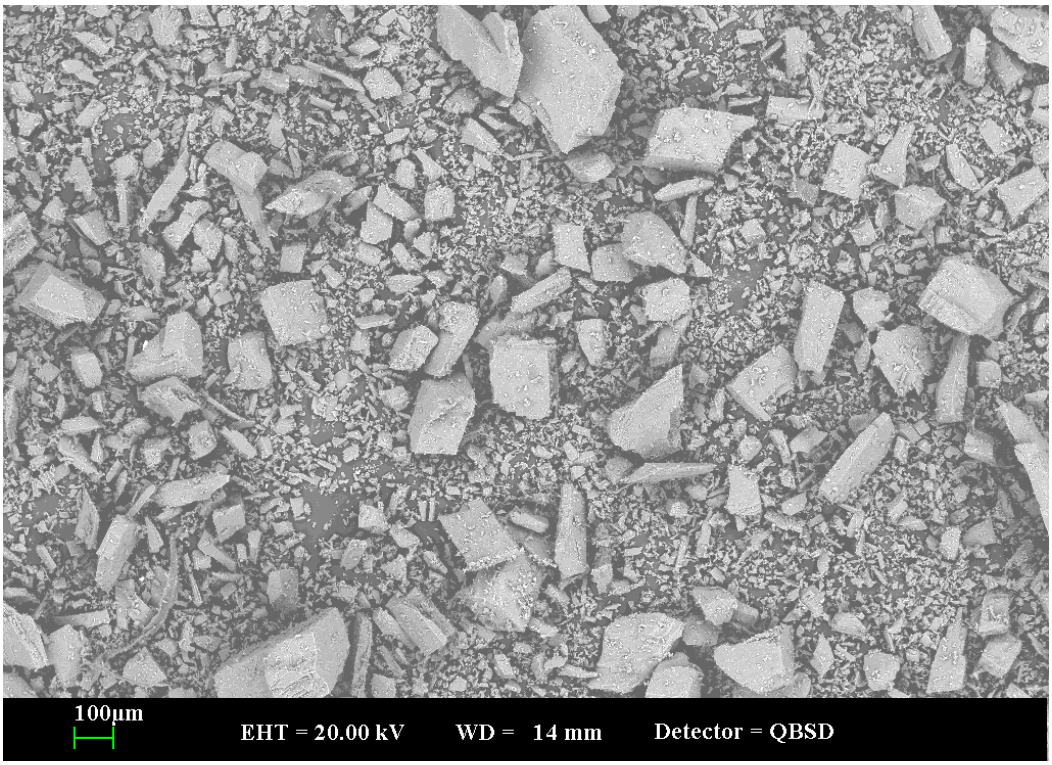

Crushed dolomite crystal, calcined to 400°C, at 100X magnification.

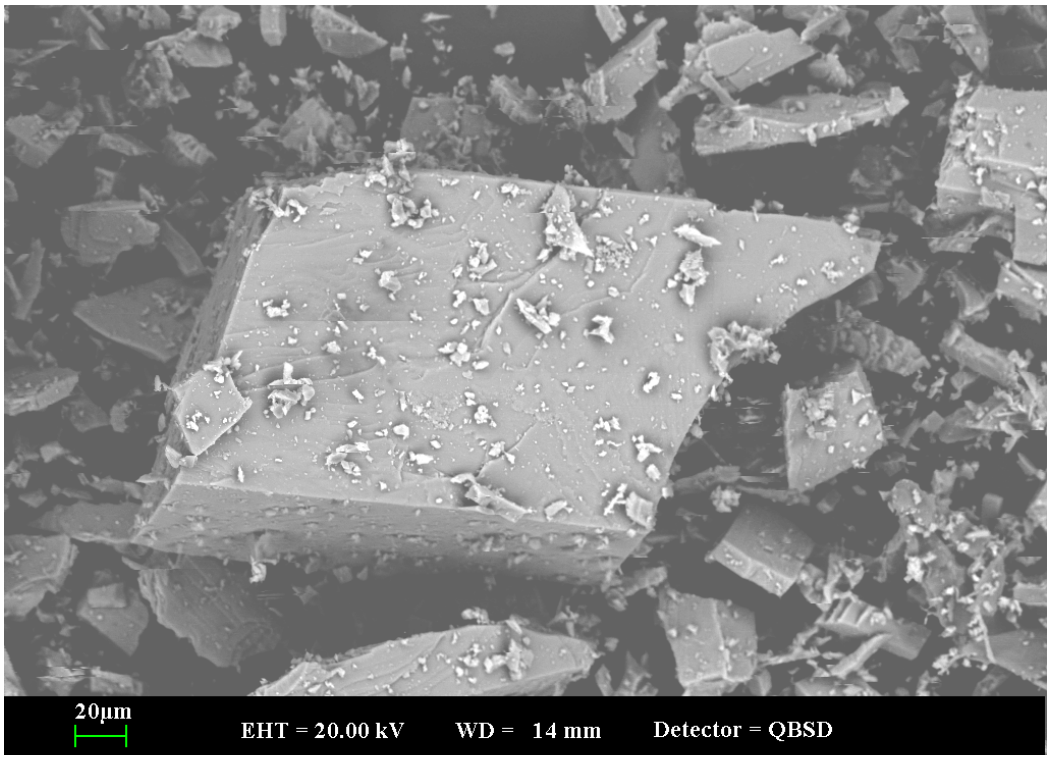

Crushed dolomite crystal, calcined to 400°C, at 646X magnification.

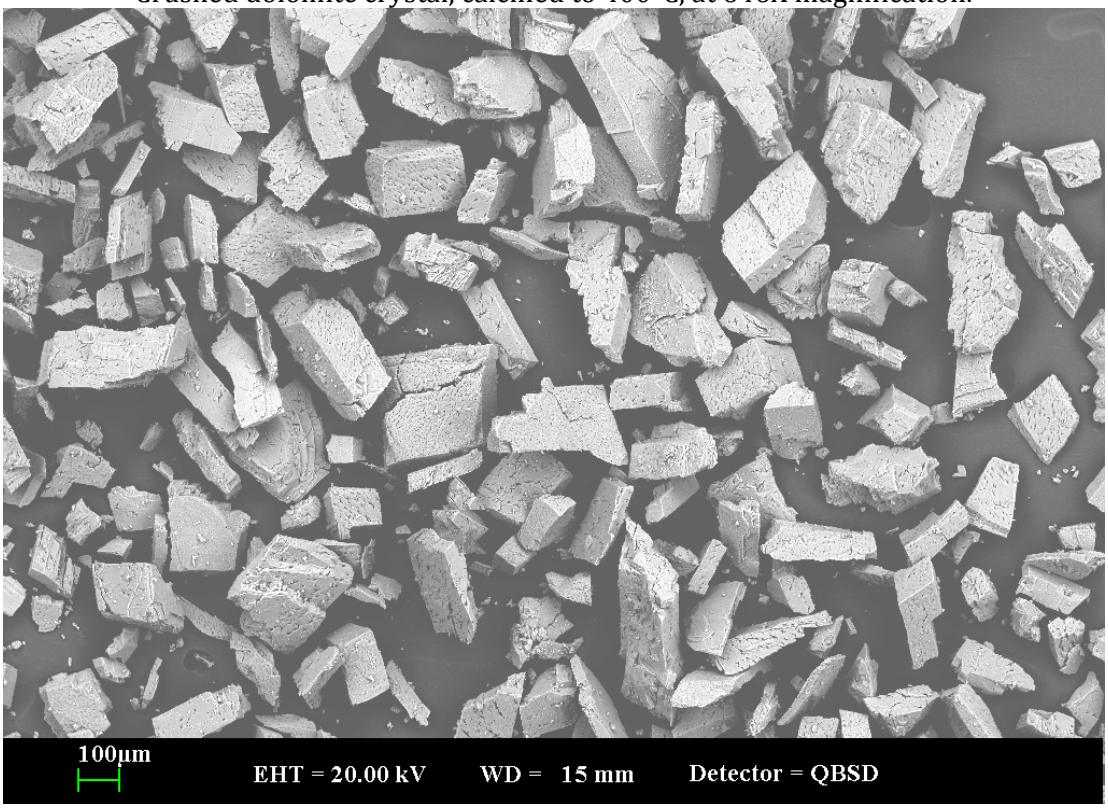

Crushed dolomite crystal, calcined to 600°C, at 100X magnification.

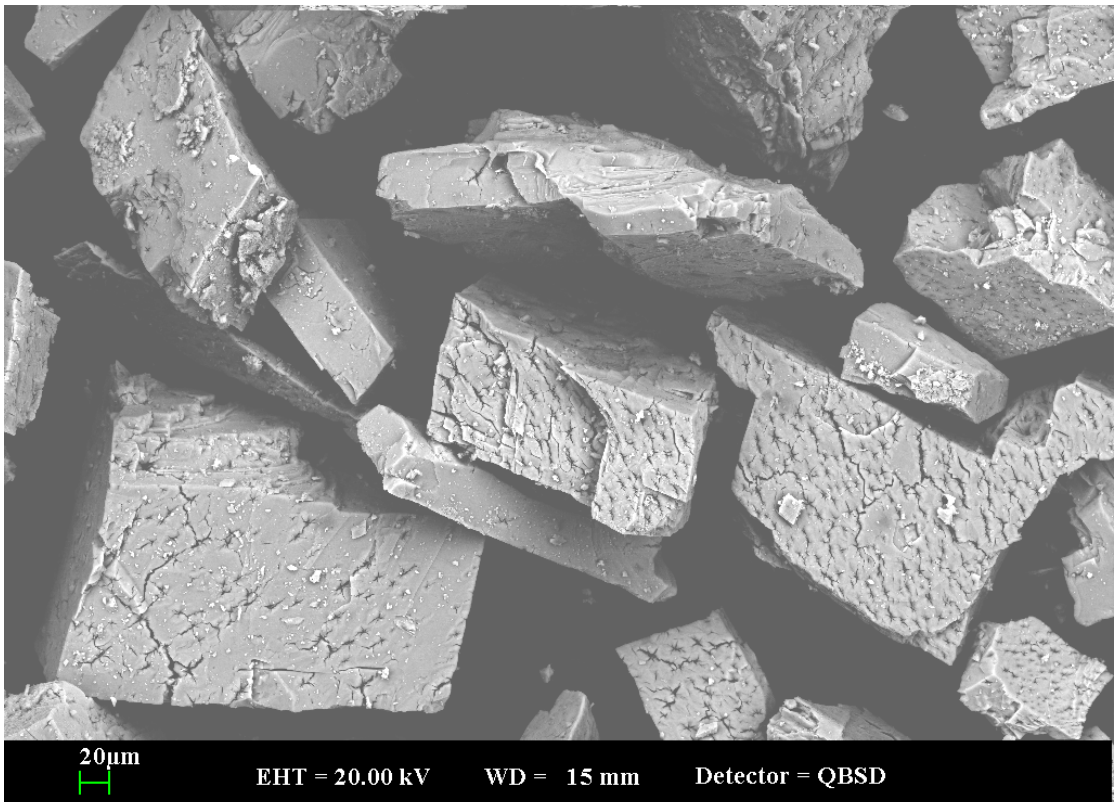

Crushed dolomite crystal, calcined to 600°C, at 348X magnification.

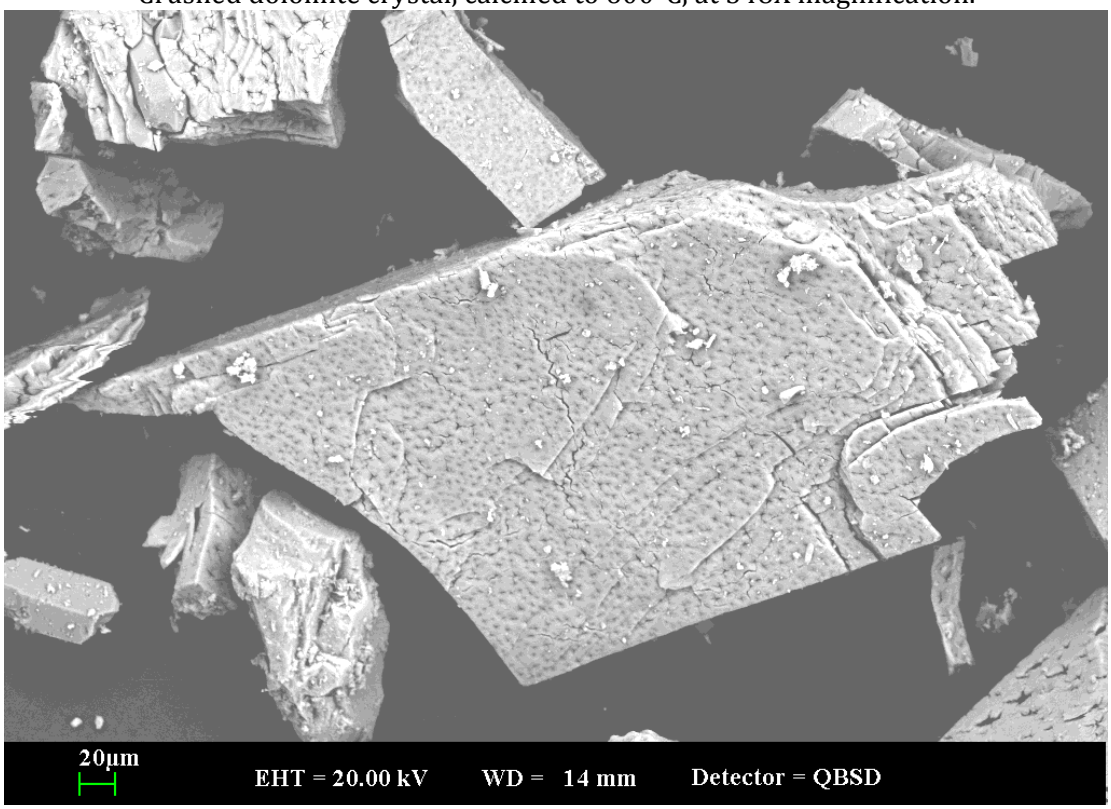

Crushed dolomite crystal, calcined to 600°C, at 435X magnification.

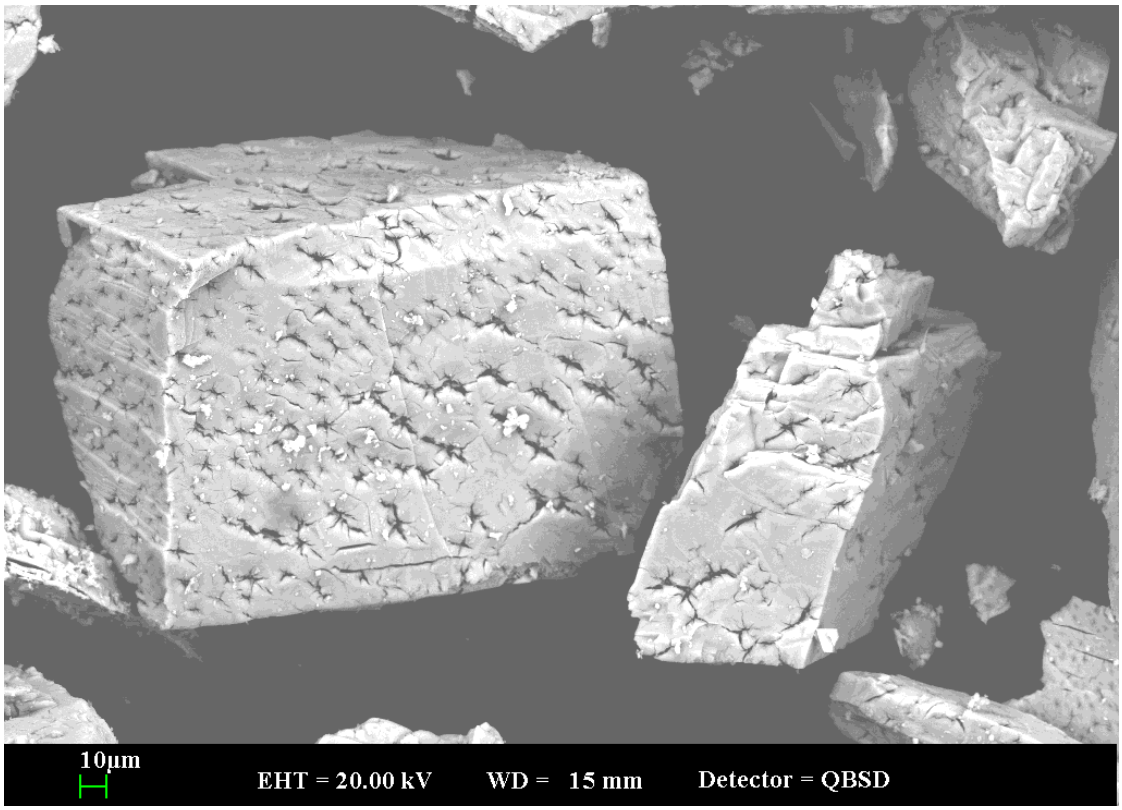

Crushed dolomite crystal, calcined to 600°C, at 615X magnification.

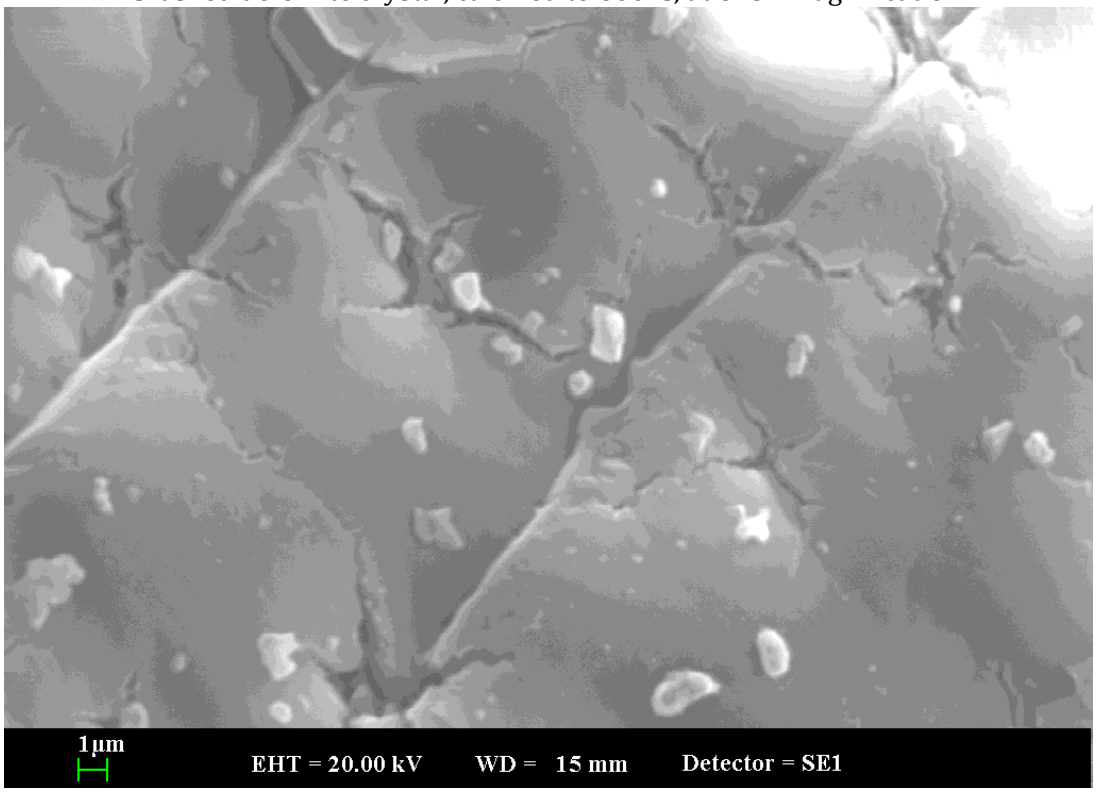

Crushed dolomite crystal, calcined to 600°C, at 7000X magnification.

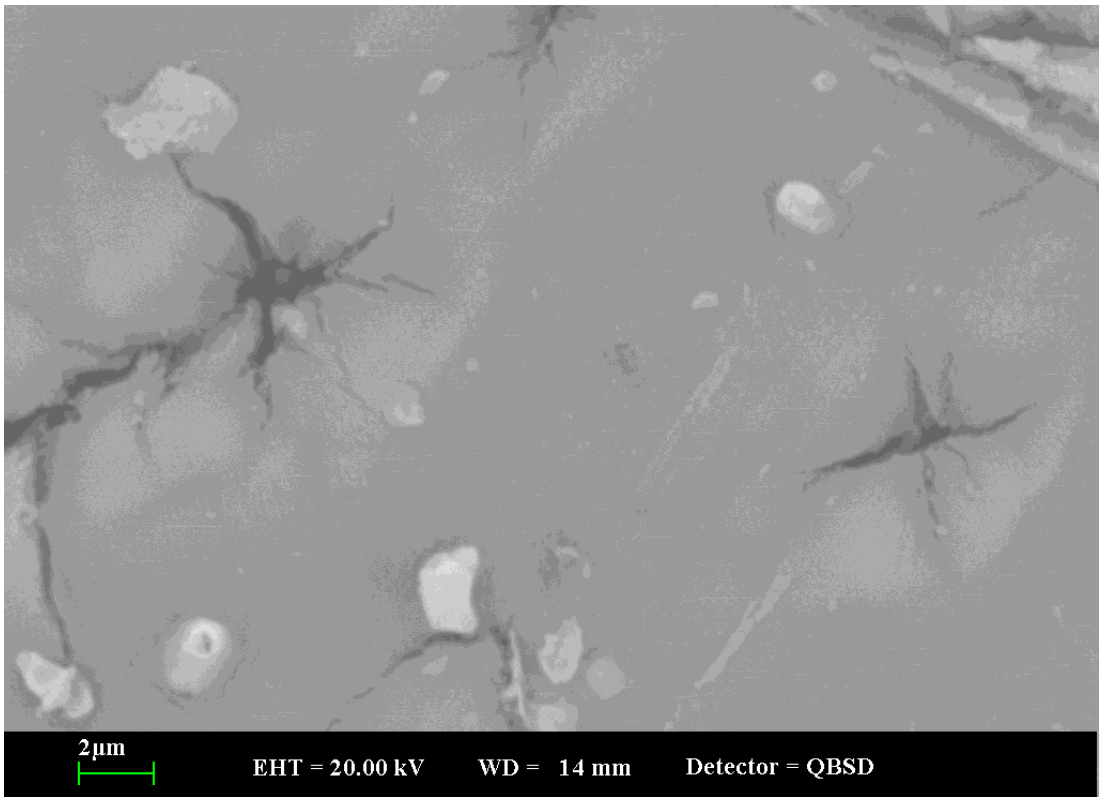

Crushed dolomite crystal, calcined to 600°C, at 9000X magnification.

Crushed dolomite crystal, calcined to 750°C, at 611X magnification.

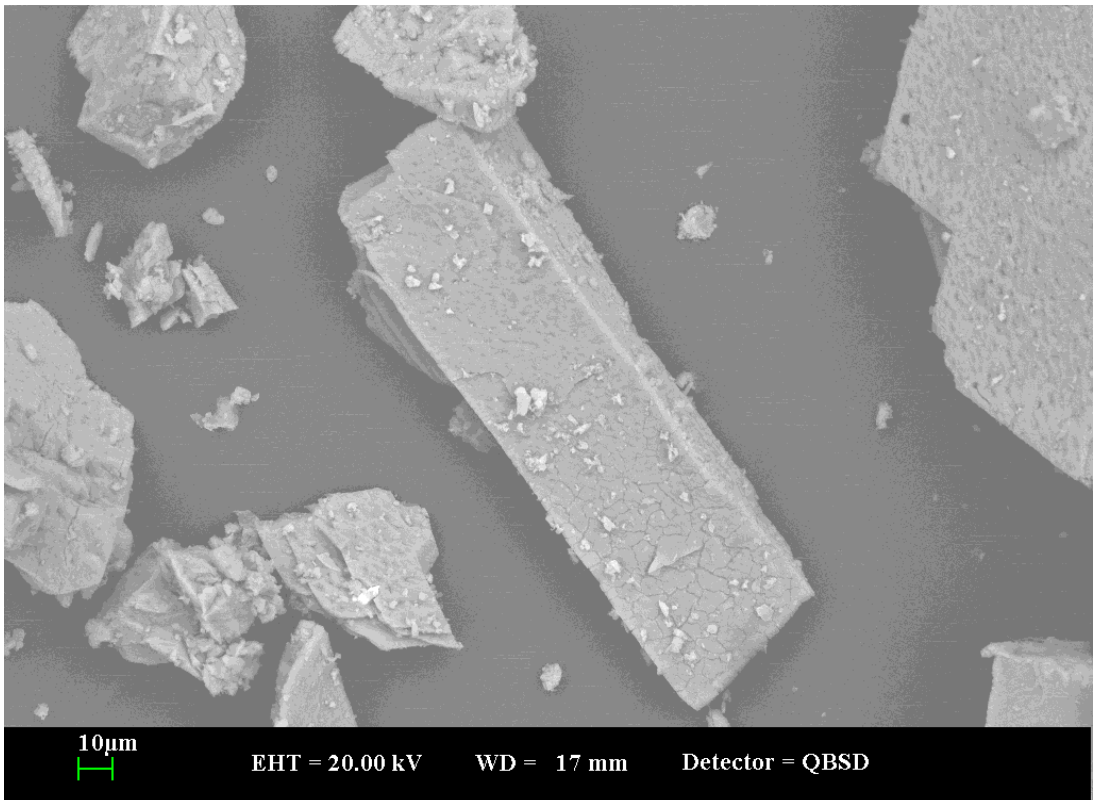

Crushed dolomite crystal, calcined to 750°C, at 840X magnification.

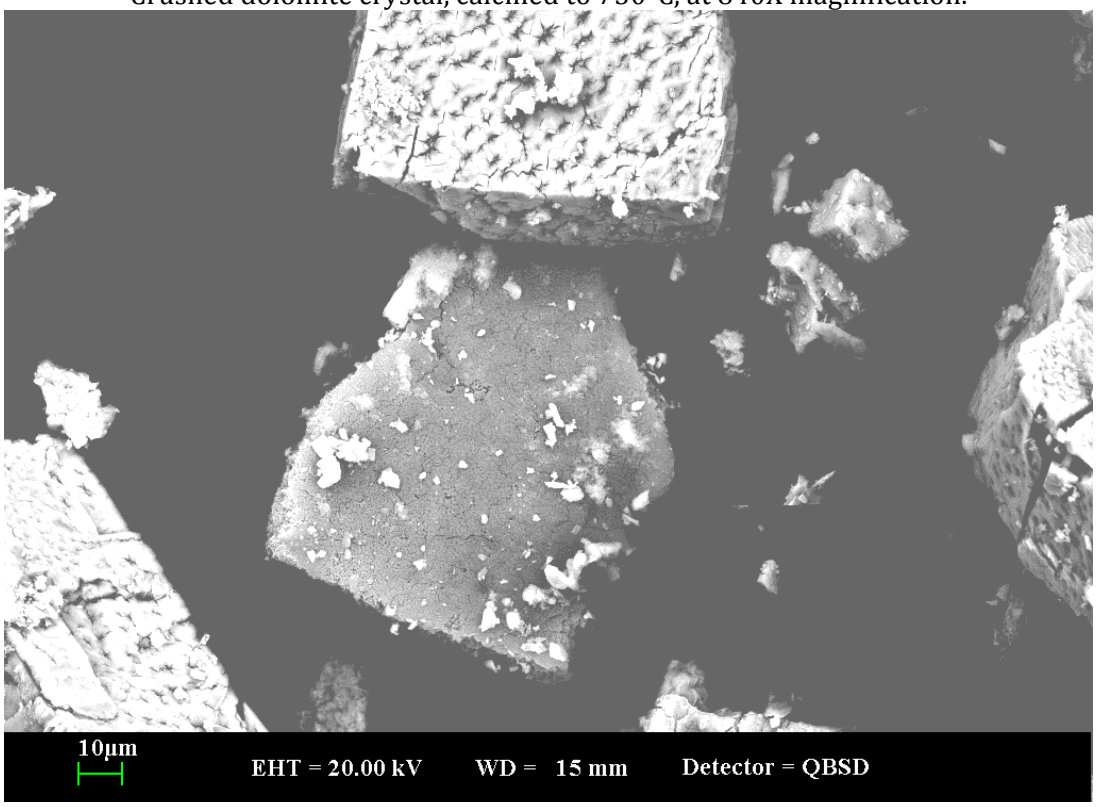

Crushed dolomite crystal, calcined to 750°C, at 1000X magnification.

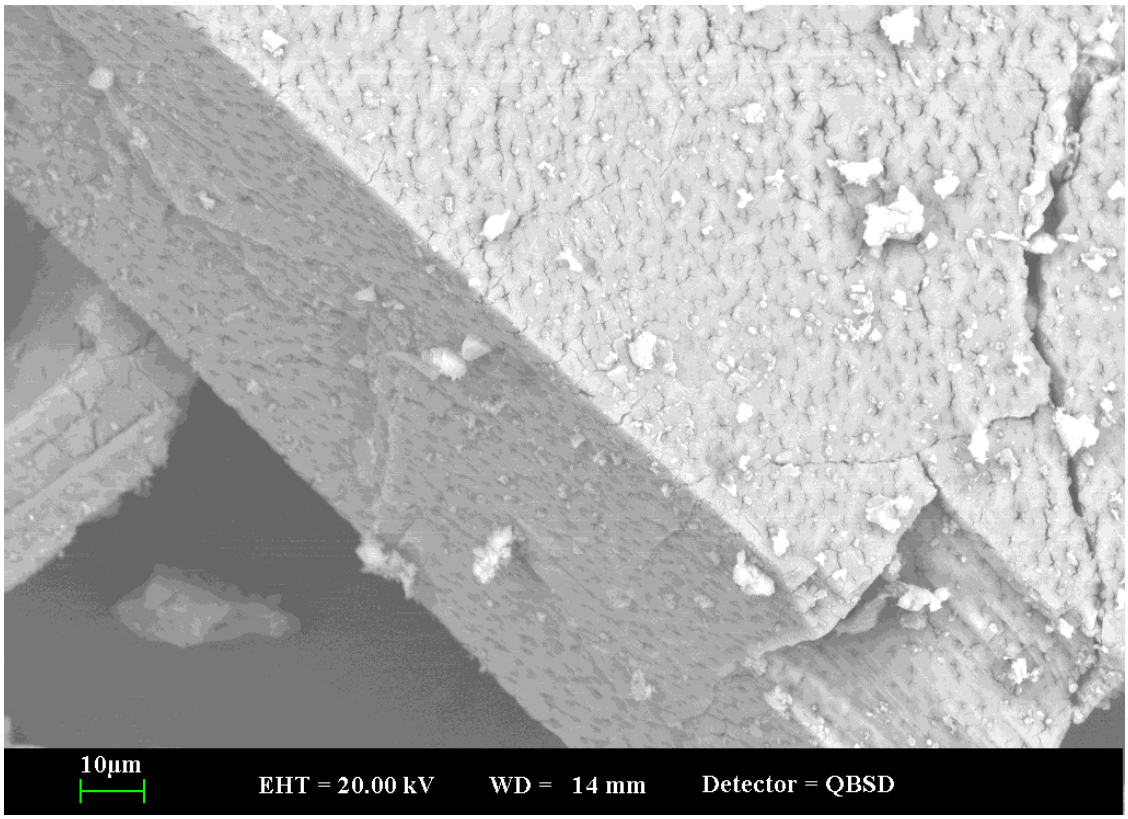

Crushed dolomite crystal, calcined to 750°C, at 1500X magnification.

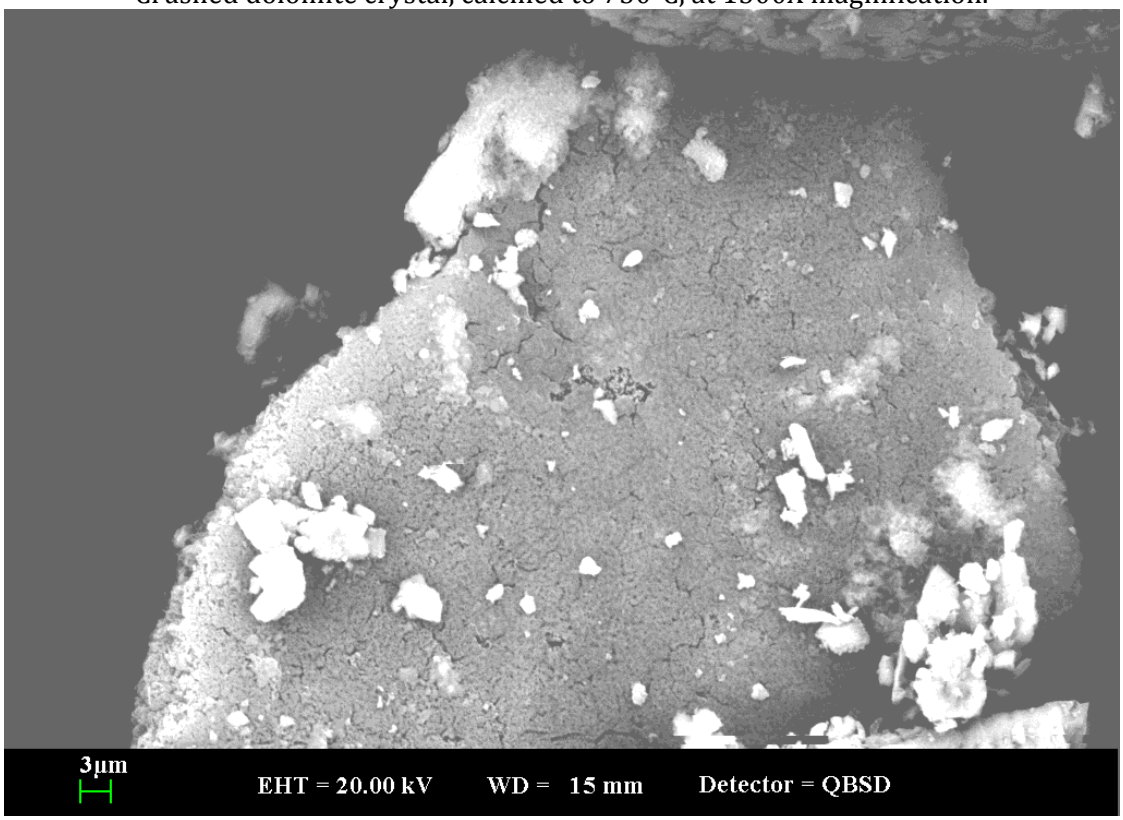

Crushed dolomite crystal, calcined to 750°C, at 2440X magnification.

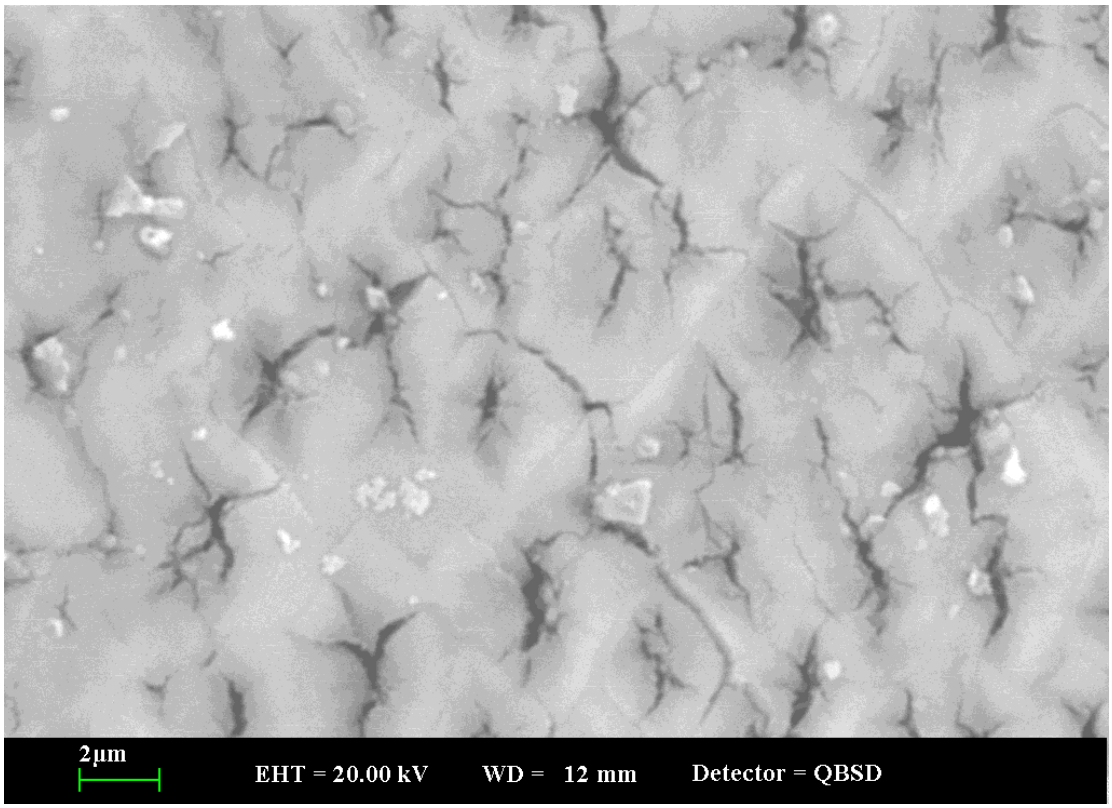

Crushed dolomite crystal, calcined to 750°C, at 9600X magnification.

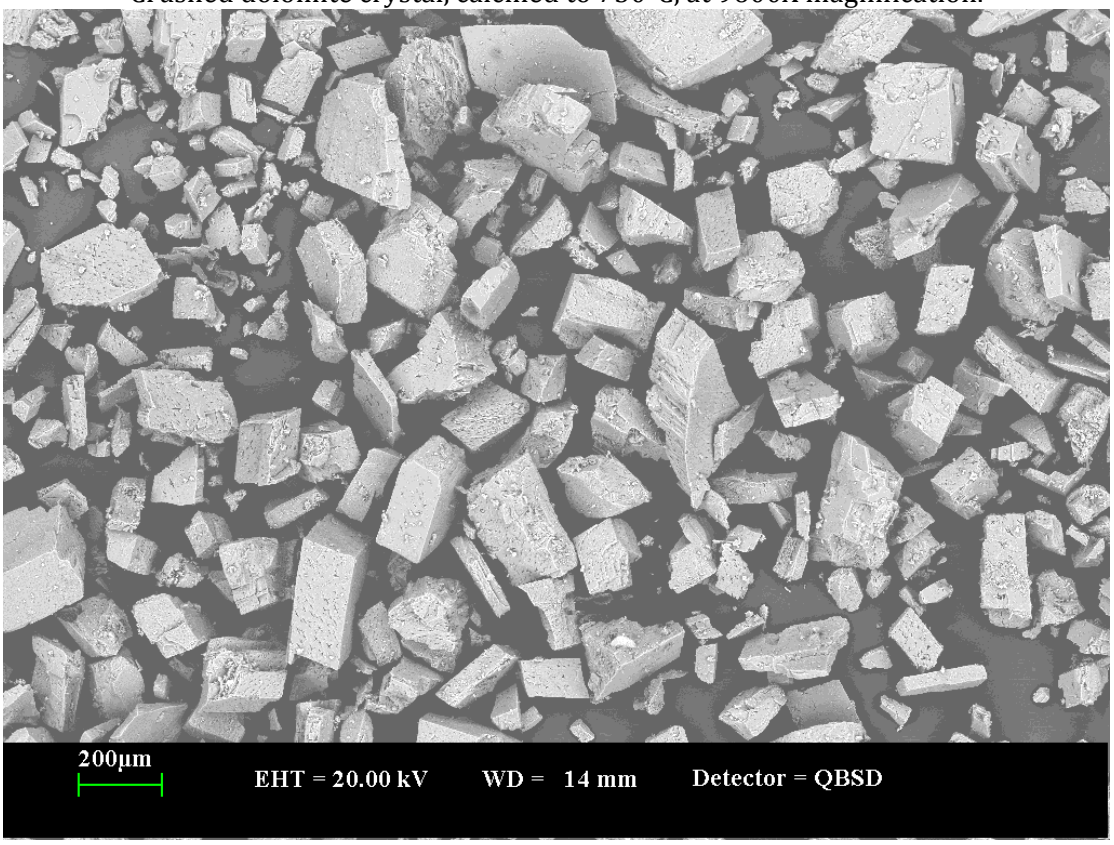

Crushed dolomite crystal, calcined to 900°C, at 100X magnification.

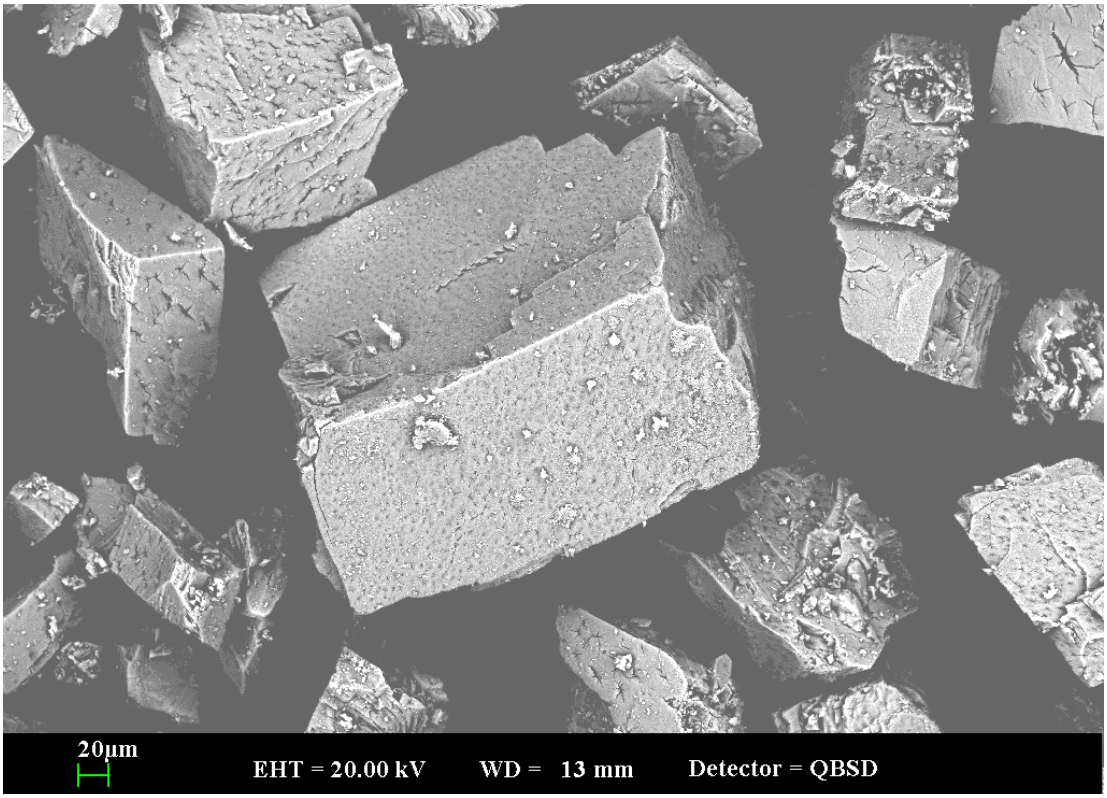

Crushed dolomite crystal, calcined to 900°C, at 368X magnification.

Kasota Stone, calcined at 900°C

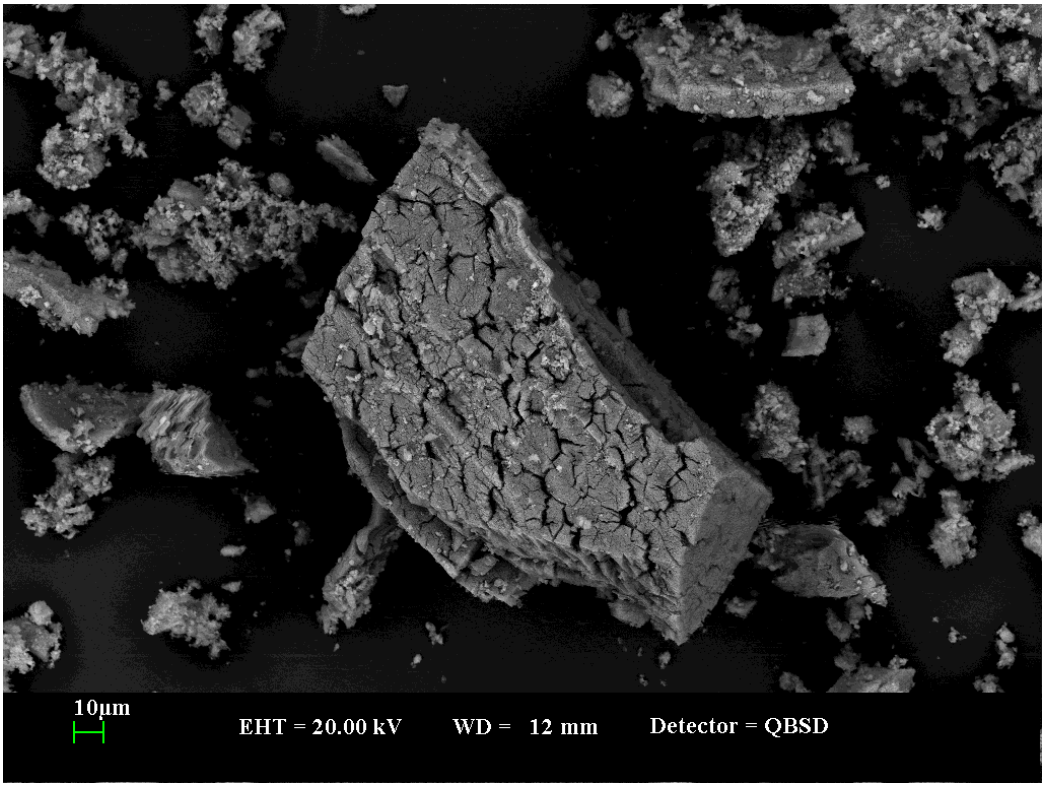

Kasota, calcined at 900°C, at 752X magnification.

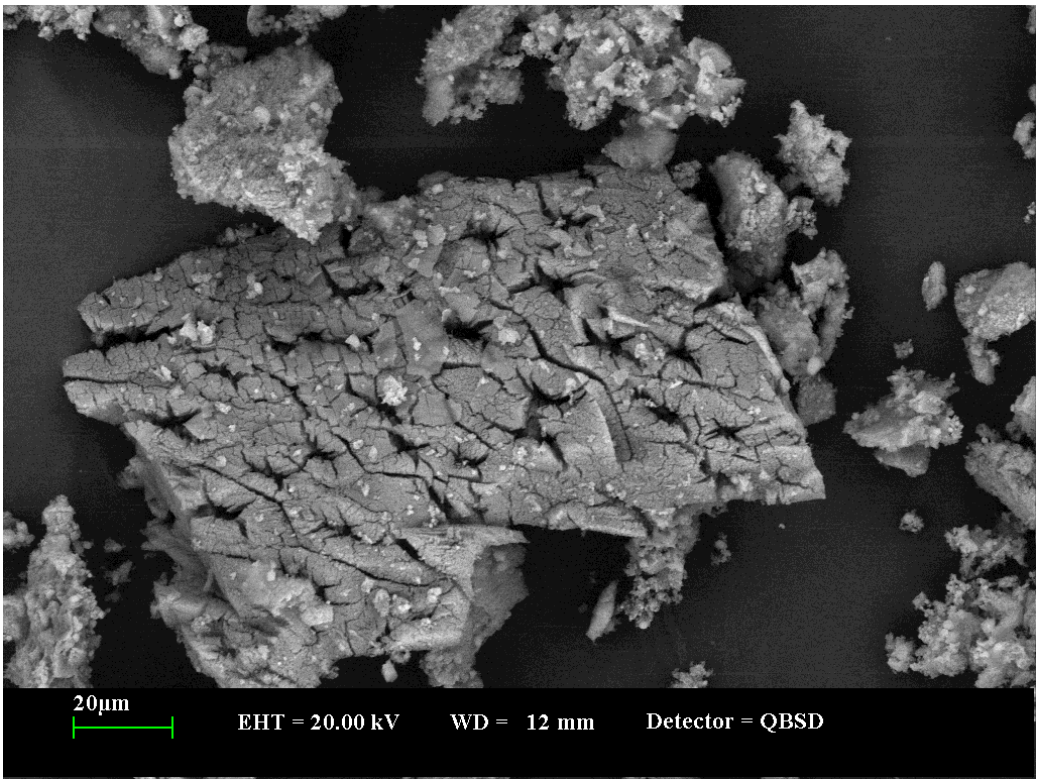

Kasota, calcined at 900°C, at 1270X magnification.

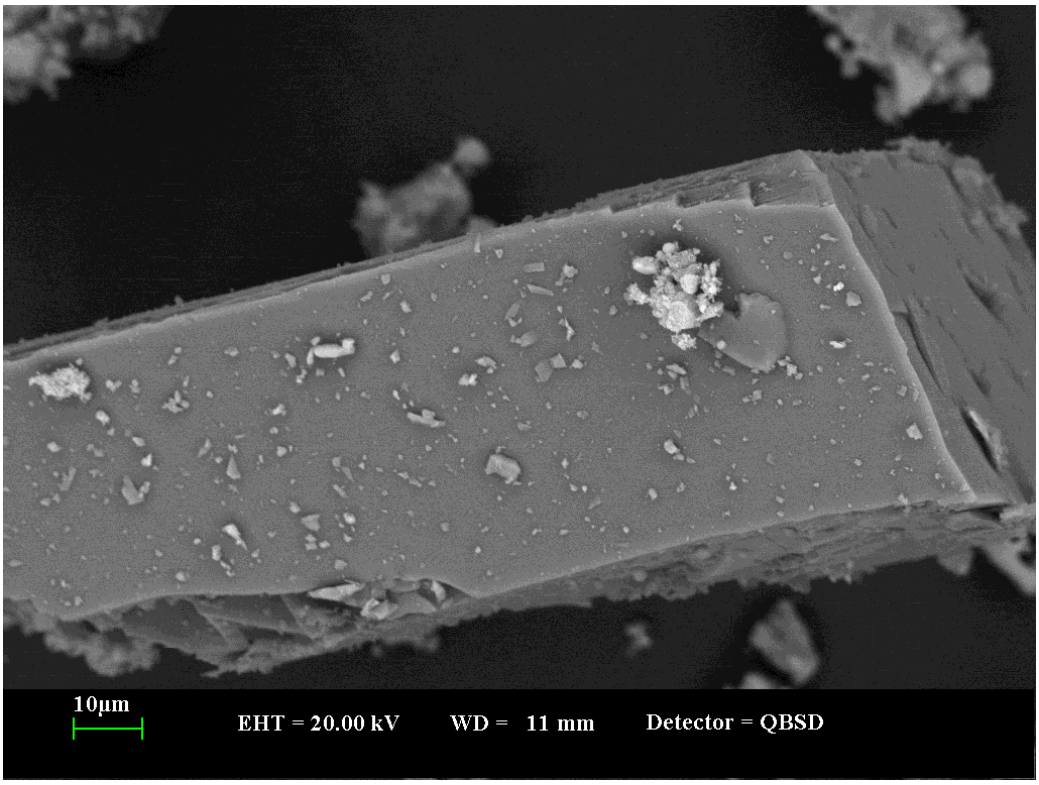

Kasota, calcined at 900°C, at 1780X magnification.

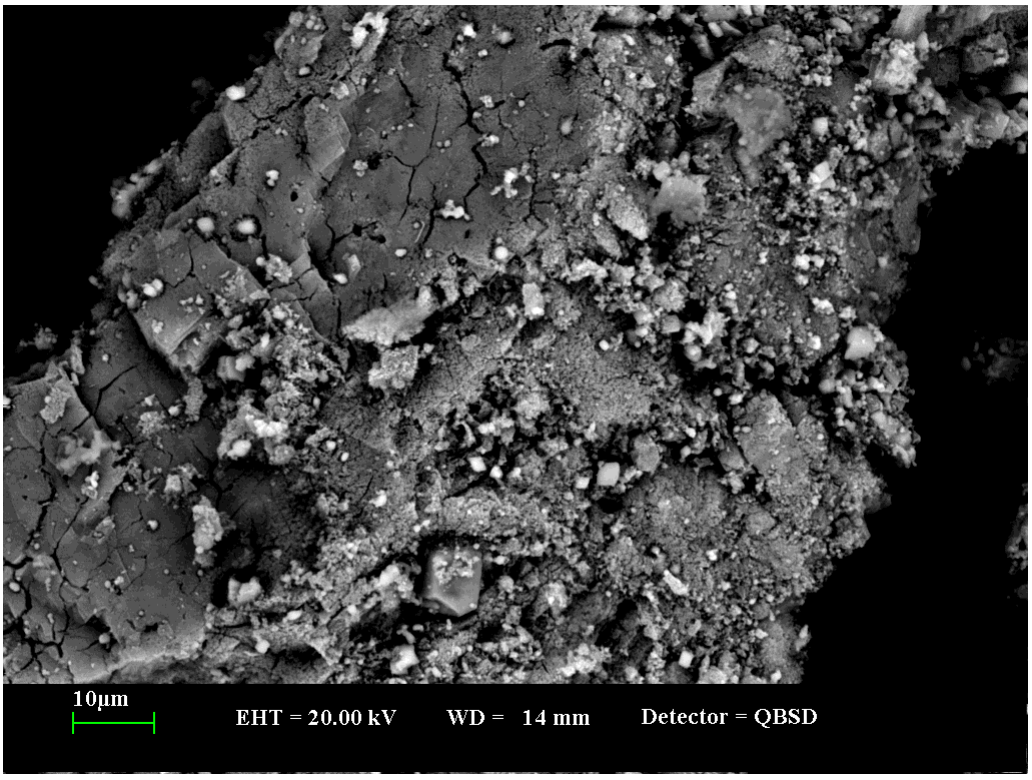

Kasota, calcined at 900°C, at 2100X magnification.

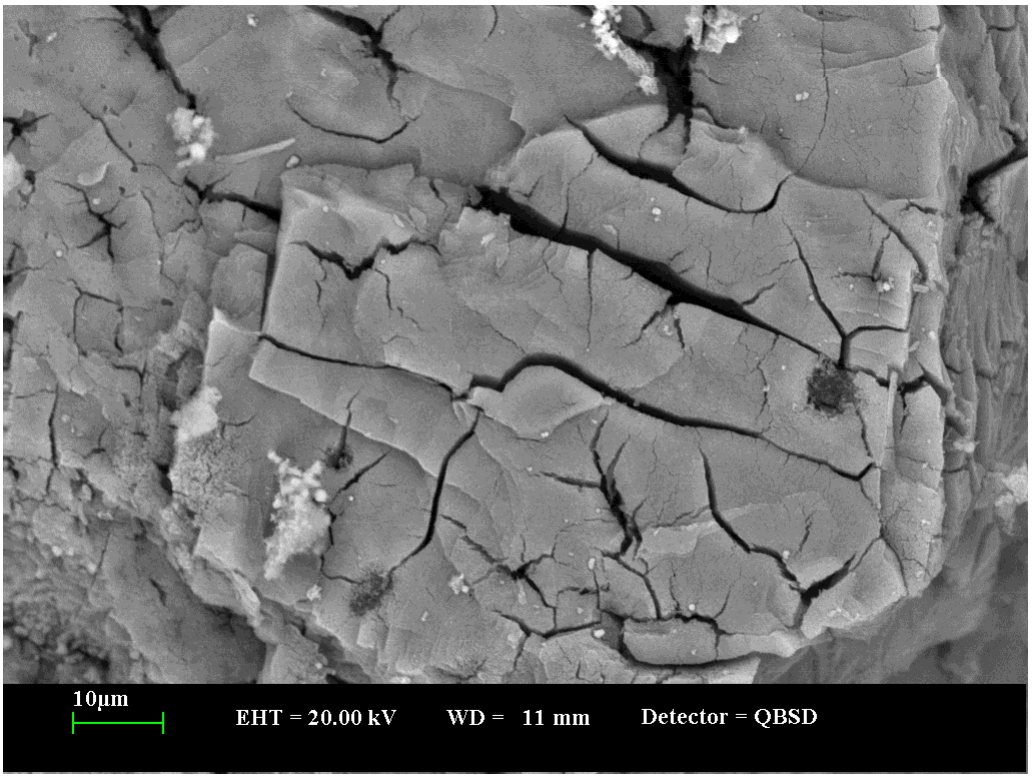

Kasota, calcined at 900°C, at 2340X magnification.

Kasota, calcined at 900°C, at 6540X magnification.

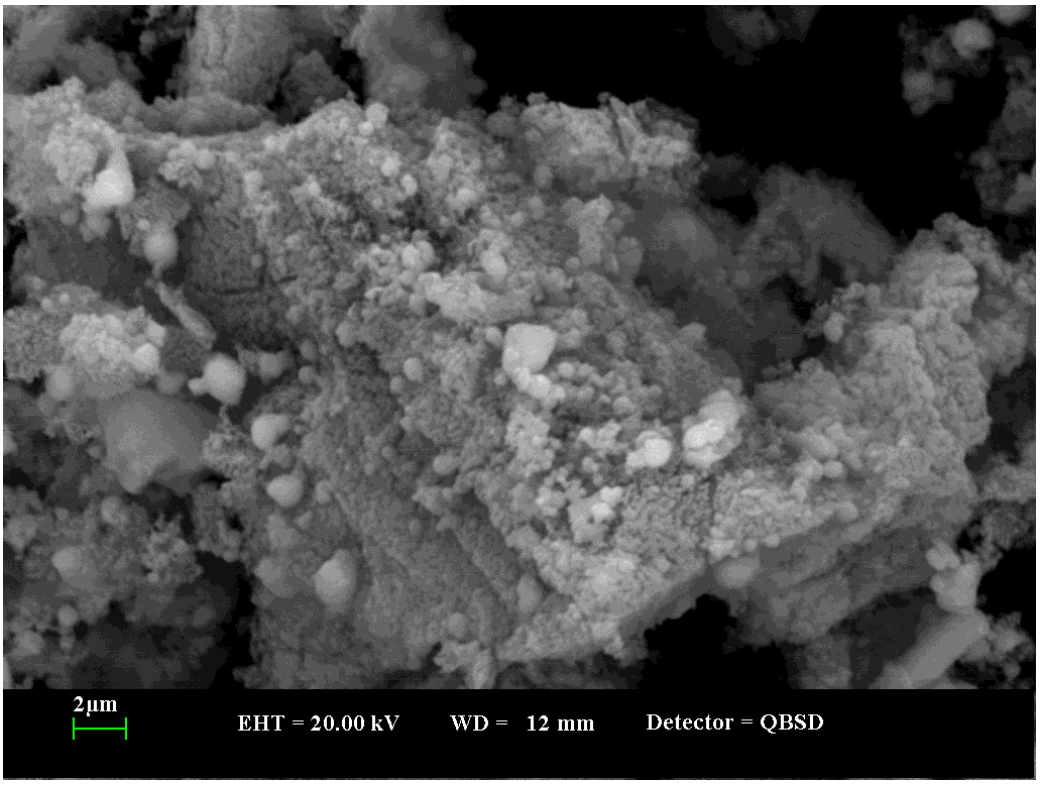

Kasota, calcined at 900°C, at 6720X magnification.

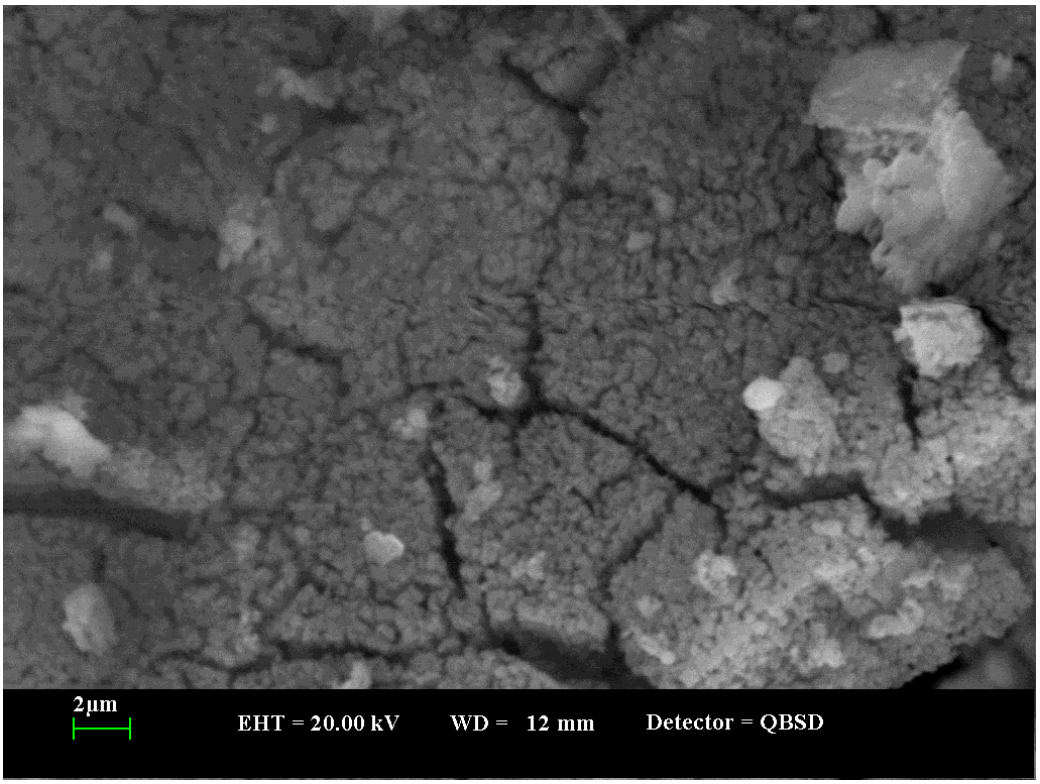

Kasota, calcined at 900°C, at 7300X magnification.

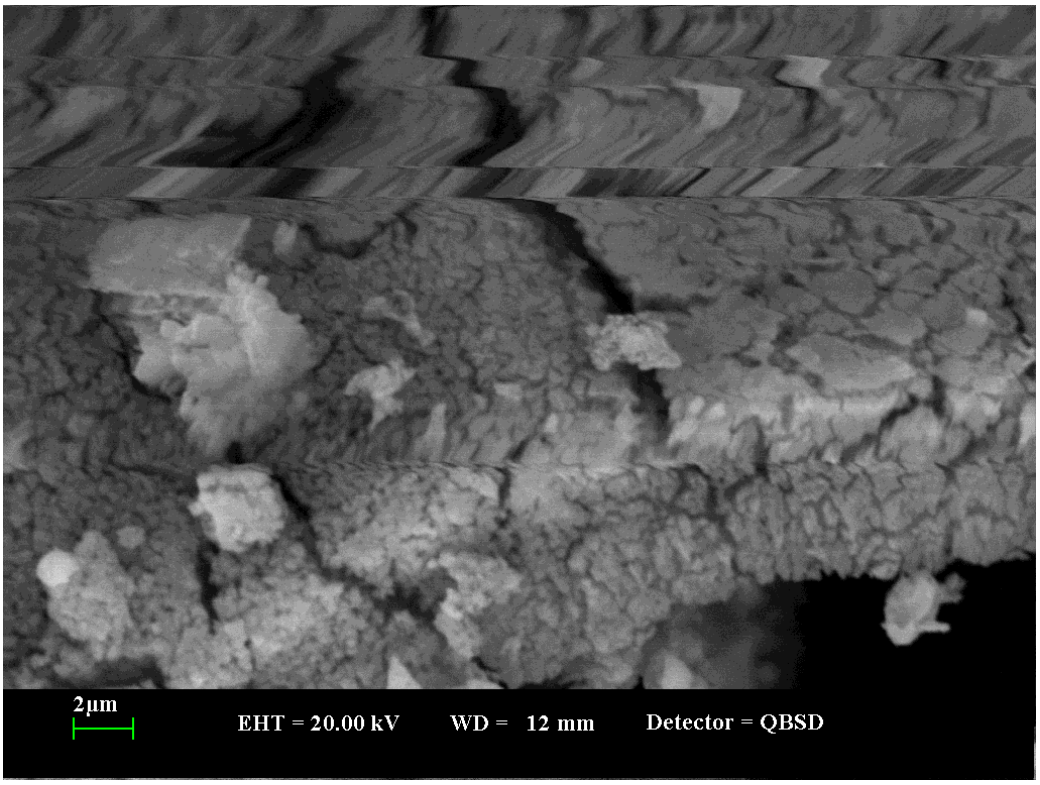

Kasota, calcined at 900°C, at 7720X magnification.

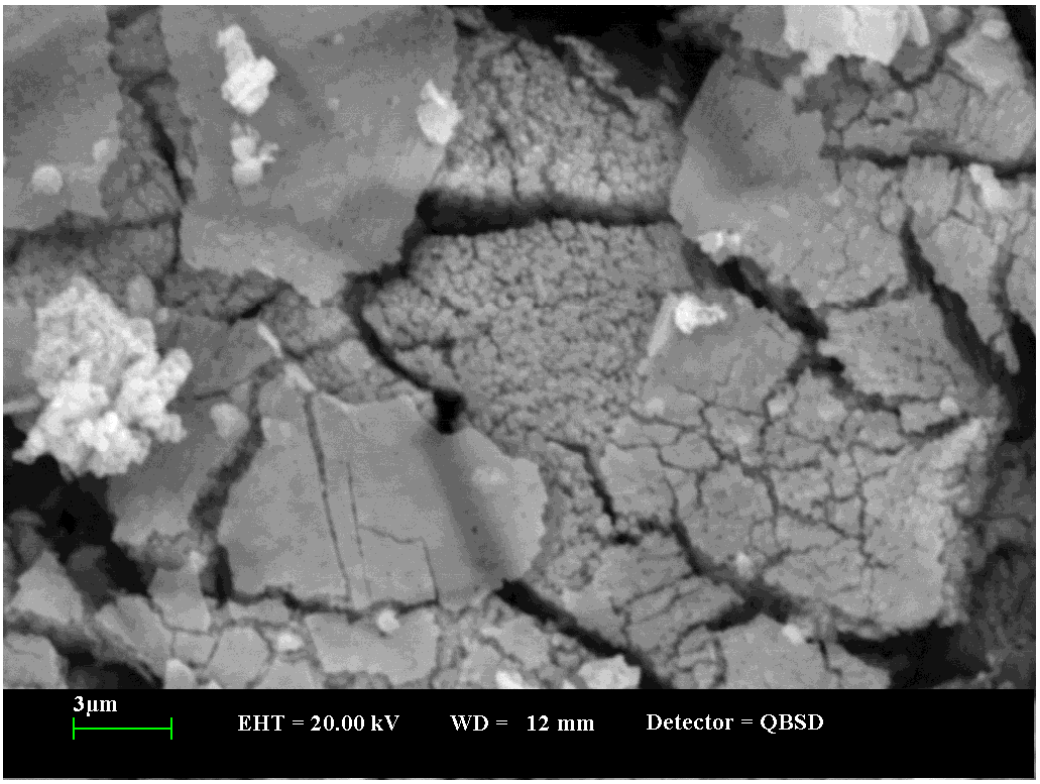

Kasota, calcined at 900°C, at 8390X magnification.

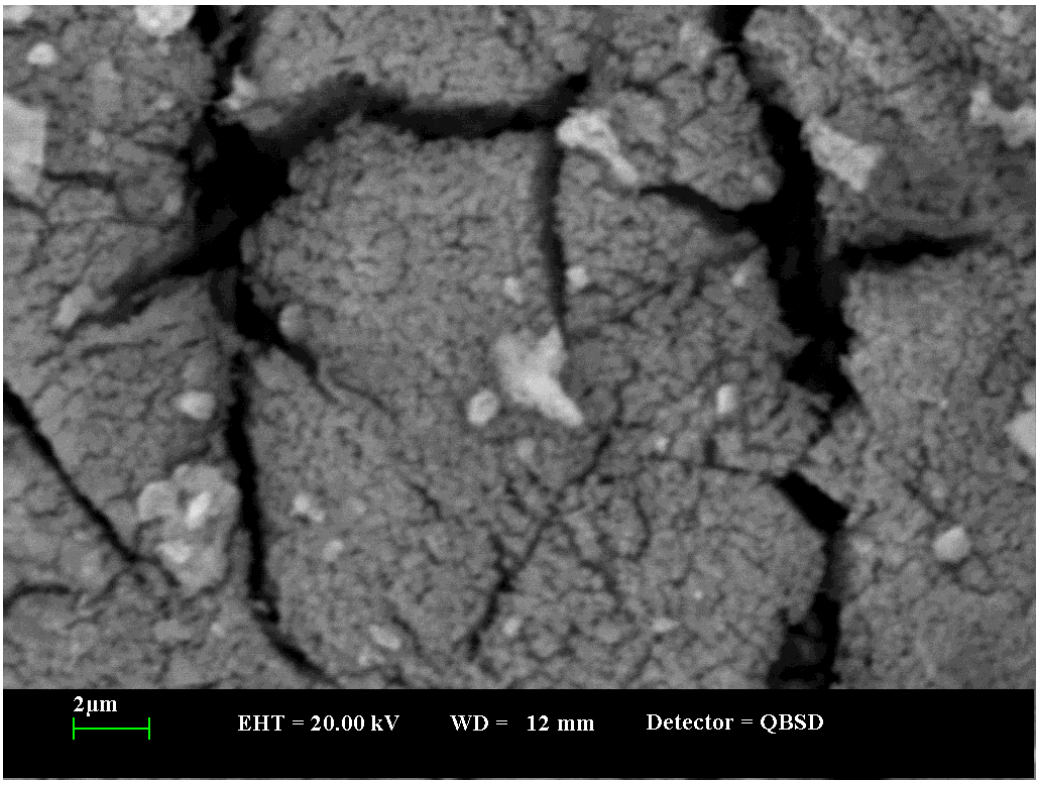

Kasota, calcined at 900°C, at 9770X magnification.

Calcite, calcined at 750°C

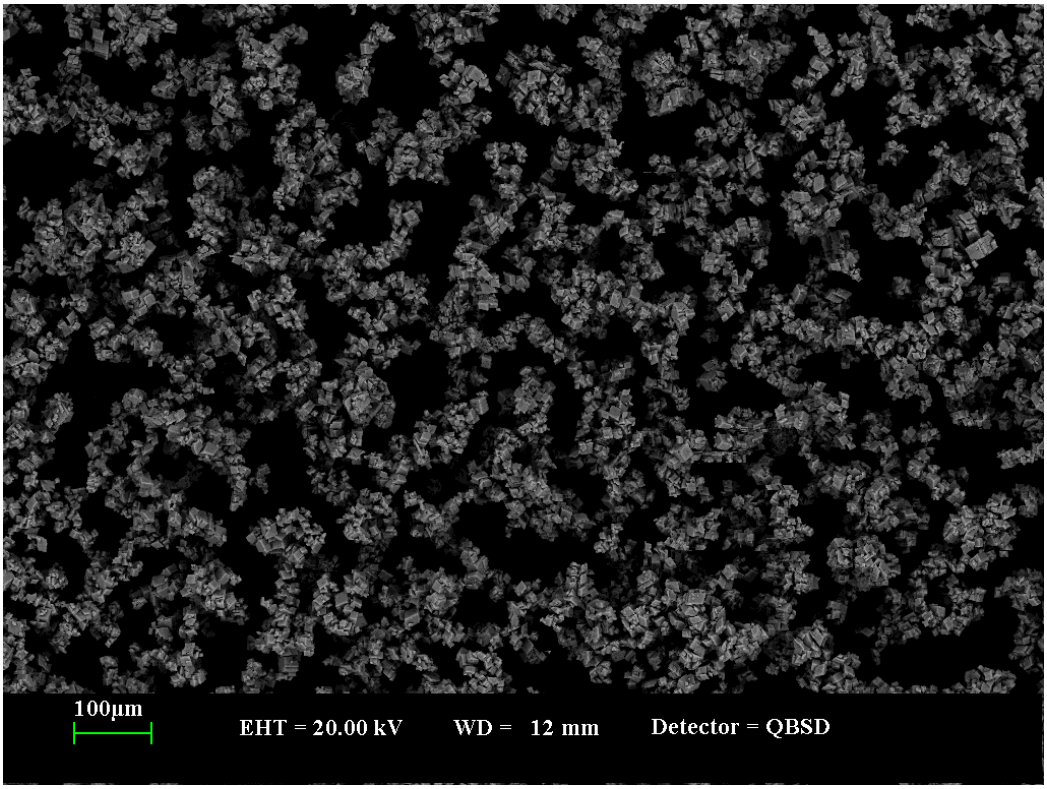

Calcite, calcined at 750°C, at 199X magnification.

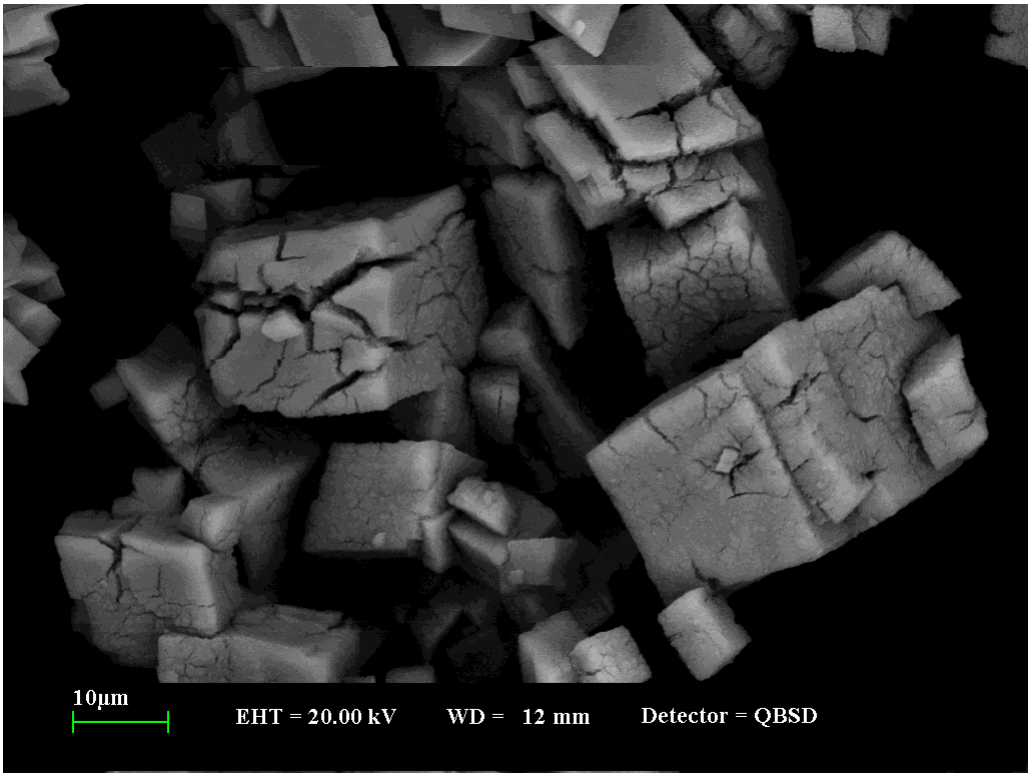

Calcite, calcined at 750°C, at 2480X magnification.

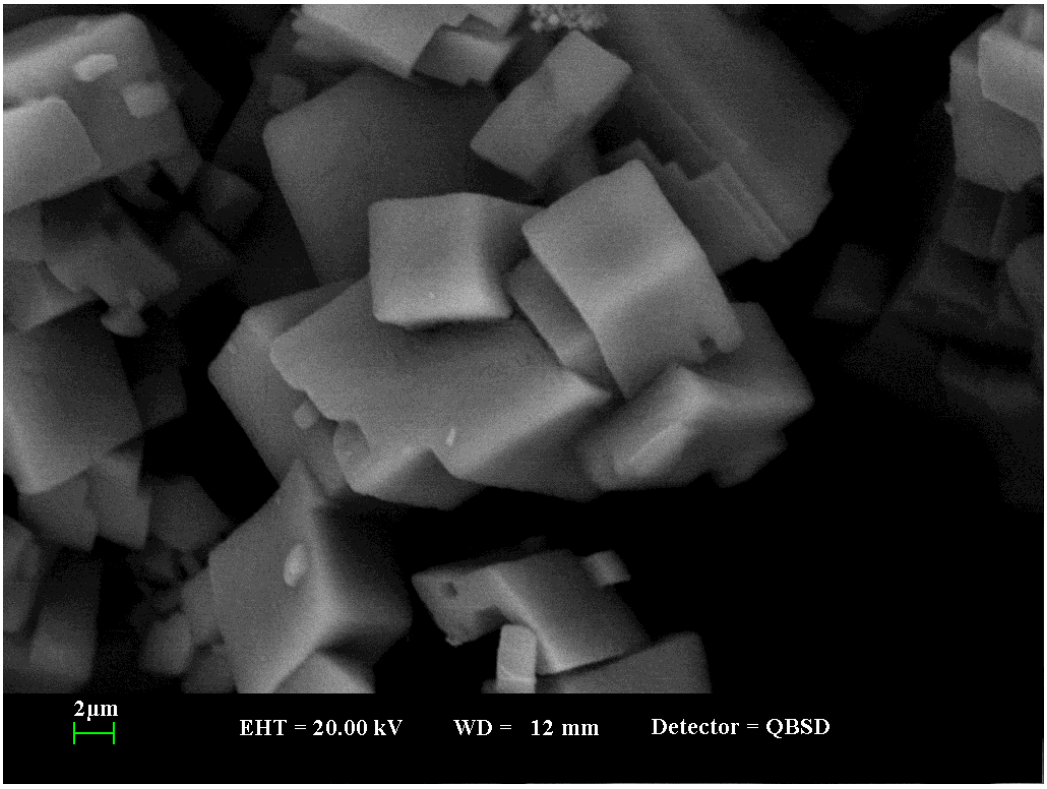

Calcite, calcined at 750°C, at 5000X magnification.

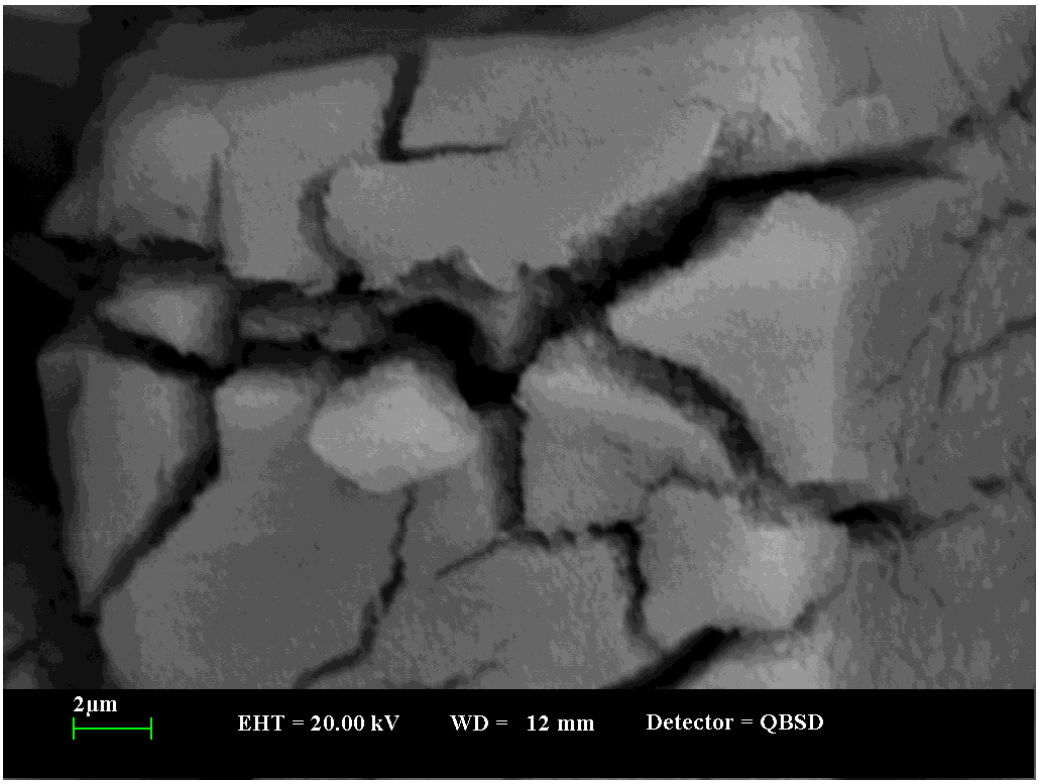

Calcite, calcined at 750°C, at 10,000X magnification.

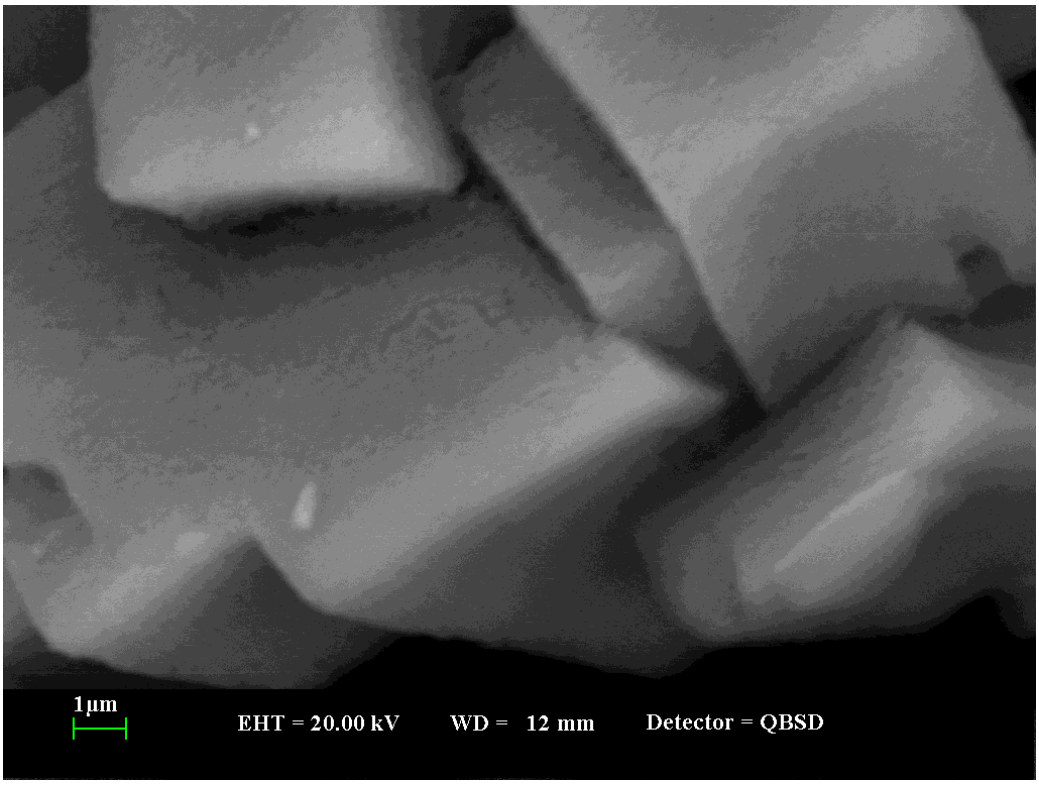

Calcite, calcined at 750°C, at 13,440X magnification.

Calcite, calcined at 750°C, at 14,000X magnification.

Commercial Dolomitic Lime

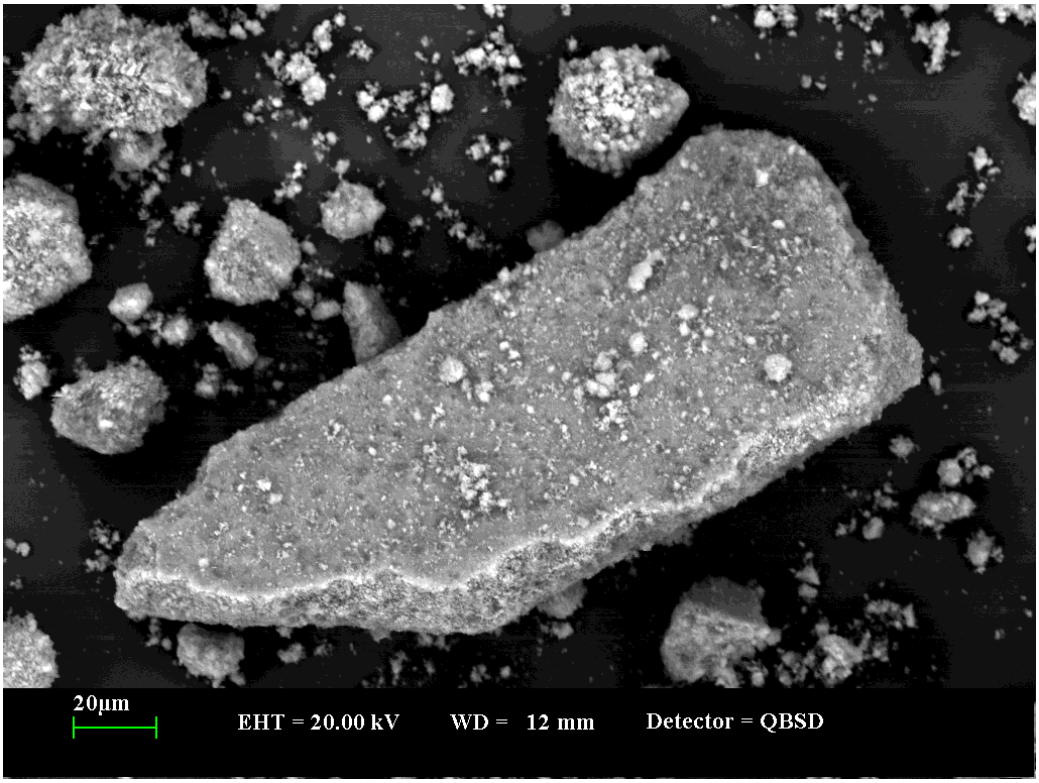

Graymont Dolomitic Lime at 1000X magnification.

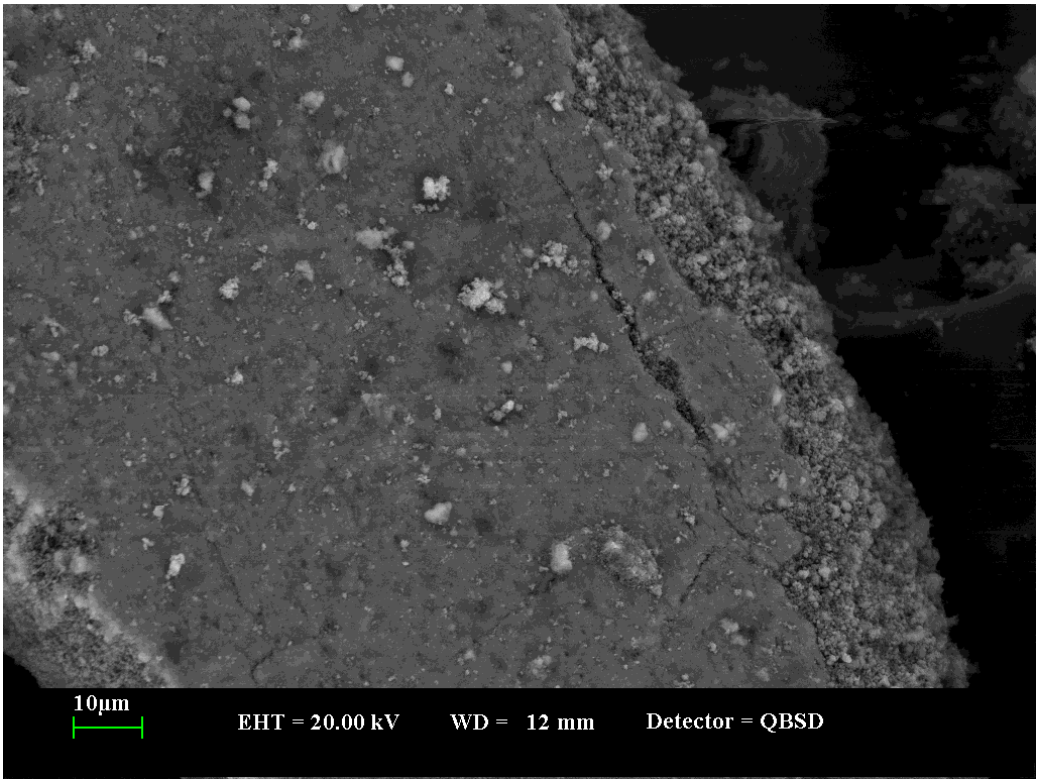

Graymont Dolomitic Lime at 1780X magnification.

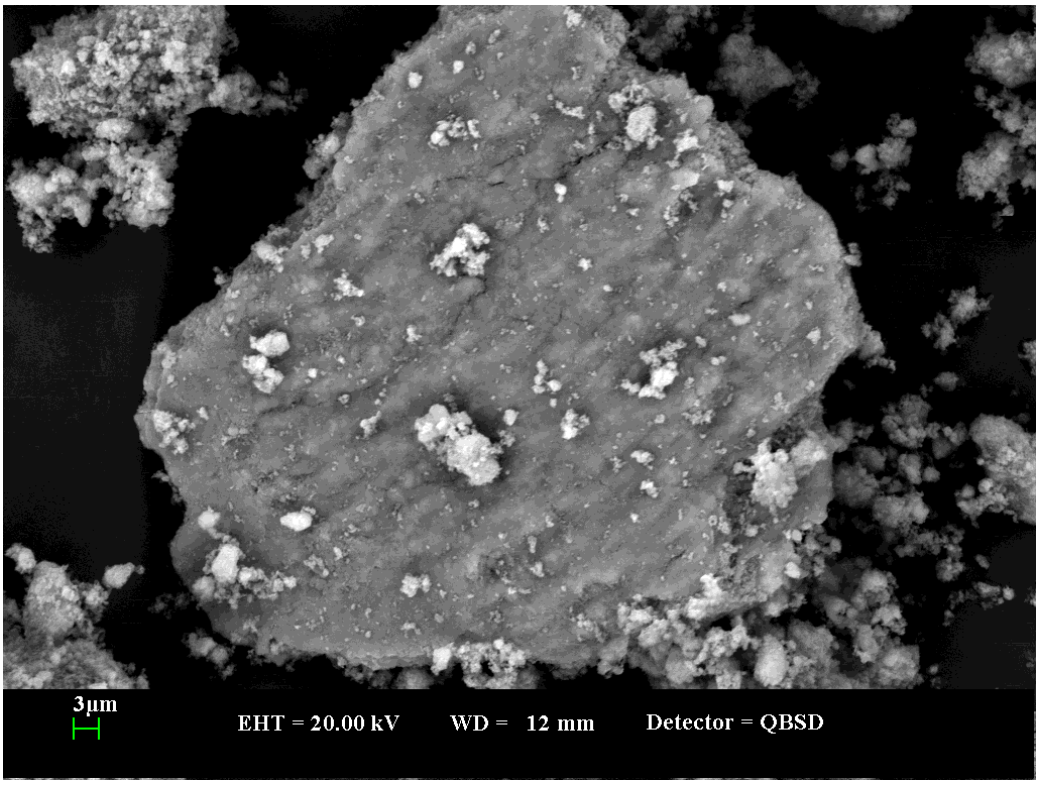

Graymont Dolomitic Lime at 2140X magnification.

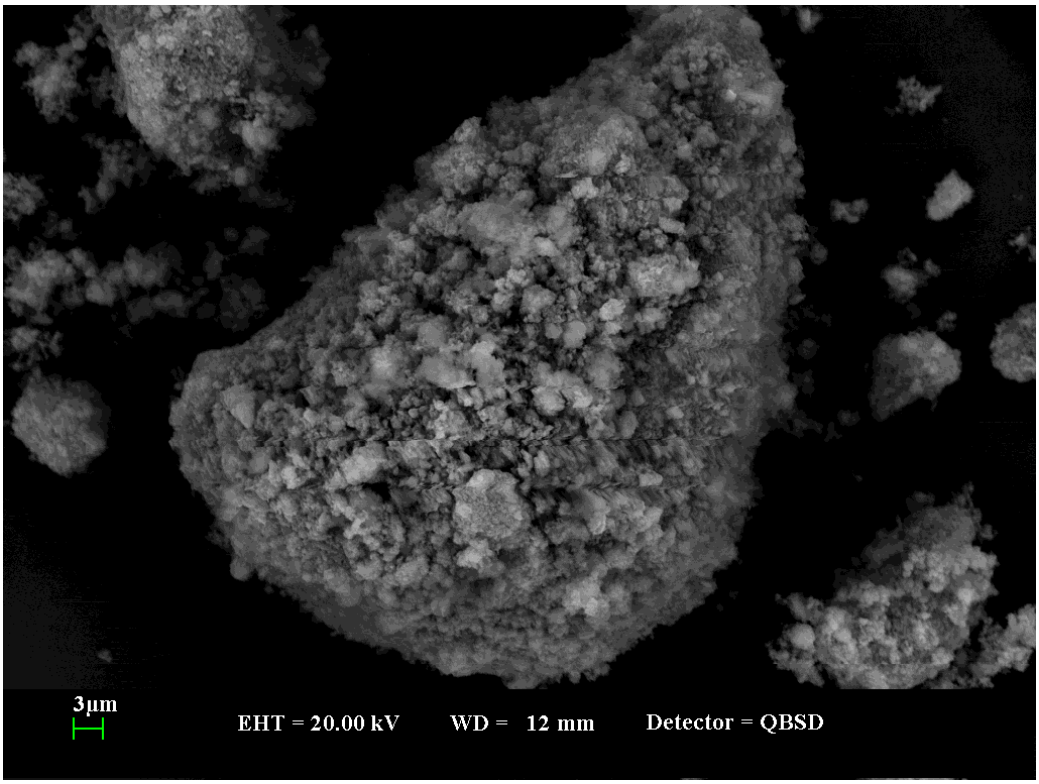

Graymont Dolomitic Lime at 2490X magnification.

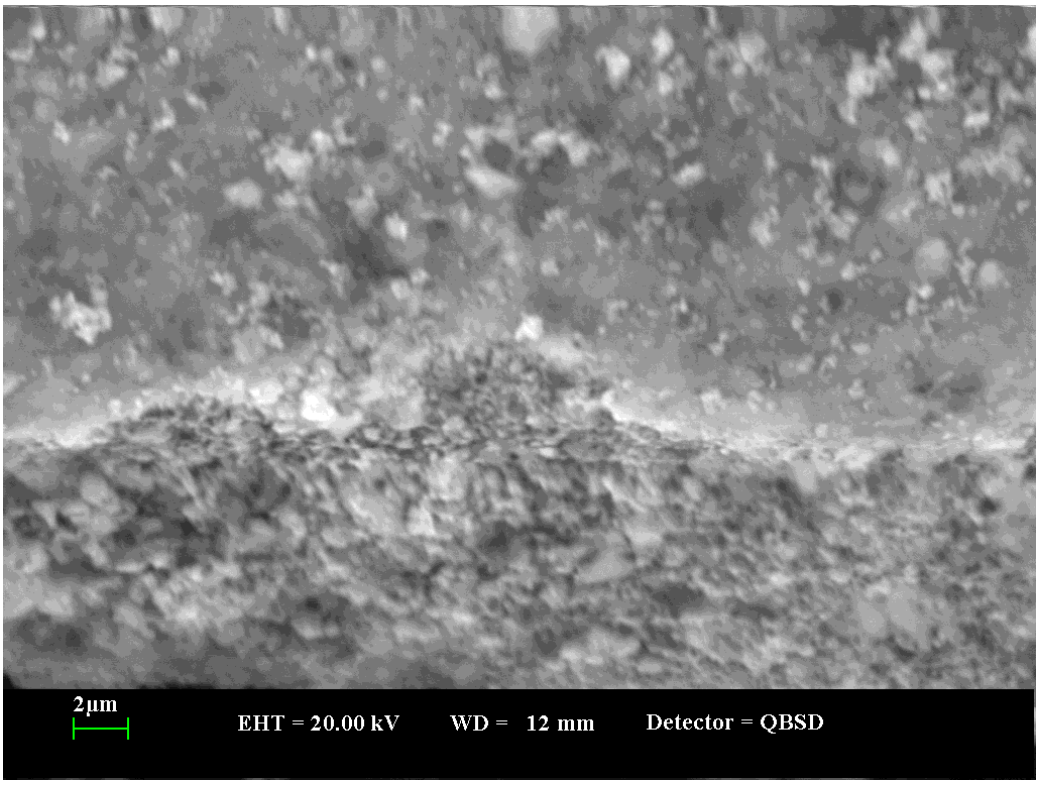

Graymont Dolomitic Lime at 7000X magnification.

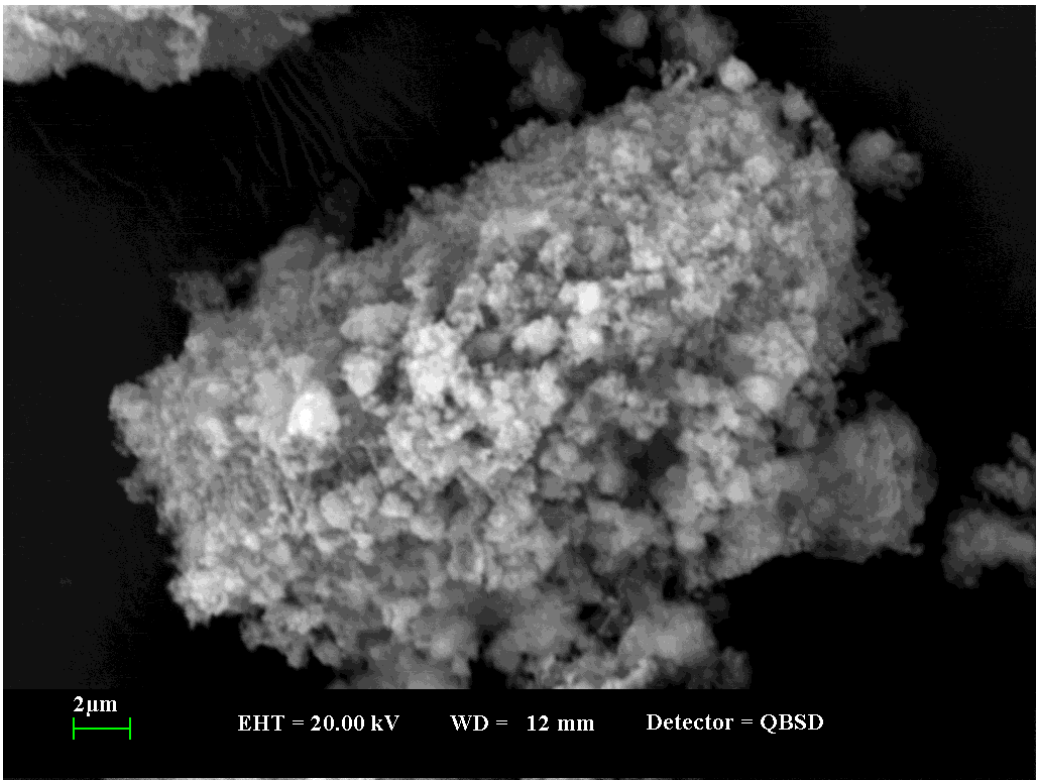

Graymont Dolomitic Lime at 7240X magnification.

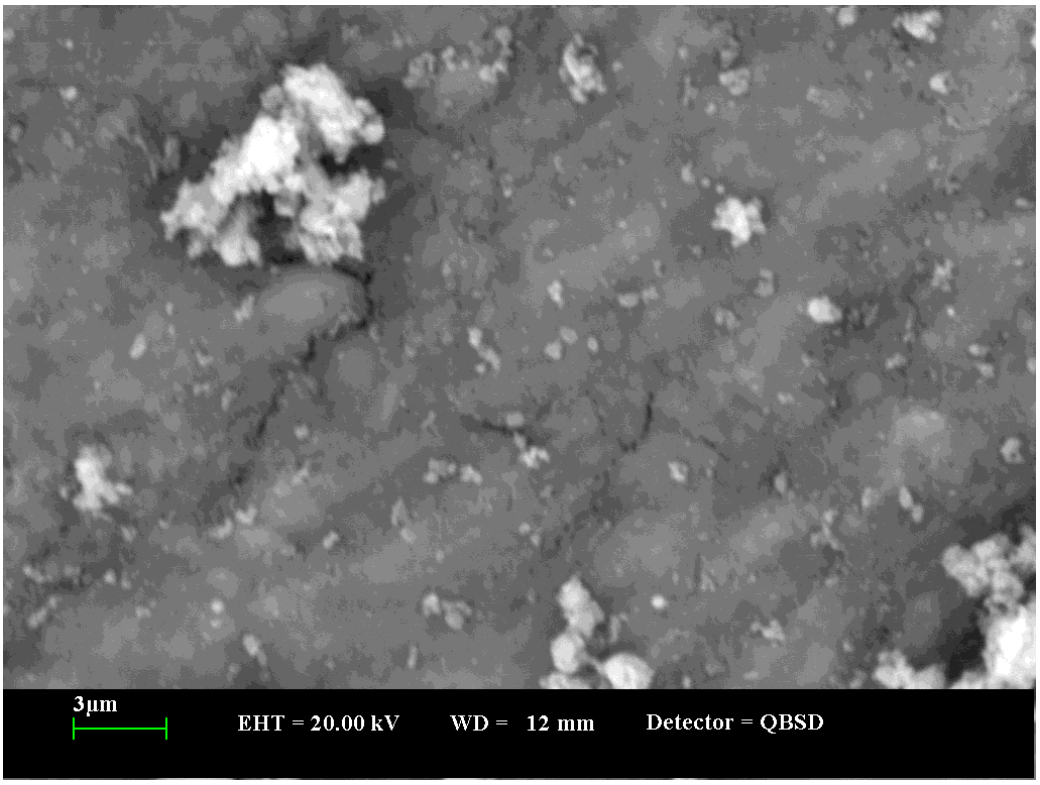

Graymont Dolomitic Lime at 7990X magnification.

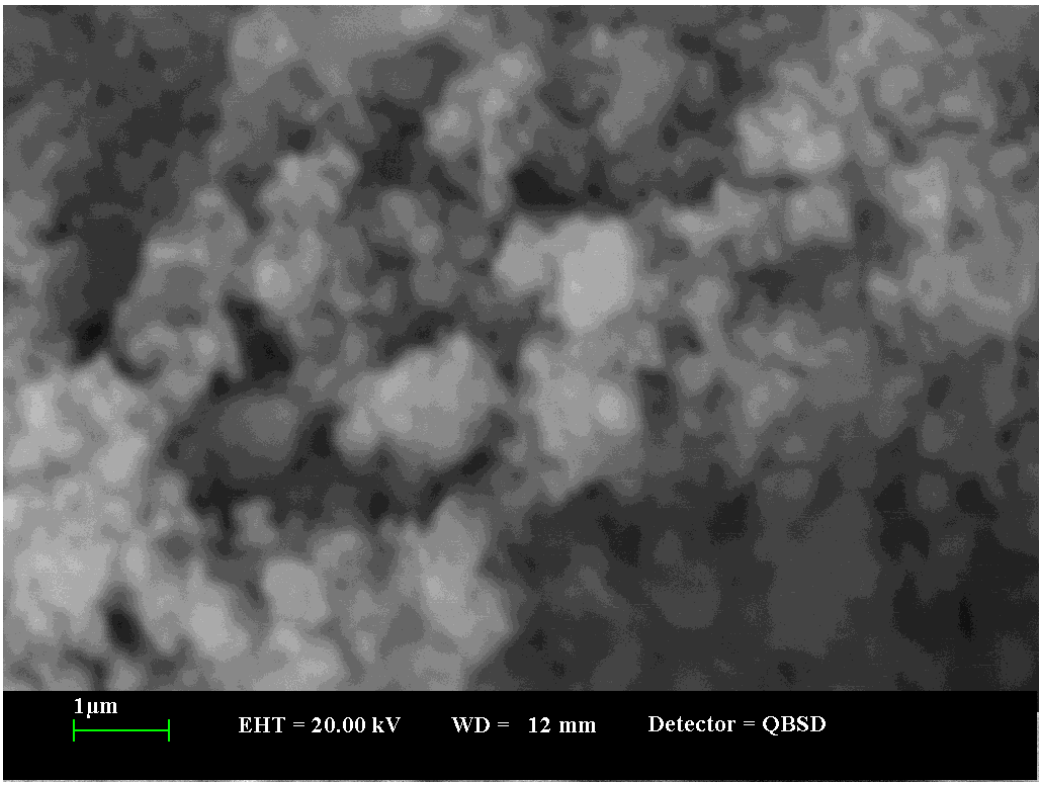

Graymont Dolomitic Lime at 24,500X magnification.

Commercial High-Calcium Lime

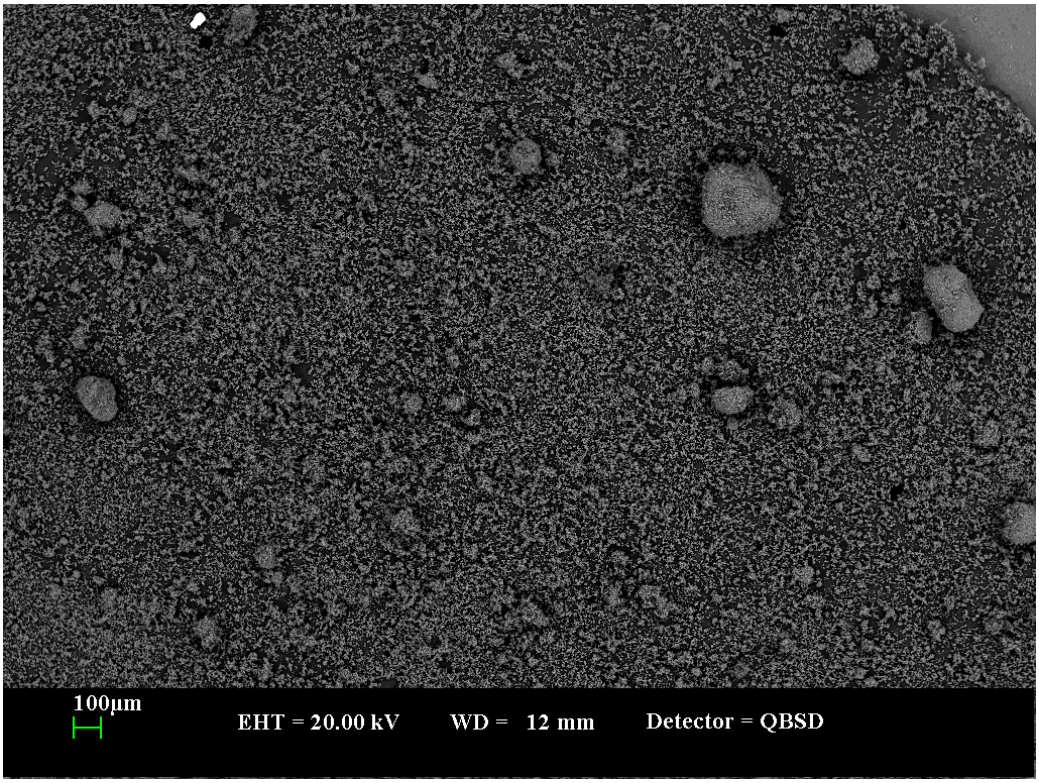

Mercer High-Calcium Lime at 69X magnification.

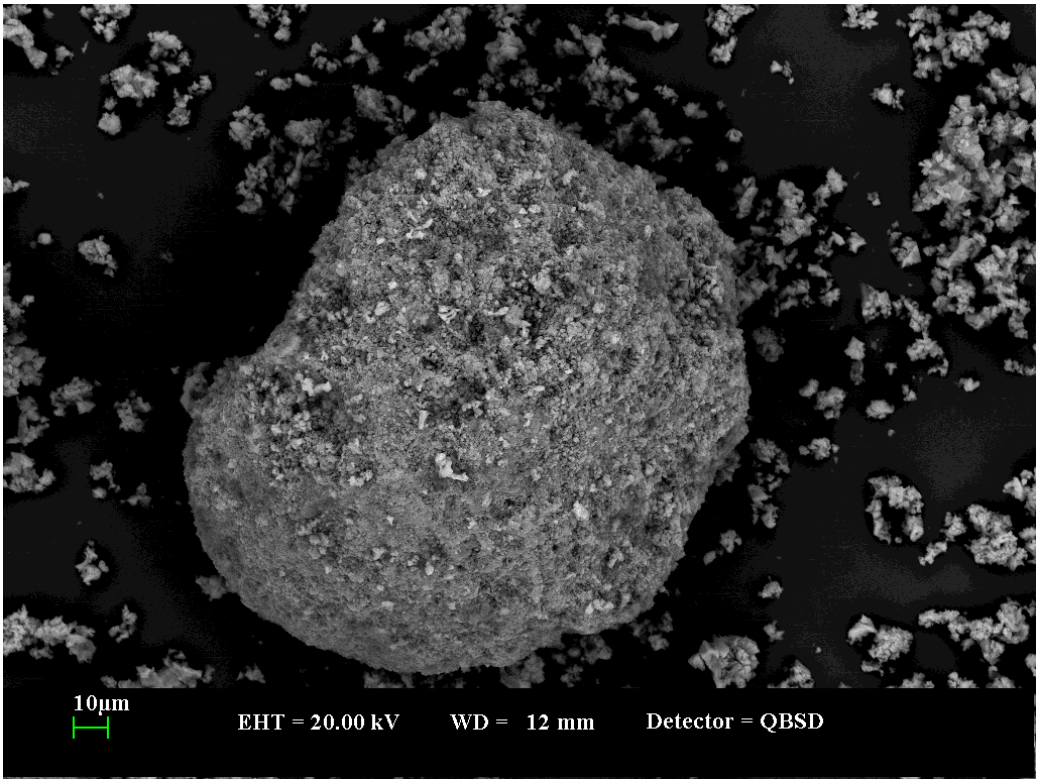

Mercer High-Calcium Lime at 888X magnification.

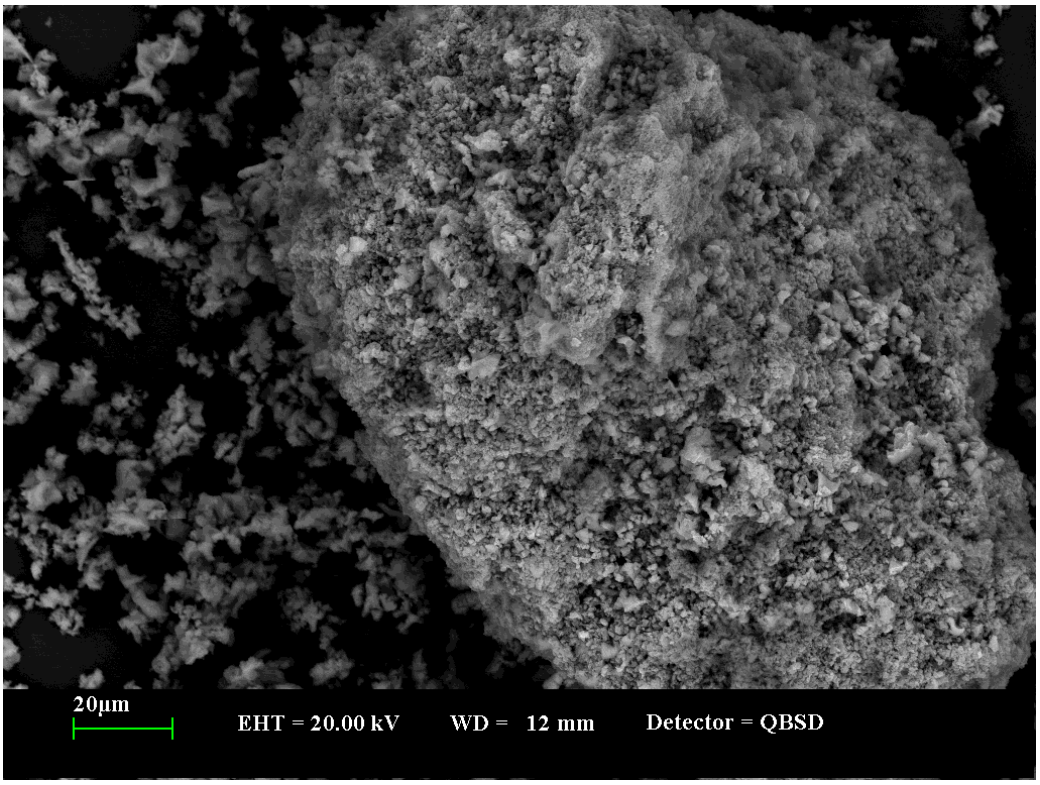

Mercer High-Calcium Lime at 1270X magnification.

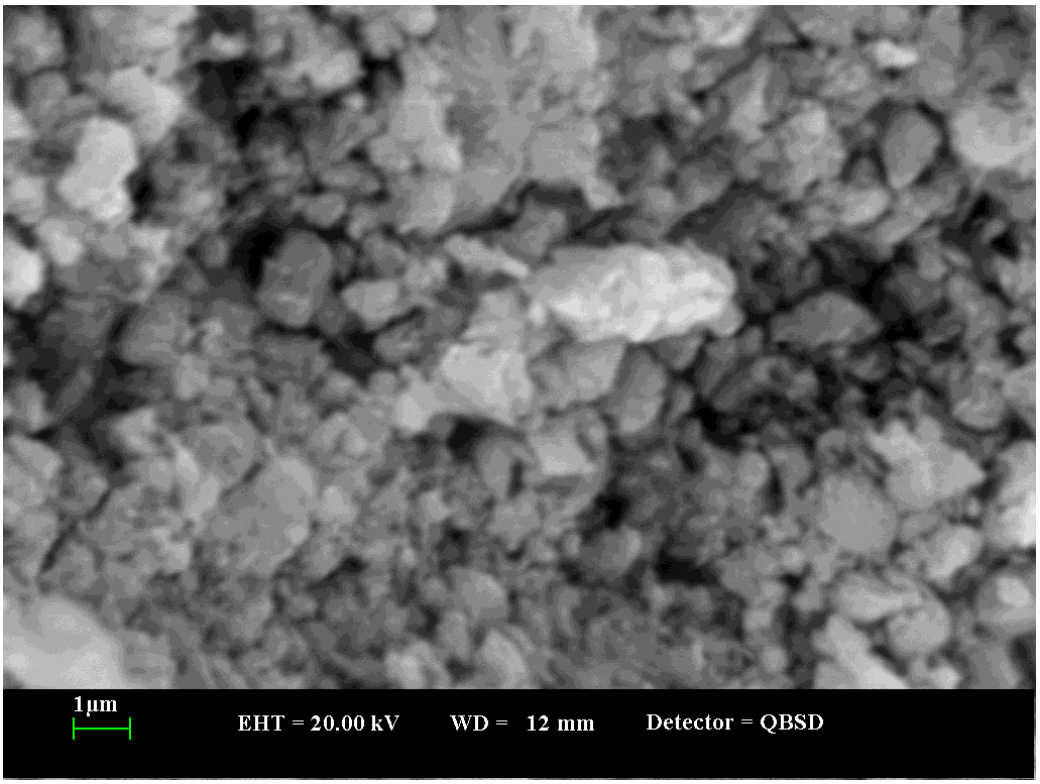

Mercer High-Calcium Lime at 14,600X magnification.